B86-183

THERMAL ANALYSIS OF HEAT EXTRACTION BOREHOLES

Per Eskilson

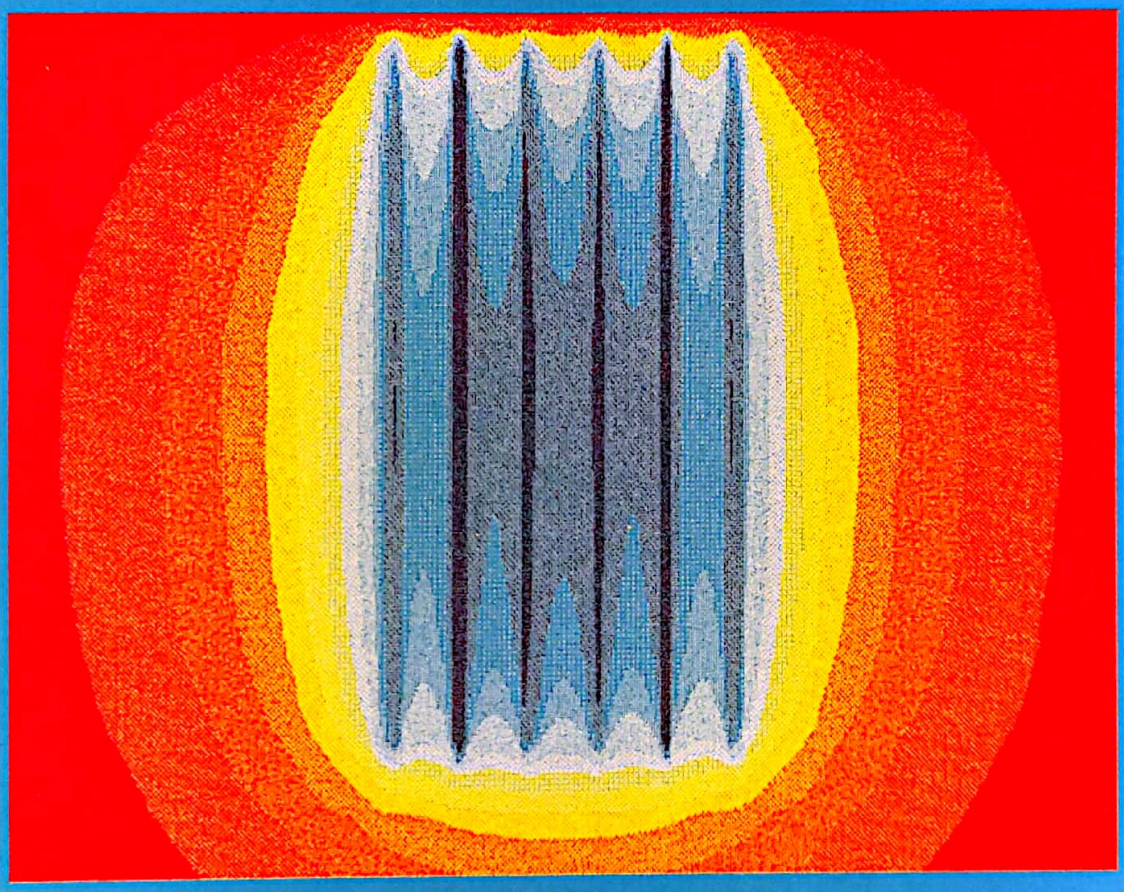

June 1987

Dep. of Mathematical Physics
University of Lund, Sweden

Thermal Analysis of Heat Extraction Boreholes

Per Eskilson

BIBLIOTH. AMSTELAED.

The figure on the front page shows the isotherms after 25 years for a system with six vertical boreholes. The heat extration rate is 127 MWh/year. The spacing between the boreholes is 11 meters, and each borehole has a depth of 115 meters. The red color indicates the undisturbed ground temperature, which is 8°C, and the dark blue represents the temperature 1°C.

Papers and reports of the thesis

- Thermal Analysis of Heat Extraction Boreholes. Summary.
- Conductive Heat Extraction by a Deep Borehole. Analytical Studies.
- Conductive Heat Extraction by a Deep Borehole. Thermal Analyses and Dimensioning Rules.
- Conductive Heat Extraction by Thermally Interacting Deep Boreholes.
- Simulation Model for Thermally Interacting Heat Extraction Boreholes.
- PC-programs for Dimensioning of Heat Extraction Boreholes.
- Response Test for a Heat Store with 25 Boreholes.
- Numerical Study of Radial and Vertical Mesh Division for a Single Heat Extraction Borehole.
- Numerical Study of the Radial Mesh Division for Two Systems with 16 and 120 Boreholes.
- Temperature Response Function g for 38 Borehole Configurations.
- Temperature Response Function g for 12 Borehole Configurations.

Organization LUND UNIVERSITY	Document name DOCTORAL DISSERTATION
	Date of issue 1987-08-19
	CODEN: Lund-MPh-87/13
Author(s) Per Eskilson	Sponsoring organization Swedish Council for Building Research, National Energy Administration

Title and subtitle

Thermal analysis of heat extraction boreholes

Abstract

The ground is a virtually unlimited, always accessible heat source and sink to heat pumps. One or many deep boreholes may be used as heat exchanger in the ground. The thesis, which presents a reasonably complete theory for the thermal processes in ground and boreholes, consists of the following papers and reports:

1. Conductive Heat Extraction by a Deep Borehole. Analytical Studies. J. Claesson, P. Eskilson, 1986. (Submitted to Journal of Heat and Mass Transfer)
2. Conductive Heat Extraction by a Deep Borehole. Thermal Analyses and Dimensioning Rules. J. Claesson, P. Eskilson, 1987.
3. Conductive Heat Extraction by Thermally Interacting Deep Boreholes. J. Claesson, P. Eskilson, 1987.
4. Simulation Model for Thermally Interacting Heat Extraction Boreholes. J. Claesson, P. Eskilson, 1987. (in Journal of Numerical Heat Transfer)
5. PC-programs for Dimensioning of Heat Extraction Boreholes. Per Eskilson, 1987.
6. Response Test for a Heat Store with 25 Boreholes. Per Eskilson, Göran Hellström, Bengt Wånggren, 1987.
7. Numerical Study of Radial and Vertical Mesh Division for a Single Heat Extraction Borehole. Per Eskilson, 1986.
8. Numerical Study of the Radial Mesh Division for Two Systems with 16 and 120 Boreholes. Per Eskilson, 1986.
9. Temperature Response Function g for 38 Borehole Configurations. Per Eskilson, 1986.
10. Temperature Response Function g for 12 Borehole Configurations. Per Eskilson, 1986

Key words
Ground-coupled heat pumps, ground heat exchanger, multiple boreholes, thermal analysis, heat transfer in the ground

Classification system and/or index terms (if any)

Supplementary bibliographical information

Language
English

ISSN and key title
Heat extraction boreholes

ISBN 91-7900-298-6

Recipient's notes

Number of pages 264

Price

Security classification

Distribution by (name and address)
Lund Institute of Technology, Dep. of Mathematical Physics, P.O. Box 118, 221 00 LUND, Sweden.

I, the undersigned, being the copyright owner of the abstract of the above-mentioned dissertation, hereby grant to all reference sources permission to publish and disseminate the abstract of the above-mentioned dissertation.

Signature Per Eskilson **Date** 30/7 - 1987

/Per Eskilson/

enl SIS 61 41 21

THERMAL ANALYSIS OF HEAT EXTRACTION BOREHOLES

PER ESKILSON
Civ.ing.,Kr.

AKADEMISK AVHANDLING
som för avläggande av teknisk doktorsexamen vid tekniska fakulteten vid Lunds universitet kommer att offentligen försvaras vid sektionen för teknisk fysik, Sölvegatan 14, sal F, fredagen den 11 september 1987, kl 9.15

Thermal Analysis of Heat Extraction Boreholes. Summary

Introduction

The oil crisis in the early 70's gave incentive for the development of alternative energy sources. Renewable sources such as solar, wind, and ocean power were were studied intensely. Heat pumps for domestic heating attracted and continues to attract quite a lot of interest. A heat pump requires a low-temperature heat source. Ambient air and surface water, which are frequently used, have the disadvantage that the temperature follows the climatic variations. In particular, problems arise, when the temperature falls below freezing. Groundwater, when available in sufficient quantities, is a very good heat source, since its temperature normally is quite stable. The ground itself is an attractive heat source, as it is virtually unlimited and always available. The ground temperature is almost constant in time except for the upper few meters.

The ground heat is extracted by some kind of heat exchanger system, which has to be constructed. Horizontal pipes at moderate depth are frequently used. Trenches are dug, pipes installed, and the trenches are refilled. In soft ground, vertical pipes may be forced down to a sufficient depth. Another possibility is to use boreholes[1]. Abandoned boreholes in rock, previously used as water wells, have often been converted to heat extraction. The depth of a heat extraction borehole is normally between 40 and 150 m, and the diameter 0.075 to 0.11 m. Large heat pumps require many boreholes. Multiple boreholes are often drilled from a small area at the ground surface, and inclined away from each other.

The heat carrier fluid flows along the borehole in one channel (or a number of channels) down to the bottom of the borehole and back upwards in another channel. The fluid is cooled, when it delivers heat to the heat pump. The cold fluid in the borehole induces conductive heat flow from the surrounding, warmer ground. The borehole may be conceived as a cold rod, to which heat flows from the surrounding ground.

Research in this field has been quite active during the last 10 years. A few conferences on ground heat storage and extraction have taken place, [1-2]. I would like to mention studies of the following authors: Andersson, Eriksson and Åbyhammar (1980), Andersson, Eriksson, and Tollin (1983), Mogensen (1983), Tollin, Andersson, Eriksson (1983), Eriksson (1984), Tollin (1984), Bose (1984), Leroy (1985), Tollin (1985), Ericsson (1985), and Franck (1986).

The performance of a ground-coupled heat pump system is determined by the heat pump characteristics, and by the thermal process in the ground with its heat exchanger. The temperature of the heat delivered from the ground must lie within a specified range depending on the heat pump, the performance of which deteriorates with falling temperatures. The ground heat exchanger must be designed so that the required heat is delivered at proper temperatures.

The construction costs of the ground heat exchangers are critical for the economical competitiveness of this type of heating system. It is imperative to find the cheapest alternatives for different geological and technical conditions. In order to optimize the systems from a technical, economical, and environmental point-of-view, it is necessary to have analytical tools by which

[1] I have not found the word borehole in English dictionaries, but bore, bore hole,and bore-hole. I have taken the liberty to write it in one word, since it is used so frequently.

the thermal behavior of any system can be assessed. The proper design and dimensioning of a particular system require a precise knowledge of the relation between temperature of delivered heat and heat extraction rate under various conditions. Reliable and easy-to-use dimensioning methods are needed to promote the use of ground-coupled heat pumps. New ideas and inventions keep appearing in this field. A firm knowledge and understanding of the thermal processes in the ground and their interaction with any conceivable heat exchanger are needed in the assessment of new ideas.

The aim of *this thesis* is to provide analytical tools by which questions and problems related to the thermal processes in ground and borehole can be answered and solved.

Ground-coupled heat pumps used for air conditioning discharge, in the cooling mode, heat to the ground. Then, the problem is to avoid too high discharge temperatures. The thermal problem of this thesis is posed in terms of heat extraction, but all results and analyses are equally applicable to heat injection to the ground, or any mixture of injection and extraction.

Thermal Analysis

The general goal of the thermal analysis is to master the response of the ground heat exchanger, i.e. the relation between heat extraction rate and temperature of the heat carrier fluid, under various conditions. The thermal analysis should also provide a basis for evaluations of new ideas and designs. Simple and reliable dimensioning rules should be established.

In order to develop the theory of heat extraction boreholes, one ought to start with basic simple cases and introduce complications step by step. Less important effects should, if possible, be analyzed seperately. Whenever possible, different thermal processes should be seperated from each other in order to obtain a more clear understanding of the complex total process.

A suitable starting point for the analysis is the basic case of a single vertical borehole. The ground heat exchanger consists of two main parts: the heat exchanger in the borehole and the ground outside the borehole.

The thermal processes of the heat exchanger in the borehole are treated in detail in other studies within our reseach group, [13-15]. The results are used in my thesis, which focuses upon the thermal processes in the ground outside the borehole.

The borehole acts as a cold vertical rod, to which heat flows from the surrounding ground by pure heat conduction. There are many many phenomena which complicate the thermal process. The boundary conditions at the ground surface are determined by the variable local climate including snow and rain. Typically, the ground consists of horizontal strata with different thermal properties. Shallow layers of soil may act as a thermal insulator. The geothermal heat flow through the earth's crust must be taken into account, since it causes a significant increase of ground temperature with depth. Moving groundwater in cracks may influence the heat flow around the borehole.

It is shown in *Paper 1* that all the complications mentioned above may be dealt with by separate analyses. The basic problem for a single borehole may be simplified to a case with homogeneous ground, and constant initial and boundary temperature. The next simplification concerns the demand of heat, which often varies strongly, for example during the day and the year. The simplest conceivable case is a heat extraction step, i.e. a constant extraction rate starting at a certain time. By superposition, any time-dependent heat extraction may be regarded as a sum of such basic extraction steps. The solution for the heat extraction step and its behavior are treated in detail in Paper 1. Superposition of the steady-state solution, step responses, and the periodic solution makes it possible to give a lucid descripion of the physical character of the heat extraction process. A novel analytical solution shows, contrary to common belief, that the effect of groundwater filtration is negligible in normal Swedish applications. The cooling of the ground due to the heat extraction may affect the vegetation. However, it is shown

with simple formulas, derived from analytical solutions, that the temperature disturbance is completely negligible in comparison with natural climatic variations.

Paper 1 deals with the mathematical analysis of the thermal processes for a single borehole, while *Paper 2*, which is based on the results of Paper 1, is devoted to physical and more technical aspects. It is shown that more than 25 years are required to attain approximate steady-state conditions (for a borehole with the depth 100 m). The extracted heat originates partly from cooling of the ground, partly from heat flow through the ground surface. It is interesting to note that only one-third of the extracted heat is supplied through the ground surface after 25 years (for the borehole depth 100 m). The time-scale of the thermal process is indeed large.

Further insight in the processes is gained by an analysis of extraction pulses. Handy formulas for the effect of a single pulse, balanced pulses, and a pulse train are derived. The futility of thermal recharge in summertime in order to improve the extraction the following winter is demonstrated.

Thermal resistances, associated with the different types of extraction components, are introduced and used systematically to relate extraction temperatures, or rather temperature drops, to heat extraction rates. The thermal resistance for the heat extraction step becomes time-dependent. The temperature drop is equal to a sum over products of thermal resistances and the corresponding intensities or amplitudes.

Three quite important parameters for heat extraction boreholes are the (average) thermal conductivity of the ground, the thermal resistance of the borehole heat exchanger, and the (average) undisturbed ground temperature. A method to measure these parameters is proposed, [6]. An application of this so-called response-test method for a case with 25 boreholes is reported in *Report 6*. The mathematics of the evaluation method for variable extraction pulses is detailed in the report.

A single borehole with a depth of 80 to 150 m is sufficient for the heating demand of a Swedish one-family house. The question of thermal influence arises, when there are many closely-spaced boreholes. This situation occurs for neighboring houses, each using a borehole, or when a large heat pump uses many boreholes as heat exchanger in the ground. For a multiple-borehole system, it is often necessary or advantageous to let the boreholes lie close to each other at the ground surface and incline them outwards away from each other in order to diminish the thermal influence. A rather common system in Sweden is a diverging bundle of 10 to 25 boreholes. The heat pump is placed close to the small borehole surface area, often in the basement of the building.

Paper 3 presents a rather complete theory for thermally interacting boreholes. Simple formulas to estimate, when the thermal influence is negligible, and when it is significant, are given. The thermal influence turns out to be of a rather insidious character, as it is totally unnoticable during the first few years, if the smallest distance between the boreholes exceeds, say, 15 m. However, the thermal influence often becomes excessive after another 5 years. The analyses and dimensioning rules of Paper 2 must be modified to account for the thermal influence. Normally, the thermal processes due to variations of extraction rate during the annual cycle and the corresponding components in the dimensioning formulas are not changed. The modifications concern the long-term heat extraction steps only. The solution for the basic extraction step is needed for a very long time period up to steady-state conditions. The corresponding thermal resistance is expressed in dimensionless form by so-called g-functions, which depend on time and on the dimensionless parameters that determine the positions of all boreholes. Based on these dimensionless step-response functions, a discussion of the thermal influence is presented in Paper 3 for various borehole configurations (row of boreholes, parallel rows, quadratic pattern, inclined boreholes etc.). The thermal performance is shown to be quite insensitive to moderate changes of the borehole directions. The question of optimal borehole configurations is touched upon. Guide-lines for optimum under geometrical constraints on the borehole positions are given.

In the case of multiple boreholes, the thermal process, and in particular the step-response functions, have to be calculated with a numerical model. A complication is the interaction between the axial convective heat flow along the fluid channels in the boreholes and the conductive heat flow in the ground. A major problem is the complicated geometry for cases with many boreholes, which may have different directions. A direct solution with conventional numerical methods cannot, with the present capacities of computers, give an accurate result. A judicious use of the inherent symmetries of the heat flow process is necessary.

An elaborate numerical model for any configuration of boreholes has been developed. The theory and ideas of the model are presented in *Paper 4*, while *Report 12* is a manual for the computer program. The three-dimensional problem is by a rather intricate superposition reduced to axi-symmetrical ones; one for each borehole or symmetry group of boreholes. The temperature in the ground is given by superposition of one contribution from each borehole. The boundary condition at the ground surface necessitates, in the case of inclined boreholes, the introduction of mirror boreholes above the ground surface. The thermal process along the borehole channels is accounted for by an analytical solution, which is incorporated in the numerical model. The model is quite flexible concering loading conditions and hydraulic coupling between the boreholes. It has been numerically validated in a number of studies. The mesh used for the axi-symmetrical solutions is studied in *Report 7*. Simple rules how to choose a proper mesh are given. The accuracy of the numerical solution is studied in *Report 8* for two cases with 16 or 120 boreholes.

The numerical model has been used extensively to compute the dimensionless response functions for various borehole configurations. The g-functions for 226 cases are given in *Reports 9* and *10*.

Quite a lot of work has been expended on PC-models. The dimensioning rules in Papers 2 and 3, and the analytical formulas in Paper 1 have been implemented on IBM-compatible personal computers. All g-functions of Reports 9-10 are accessible.

Papers and reports in the thesis

- Papers to be published.

  1. Conductive Heat Extraction by a Deep Borehole. Analytical Studies. J. Claesson, P. Eskilson, 1986. (Submitted to Journal of Heat and Mass Transfer)
  2. Conductive Heat Extraction by a Deep Borehole. Thermal Analyses and Dimensioning Rules. J. Claesson, P. Eskilson, 1987.
  3. Conductive Heat Extraction by Thermally Interacting Deep Boreholes. J. Claesson, P. Eskilson, 1987.
  4. Simulation Model for Thermally Interacting Heat Extraction Boreholes. J. Claesson, P. Eskilson, 1987. (Accepted for publication in Journal of Numerical Heat Transfer)

- Reports.

  5. PC-programs for Dimensioning of Heat Extraction Boreholes. Per Eskilson, 1987.
  6. Response Test for a Heat Store with 25 Boreholes. Per Eskilson, Göran Hellström, Bengt Wånggren, 1987.
  7. Numerical Study of Radial and Vertical Mesh Division for a Single Heat Extraction Borehole. Per Eskilson, 1986.
  8. Numerical Study of the Radial Mesh Division for Two Systems with 16 and 120 Boreholes. Per Eskilson, 1986.

9. Temperature Response Function g for 38 Borehole Configurations. Per Eskilson, 1986.

10. Temperature Response Function g for 12 Borehole Configurations. Per Eskilson, 1986

- Departmental reports not included in the dissertation.

11. Bergvärme. Termiska analyser (Heat Extraction Boreholes. Thermal Analyses). Per Eskilson, 1986.

12. Superposition Borehole Model. Manual for Computer Code. Per Eskilson, 1986.

References

1. Swedish Council for Building Research, Proceedings of International Conference on Subsurface Heat Storage in theory and practice, Stockholm, June 6-8, 1983, BFR-Document D16-17:1983, Svensk Byggtjänst, Box 7853, S-103 99 Stockholm, Sweden.

2. Public Works Canada, Enerstock 1985, III International Conference on Energy Storage for Building Heating and Cooling, September 22-26, Toronto, Canada.

3. Andersson, S., A. Eriksson, and T. Åbyhammar, Utvinning av värme ur bergborrade brunnar (Extraction of heat from boreholes in hard rock), Swedish Council of Building Research, Report R142:1980, Svensk Byggtjänst, Box 7853, S-103 99 Stockholm, Sweden.

4. Ericsson, L.O., Värmeutbyte mellan berggrund och borrhål vid bergvärmesystem (Heat exchange between crystalline bedrock and borehole in an energy well system), Thesis, Publ. A52:1985, Department of Geology, Chalmers Institute of Technology, S-412 96 Gothenburg, Sweden, 1985.

5. Franck P.Å. ,A Study of Heat Pump Systems with Low Temperature Seasonal Heat Storage in Clay. Thesis, Dep. of Heat and Power Techology, Chalmers University of Technology, S-412 96 Gothenburg, Sweden, 1986.

6. Mogensen P., Fluid to Duct Wall Heat Transfer in Duct System Heat Storages. Appearing in Reference 1.

7. Tollin, J., S. Andersson, and A. Eriksson, Utvinning av värme ur bergborrade brunnar. Fältmätningar och erfarenheter (Heat extraction from boreholes in hard rock. Field measurements and experiences.), Swedish Council of Building Research, Report R148:1983, Svensk Byggtjänst, Box 7853, S-103 99 Stockholm, Sweden.

8. Eriksson, A., Energibrunnar för villa och småhusbebyggelse. Kortfattad informationsskrift. (Heat extraction boreholes for one-family houses. Brief information.) Swedish Council of Building Research, Report G27:1984, Svensk Byggtjänst, Box 7853, S-103 99 Stockholm, Sweden.

9. Tollin, J., Bergvärme för små hus. Dimensionering (Heat extraction boreholes for one-family houses. Dimensioning.) Swedish Council of Building Research, Report R183:1984, Svensk Byggtjänst, Box 7853, S-103 99 Stockholm, Sweden.

10. Bose, J.E., J.D. Parker, and F.C. McQuiston, Design/Data Manual for Closed-Loop Ground-Coupled Heat Pump Systems, ASHREA, 1791 Tullie Circle, NE, Atlanta, GA 30329, USA, 1985.

11. Leroy G., Response transitoire d'un echangeur cylindrique vertical dans le sol. Caracterisation thermique due terrain.
Appearing in Reference 2

12. Tollin J., Heat Pump with a Hard Rock Well Equipped for Thermal Recharge.
Appearing in Reference 2.

13. Bennet J. , J. Claesson, G. Hellström, Multipole Method to Compute the Conductive Heat Flows to and between Pipes in a Composite Cylinder, Notes on Heat Transfer 3-1987, Dep. of Building Technology and Mathematical Physics, University of Lund, Box 118, S-221 00 Lund, Sweden, 1987.

14. Claesson J. , G. Hellström, Thermal Resistances to and between Pipes in a Composite Cylinder, Dep. of Mathematical Physics and Building Physics, University of Lund, Box 118, S-221 00 Lund, Sweden, 1987.

15. Claesson J. , G. Hellström, The Effect of the Temperature Variation along the Pipes in a Heat Exchanger in the Ground, Dep. of Mathematical Physics and Building Physics, University of Lund, Box 118, S-221 00 Lund, Sweden, 1987.

PREPRINT

(Submitted to the International Journal of Heat and Mass Transfer)

Conductive Heat Extraction by a Deep Borehole. Analytical Studies.

Johan Claesson
Per Eskilson

March 1987

Departments of Mathematical Physics
and Building Technology
University of Lund
Box 118
S-221 00 Lund, Sweden

TABLE OF CONTENTS

Section	Page
Abstract	1
Nomenclature	2
1 Introduction	3
2 Assumptions and simplifications	4
3 Effect of the geothermal gradient	5
4 Mathematical formulation	8
5 Heat extraction step	9
6 Steady-state solution	11
7 Approximations for the g-function	12
8 Periodic heat extraction	13
9 Superposition using the basic solutions	14
10 Effect of groundwater filtration	16
11 Disturbance at the ground surface	19
Appendix. Analytical solutions using line sinks	21
References	25

Abstract

The thermal processes in the ground, when heat to support a heat pump is extracted by conduction to a deep borehole, are analysed. Simple formulas that relate the required extraction temperature to any prescribed heat extraction are obtained by superposition of steady-state (for which a ubiquitous error is corrected), periodic, and extraction step solutions. The effect of groundwater filtration and the thermal disturbance at the ground surface are shown to be negligible in many applications.

q	heat extraction step
s	steady-state
surf	ground surface
sw	steady-state and groundwater filtration
w	water

1 Introduction

A way to extract heat from the ground to support a heat pump for domestic heating is to use a deep borehole, preferably in rock with high thermal conductivity. The depth of the borehole may be 40-150 meters. Many systems of this kind have been built in the United States and Canada, and about 5,000 systems are now in operation in Sweden.

The heat carrier fluid is heated by the rock, while it flows down to the bottom of the borehole in a channel and back upwards in another channel. The cold borehole extracts heat from the surrounding rock by pure heat conduction. The most common alternative in Sweden is to use a closed loop for the heat carrier fluid in the borehole. A U-shaped plastic tube may be used, see Figure 1. A second alternative is to use the groundwater in the borehole directly as heat carrier fluid. A single pipe down to the bottom is needed. The heat extraction temperature must then be above 0 °C in order to avoid freezing.

The borehole and a few notations are shown in Figure 1. An upper part down to the depth D is regarded as thermally insulated. The total heat extraction rate is $q(t) \cdot H$ (W). Here $q(t)$ (W/m) denotes the average heat extraction rate per meter borehole. The temperature at the borehole wall is denoted T_b.

The aim of our studies is to obtain formulas for the relation between the heat extraction rate $q(t)$ and the required borehole temperature $T_b(t)$. The results are also applicable for the case of heat injection to the ground. The formulas presented here are applied in [1] to obtain dimensioning rules for a single borehole, and in [2] for a system of thermally interacting boreholes. Thermal problems such as the disturbance near the ground surface, the long-term behaviour, and the effect of moving groundwater are discussed here, and from a more applied point of view in

[1] and [2]. The local thermal processes within the borehole, which are not discussed here, are dealt with in detail in [3] and [4]. A more detailed report of our studies is [5], which is written in Swedish.

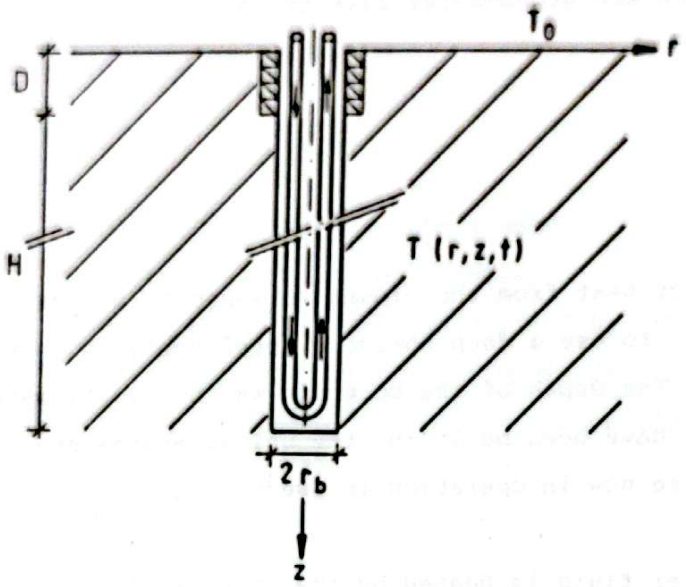

Figure 1. Heat extraction borehole.

2 Assumptions and simplifications

The thermal process in the ground with all its possible complications may in the present applications be simplified quite a lot. The temperature at the ground surface varies strongly during the day and the year. The amplitude of periodic surface variations decreases as e^{-z/d_p} downwards. The penetration depth d_p (8.3) is a few meters for the annual variation. This disturbance in the top few meters can be neglected, since the length of the borehole is around 100 meters. It is quite sufficient to use the annual mean air temperature T_o as boundary condition at the ground surface. All other complications at the ground surface such as air-to-ground thermal resistance, freezing, and snow may by the same reason be neglected.

The ground is assumed to be homogeneous. In practice there is often a different top-soil layer. Consider as an example the case with granite (λ=3.5 W/mK) and a 5 meter thick top-soil layer (λ=1.5 W/mK). A numerical simulation shows that the lower conductivity of the top layer changes the thermal performance with less than 2%. A top-soil layer with a thickness less than, say, 10 m can therefore be neglected.

The uppermost part of the borehole, $0 < z < D$, is treated as thermally insulated. The depth D may in the actual case be the groundwater level or the depth of an insulated casing. The exact value of D, for a fixed active borehole length H, is however not important. In a numerical simulation we varied D from 2 to 8 meters. The change of the extraction temperature was less than 0.1°C. The value of D is in the following numerical examples 4 or 5 m.

The thermal process within the borehole and the interaction with the temperatures in the ground in the immediate vicinity of the borehole are analysed in [3] and [4]. The temperature of the heat carrier fluid varies along the downward and upward channels. At each level z and time t there is a local, essentially steady-state process for the heat flows between the fluid channels and the ground near the borehole. Let T_b denote the average wall temperature over the borehole height, $D < z < D+H$. Strictly speaking there is also an average around the pheriphery of the borehole. The inlet and outlet temperatures of the heat carrier fluid are related to T_b with explicite formulas in [3-4], and [1]. We will here only consider the thermal problem from the borehole wall and outwards in the ground. The temperature T_b at the borehole wall is constant over the borehole height, but it will of course vary with time.

3 Effect of the geothermal gradient

The temperature at the ground surface is equal to the annual average value T_o of the air temperature. Let the geothermal gradient be α (K/m). The initial and boundary conditions are then:

$$T\Big|_{t=0} = T_o + \alpha \cdot z \qquad T\Big|_{z=0} = T_o \tag{3.1}$$

An example with H=146 m, D=4 m, λ=3.5 W/mK, and α=0.0162 °C/m is shown in Figure 2a (case a). The constant heat extraction rate is 1712 W (= 15 MWh/year). The computed isotherms after 25 years are shown. The calculation is made with the simulation model described in [6,7].

The thermal problem is simplified, if a constant common value for the initial and boundary temperature can be used. If the geothermal gradient in (3.1) is neglected, this temperature becomes T_o. A much better choice is to use the undisturbed mean temperature T_{om} along the borehole length H:

$$T_{om} = T_o + \alpha \cdot (D+H/2) \qquad (3.2)$$

Figure 2b shows the computed isotherms after 25 years with this simplified boundary and initial condition according to (4.2) (case b). All other data are the same as in case a. The borehole temperature differs only with 0.01 °C. The difference between the problems of Figure 2a and 2b is shown by Figure 2c. The temperature field is almost anti-symmetric around the depth D+H/2 at the mid-point of the borehole. The ground surface disturbs somewhat this anti-symmetry, but the error for the borehole temperature using the simplification (4.2) is negligable. The simplified boundary and initial conditions (4.2) are used in the following in the analysis of relations between heat extraction rates and borehole temperatures.

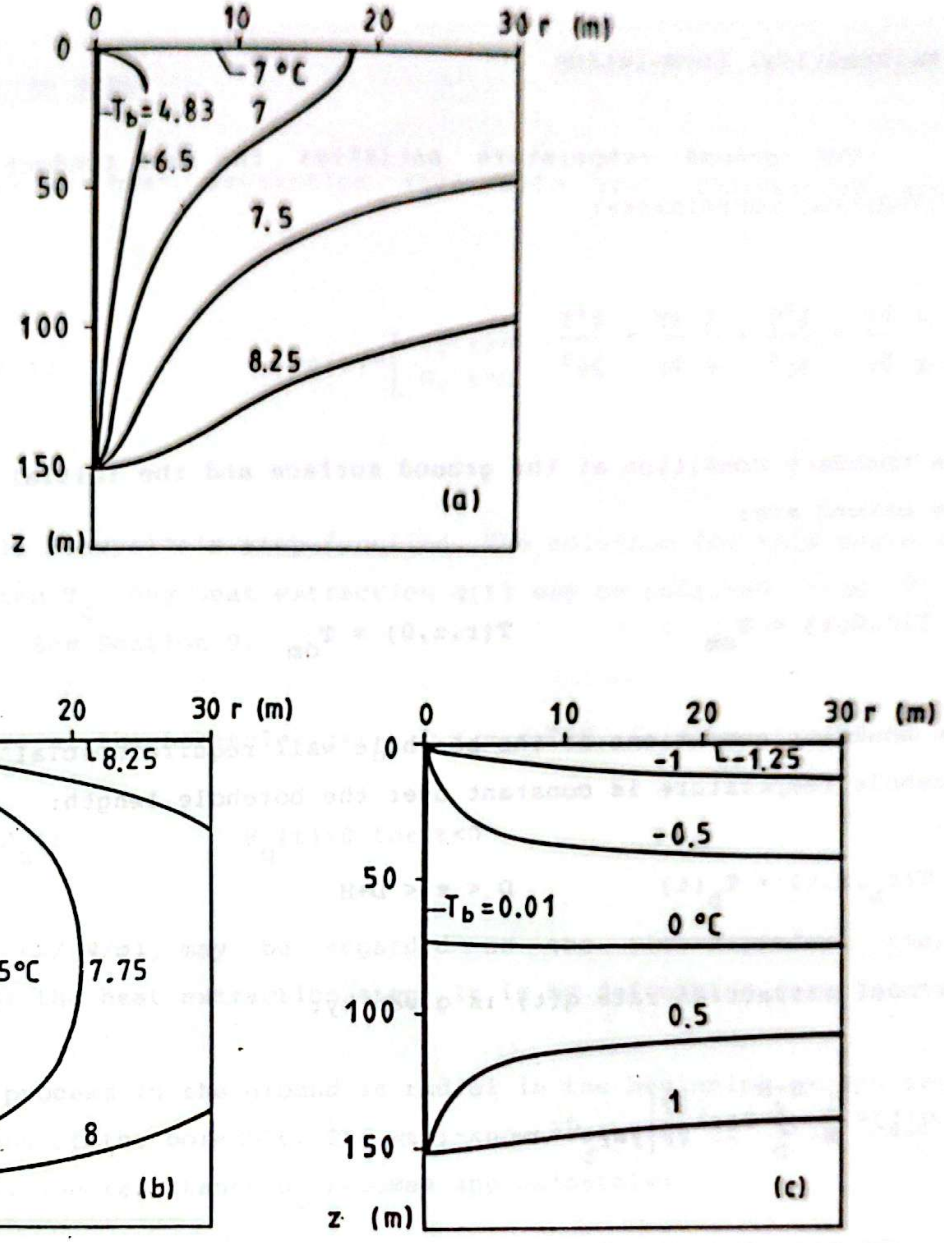

Figure 2. Isotherms after 25 years with boundary and initial conditions according to (3.1) (a) and (4.2) (b). The difference between (a) and (b) is given by (c).

4 Mathematical formulation

The ground temperature satisfies the heat conduction equation in cylindrical coordinates:

$$\frac{1}{a}\frac{\partial T}{\partial t} = \frac{\partial^2 T}{\partial r^2} + \frac{1}{r}\frac{\partial T}{\partial r} + \frac{\partial^2 T}{\partial z^2} \qquad (4.1)$$

The boundary condition at the ground surface and the initial condition in the ground are:

$$T(r,0,t) = T_{om} \qquad T(r,z,0) = T_{om} \qquad (4.2)$$

The boundary conditions at the borehole wall require special attention. The borehole temperature is constant over the borehole length:

$$T(r_b,z,t) = T_b(t) \qquad D < z < D+H \qquad (4.3)$$

The heat extraction rate q(t) is given by:

$$q(t) = \frac{1}{H}\int_D^{D+H} 2\pi r\lambda \frac{\partial T}{\partial r}\bigg|_{r=r_b} dz \qquad (4.4)$$

To complete the boundary condition we can prescribe $T_b(t)$ or q(t). The second alternative is much more convenient in our applications. Our thermal problem is then defined by (4.1-4) with a prescribed total heat extraction rate $H \cdot q(t)$. A main goal is to get $T_b(t)$.

5 Heat extraction step

Consider a heat extraction step with zero undisturbed ground temperature:

$$q(t) = q_1 \cdot He(t) \qquad He(t) = \begin{cases} 1, & t>0 \\ 0, & t<0 \end{cases} \qquad (5.1)$$

$$T_{om} = 0$$

Here He(t) is Heavyside's step-function. The solution for this basic step pulse is denoted T_q. Any heat extraction q(t) may be obtained from T_q by superposition. See Section 9.

The temperature at the borehole, $r=r_b$, $D < z < D+H$, is proportional to q_1:

$$T_{q,b} = -q_1 \cdot R_q(t) \qquad R_q(t)=0 \text{ for } t<0 \qquad (5.2)$$

The factor R_q (K/(W/m)) may be regarded as the time-dependent thermal resistance for the heat extraction step. It is by definition zero for t<0.

The thermal process in the ground is radial in the beginning except around the end regions of the borehole. The well-known solution of this case is given in [8A]. The resistance R_q becomes approximately:

$$R_q \approx R'_q = \frac{1}{4\pi\lambda} E_1(r_b^2/(4at)) \approx \frac{1}{4\pi\lambda}\left[\ln(4at/r_b^2)-\gamma\right] \qquad (5.3)$$

$$(5r_b^2/a < t < t_s/10) \qquad \gamma=0.5772$$

The lower limit $5r_b^2/a$, which in our applications becomes a few hours, is necessary for the use of a line sink at r=0 instead of a flow at $r=r_b$. The approximation of the exponential integral E_1 with the logarithmic expression is then valid [9A]. The upper limit, $t_s/10$, which in our applications becomes a few years, ensures essentially radial flow. See below.

For larger times it is necessary to consider three-dimensional effects. The general solution for the heat extraction step (5.1) is cylindrically symmetric: $T_q=T_q(r,z,t)$. The following dimensionless variables are used in the dimensional analysis:

$$r'=r/H \qquad z'=z/H \qquad t'=at/H^2 \qquad T'=\frac{2\pi\lambda}{q_1}\cdot T_q \tag{5.4}$$

The boundary condition (4.4) becomes:

$$1 = \int_{D/H}^{1+D/H} (r_b/H)\cdot\left.\frac{\partial T'}{\partial r'}\right|_{r'=r_b/H} dz' \qquad t'>0 \tag{5.5}$$

It follows from (5.5) that T' depends on the two dimensionless parameters r_b/H and D/H. The variation with D/H can according to the discussion above be neglected. The temperature $T_{q,b}$ at the borehole wall is independent of z. It is therefore a function of at/H^2 (or t/t_s) and r_b/H only. The resistance R_q of (5.2) is thus in general given by an expression of the type:

$$R_q(t) = \frac{1}{2\pi\lambda}\cdot g(t/t_s, r_b/H) \qquad t_s=\frac{H^2}{9a} \tag{5.6}$$

The dimensionless response function g for a step pulse is equal to -T' taken at $r'=r_b/H$. It is zero for $t/t_s<0$. The g-function has been computed numerically using the model [6,7] for $r_b/H= 0.0005$. See Figure 3. The variation of g with r_b/H is simple:

$$g(t/t_s, r_b^*/H) = g(t/t_s, r_b/H) - \ln(r_b^*/r_b) \tag{5.7}$$

The logarithm is essentially the thermal resistance of the annulus $r_b < r < r_b^*$. Numerical studies have shown that the error using (5.7), i.e. a radial steady-state approximation in the small annulus near the borehole, is less than 0.3% [5].

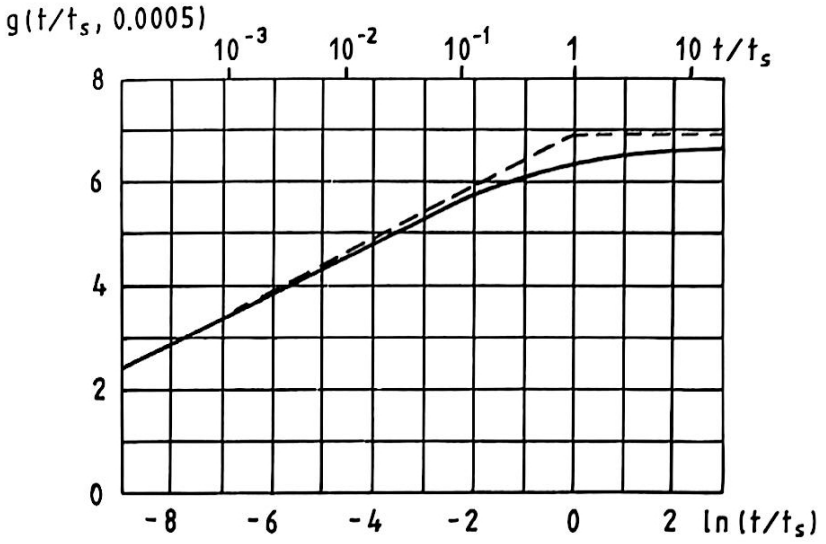

Figure 3. Dimensionless temperature-response function g for the heat extraction step (5.1).

6 Steady-state solution

The temperature T_q approaches the steady-state solution, when t tends to infinity. Let $T_s(r,z)=T_q(r,z,\infty)$ be this solution for a constant heat extraction $q=q_o$ and zero surface and undisturbed ground temperature ($T_{om}= 0$). The steady-state problem can be solved analytically, if the borehole is approximated by a line-sink with constant heat extraction per unit length. This boundary condition is somewhat different from the one given by (4.3-4). However, numerical calculations have shown [5] that the average temperature over the borehole length becomes almost identical for the two types of boundary condition.

The steady-state line-sink solution is given by the integral (A.2) in the Appendix. The borehole temperature is approximately given by the temperature at $r=r_b$ for the average borehole depth $z=H/2$ according to (A.3). However, the temperature $T_s(r_b,z)$ of (A.2) varies somewhat along the borehole, and the boundary condition (4.3) is not satisfied exactly. An improved approximation is discussed in the Appendix. The borehole temperature is proportional to q_o:

$$T_{s,b}= -q_o \cdot R_s \qquad (6.1)$$

The steady-state resistance R_s is from (A.4):

$$R_s = \frac{1}{2\pi\lambda} \cdot \ln\left(\frac{H}{2r_b}\right) \qquad (r_b << H) \tag{6.2}$$

An erroneous formula with the logarithm $\ln(2H/r_b)$ instead of $\ln(H/(2r_b))$ is given in many standard works on heat transfer [10, 11, 12, 13, 14]. The difference is in our applications around 20% ($\ln(4)/\ln(1000) = 0.20$). The erroneous formula refers in fact to the case with zero heat flux at the ground surface instead of zero temperature. It is obtained by considering a single line sink $-H < z < H$ and taking the value at $z=0$, $r=r_b$ [14]. The original references to [10, 11, 12] and [13] are [15] and [16] respectively. In both these original references the boundary condition with zero heat flux at the ground is considered. The error appears to be due to a misunderstanding of the boundary condition in the original references.

7 Approximations for the g-function

Expressions (5.3) and (6.2) give two asymptotic approximations for the g-function (5.6):

$$g(t/t_s, r_b/H) \approx \begin{cases} \ln\left(\frac{H}{2r_b}\right) + \frac{1}{2}\ln\left(\frac{t}{t_s}\right) & , \; 5r_b^2/a < t < t_s \\ \ln\left(\frac{H}{2r_b}\right) & , \; t > t_s \end{cases} \qquad t_s = \frac{H^2}{9a} \tag{7.1}$$

The break time or steady-state time t_s is obtained by taking (5.3) and (6.2) equal. The approximation (7.1) is shown by the two dashed lines in Figure 3. The maximum error of the approximation is 7% at $t=t_s$. A borehole with the data (9.6) has a steady-state time t_s of 26 years. The radial solution (5.3) can therefore in normal applications be used for many years, before vertical effects become important.

8 Periodic heat extraction

Another basic case is a sinusoidal heat extraction with a period time t_p. The undisturbed ground temperature is zero:

$$q(t) = q_p \cdot \sin(2\pi t/t_p) \qquad T_{om} = 0 \tag{8.1}$$

The range of this periodic solution T_p is only a few meters out from the borehole for the annual variation, t_p=1 year. Three-dimensional end effects can then be neglected. The solution of the radial, periodic problem is given by [8B]. The temperature at the borehole wall may be written in the following way:

$$T_{p,b} = -q_p \cdot R_p \cdot \sin\{2\pi(t/t_p - \phi_p)\} \tag{8.2}$$

Here R_p (K/(W/m)) is the amplitude of the thermal resistance for the periodic heat extraction (8.1) and ϕ_p the phase lag given as a fraction of the period time t_p. The quantities R_p and ϕ_p are given by complex-valued Kelvin functions with the argument r'_{pb}:

$$r'_{pb} = r_b\sqrt{2}/d_p \qquad d_p = \sqrt{at_p/\pi} \tag{8.3}$$

The length d_p is a measure of the penetration depth for a periodic boundary temperature. The argument r'_{pb} is in our applications small. An approximation to the first terms of the series expansion of the Kelvin function gives the following expressions for R_p and ϕ_p:

$$R_p(r'_{pb}) = \frac{1}{2\pi\lambda}\sqrt{(\ln(2/r'_{pb})-\gamma)^2 + \pi^2/16} \qquad r'_{pb} < 0.1 \tag{8.4}$$

$$\phi_p(r'_{pb}) = \frac{1}{2\pi}\cdot\arctan\left\{\frac{\pi/4}{\ln(2/r'_{pb})-\gamma}\right\}$$

9 Superposition using the basic solutions

Any heat extraction q(t) can be obtained from the basic cases above by superposition. Consider as an example the rather general case of N piecewise constant values $q(t)=q_i$, $t_i < t < t_{i+1}$:

$$q(t)= \sum_{i=1}^{N} (q_i - q_{i-1})\cdot He(t-t_i) \qquad (q_o = 0) \tag{9.1}$$

The temperature below T_{om} at the borehole wall is obtained by superposition of the contributions from each step:

$$T_b(t) = T_{om} - \sum_{i=1}^{N} (q_i - q_{i-1})\cdot R_q(t-t_i) \tag{9.2}$$

Here R_q is given by (5.6) or (5.3). It shall be remembered that $R_q(t-t_i)$ is zero for $t<t_i$. The general formula for any q(t) that starts at t=0 is by superposition:

$$T_b(t) = T_{om} - q(0)\cdot R_q(t) - \int_0^t \frac{dq}{dt'}\cdot R_q(t-t')dt' \tag{9.3}$$

$(q(t)=0,\ t < 0)$

In the thermal analysis and dimensioning of heat extraction boreholes it is often sufficient and advisable to use a rather simple representation of q(t) in order to get lucid and handy expressions. The three components of Figure 4a are ususally sufficient for dimensioning. There is an average extraction rate q_o and a periodic component with the amplitude q_p and the period t_p= 1 year. There is a superimposed extraction pulse q_1 with the duration t_b-t_a during the coldest period of the year. The heat extraction function is then for year n:

$$q(t) = q_o + q_p\cdot\sin(2\pi t/t_p) + q_1\cdot[He(t-t_a) - He(t-t_b))] \tag{9.4}$$

The effect of the pulses from previous years can be neglected. The temperatures due to the three parts of heat extraction are given by (6.1), (8.2), and (5.2). The temperature at the borehole wall becomes:

$$T_b(t) = T_{om} - q_o \cdot R_s - q_p \cdot R_p \sin\{2\pi(t/t_p - \phi_p)\} - q_1 [R_q(t-t_a) - R_q(t-t_b)] \quad (9.5)$$

A numerical example with typical Swedish data is:

$$\lambda = 3.5 \text{ W/mK} \qquad a = 1.62 \cdot 10^{-6} \text{ m}^2/\text{s} \qquad T_{om} = 8 \text{ °C} \quad (9.6)$$

$$2r_b = 0.11 \text{ m} \qquad H = 110 \text{ m} \qquad t_p = 1 \text{ year}$$

Then we have:

$$R_s = 0.314 \text{ K/(W/m)} \qquad R_p = 0.188 \text{ K/(W/m)} \qquad \phi_p = 11/365 \quad (9.7)$$

$$R_q(t) = 0.106 + 0.023 \cdot \ln(t/t_{day}) \text{ K/(W/m)}$$

Here t/t_{day} is the number of days for a heat extraction step. Consider the following heat extraction, which is shown in Figure 4a:

$$q_o = 20 \text{ W/m} \qquad q_p = 15 \text{ W/m} \qquad q_1 = 10 \text{ W/m} \quad (9.8)$$

$$t_a = (n + \tfrac{5}{24}) \cdot t_p \qquad t_b = (n + \tfrac{7}{24}) \cdot t_p$$

The temperature contribution from the average component q_o is $-q_o \cdot R_s = -20 \cdot 0.314 = -6.3$ °C. The borehole temperature (9.5) is shown in figure 4b. The lowest extraction temperature at the end of the extraction pulse is -2.9 °C.

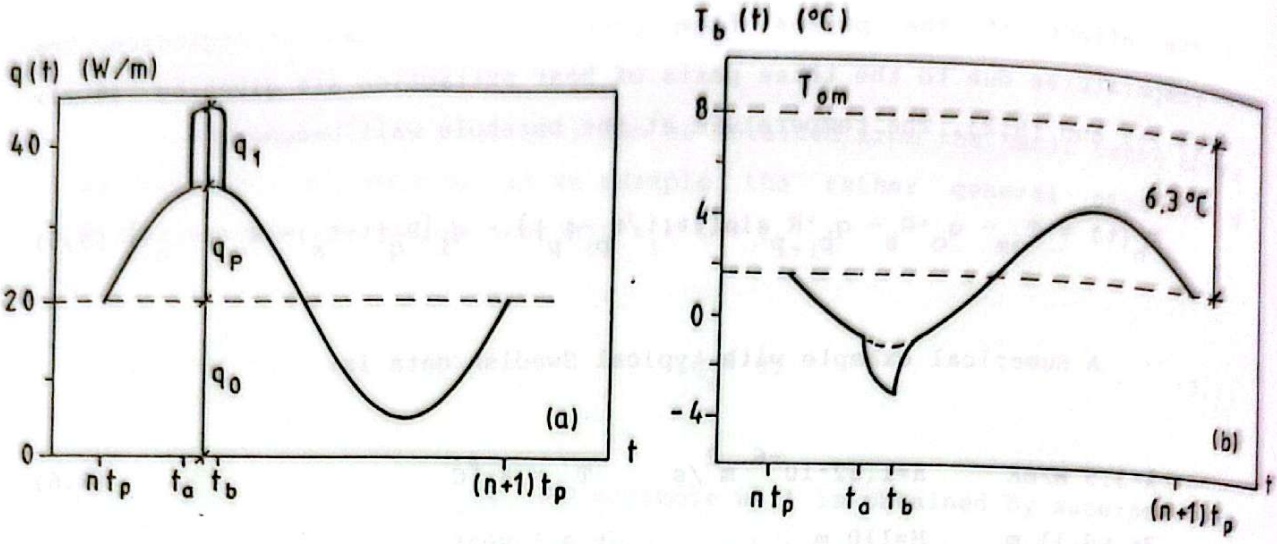

Figure 4. Heat extraction function (a) and borehole temperature (b) for the example (9.6-8).

10 Effect of groundwater filtration

The heat conduction is disturbed by moving groundwater in cracks and other permeable zones. The flow is strongly variable locally. It is common practice in groundwater hydrology to consider the average flow for suitably chosen represenative volumes and to treat the ground as a homogeneous porous medium. With this type of idealization, we assume a constant groundwater flow in the x-direction:

$$\bar{q}_w = q_w \cdot \hat{x} \qquad q_w = K \cdot I \tag{10.1}$$

The groundwater table is assumed to lie close to the ground surface compared to H. The region above this level is neglected, and we assume (10.1) to be valid for $0 < z < \infty$. The flow intensity q_w (m/s, or to be more precise $m^3_{water}/m^2,s$) is equal to the (average) hydraulic conductivity K (m/s) times the gradient of the water table I (m/m) [17]. We only consider the steady-state case, Figure 5. The solution $T_{sw}(x,y,z)$ for the constant heat extraction q_o and zero surface and undisturbed ground temperature ($T_{om}=0$) is no longer cylindrically symmetric.

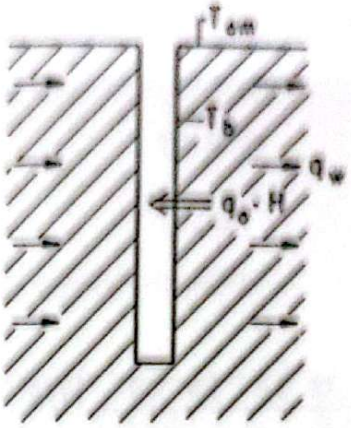

Figure 5. Steady-state heat extraction when groundwater filtration is allowed for.

The conductive-diffusive heat balance equation is:

$$\nabla\cdot(\lambda\nabla T - Tc_w\rho_w\bar{q}_w) = 0 \tag{10.2}$$

or, introducing the length ℓ:

$$\nabla^2 T - \frac{2}{\ell}\frac{\partial T}{\partial x} = 0 \qquad \ell = \frac{2\lambda}{\rho_w c_w q_w} \tag{10.3}$$

The point-source solution to (10.3) is given by [8C]. Integration gives T_{sw} according to (A.5). The temperature at the borehole wall is proportional to q_o:

$$T_{sw,b} = -q_o \cdot R_{sw} \tag{10.4}$$

The thermal resistance R_{sw} is according to (A.11) and the subsequent discussion:

$$R_{sw} = \frac{1}{2\pi\lambda}\left[\ln\left(\frac{H}{2r_b}\right) - P_w\left(\frac{H}{\ell}\right)\right] \qquad \ell >> r_b \tag{10.5}$$

The logarithm gives the steady-state resistance (6.2). The correction term $P_w(H/\ell)$ is given by (A.12-13) and shown in Figure 6.

The following approximations may be used for small and large arguments:

$$P_w(s) \approx \frac{3}{16} s^2 - \frac{1}{12} s^3 \qquad (s<0.5) \qquad (10.6)$$

$$P_w(s) \approx \ln(\frac{s}{2}) + \gamma - \frac{1}{2}\ln(3) \qquad (s>10) \qquad (10.7)$$

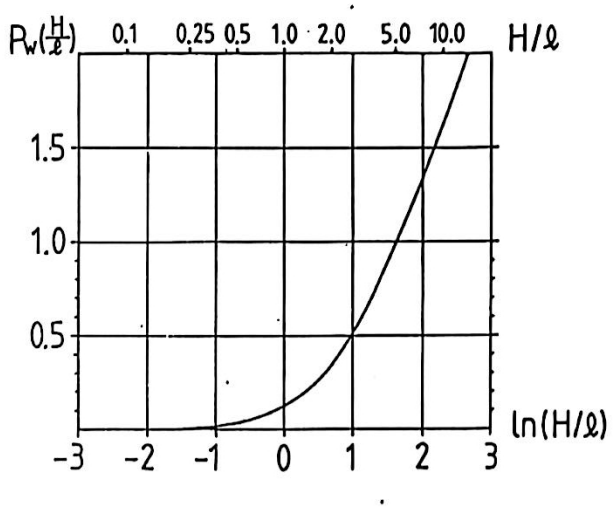

Figure 6. Function giving the effect of groundwater flow in the thermal resistance formula (10.5).

The influence of the groundwater flow is illustrated with following example:

$$H=110 \text{ m} \qquad 2r_b = 0.11\text{m} \qquad K=10^{-6} \text{ m/s} \qquad I = \frac{1}{66} \text{ m/m} \qquad (10.8)$$

The chosen value of K is very high for rock. The hydraulic gradient I is also quite high. Then we have:

$$\ell = \frac{2 \cdot 3.5}{4.2 \cdot 1/66} = 110 \text{ m} \qquad \frac{H}{\ell} = 1$$

$$P_w(1) = 0.124 \qquad \frac{P_w(1)}{\ln(H/2r_b)} = 0.02 \qquad (10.9)$$

The extreme data (10.8) give an influence of 2 %.

The general conclusion is that the effect of natural groundwater movements, which are resonably homogeneously spread over the ground volume , is negligible.

11 Disturbance at the ground surface

The heat extraction increases the heat flow through the ground surface compared to undisturbed, natural conditions. This thermal disturbance $q_{surf}(r,t)$ (W/m^2) is a function of radial distance and time.

Consider the case of a heat extraction step q_1 for $t>0$, (5.1). The line-sink approximation (A.1) gives with good accuracy the temperature disturbance. The derivative $\partial T_q/\partial z\big|_{z=0}$ gives the heat flow. This derivative is readily changed to the derivative with respect to the integration variable s. The integration in s becomes quite simple, and we get the following expression:

$$q_{surf}(r,t)=\frac{q_1}{2\pi}\left[\frac{1}{\sqrt{r^2+D^2}}\operatorname{erfc}\left(\frac{\sqrt{r^2+D^2}}{\sqrt{4at}}\right) - \frac{1}{\sqrt{r^2+(D+H)^2}}\operatorname{erfc}\left(\frac{\sqrt{r^2+(D+H)^2}}{\sqrt{4at}}\right)\right] \qquad (11.1)$$

The steady-state heat flux becomes:

$$q_{surf}(r,\infty) = \frac{q_1}{2\pi}\left[\frac{1}{\sqrt{r^2 + D^2}} - \frac{1}{\sqrt{r^2 + (D+H)^2}}\right] \qquad (11.2)$$

This is the maximum heat flow at the ground surface. Numerical examples show that the disturbance q_{surf} becomes quite small. The thermal disturbance at the ground surface from a heat extraction borehole is normally negligible [1,5]. The temperature disturbance, which is superimposed on undisturbed natural conditions with the annual and daily variations, can for moderate depths be estimated by the formula:

$$T_{dist}(r,z,t) \approx -q_{surf}(r,t)\cdot\frac{z}{\lambda} \qquad (z < D,\ z < H/40) \qquad (11.3)$$

Combining (11.2-3) we get the following simple formula to estimate the maximum disturbance:

$$-T_{dist}(r,z,t)\Big|_{max} = \frac{q_1}{2\pi\lambda} \frac{z}{\sqrt{r^2 + D^2}} \qquad (z < D, \quad z < H/40) \qquad (11.4)$$

The total heat flow through the ground surface due to the heat extraction is obtained by integration of (11.1):

$$Q_{surf} = \int_0^\infty 2\pi r \cdot q_{surf}(r,t)dr = q_1\sqrt{4at} \cdot \{ierfc(D/\sqrt{4at}) - ierfc((D+H)/\sqrt{4at})\}$$

$$ierfc(s) = \frac{1}{\sqrt{\pi}} e^{-s^2} - s \cdot erfc(s) \qquad (11.5)$$

Acknowledgement. The suport by the Swedish Council for Building Research and the National Energy Administration is gratefully acknowledged.

Appendix. Analytical solutions using line sinks

Quite good approximate solutions for T_q, T_s, and T_{sw} are obtained by approximating the borehole with a line sink at r=0, D < z < D+H. The zero temperature at the boundary z=0 is obtained by adding a mirror source at r=0, -D-H < z < -D.

Heat extraction step

The temperature due to a continuous point source, that emits heat from t=0, is given by [8D]. The integral along the borehole and its mirror gives the solution:

$$T_q(r,z,t) = -\frac{q_l}{4\pi\lambda}\int_D^{H+D}\{\frac{1}{r_+}\,\mathrm{erfc}(\frac{r_+}{\sqrt{4at}}) - \frac{1}{r_-}\,\mathrm{erfc}(\frac{r_-}{\sqrt{4at}})\}ds \qquad (A.1)$$

$$r_+ = \sqrt{r^2 + (z-s)^2} \qquad r_- = \sqrt{r^2 + (z+s)^2} \qquad r = \sqrt{x^2 + y^2}$$

The integral (A.1), which contains the complementary error function erfc, may be solved numerically.

Steady-state heat extraction

The steady-state solution $T_s(r,z)$ is obtained from (A.1) in the limit t=∞:

$$T_s(r,z) = -\frac{q_o}{4\pi\lambda}\int_D^{H+D}\{\frac{1}{r_+} - \frac{1}{r_-}\}ds \qquad (A.2)$$

The integration of (A.2) is straightforward. We may in our applications put D equal to zero.

The borehole temperature at the midpoint depth (z=H/2, D=0) becomes, using the fact that $r_b << H$:

$$T_{s,b} = - \frac{q_o}{2\pi\lambda} \ln(\frac{H}{r_b\sqrt{3}}) \qquad (r_b << H) \qquad (A.3)$$

The temperature $T_s(r_b,z)$ differs somewhat from (A.3) in particular near the end regions (z=0 and z=H). The temperature from the line sink, i.e. the integral of $1/r_+$ is in fact constant on rotational ellipsoids around the line sink. The real isotherms are therefore ellipsoids which are slightly deformed by the mirror source, i.e. by the integral of $1/r_-$. Our main intrest is the relation between the heat loss q_o and the temperature of the isotherm that approximates the borehole wall. A somewhat better approximation than (A.3) of the borehole temperature is obtained, if we choose an isotherm so that the volume of the ellipsoid is equal to that of the borehole [18]. The boundary is then deformed under volume conservation. The radius r_e of the ellipsoid with the same volume is $r_e=\sqrt{1.5}r_b$ ($\pi r_b^2 H=4\pi r_e^2 H/(3\cdot 2)$). We get the following approximation, where r_e replaces r_b in (A.3):

$$T_{s,b} = - \frac{q_o}{2\pi\lambda} \ln(\frac{H}{r_b\sqrt{4.5}}) \qquad (r_b << H) \qquad (A.4)$$

The numerical factor $\sqrt{4.5} \approx 2.1$ is simplified to 2 in (6.2), since the decimal is not significant.

Heat extraction in moving groundwater

The steady-state point source solution for the convective-diffusive equation (10.3) in an infinite region is given by [8C]. The temperature from a line sink along the borehole and a mirror line source becomes:

$$T_{sw}(x,y,z) = - \frac{q_o}{4\pi\lambda} e^{x/\ell} \int_D^{D+H} [\frac{e^{-r_+/\ell}}{r_+} - \frac{e^{-r_-/\ell}}{r_-}] \, ds \qquad (A.5)$$

Here r_+ and r_- are given in (A.1). The integral may be solved numerically.

We are in particular intrested in the temperatures near and at the borehole $r=r_b$. The first term of (A.5) with integration over $-\infty < z < \infty$ gives $2K_o(r/\ell)$, which respresents the two-dimensional line source, [8C]. We may then with D=0 rewrite (A.5) in the following way:

$$T_{sw}(x,y,z) = -\frac{q_o}{2\pi\lambda}\cdot e^{x/\ell}\Big[K_o(r/\ell) - \int_0^\infty \frac{1}{r_-} e^{-r_-/\ell}\,ds \qquad (A.6)$$

$$- \frac{1}{2}\int_H^\infty \frac{1}{r_+} e^{-r_+/\ell}\,ds + \frac{1}{2}\int_H^\infty \frac{1}{r_-} e^{-r_-/\ell}\,ds\Big]$$

We have in the present applications:

$$r_b << \ell \qquad (A.7)$$

The temperature at the borehole, $r=r_b$, $0 < z < H$, is readily obtained with the following approximations:

$$e^{x/\ell} \approx 1 \qquad K_o(r_b/\ell) \approx \ln(2\ell/r_b) - \gamma \qquad (A.8)$$

$$r_+ \approx s - z \qquad r_- \approx s + z$$

The approximation of the modified Bessel function K_o is given by [9B]. The integrals now give the exponential integral function E_1, and we have with good accuracy:

$$T_{sw,b} = -\frac{q_o}{2\pi\lambda}\left\{\ln\left(\frac{2\ell}{r_b}\right) - \gamma - E_1\left(\frac{z}{\ell}\right) - \frac{1}{2}E_1\left(\frac{H-z}{\ell}\right) + \frac{1}{2}E_1\left(\frac{H+z}{\ell}\right)\right\} \qquad (A.9)$$

$(r=r_b,\ 0 < z < H)$

We have in particular for z=H/2 introducing the function (A.13):

$$T_{sw,b} = -\frac{q_o}{2\pi\lambda}\left\{\ln\left(\frac{H}{2r_b}\right) + \ln\left(\frac{2}{\sqrt{3}}\right) - \frac{3}{2}E_1\left(\frac{H}{2\ell}\right) + \frac{1}{2}E_1\left(\frac{3H}{2\ell}\right)\right\} \qquad (A.10)$$

This may be written in the following way:

$$T_{sw,b} = - q_o \cdot \frac{1}{2\pi\lambda}\left[\ln\left(\frac{H}{r_b\sqrt{3}}\right) - P_w\left(\frac{H}{\ell}\right)\right] \tag{A.11}$$

Here we have used the notations:

$$P_w(H/\ell) = \frac{3}{2}\cdot E_\ell(H/2\ell) - \frac{1}{2} E_\ell(3H/2\ell) \tag{A.12}$$

$$E_\ell(s) = \ln(s) + \gamma + E_1(s) \tag{A.13}$$

Formula (A.11) is obtained by taking the temperature at $z=H/2$, $r=r_b$. It is in accordance with (A.3). The somewhat better ellipsoid approximation gave instead of $\sqrt{3}$ the factor 2, which is used in (10.5).

References

1. J. Claesson, P. Eskilson, Conductive Heat Extraction by a Deep Borehole. Thermal Analyses and Dimensioning Rules. Dep. of Mathematical Physics, University of Lund, Box 118, S-221 00 Lund, Sweden (1987).

2. J. Claesson, P. Eskilson, Conductive Heat Extraction by Thermally Interacting Deep Boreholes. Dep. of Mathematical Physics, University of Lund, Box 118, S-221 00 Lund, Sweden (1987).

3. J. Claesson, G. Hellström . Thermal Resistances to and between Pipes in a Composite Cylinder, Dep. of Mathematical Physics, University of Lund, Box 118, S-221 00 Lund, Sweden (1987). (To be published.)

4. J. Claesson, G. Hellström, The Effect of the Temperature Variation along the Pipes in a Heat Exchanger in the Ground, Dep. of Mathematical Physics, University of Lund, Box 118, S-221 00 Lund, Sweden (1987). (To be published.)

5. J. Claesson et. al., Markvärme. En handbok om termiska analyser (Ground Heat Systems. A Handbook on Thermal Analyses), BFR-report T16-T18:1985, (900pp. 460 fig.), Svensk Byggtjänst, Box 7853, S-103 99, Stockholm (1985).

6. J. Claesson, P. Eskilson, Simulation Model for Thermally Interacting Heat Extraction Boreholes, Department of Mathematical Physics, University of Lund Box 118, S-221 00 Lund, Sweden (1987). (Submitted to Journal of Numerical Heat Transfer)

7. P. Eskilson, Superposition Borehole Model. Manual for Computer Code, Dep. of Mathematical Physics, University of Lund, Box 118, S-221 00 Lund, Sweden (1986).

8. H.S. Carslaw, J.C. Jaeger, Conduction of Heat in Solids, Oxford (1959). 8A: p261, 8B: p263, 8C: p267, 8D: p261.

9. M. Abramowitz, I.A. Stegun, Handbook of Mathematical Functions, (AMS 55, National Bureau of Standards, (1970). 9A: p229, 9B: p375.

10. F. Kreith, Principles of Heat Transfer, International Textbook Co., Scranton, Pa., (1958), p. 88.

11. J. Sunderland, K. Johnson, ASHRAE Transactions, Vol 10 (1964), pp. 238-239.

12. D.R. Pitts, L.E. Sissom, Theory and Problems of Heat Transfer, McGraw Hill (1977), p. 54.

13. J. P. Hartnett, W. M. Rohsenow, Handbook of Heat Transfer, McGraw Hill (1973), p. 3-120.

14. E.R.G. Eckert, R.M. Drake, Analysis of Heat and Mass Transfer, McGraw-Hill (1972), pp. 103-106.

15. R. Rüdenberg, Die Ausbreitung der Luft und Erdfelder um Hochspannungsleitungen besonderes bei Erd- und Kurzschlüssen, Electrotechnische Z., Vol. 46 (1925), pp. 1342-1346.

16. S. Kutateladze, Fundamentals of Heat Transfer (English ed.), Academic Press Inc., New York (1963), p. 94.

17. J. Bear, Hydraulics of Groundwater, McGraw-Hill (1979).

18. J. Claesson, T. Bengtsson, Stationary Heat Losses from a Spherical or Ellipsoidal Heat Storage Volume Deep in the Ground, Department of Mathematical Physics, University of Lund, Box 118, S-221 00 Lund, Sweden (1978).

CONDUCTIVE HEAT EXTRACTION BY A DEEP BOREHOLE.
THERMAL ANALYSES AND DIMENSIONING RULES.

Johan Claesson
Per Eskilson
Department of Building Technology, Lund Institute of Technology
Box 118, S-221 00 Lund, Sweden

Mars 1987

Acknowledgement: The support by the Swedish Council for Building Research and the National Energy Administration is gratefully acknowledged.

Contents

Abstract 3

Nomenclature 4

1 INTRODUCTION 5

2 THERMAL PROCESS AND SIMPLIFICATIONS 6
- 2.1 Stratified ground . . . 6
- 2.2 Ground Surface . . . 6
- 2.3 Effective undisturbed ground temperature . . . 6
- 2.4 Boundary conditions at the borehole . . . 7
- 2.5 Effect of groundwater movements . . . 7

3 HEAT EXTRACTION STEP 9
- 3.1 Borehole temperature . . . 9
- 3.2 Long-term thermal disturbance in the ground . . . 10
- 3.3 Thermal disturbance near the ground surface . . . 11
- 3.4 Heat supply from ground and through ground surface . . . 12

4 PULSE ANALYSIS 14
- 4.1 Superposition of heat extraction steps . . . 14
- 4.2 Single pulse . . . 14
- 4.3 Two balanced pulses . . . 16
- 4.4 Balanced pulse train . . . 16
- 4.5 Pulsated versus constant extraction . . . 17

5 LOCAL PROCESSES IN THE BOREHOLE 19
- 5.1 Time-scales . . . 19
- 5.2 Borehole thermal resistance . . . 19
- 5.3 Temperature variations along the borehole . . . 21

6 DIMENSIONING RULES 22
- 6.1 Simplified heat extraction . . . 22
- 6.2 Stepwise heat extraction . . . 23
- 6.3 PC-models . . . 24

7 DISCUSSIONS OF PARAMETERS 25
- 7.1 Three important parameters: λ, R_b, T_{om} . . . 25
- 7.2 Heat extraction $q(t)$ . . . 25
- 7.3 Pumping rate . . . 25
- 7.4 Negligible parameters and effects . . . 26
- 7.5 Response test . . . 26
- 7.6 Thermal resistance analysis . . . 27

References 29

Abstract

The ground together with a deep borehole as heat exchanger may be used as heat source and sink to a heat pump. The paper presents an extensive analysis of such a heat extraction (or injection) borehole. The effects of stratification of the ground, climatic variations, geothermal gradient, and groundwater filtration are dealt with. A basic tool for the analysis is the solution for a heat extraction step. The thermal disturbance at and near the ground surface is shown to be negligible. Thermal recharge in order to improve the heat extraction capacity a few months later is shown to be futile. The thermal processes in the borehole are with good approximation represented by a single borehole resistance. Simple dimensioning formulas that relate the heat extraction rate to the required extraction temperatures are given. They are based on superpositions of steady-state, periodic, and extraction step solutions. A response-test method is proposed for the determination of three important parameters: average thermal conductivity in the ground, borehole thermal resistance, and average undisturbed ground temperature.

Nomenclature

a	thermal diffusivity
c	heat capacity
D	depth of thermally insulated upper part of the borehole
g	response function for the heat extraction step, (10,11)
H	borehole length over which heat extraction takes place
q	heat extraction rate (W/m, average over the borehole)
r	radial distance
r_b	borehole radius
R	thermal resistances (K/(W/m))
R_b	thermal resistance between fluid and borehole wall
R_q	thermal resistance due to a heat extraction step
t	time
t_b	borehole steady-state time, (32)
t_s	steady-state extraction time, (17)
T	temperature in the ground
T_b	temperature at the borehole wall
T_f	temperature of heat carrier fluid
T_{om}	effective undisturbed ground temperature
V_f	pumping rate (m^3/s)
z	depth from the ground surface

Greek symbols

γ	Euler's constant ($\simeq 0.5772$)
λ	thermal conductivity
ρ	density
$\Delta T, \Delta T'$	temperature drop, (19)

Subscripts

b	borehole wall
f	fluid
p	periodic
q	heat extraction step
s	steady-state
w	groundwater

1 INTRODUCTION

The ground may be used as heat source and sink to heat pumps. Heat is extracted from the ground in the heating mode and injected in the cooling mode. The ground heat exchanger may use buried horizontal pipes or deep boreholes. This paper concerns thermal analysis and dimensioning rules for the latter type.

Many systems using deep boreholes have been built in the United States and Canada, and about 5000 systems for heat extraction are in operation in Sweden. The Swedish systems use boreholes in rock with high thermal conductivity. The depth of the boreholes is 40 to 150 m, and the diameter is 0.075 to 0.11 m. The heat carrier fluid is heated by the surrounding ground, while it flows down to the bottom of the borehole in one channel and back upwards in another channel. The cold borehole extracts heat from the surrounding ground by pure heat conduction. The thermal problem is here posed in terms of heat extraction, but all results and analyses are equally applicable to heat injection or any mixture of injection and extraction.

There are many different heat collector designs. The most common type in Sweden is a U-shaped plastic tube in the borehole, Figure 1. More than two channels are often used. The volume of the borehole outside the pipes contains groundwater, or a backfilling with for example sand in order to increase the thermal contact between the pipes and the borehole wall. The water may be used directly as heat carrier. Then, a single pipe down to the bottom of the borehole is used. Designs with a closed loop for a separate heat carrier fluid have the advantage that extraction temperatures below 0°C may be used. Temperatures down to -5°C during peak extraction periods are common in the Swedish systems. An interesting new concept is to use direct evaporation of the working fluid in copper pipes in the borehole.

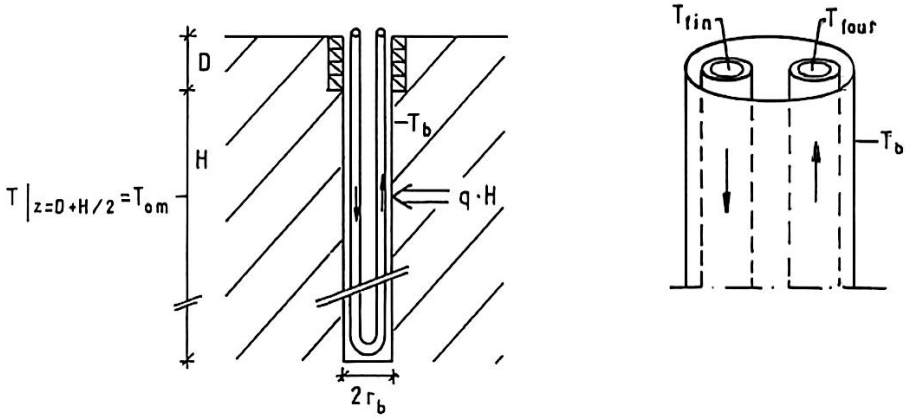

Figure 1. Heat extraction borehole.

A general design manual for ground-coupled heat pumps has been compiled by Bose et al, [1]. The present paper deals with questions and problems associated with the thermal processes in the ground and the borehole. Questions such as thermal influence at the ground surface, long-term behaviour and effect of groundwater filtration are dealt with. The key processes and parameters for the thermal performance are identified. Secondary and insignificant processes and simplifications are discussed. The proper design of these systems requires a precise knowledge of the relation between the fluid temperature and the heat extraction rate under various conditions. Simple dimensioning rules, which may be used for calculations by hand or on a personal computer, are presented. This paper is based on the analytical solutions and other results of [2]. A subsequent paper [3] deals with the case of thermally interacting boreholes. Many details and special studies are reported in [4]. The dimensioning rules and the other final formulas presented here and in [2,3] have been implemented on a personal computer (IBM compatible, MS-DOS) for simple interactive use, [5].

2 THERMAL PROCESS AND SIMPLIFICATIONS

The thermal process in the ground and the borehole involves many complications. It is of great help for the further analysis to identify secondary and insignificant processes, which may be neglected in the formulation of the basic problem or dealt with by separate analyses. The results from [2] are used to this end.

2.1 Stratified ground

The ground is often stratified. The thermal conductivity, which is one of the most important parameters for the thermal performance, is then a function of depth: $\lambda = \lambda'(z)$. The average thermal conductivity over the active heat extraction region, $D < z < D + H$, is:

$$\lambda = \frac{1}{H} \int_D^{D+H} \lambda'(z) dz \tag{1}$$

We have in numerical simulations compared cases with a stratified ground to the corresponding homogeneous case with λ given by (1). An example is a case with $\lambda' = 2.5$ W/(m·K) for $0 < z < D + H/2$ and $\lambda' = 4.5$ for $z > D + H/2$, and the homogeneous case with $\lambda = 3.5$. The difference in heat extraction temperatures became less than 0.04°C [4], when typical Swedish data are used for the other parameters. The average volumetric heat capacity over the borehole depth should be used. The error, when the ground is treated as homogeneous with λ given by (1), is negligible in the present applications. The ground may now be treated as homogeneous. The temperature $T(r, z, t)$ in the ground satisfies the heat conduction equation in cylindrical coordinates:

$$\frac{1}{a} \cdot \frac{\partial T}{\partial t} = \frac{\partial^2 T}{\partial r^2} + \frac{1}{r} \cdot \frac{\partial T}{\partial r} + \frac{\partial^2 T}{\partial z^2} \tag{2}$$

2.2 Ground Surface

The temperature at the ground surface varies strongly during the day, from day to day, and during the year. These variations at the ground surface are attenuated downwards in the ground. The length d_p, (39), which depends on the period time t_p, is a measure of the penetration depth. The annual variation gives the largest penetration depth, which characteristically is a few meters. These variations in the top-soil layer are negligible for the thermal response of the deep borehole. It is sufficient to use the annual mean temperature as boundary condition at the ground surface. Other complications at the ground surface such as air-to-ground thermal resistance, freezing, rain, and snow may by the same reason be neglected.

2.3 Effective undisturbed ground temperature

The undisturbed ground temperature increases with at most a few degrees centigrade from the ground surface down to the bottom of the borehole due to the geothermal gradient. It is shown in [2] that only an average undisturbed ground temperature, T_{om}, is of importance for the heat extraction. The temperature T_{om} is normally with good accuracy equal to the undisturbed ground temperature at the mid-depth, $z = D + H/2$, of the borehole. Experimentally, it is determined by circulating the heat carrier fluid without heat extraction or injection. The circulating fluid assumes after a short transient period a steady temperature T_{om}. Heat is then flowing to the lower half of the borehole from the surroundings, which have a temperature above T_{om}, and the same amount of heat is flowing from the borehole to the somewhat colder surroundings in the upper half. In a precise analysis, one should account for the effect of the heat input from the circulation pump, which causes a slow increase of the fluid temperature. This is easily done

using formula (10) and (14) with $-q_1 H$ equal to the heat input from the circulation pump. The temperature T_{om} will be called the effective undisturbed ground temperature. The simplified initial condition in the ground is now:

$$T(r, z, 0) = T_{om} \tag{3}$$

The temperature T_{om}, instead of the somewhat lower mean annual temperature at the ground surface, is also to be used as boundary condition at $z = 0$, [2]:

$$T(r, 0, t) = T_{om} \tag{4}$$

The errors in heat extraction performance, when the simplified initial and boundary conditions (3-4) are used instead of more precise ones with a geothermal gradient and variations at $z = 0$, are characteristically less than 1% [4].

2.4 Boundary conditions at the borehole

The uppermost part of the borehole, $0 < z < D$, may be thermally insulated. The small heat flow through the insulation is neglected. The radial derivative becomes zero:

$$\frac{\partial T}{\partial r} = 0 \qquad r = r_b, \quad 0 < z < D \tag{5}$$

The depth $z = D$ may be the groundwater level. The boundary condition (5) is valid for this case, if the small heat flow to the pipes through the air gap in the borehole is neglected. The precise value of D (for variations between, say, 1 and 5 m) for a fixed active heat extraction length H is not important, [2].

The thermal process in the ground is coupled to the convective-diffusive processes in the borehole. This coupling with its heat flows to and between the fluid channels and its temperature variations along the borehole is discussed in Section 5. We will first deal with the thermal process in the ground for a constant temperature $T_b(t)$ along the borehole wall:

$$T(r_b, z, t) = T_b(t) \qquad D < z < D + H \tag{6}$$

The average heat extraction $q(t)$ per meter borehole (W/m) is given by the integral:

$$q(t) = \frac{1}{H} \int_D^{D+H} 2\pi r_b \cdot \lambda \left. \frac{\partial T}{\partial r} \right|_{r=r_b} dz \tag{7}$$

The total heat extraction rate is $H \cdot q(t)$ (W). It is negative during periods of heat injection to the ground.

The thermal problem may be formulated with a given extraction temperature $T_b(t)$. The problem is then defined by (2-6). The heat extraction rate (7) is obtained from the solution. However, it is much better to start with a given heat extraction rate $q(t)$. The simplicity of the presented dimensioning formulas is due to this better way to pose the problem. The thermal problem is then defined by (2-7) with a given heat extraction rate $q(t)$. The extraction temperature $T_b(t)$ is obtained from the solution.

2.5 Effect of groundwater movements

The heat conduction with the governing equation (2) is disturbed by moving or filtrating groundwater in cracks and permeable strata. The effect of a reasonably homogeneous, horizontal groundwater flow is analyzed in [2]. A simple formula for the steady-state heat extraction rate is derived. The effect of the groundwater flow is negligible if:

$$\frac{H\rho_w c_w q_w}{2\lambda} < 1 \tag{8}$$

Here q_w (m/s or, to be precise, m^3 of water/($m^2 \cdot$ s)) is the Darcy velocity of the groundwater flow, [6]. The groundwater flow q_w must be quite strong, before the limit (8) is exceeded. The ground has to be highly permeable and the hydraulic gradient high. Therefore, the condition (8) should be met for reasonable values for hard rock with its normally very low permeability, [2].

There may in certain cases be a groundwater flow along the borehole between two permeable strata with different hydraulic heads. This may influence the heat extraction performance considerably, provided that the water flow is large enough, and the influenced segment of the borehole is long enough.

3 HEAT EXTRACTION STEP

The given heat extraction $q(t)$ (or injection for $q(t) < 0$) in the problem defined by (2-7) may be any function of time. The simplest case is a constant rate q_1 (W/m) starting at $t = 0$. This heat extraction step is expressed with Heavyside's step function He:

$$q(t) = q_1 \cdot He(t) \qquad He(t) = \begin{cases} 1 & t > 0 \\ 0 & t \leq 0 \end{cases} \tag{9}$$

The temperature solution for any $q(t)$ may be obtained from the solution for the heat extraction step by superposition using Duhamel's theorem, [7]. The general superposition integral for the borehole temperature $T_b(t)$ is given in [2]. The superposition technique is here used to get the solution for any piece-wise constant $q(t)$. The solution or response for the heat extraction step is a fundamental tool for the further analysis.

3.1 Borehole temperature

The borehole temperature $T_b(t)$ is of particular interest, being the response felt by the heat pump. The dimensional analysis in [2] showed that $T_b(t)$ may be written in the following way:

$$T_b(t) = T_{om} - q_1 \cdot R_q \tag{10}$$

$$R_q = \frac{1}{2\pi\lambda} \cdot g(t/t_s, r_b/H) \tag{11}$$

The factor R_q (K/(W/m)) may be regarded as a time-dependent thermal resistance for a unit heat extraction step. The dimensionless step response function g depends on t/t_s and r_b/H (and on D/H, but this dependence is negligible, [2]). The time t_s is defined by (17). The resistance R_q and the g-function are by definition zero for negative t/t_s. The variation of g with the second argument is simple, [2]. For two radii r_b and r_b^* we have:

$$g(t/t_s, r_b^*/H) = g(t/t_s, r_b/H) - \ln(r_b^*/r_b) \tag{12}$$

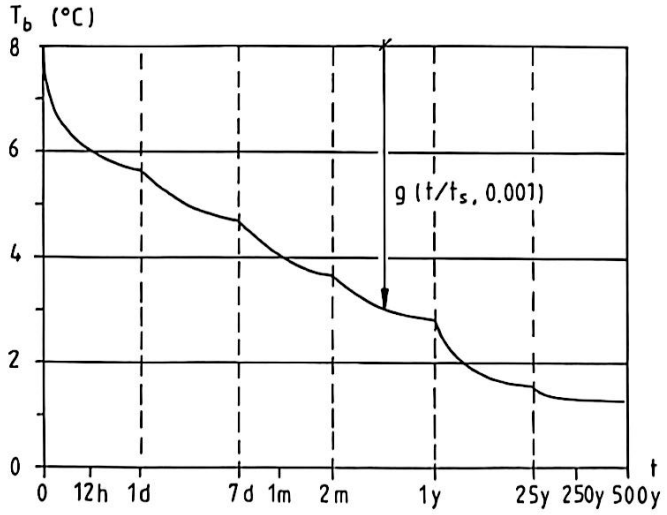

Figure 2. Borehole temperature for a heat extraction step for the data (13). Time-scales from days (d) to years (y).

Consider the following example with typical Swedish data:

$$\begin{array}{lll} H = 110\ \text{m} & D = 5\ \text{m} & 2r_b = 0.11\ \text{m} \\ \lambda = 3.5\ \text{W/m·K} & a = 1.62 \cdot 10^{-6}\ \text{m}^2/\text{s} & T_{om} = 8\ ^\circ\text{C} \\ q_1 = 22\ \text{W/m} & R_b = 0.1\ \text{K/(W/m)} & \end{array} \tag{13}$$

The constant heat extraction $q_1 = 22$ W/m gives 21000 kWh per year. This case has been solved numerically with the model [8,9]. The borehole temperature from the first few hours up to 500 years is shown in Figure 2. The curve also gives $g(t/t_s, 0.001)$ as indicated by the arrow in the figure, since $q_1/(2\pi\lambda) \simeq 1.0$ in this example (the time t_s becomes 26 years).

The temperature decrease is quite rapid during the first hours. The time-scales are interesting. One third of the total temperature drop to steady-state conditions occurs during the first day, and two thirds during the first two months. Only 5% of the total drop occurs from 25 to 500 years. The steady-state extraction temperature is essentially obtained after, say, five years.

The fundamental response function g has, in a logarithmic time-scale, two asymptots, which provide quite good approximations, [2]:

$$R_q \simeq R'_q = \frac{1}{2\pi\lambda}\left\{\ln(\sqrt{4at}/r_b) - \gamma/2\right\} \qquad \begin{array}{l} t_b \le t \le t_s \\ (t_b \le t \le 0.1t_s) \end{array} \tag{14}$$

$$R_q \simeq R_s = \frac{1}{2\pi\lambda}\ln(H/(2r_b)) \qquad \begin{array}{l} t \ge t_s \\ (t \ge 10t_s) \end{array} \tag{15}$$

Here $\gamma \simeq 0.5772$ is Euler's constant. The first expression is obtained in a radial heat flow approximation using a line sink. It is not valid for very short times, when the heat capacities inside the borehole is of importance. There is the following lower limit associated with the borehole radius, [2]:

$$t_b = \frac{5r_b^2}{a} + \pi r_p^2 \cdot 2H/V_f \simeq \frac{5r_b^2}{a} \tag{16}$$

The first term, $5r_b^2/a$, is characteristically 2-3 hours; see example (13). The second term, which is the circulation time for the fluid in the pipes, is characteristically a few minutes. It can normally be neglected. The radial approximation $R'_q(t)$ and the steady-state thermal resistance R_s coincide at the (steady-state) time t_s. This gives:

$$t_s = \frac{H^2}{9a} \tag{17}$$

This time becomes 26 years for the data (13). The expressions (14) and (15) are valid with very good accuracy for $t \le 0.1t_s$ and $t > 10t_s$, respectively. More precise values, obtained from a numerical calculation, differ with up to 7% in the intermediate interval $0.1t_s < t < 10t_s$, [2].

3.2 Long-term thermal disturbance in the ground

Heat extraction and injection will change the ground temperatures. This thermal disturbance depends on the given $q(t)$. The temperature variations near the borehole follows the temporal variations of $q(t)$. The radial range of the variations during the year is shown in [3] to be a few meters for all ground materials. The thermal disturbance in the ground outside a cylinder with a radius of, say, 3 m around the borehole is determined by the average annual heat extraction rate, which is roughly constant from year to year. Thus, the thermal disturbance for $r > 3$ m is given by the heat extraction step with q_1 equal to the average annual heat extraction rate.

Consider the example (13), for which $q_1 = 22$ W/m is the average annual extraction rate. Figure 3 shows the computed positions for the isotherm $T = 7^\circ$C, i.e. 1°C below the undisterbed

ground temperature T_{om}. The largest distance from the isotherm to the borehole is 4, 9, 18, 23, and 27 m after 1, 5, 15, 100, and 1000 years respectively. The corresponding borehole temperatures, given in the table below the isotherms, are virtually constant after 25 years. The isotherm for t = 1000 y lies close to the steady-state one. The figure illustrates the gradual change from an essentially radial process during the first years to a three-dimensional one after, say, 10 years, and finally to a virtually steady-state process after some 25 (near the borehole) to 100 years (further out in the ground).

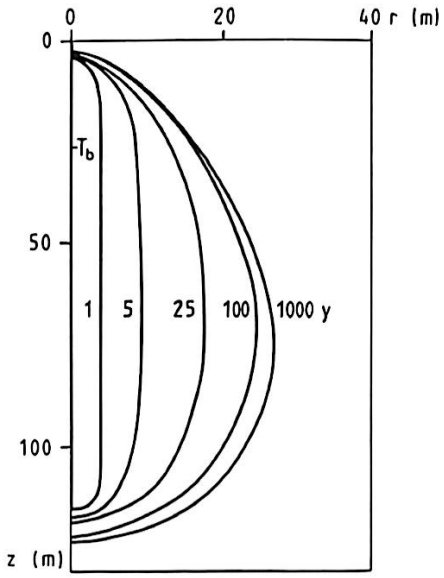

Time (y)	1	5	25	100	1000
T_b (°C)	2.77	2.07	1.55	1.33	1.27

Figure 3. Propagation of the isotherm $T = T_{om} - 1 = 7$°C.
The table gives the borehole temperature.
Data (13).

The borehole may be used for any combination of extraction and injection during the annual cycle. The thermal disturbance outside r = 3 m is determined by the annual average extraction rate only. A balanced system, for which equal amounts of heat are extracted and injected during each year, does not have virtually any thermal disturbance outside r = 3 m.

3.3 Thermal disturbance near the ground surface

The thermal disturbance at and near the ground surface may change the conditions for vegetation. The variations in $q(t)$ during the year are only felt in the vicinity of the borehole. They are essentially negligible in the top-soil layer even close to the borehole, if the heat extraction starts at, say, two meter's depth or further down ($D \geq 2$ m). Then, the thermal disturbance is determined by the basic heat extraction step with q_1 equal to the average heat extraction rate during the year.

The result of a numerical calculation is shown in Figure 4. The temperature disturbance, T_{dist}, is shown at the depth z = 1 m for the case (13) for t = 1, 5, 25, and ∞ years. The largest disturbance near the borehole is -0.2°C only. This disturbance is superimposed on the natural,

undisturbed temperatures with their strong variations during the year.

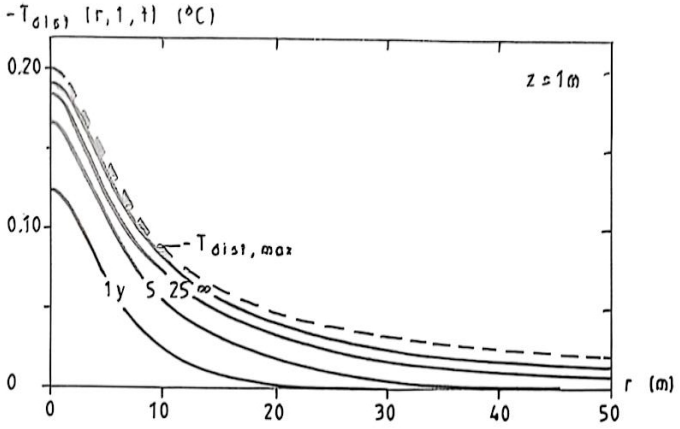

Figure 4. Thermal disturbance at the depth $z = 1$ m due to a heat extraction borehole. Data (13).

An analytical solution for the heat extraction step is given in [2]. Simple formulas for the heat flux at the ground surface and the temperature near the ground surface are given. The following estimation of the maximal disturbance is derived:

$$T_{dist,max} = -\frac{q_1}{2\pi\lambda} \cdot \frac{z}{\sqrt{r^2 + D^2}} \qquad (z < D, z < H/40) \tag{18}$$

The dashed line in Figure 4 shows this estimate for example (13). The thermal resistance at the ground surface is here neglected. Let α (W/m^2· K) be the heat transfer coefficient between the ground surface and the free air. A soil layer with the thickness $z_o = \lambda/\alpha$ has the same thermal resistance ($1/\alpha = z_o/\lambda$). The effect of the surface resistance is accounted for, if z is replaced by $z + z_o$ in (18). The order of magnitude of z_o is 0.1 m. In Figure 4 the disturbance is at most -0.2°C at $z = 1$ m. The disturbance at the ground surface becomes one tenth of this for $z_o = 0.1$ m.

The example above shows that the order of magnitude of the thermal disturbance in the top-soil layer is at most 0.2°C, and at the ground surface 0.02 °C. These temperature changes are completely negligible in comparison to natural variations. The thermal disturbance from a single heat extraction borehole on the environment is negligible.

3.4 Heat supply from ground and through ground surface

The extracted heat is obtained by cooling of the ground around the borehole. The cooling will induce a heat flux from the air through the ground surface. The relative contributions from these two sources are obtained from the heat extraction step with q_1 equal to the annual average heat extraction rate. The superimposed variation, $q(t) - q_1$, represents a balanced extraction and injection. A simple formula for the total heat flux, $Q_{surf}(t)$ (W), through the ground surface is given in [2]. The fraction $\eta = Q_{surf}/(H \cdot q_1)$ represents the heat taken from the air, while the remaining part $1 - \eta$ is the fraction obtained by cooling of the ground. Table 1 gives η as a function of time with a, D and H taken from (13). The time-scale is noteworthy. After 25 years only 32% of the heat comes from the air, while the remaining 68% is due to cooling of the ground. About one half is obtained from the air after 100 years, and after 1000 years there is still 15% from cooling of the ground.

t (years)	1	5	25	100	500	1000
η	0.04	0.12	0.32	0.57	0.79	0.85

Table 1. Fraction of the extracted heat that is supplied through the ground surface.

4 PULSE ANALYSIS

The given heat extraction may normally with sufficient accuracy be represented by piecewise constant values. We will here consider certain basic cases, from which insight is gained and important conclusions may be drawn. The temperature drop from the undisturbed level T_{om} is denoted ΔT, while $\Delta T'$ denotes a dimensionless drop:

$$\begin{aligned} \Delta T &= T_{om} - T_b(t) \\ \Delta T' &= \Delta T \cdot (4\pi\lambda)/q_1 \end{aligned} \tag{19}$$

4.1 Superposition of heat extraction steps

Let the extraction function $q(t)$ consist of N steps:

$$q(t) = \sum_{n=1}^{N} (q_n - q_{n-1}) \cdot He(t - t_n) \qquad (q_o = 0) \tag{20}$$

Then $q(t)$ is equal to 0 for $t \leq t_1$, q_n for $t_n < t \leq t_{n+1}$ $(n = 1, ..., N-1)$, and q_N for $t > t_N$. The temperature at the borehole wall is obtained by superposition of the contributions from each step, [2]:

$$T_b(t) = T_{om} - \sum_{n=1}^{N} (q_n - q_{n-1}) \cdot R_q(t - t_n) \qquad (q_o = 0) \tag{21}$$

The resistance $R_q(t)$, which is zero for negative t, is given by the approximations (14-15), or by a complete, more exact curve in [2]. Formula (14) is valid with very good accuracy for $t_b < t - t_n < 0.1t_s$ $(n = 1, ..., N)$, which in example (13) is an interval from 3 hours to 3 years.

4.2 Single pulse

Figure 5A shows a single pulse with the length t_1. The temperature drop at the end of the pulse, $t = 0$, is from (10), (14) and (19):

$$\Delta T = \frac{q_1}{4\pi\lambda} \cdot \left\{ \ln(4at_1/r_b^2) - \gamma \right\} \qquad (t_b < t_1 < 0.1t_s) \tag{22}$$

The second factor is the dimensionless temperature drop $\Delta T'$. Table 2 gives values for different t_1 with a and r_b from (13). The temperature factor $q_1/(4\pi\lambda)$ is 0.5°C for the data (13). The value of $\Delta T'$ falls in the interval 3 to 10.

t_1	3h	6h	1d	1w	1m	6m	1y
$\Delta T'$	2.6	3.3	4.6	6.5	8.1	9.9	10.5

Table 2. Dimensionless temperature drop at the end of a pulse with the length t_1.

The recovery after the single pulse of Figure 5A is from (14) and (21) obtained as the difference between two logarithms in time to the beginning $(t + t_1)$ and end (t) of the pulse:

$$\Delta T = \frac{q_1}{4\pi\lambda} \cdot \ln\left(\frac{t + t_1}{t}\right) \qquad (t_b < t < 0.1t_s - t_1) \tag{23}$$

The second factor is the dimensionless temperature drop $\Delta T'$, which depends on t/t_1 only. Table 3 gives a few values.

t/t_1	0.1	0.25	0.5	1	3	5	10
$\Delta T'$	2.4	1.6	1.1	0.69	0.29	0.18	0.10

Table 3. Dimensionless temperature drop $\Delta T'$ after a single pulse.

The values in Table 3 should be compared with those in Table 2. The remaining temperature drop after one pulse length ($t = t_1$) is of the order of 10% of the temperature drop at the end of pulses with the length 1 day to 6 months. Only around 3% remains after three pulse lengths ($t = 3t_1$).

Any pulse train can be expressed by a superposition of single pulses. With the two formulas (22) and (23) we already have aquired a good knowledge of the behaviour of the borehole temperature $T_b(t)$.

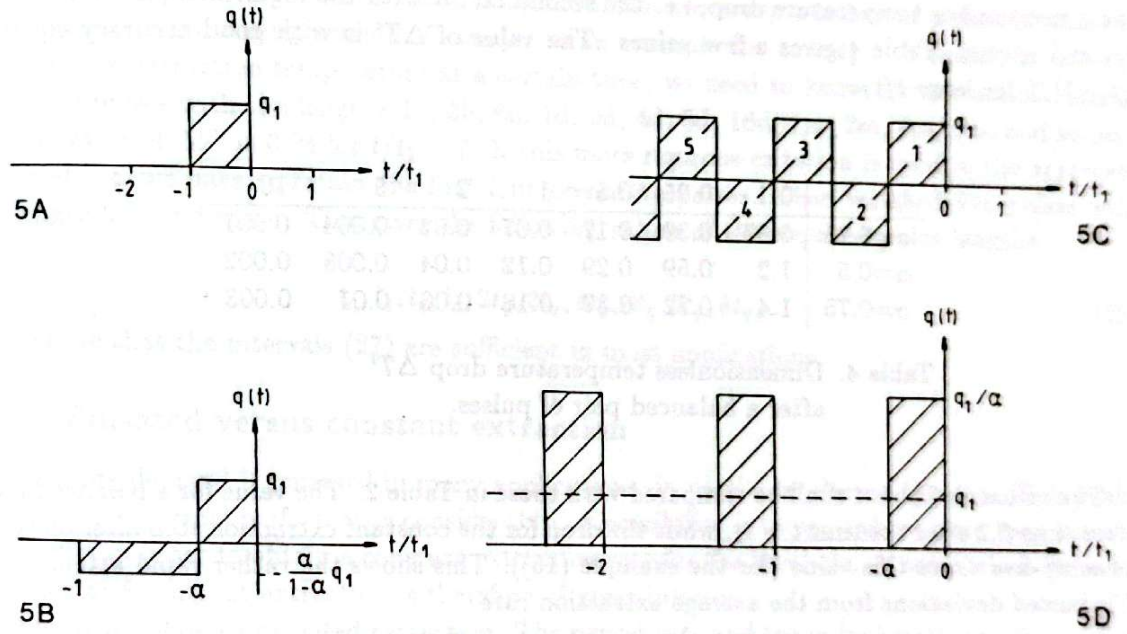

Figure 5. Considered extraction pulses.

The heat extraction conditions during the periods of maximum extraction rate (nomally in wintertime) are improved, if the borehole is recharged during the summer. The improvement due to summer recharge is easily assessed with the formulas above. The temperature decline after a recharge pulse is given by (23). Let us take the data (13) and a recharge pulse $q(t) = -22$ W/m, i.e. injection of 2.42 kW, during three months. The increase of the borehole temperature due to the recharge becomes:

$$t_1 = 3 \text{ months} \quad t = 3 \text{ months} : \Delta T = \frac{22}{4\pi \cdot 3.5} \ln\left(\frac{3+3}{3}\right) = 0.35°C$$
$$t = 6 \text{ months} : \Delta T = 0.5 \ln\left(\frac{6+3}{6}\right) = 0.2°C \qquad (24)$$

The maximal temperature drops ΔT in a normal application may be around 5 to 10°C. The above recharge will diminish these drops with around 4%. This means that 4% more heat may be extracted for the same lowest extraction temperature.

The above example shows that the gain from recharge is quite small. It is in most cases not economical to recharge heat in order to improve the situation some months later.

4.3 Two balanced pulses

Strictly speaking, the borehole temperature $T_b(t)$ depends on all variations of the heat extraction rate before the concidered time t. The average extraction rate is always important, while the superimposed variations are attenuated with time. The variable extraction rate may be represented by the average extraction rate and superimposed balanced pairs of pulses; i.e. an injection and an extraction pulse involving equal amounts of heat.

We will analyse the effect of a single balanced pair of pulses of the type shown in Figure 5B. The length of the pulses are αt_1 and $(1-\alpha)t_1$, $0 < \alpha < 1$, and the injection and extraction rates are q_1 and $-\alpha q_1/(1-\alpha)$ respectively. Here, the sum (20) involves four terms. The temperature drop becomes:

$$\Delta T = \frac{q_1}{4\pi\lambda}\left\{\ln\left(\frac{t+\alpha t_1}{t}\right) - \frac{\alpha}{1-\alpha}\ln\left(\frac{t+t_1}{t+\alpha t_1}\right)\right\} \qquad (t_b < t < 0.1t_s - t_1) \qquad (25)$$

The dimensionless temperature drop, i.e. the second factor with the logarithms, is a function of t/t_1 and α only. Table 4 gives a few values. The value of $\Delta T'$ is with good accuracy equal to $\alpha(t_1/t)^2/2$ for large t/t_1.

t/t_1	0.1	0.25	0.5	1	2	5	10
α=0.25	0.87	0.39	0.17	0.07	0.02	0.004	0.001
α=0.5	1.2	0.59	0.29	0.12	0.04	0.008	0.002
α=0.75	1.4	0.72	0.37	0.16	0.06	0.01	0.003

Table 4. Dimensionless temperature drop $\Delta T'$ after a balanced pair of pulses.

The values in Table 4 shall be compared with those in Table 2. The value for a balanced pair is less than 0.2 after the time $t = t_1$, while the drop for the constant extraction step after one day is twenty-five times this value (for the example (13)). This shows the rather rapid attenuation of balanced deviations from the average extraction rate.

4.4 Balanced pulse train

The influence of previous pulses may be illustrated further with the balanced pulse train shown in Figure 5C. Each pulse has the time length t_1. The extraction and injection rates are equal.

The dimensionless temperature drop $\Delta T'$ at $t = 0$, i.e. at the end of an extraction pulse contains contributions from the last pulse 1 and from the other pulses 2, 3 and so on. The contribution from pulse 1 is, for example (13), given by Table 2. The value of $\Delta T'$ lies between 2.6 and 10 for t between 3 hours and 6 months. The balanced contribution from pulse 2 and 3 becomes 0.29 (Table 3 with $\alpha = 0.5$, $t/(2t_1) = 0.5$). The contribution from pulse 4 and 5 is 0.06. The contribution from pulse 6 to N is, for $N > 10$, very close to the contribution from 6 to $N = \infty$, which is 0.10. The total contribution from pulse 2 to a large N is 0.45. This is to be compared with the contribution between 2.6 and 10 for pulse 1. The error, when all the balanced pairs from 2 and 3, 4 and 5, and so on are neglected, is thus around 10%.

The examples in Sections 4.2-4 provide guidelines for the necessary resolution in $q(t)$ in order to make an accurate calculation. The formulas and analyses above are not valid for variations on a time-scale below t_b, which may be somewhat below 3 hours. This time defines the highest resolution for which $q(t)$ is given. Let t_q denote a smallest pulse time. It must exceed t_b:

$$t_q > t_b \qquad (26)$$

The given function $q(t)$ is given by one constant value for each basic time interval t_q.

The value of $\Delta T'$ for a balanced pair of pulses is 0.12 for $t/t_1 = 1$ and 0.04 for $t/t_1 = 2$ (Table 3, $\alpha = 0.5$). A reasonable criterion is to neglect a balanced pulse pair for $t \geq t_1$, i.e. if the time t to the end of the pulse pair is greater than or equal to the length t_1 of the pulse pair. The first and second preceding pulses are retained. The next two pulses 3 and 4 have together the length $t_1 = 2t_q$, and their effect is considered after the time $t = 2t_q$. We therefore use only the average of pulse 3 and 4. Pulses 5 and 6, and so on, are brought together in the same way. Consider then the pulses 5+6 and 7+8. The balanced part may again be neglected, since it is considered after the time $t = 4t_q$. This argument may be applied for all preceding pulses. The result is that we only need to consider average extraction values during pulses, the lengths of which are doubled for each pulse (except the first one):

$$t_q, t_q, 2t_q, 4t_q, 8t_q, \ldots \tag{27}$$

This geometric series increases rapidly. Therefore, the necessary number of pulses in order to represent $q(t)$ is surprisingly small. Consider as an example the case $t_q = 3$ hours. In order to calculate the extraction temperature at a certain time, we need to know the extraction rate for preceding pulses with the lengths 3h, 3h, 6h, 1d, 2d, 4d, 8d, 16d, 1m, 2m, 4m, 8m, and so on.

The value of $\Delta T'$ is 0.04 for $t/t_1 = 2$. If this more rigorous criterion is used in the argumentation above, we have to retain the first four preceding pulses. Then we need two pulses with the length $2t_q$, and so on. This gives the following values of the required pulse lengths:

$$t_q, t_q, t_q, t_q, 2t_q, 2t_q, 4t_q, 4t_q, 8t_q, 8t_q, \ldots \tag{28}$$

We believe that the intervals (27) are sufficient in most applications.

4.5 Pulsated versus constant extraction

The heating demand is pulsated in many applications, in particular during the day. High peaks decrease the thermal performance considerably. A possibility is to use a short term heat storage as a buffer in order to obtain a constant extraction rate for the borehole. A comparison between pulsated and constant extraction is therefore of great interest.

Figure 5D shows a pulsated extraction. The period is t_1 and the pulse length αt_1, $0 < \alpha < 1$. The extraction rate of the pulses is q_1/α. The corresponding constant extraction rate is q_1 (dashed line). We are interested in the difference of the borehole temperature at the end of a pulse, i.e. at $t = 0$, between the pulsated case and the case with constant extraction. This difference depends on the number of preceding pulses. It becomes with good accuracy equal to the value for an infinite pulse train after about five pulses. Quite simple formulas for the borehole temperatures for a balanced, infinite pulse train are derived in [10]. The difference in temperature drop at $t = 0$ (Figure 5D) between the pulsated case and the constant extraction is:

$$\Delta T = \frac{q_1}{4\pi\lambda}\left\{\left(\frac{1}{\alpha}-1\right)\left(\ln\left(\frac{4a\alpha t_1}{r_b^2}\right)-\gamma\right)+\ln(\alpha)-\frac{\ln(\Gamma(1+\alpha))}{\alpha}\right\} \qquad (\alpha t_1 > r_b) \tag{29}$$

Here $\Gamma(1+\alpha)$ is the gamma function, which is tabulated in [11]. The first part represents the temperature drop of the excess pulse $q_1/\alpha - q_1$ during the time $-\alpha t_1 < t < 0$. The remaining part, which is a small correction, depends on α. A few values are given in Table 5. The values in Table 5 are rather small compared to the values of the constant extraction pulse in Table 2, except for very small α. The effect of pulsation instead of constant extraction is therefore approximately equal to the extra temperature drop due to the excess extraction rate $q_1/\alpha - q_1$ during the pulse.

α	0.1	0.2	0.3	0.4	0.5	0.6	0.7	0.8	0.9	1
$\ln(\alpha) - \ln(\Gamma(1+\alpha))/\alpha$	-1.8	-1.2	-0.84	-0.62	-0.45	-0.32	-0.22	-0.13	-0.06	0

Table 5. Correction term in formula (29).

Consider example (13). A pulsated extraction during 8 of the 24 hours ($\alpha = 1/3$) is compared to the constant extraction. The temperature drop for the constant extraction is after, for example, one year $10.5 \cdot 0.5 = 5.25°C$ according to Table 2. The extra temperature drop due to pulsation is from (29):

$$\Delta T = 0.5 \cdot \{(3-1) \cdot 2.45 - 0.76\} = 2.1°C \tag{30}$$

The decrease of heat extraction referred to the same temperature drop becomes $1 - 5.25/(5.25 + 2.1) = 0.29$, i.e. 29%.

5 LOCAL PROCESSES IN THE BOREHOLE

The detailed thermal processes in the borehole and its immediate vicinity are quite complex. It is necessary to consider their time-scales in order to identify the basic parameters.

5.1 Time-scales

The time for the heat carrier fluid to circulate through the borehole is given by the second term of (16). It gives a time-scale for a change of inlet conditions to be felt along the whole borehole. These transient, axial effects with a time-scale of a few minutes are not considered in this study.

The response to variations on a time-scale below 1-2 hours will depend on the heat capacities of heat carrier fluid, pipings, heat exchanger etc. This problem, associated with the specific equipment above ground, should be studied by practical experiments. These short-time effects are not considered here.

A change of the temperature in the heat carrier fluid in the pipes will induce a transient local process in the borehole outside the pipes. The time-scale to obtain approximate local steady-state conditions in the borehole may be assessed in the following way. Consider a change ΔT of fluid temperature in the pipes. The amount of heat to change the borehole temperature with ΔT is of the order $\pi r_b^2 \cdot \rho_w c_w \cdot \Delta T$ (J/m). It is shown below that the order of magnitude of the heat flux from the pipes is $\Delta T / R_b$ (W/m). The quotient gives a time-scale t_b' to obtain local steady-state conditions in the borehole:

$$t_b' = \frac{\pi r_b^2 \cdot \rho_w c_w \cdot \Delta T}{\Delta T / R_b} = \frac{r_b^2}{a} \cdot \frac{\rho_w c_w}{\rho c} \cdot \pi \lambda R_b \tag{31}$$

The second factor $\rho_w c_w / (\rho c)$, which is the ratio between the heat capacity of ground water and ground material, is approximately 2. The borehole resistance R_b is characteristically equal to 0.1 K/(W/m) or less. The last factor with λ equal to, say, 3.3 W/(mK) is then about 1. It is reasonable to take $2.5 t_b' \simeq t_b$ according to (16) as the criterion for attaining local steady-state in the borehole and its immediate vicinity. We introduce the following (borehole) time:

$$t_b = \frac{5 r_b^2}{a} \tag{32}$$

We do not consider variations of the heat extraction rate $q(t)$ on a time-scale below t_b.

5.2 Borehole thermal resistance

The temperature of the heat carrier fluid varies along the downward and upward channels. At each depth z and time t, there is a local steady-state process with heat flows between the pipes and the ground around the borehole. These flows balance the convective heat flow along the pipes. The exact equations for heat balance in the borehole are given in [8].

The heat flow problem between the fluid in the pipes and the surrounding ground is essentially two-dimensional in the plane perpendicular to the borehole. The relations between temperatures and heat flows may be represented by a heat flow circuit, [8], with thermal resistances between nodes at the bulk fluid temperatures in the pipes and at the borehole wall.

Natural convection in the groundwater in the borehole may be important. Then, the thermal resistances should be measured in laboratory experiments. Field experiences indicate that the effect of natural convection is small at low temperatures around 4°C, where the variation of water density with temperature has its minimum. The borehole outside the pipes is in many cases filled with a solid material that prevents natural convection. The local heat flow problem outside the pipes is then one of pure heat conduction. This case is solved analytically in [12]. So-called multipole expansions are used to fit the solution around each pipe and around an

outer circular boundary in the ground. A PC-model (IBM-compatible, MS-DOS), which gives the solution very rapidly, is available. The model is used extensively in [13], in which these local resistances are given and discussed for many cases of practical importance.

The variation of temperature along the pipes depends on the pumping rate V_f. It becomes negligible, when V_f is very high. This case with a single temperature $T_f(t)$ for the heat carrier fluid is discussed here, while the necessary modifications for small V_f are dealt with in the next section. The thermal resistance circuit is then reduced to a single resistance between T_f and T_b. We have the fundamental relation:

$$T_b - T_f = q \cdot R_b \tag{33}$$

The borehole thermal resistance R_b (K/(W/m)) between heat carrier fluid is one of the most important parameters of a heat extraction borehole. It is important to design the heat exchanger so that R_b becomes as small as possible.

The model in [12] uses a circle in the ground outside the borehole periphery as outer boundary. This means that the effect of the outside ground with its different thermal conductivity is accounted for. The borehole resistance R_b includes this effect, and T_b should be interpreted as the mean temperature around the borehole periphery, [13].

The total thermal resistance R_b depends on λ, r_b, the thermal conductivity λ_b in the borehole outside the pipes, and the number of pipes and their positions in the borehole. It also depends on the thermal resistances R'_p over the borehole wall and R_{fc} between the bulk fluid in the pipes and the inner pipe wall with different expressions for laminar and turbulent flow.

As an illustration we take a case with two pipes (polyethelene, medium density) with water outside the pipes. Natural convection is not considered. The calculation is performed for laminar and turbulent flow in the pipes. A third case with temperatures below 0°C and the water frozen to ice is also included. The following data are used:

$$\begin{array}{lll} \lambda = & 3.5 \text{ W/(mK)} & r_b = 0.0575 \text{ m} \\ \lambda_b = & 0.56 \text{ W/(mK)} & \text{(water)} \\ \lambda_b = & 2.0 \text{ W/(mK)} & \text{(ice)} \end{array} \tag{34}$$

pipe: outer radius 16 mm
wall thickness 2.1 mm
wall thermal conductivity 0.36 W/(mK)

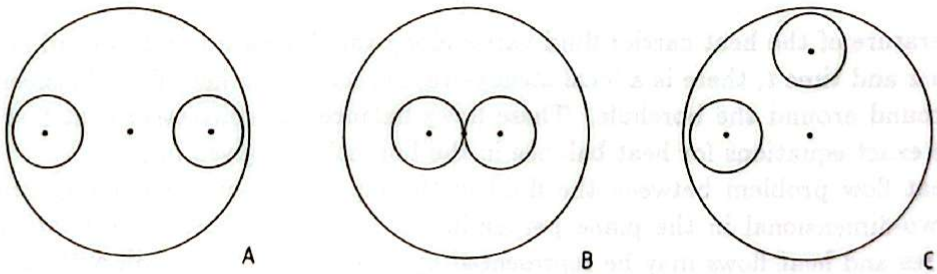

Figure 6. Considered pipe configurations.

Formulas from [13] give R'_p =0.062 K/(W/m), and R_{fc} = 0.142 for laminar flow and R_{fc} = 0.008 for turbulent flow (Re = 7500, Pr = 13.4). Three pipe configurations according to Figure 6 are considered. The spacing between pipes and borehole wall is 2 mm in case A and C. The 9 cases have been computed with the model [12]. The obtained borehole resistances R_b are given in Table 6.

	A	B	C
unfrozen, laminar	0.210	0.362	0.227
unfrozen, turbulent	0.132	0.279	0.148
frozen, turbulent	0.042	0.075	0.051

Table 6. Computed borehole resistance R_b (K/(W/m)) for the configurations of Figure 6.

It should be remembered that the natural convection, which may occur in the unfrozen cases and then giving a smaller R_b, is neglected in these calculations. It is clear that laminar flow in the pipes should be avoided. It is also clear that the increase of λ_b from 0.56 in the unfrozen case to 2.0 in the frozen case reduces R_b considerably. The importance of position is also shown. The pipes should be kept close to the wall by a suitable device in order to reduce the flow paths through the water as much as possible. These questions about how to diminish R_b are discussed further in [12].

The Swedish field experiences indicate values around $R_b = 0.1$ K/(W/m) for a typical case with two plastic pipes in a borehole.

5.3 Temperature variations along the borehole

The temperatures in the fluid channels and in the ground outside vary along the borehole. These variations are studied analytically in [14]. A simple formula is deduced for the case with a uniform ground temperature. It has been tested with very good agreement [4] against a more exact numerical model [9], in which the ground temperature varies along the borehole. The simplified formulas below may therefore be used without restrictions.

The inlet and outlet fluid temperatures are given by:

$$T_{f,in} = T_f - \frac{qH}{2c_f\rho_f V_f} \qquad T_{f,out} = T_f + \frac{qH}{2c_f\rho_f V_f} \tag{35}$$

Here V_f (m_f^3/s) is the pumping rate. These formulas imply that $T_f(t)$ is the mean value of $T_{f,in}$ and $T_{f,out}$. Formula (33) is valid with a modified thermal resistance R_b', which accounts for the effect of variation of fluid temperature along the borehole [14]:

$$T_b(t) - T_f(t) = q(t) \cdot R_b' \tag{36}$$

The heat extraction rate $q(t)$ and the temperature $T_b(t)$ are average values along the borehole.

Exact formulas for the modified borehole resistance R_b' are given in [14]. The ratio R_b'/R_b depends on the pumping rate V_f and on the thermal resistances of the heat flow circuit. These resistances are easily computed with the model [12]. Numerical examples show that the difference between R_b and R_b' is rather small (less than 10%) in normal applications. Then, it is sufficient to use R_b instead of R_b'.

6 DIMENSIONING RULES

The dimensioning rules proposed here are based on a given heat extraction rate $H \cdot q(t)$ (W) and a given lowest extraction temperature $T_{f,min}$ for the temperature $T_f(t)$ of the heat carrier fluid. Input parameters are λ, T_{om}, and a for the ground, r_b, H, and R_b for the borehole and its heat exchanger, and the given $q(t)$. The dimensioning formulas below give the lowest fluid temperature. The borehole depth H or some other input variables are adjusted, until the prescribed value of $T_{f,min}$ is obtained.

The cooling mode with heat injection to the ground is in many applications the critical one in the dimensioning. Then, there is a prescribed highest injection temperature $T_{f,max}$ instead. The formulas below (and PC-models) are directly applicable by using negative values for $q(t)$.

6.1 Simplified heat extraction

It is often sufficient to use a rather simple form for the extraction rate $q(t)$. Figure 7 shows such a case with a constant component q_o and a superimposed periodic component with the amplitude q_p and the period t_p (normally one year). There is also a superimposed heat extraction pulse with the strength q_1 and the length t_1. This pulse occurs at the time of largest periodic extraction.

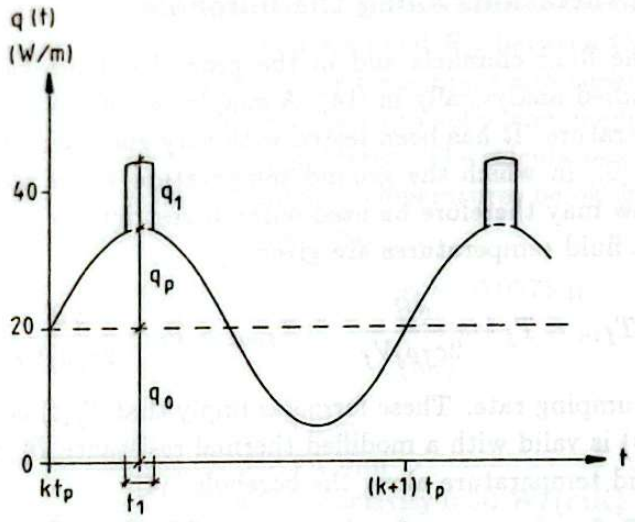

Figure 7. Prescribed heat extraction (constant+periodic +pulse). The k:th period is shown.

The borehole temperature, based on analytical solutions for the three components, is given in [2]. The largest contribution from the pulse occurs at the end of it, while the largest effect from the periodic components occurs some time after its extraction maximum. We assume that these largest effects occur roughly at the same time. Then from [2] and (33), the lowest fluid extraction temperature is:

$$T_{f,min} = T_{om} - q_o \cdot R_s - q_p \cdot R_p - q_1 \cdot R'_q(t_1) - (q_o + q_p + q_1) \cdot R_b \tag{37}$$

Here R_s (K/(W/m)) is the steady-state thermal resistance of the heat extraction borehole and R_p the amplitude of the periodic thermal resistance, [2]:

$$R_s = \frac{1}{2\pi\lambda} \cdot \ln\left(\frac{H}{2r_b}\right) \qquad (r_b << H) \tag{38}$$

$$R_p = \frac{1}{2\pi\lambda}\sqrt{(\ln(2/r'_{pb}) - \gamma)^2 + \pi^2/16} \qquad r'_{pb} = r_b\sqrt{2}/d_p < 0.1 \qquad d_p = \sqrt{at_p/\pi} \tag{39}$$

The resistance $R_q'(t_1)$ for the pulse is given by (14).

Formula (37) is quite instructive. The temperature drop $T_{om} - T_{f,min}$, required to sustain the largest heat extraction, has a steady-state term $q_o \cdot R_s$ from the constant (i.e. average) extraction, and corresponding terms from the periodic and step components. Finally, there is a term $q(t) \cdot R_b$ for the drop in the borehole. The thermal resistances R_s, R_p, R_q, and R_b give the temperature drop for a unit extraction rate.

Consider as example the data (13). The resistances become from (38), (39), and (14):

$$\begin{aligned} R_s &= 0.314 \text{ K/(W/m)} \qquad R_p = 0.188 \text{ K/(W/m)} \\ R_q'(t_1) &= 0.106 + 0.023 \cdot \ln(t_1/t_d) \text{ K/(W/m)} \qquad t_d = 1 \text{ day} \end{aligned} \tag{40}$$

Here t_1/t_d is the length of the pulse in days. With the extraction components of Figure 7 ($q_o = 20$, $q_p = 15$, $q_1 = 10$ W/m) we get for $t_1/t_d = 1$:

$$\begin{aligned} T_{om} - T_{f,min} &= 20 \cdot 0.314 + 15 \cdot 0.188 + 10 \cdot 0.106 + (20 + 15 + 10) \cdot 0.1 \\ &= 6.28 + 2.82 + 1.06 + 4.5 = 14.66 \text{ K} \end{aligned} \tag{41}$$

For $t_1/t_d = 30$ we have:

$$T_{om} - T_{f,min} = 6.28 + 2.82 + 1.84 + 4.5 = 15.44 \text{ K} \tag{42}$$

This example shows the importance of the borehole resistance R_b, which here accounts for one third of the temperature drop.

Dimensioning using formula (37) is simple. Suppose that $Q_o = q_o \cdot H$, $Q_p = q_p \cdot H$ and $Q_1 = q_1 \cdot H$ are given, and the borehole depth is to be chosen. The depth H is obtained directly from (37) with a given $T_{f,min}$ by scaling (R_s depends rather weakly on H).

It is often possible to use a still simpler extraction $q(t)$ by putting q_p or q_1 to zero. It is straight-forward to extend the method to more than one periodic component and more pulses. The total variation during the period time must be considered in order to obtain $T_{f,min}$, since the largest contributions from different terms normally occur at different times.

6.2 Stepwise heat extraction

A second alternative, which is quite simple to use with the PC-models described in the next section, is to use any sequence of stepwise constant values for the given heat extraction:

$$\begin{aligned} q(t) = q_n \qquad & t_n < t \le t_{n+1} \\ & n = 1, \ldots, N_{max} \end{aligned} \tag{43}$$

The total number of steps is N_{max}. The lowest extraction temperature is given by the minimum of the temperatures at the end of pulses:

$$T_{f,min} = \min_{1 \le N \le N_{max}} \left\{ T_{om} - q_N \cdot R_b - \sum_{n=1}^{N} (q_n - q_{n-1}) \cdot R_q(t_{N+1} - t_n) \right\} \qquad (q_o = 0) \tag{44}$$

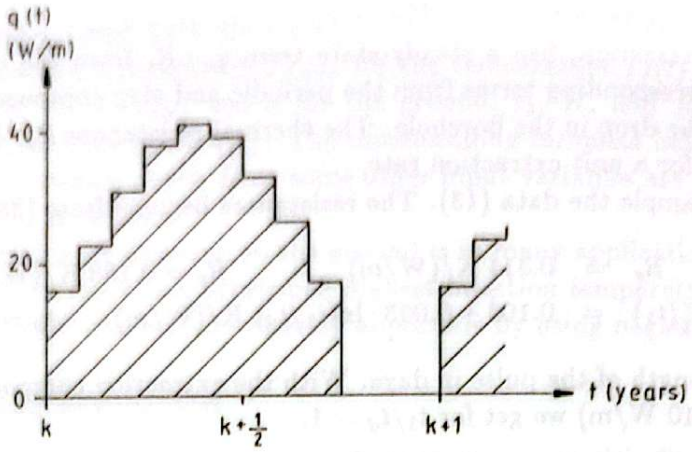

Figure 8. Prescribed monthly values.

Figure 8 shows a typical example with given monthly values, which are repeated each year. The data of (13) are used. The highest extraction rate is 41 W/m during the fifth month. The total heat extraction becomes 21 MWh per year. The lowest extraction temperature, (44), is shown in Table 7 for different years.

year	1	2	3	25	100
$T_{f,min}$ (°C)	-4.8	-5.2	-5.6	-6.2	-6.4

Table 7. Lowest extraction temperature. Data according to (13) and Figure 8.

The borehole is in this case frozen during the period of highest extraction each year. A smaller value for R_b may be valid in accordance with Table 6. A decrease from $R_b = 0.1$ to $R_b = 0.05$ K/(W/m) corresponds to an increase (0.1-0.05)· 41 = 2.05 °C for $T_{f,min}$.

6.3 PC-models

The dimensioning rule (37) has been implemented for use on a personal computer (IBM-PC and compatible computers, MS-DOS). Another PC-model calculates iteratively from (44) the required borehole length H for a given lowest extraction temperature (or a given highest temperature in the case of dimensioning for heat injection to the ground). The interactive models, [5], are rapid and quite simple to run.

The formulas in [2] for heat flow through the ground surface and the effect of groundwater flow are also implemented as small programs. The two disks of the PC-models also contain the corresponding dimensioning rules in [3] for multiple, thermally interacting boreholes.

7 DISCUSSIONS OF PARAMETERS

7.1 Three important parameters: λ, R_b, T_{om}

The thermal resistances R_q, R_s and R_p are inversely proportional to the thermal conductivity of the ground, λ. This means that the thermal performance is essentially proportional to λ, which therefore is a very important parameter. Granite with $\lambda = 3.3$ is three times better than a clay soil with $\lambda = 1.1$. The Swedish heat extraction boreholes lie almost exclusively in rock with high thermal conductivity.

A second, very important parameter is the borehole thermal resistance R_b between the heat carrier fluid and the borehole wall. It may be measured in field or laboratory experiments, or calculated theoretically with the model [12], provided that natural convection does not take place or is insignificant. The example (41) shows that the borehole thermal resistance may account for one third of the temperature drop. It is important to design the borehole heat exchanger carefully. Quite a lot of work has been done to this aim. A detailed discussion of various designs is given in [13]. For example, low-density polyethylene with low thermal conductivity should be avoided, since the thermal resistance over the pipe walls is quite important. Table 5 shows that laminar flow also is to be avoided. The water in the borehole with its low thermal conductivity (0.56 W/(mK)) is an other problem. One shall try to reduce the length of the heat flows paths through the water by pushing the pipes against the borehole wall. Compare case A and B in Figure 6 and Table 6. Freezing is advantageous, since the thermal conductivity then increases to around 2 W/(mK), Table 6. Another possibility is to replace the water by some filling material with higher thermal conductivity. The thermal resistances in the ground are of course not affected by the design of the heat exchanger in the borehole. Thus, the largest gain for a very good heat exchanger with $R_b \simeq 0$ is to eliminate the last term in (37). The other parts of the total temperature drop are not affected.

A third important parameter is the effective undisturbed ground temperature T_{om}, which is an average over the borehole depth. The heat extraction works against this temperature, and it is essentially proportional to the difference $T_{om} - T_f$. Consider for example a northern climate with $T_{om} = 8°$ C and a southern one with $T_{om} = 18$°C in a case with $T_{f,min} = 3$°C. The available temperature drop, and hence the extraction capacity, is three times larger in the southern climate. The undisturbed ground temperature lies between 2 and 10°C in northern climates such as the Swedish one. The temperature interval above freezing becomes quite small. Therefore, the Swedish systems almost exclusively use closed systems for the heat carrier brine allowing temperatures below 0°C. The lowest extraction temperatures may lie in an interval from -10 to -2°C.

7.2 Heat extraction $q(t)$

The average extraction rate q_o and the variations $q(t) - q_o$ of the given heat extraction rate are quite important. Short, strong pulses are costly. The effect of pulsation versus constant extraction is given by (29). An example with extraction during 8 hours each day gave a decrease of heat extraction capacity with 30%.

The effect of recharge in the summer on the extraction during the following winter is quite small (4% improvement in a particular example). The total cost for recharge must therefore be very small, if recharge is to be economically justified.

7.3 Pumping rate

The pumping rate V_f of the heat carrier fluid should be large enough to ensure turbulent flow in the pipes. The pumping work increases strongly with V_f, so one should not greatly exceed

the limit of turbulence. An advantage of high pumping rates is that the difference $T_{f,out} - T_{f,in}$ diminishes, (35).

The question, which flow direction to choose, arises, when the upward and downward channels are unsymmetrical. An example is an open system with an inner pipe and the borehole annulus as the second channel. It is shown in [14] that the thermal response is exactly the same in the two cases (R_b' in (36) is always an even function of V_f). This may be somewhat surprising, since the temperature profiles along the borehole are quite different in the two cases.

7.4 Negligible parameters and effects

It has been shown that many parameters and effects are negligible or rather insignificant for the thermal performance of the extraction borehole. We will as a summary enumerate them here.

- Stratified ground. Deviations from the average thermal conductivity are negligible.
- Ground surface. Temperature variations, snow etc are negligible.
- Geothermal gradient. Temperature deviations from the effective undisturbed ground temperature T_{om} due to the geothermal gradient are negligible.
- Variations of the thermally insulated upper part between, say, 1 to 5 m with constant H are negligible.
- The effect of groundwater filtration is negligible, if criterion (8) is met.
- The thermal impact of a heat extraction borehole near and at the ground surface is completely negligible compared to natural variations.
- Borehole time-scale. Transient thermal effects in the borehole and the heat carrier fluid are insignificant on a time-scale above t_b, (32).

7.5 Response test

The important parameters λ, R_b and T_{om} may be determined experimentally with a so-called response test. The undisturbed ground temperature is determined by pumping without heat injection as described in Section 2.3. After that, a constant heat injection rate ($q(t) = -q_1$) is applied, for example with an electrical heater, during a few days. The temperature varies, after an short initial period, linearly with $\ln(t)$ in accordance with (14). The slope gives λ from the equation:

$$\frac{dT_f}{d\tau} = \frac{q_1}{4\pi\lambda} \qquad \tau = \ln(t) \tag{45}$$

The response test method uses the same principle as the hot wire method, which has a line heat source with a length of around 10 cm. There is a difference in time and length scales, since the borehole has a length of around 100 m. The borehole resistance R_b is obtained from the difference $q_1 \cdot R_b = T_f(t) - T_b(t)$ with $T_b(t)$ given by (14). It is an important task to develop a laboratory method to measure R_b under controlled conditions. A cylinder of a few meter's height with the heat exchanger along the axis has to be built , and R_b is measured under steady-state conditions.

A few response tests have been made in Sweden. The largest one concerns a multiple borehole system with 25 boreholes and a total borehole length of 2000 m. The experiment and the evaluation technique in the case of several pulses are reported in [15].

7.6 Thermal resistance analysis

The analysis in Section 6.1 illustrates that the different thermal resistances represent the thermal processes in a very lucid way. The resistances R_b, R_s, and $R_q(t)$ are especially important. Consider a constant heat extraction rate q_o (or the average component). The steady-state temperature drop after very long time, $t > t_s$, is:

$$\Delta T = q_o \cdot (R_b + R_s) \tag{46}$$

In example (13) we have $R_b = 0.1$ and $R_s = 0.3$. This means that one fourth of the temperature drop occurs at the borehole and the remaining three fourth in the ground.

A large part of the temperature drop in the ground occurs close to the borehole due to the steep gradients here. Consider the region between the borehole and a radius r^*: $r_b < r < r^*$. The steady-state thermal resistance of this annulus is:

$$R^* = \frac{1}{2\pi\lambda} ln\left(\frac{r^*}{r_b}\right) \qquad \text{(K/(W/m))} \tag{47}$$

Table 8 gives R^* for the case (13). These values are to be compared with $R_s = 0.3$. One third of R_s lies in the region out to $r^* = 0.5$ m and two thirds out to $r^* = 5$ m. Let $R_{s,0.5}$ denote the radius for which R^* equals $0.5R_s$. We have from (47) and (38):

$$r_{s,0.5} = \sqrt{Hr_b/2} \tag{48}$$

This gives in case (13) $r_{s,0.5} = 1.7$ m.

r^* (m)	0.055	0.2	0.5	1	1.7	5	10
R^* (K/(W/m))	0	0.059	0.10	0.13	0.16	0.21	0.24

Table 8. Steady-state thermal resistance from the borehole to the radius r^*. Data according to (13).

An increase of the borehole radius to, for example, 0.5 m will reduce R_s from 0.3 to 0.2. The annulus $0.055 < r < 0.5$ m is now a part of the enlarged borehole. Its contribution to the borehole resistance R_b will depend on the heat exchanger design. The cost of drilling increases strongly with the radius r_b. Therefore we suggest that one should try smaller borehole radii with a trade-off between drilling cost and borehole length.

The steady-state formula (38) is only valid after long time, $t > t_s$ with $t_s = 26$ years in case (13). The temperature drop after the time t for a constant pulse q_1 is:

$$\Delta T = q_1 \cdot (R_b + R_q(t)) \tag{49}$$

Table 9 gives $R_q(t)$ from (14) for case (13), for which the numerical expression (41) is valid.

t	1d	9d	2m	1y	5y
$R_q(t)$ (K/(W/m))	0.11	0.16	0.20	0.24	0.28

Table 9. Thermal resistance of an extraction step. Data according to (13).

The values of Table 9 are to be compared with the steady-state value $R_s = 0.314$. Half this value is attained after 9 days. Let in general $t_{q,\alpha}$ denote the time, when R_q is equal to $\alpha \cdot R_s$, $0 < \alpha < 1$. Then we have from (14) and (38), using the definition (17) for t_s:

$$t_{q,\alpha} = t_s \cdot \left(\frac{2r_b}{H}\right)^{2-2\alpha} \tag{50}$$

In particular we have for $\alpha = 0.5$:

$$t_{q,0.5} = t_s \cdot \frac{2r_b}{H} = \frac{H \cdot 2r_b}{9a} \tag{51}$$

References

[1] J.E. Bose, J.D. Parker, F.C. McQuiston, Design/Data Manual for Closed-Loop Ground-Coupled Heat Pump Systems, ASHREA, 1791 Tullie Circle, Atlanta, GA 30329, USA, 1985.

[2] J. Claesson, P. Eskilson, Conductive Heat Extraction by a Deep Borehole. Analytical Studies. Dep. of Mathematical Physics and Building Technology, University of Lund, Box 118, S-221 00 Lund, Sweden. (Submitted to Journal of Heat and Mass Transfer)

[3] J. Claesson, P. Eskilson, Conductive Heat Extraction by Thermally Interacting Deep Boreholes. Dep. of Mathematical Physics and Building Physics, University of Lund, Box 118, S-221 00 Lund, Sweden, 1987.

[4] J. Claesson et. al., Markvärme. En handbok om termiska analyser (Ground Heat Systems. A Handbook on Thermal Analyses), BFR- Rapport T16:1985, (in Swedish, 900 pp. 460 fig.), Svensk Byggtjänst, Box 7853, S-103 99 Stockholm, 1985.

[5] P. Eskilson, PC-programs for Dimensioning of Heat Extraction Boreholes, Dep. of Building Technology and Mathematical Physics, University of Lund, Box 118, S-221 00 Lund, 1987.

[6] J. Bear, Hydraulics of Groundwater, McGraw-Hill, 1979.

[7] H.S. Carslaw, J. C. Jaeger, Conduction of Heat in Solids. Oxford Univ. Pr., 1957. Ch 1.

[8] J. Claesson, P. Eskilson, Simulation Model for Thermally Interacting Heat Extraction Boreholes, Department of Mathematical Physics, University of Lund, Box 118, S-221 00 Lund, Sweden, 1987. (Submitted to Journal of Numerical Heat Transfer)

[9] P. Eskilson, Superposition Borehole Model. Manual for Computer Code, Dep. of Mathematical Physics, University of Lund, Box 118, S-221 00 Lund, Sweden, 1986.

[10] J. Claesson, P. Eskilson, Analysis of Pulse Train for a Heat Extraction Borehole, Dep. of Building Technology and Mathematical Physics, University of Lund, Box 118, S-221 00 Lund, Sweden (Notes on Heat Transfer, to be published).

[11] M. Abramowitz, I. Stegun, Handbook of Mathematical Functions, National Bureau of Standards, USA, 1967.

[12] J. Bennet, J. Claesson, G. Hellström, Multipole Method to Compute the Conductive Heat Flows to and between Pipes in a Composite Cylinder, Notes on Heat Transfer 3-1987, Dep. of Building Technology and Mathematical Physics, University of Lund, Box 118, S-221 00 Lund, Sweden, 1987.

[13] J. Claesson, G. Hellström, Thermal Resistances to and between Pipes in a Composite Cylinder, Dep. of Mathematical Physics and Building Physics, University of Lund, Box 118, S-221 00 Lund, Sweden, 1987. (To be published.)

[14] J. Claesson, G. Hellström, The Effect of the Temperature Variation along the Pipes in a Heat Exchanger in the Ground, Dep. of Mathematical Physics and Building Physics, University of Lund, Box 118, S-221 00 Lund, Sweden, 1987. (To be published.)

[15] P.Eskilson, G. Hellström, B. Wånggren, Response Test for a Heat Store with 25 Boreholes, Notes on Heat Transfer 9-1987, Dep. of Building Technology and Mathematical Physics, University of Lund, Box 118, S-221 00 Lund, Sweden, 1987.

CONDUCTIVE HEAT EXTRACTION BY THERMALLY INTERACTING DEEP BOREHOLES

Johan Claesson
Per Eskilson
Department of Building Technology, Lund Institute of Technology
Box 118, S-221 00 Lund, Sweden

June 1987

Acknowledgement: The support by the Swedish Council for Building Research and the National Energy Administration is gratefully acknowledged.

Contents

Abstract 3

Nomenclature 4

1 INTRODUCTION 5

2 THERMAL PROBLEM 6
- 2.1 Thermal process in the ground 6
- 2.2 Thermal process in the boreholes 6
- 2.3 Average borehole temperatures 7

3 ESTIMATES OF THERMAL INFLUENCE 9

4 HEAT EXTRACTION STEP 12

5 DIMENSIONING RULES 13

6 THERMAL INFLUENCE AND RESPONSE FUNCTIONS 15
- 6.1 Two examples with 2 and 16 boreholes 15
- 6.2 Vertical boreholes in a row 16
- 6.3 Parallel rows of boreholes 17
- 6.4 Quadratic borehole pattern 18
- 6.5 Inclined boreholes 18
- 6.6 An optimal configuration 19
- 6.7 Character of g-functions 19
- 6.8 Distribution of extracted heat on the boreholes 20

7 CHOICE OF BOREHOLE CONFIGURATION 23

References 25

Abstract

The ground is a virtually unlimited, always available heat source and sink for heat pumps. Deep boreholes may be used as heat exchanger in the ground. In sequel to a previous study of the single borehole, the paper presents an extensive analysis for thermally interacting extraction/injection boreholes. The thermal influence, which has a very large time-scale, may strongly decrease the heat extraction capacity after 5 years, while being unnoticable during the first year (in, for example, a case with 10 boreholes and 10 m spacing). Formulas to estimate the influence for diffent number, spacing, and depth of the boreholes are given. The long-term extraction characteristics are determined by the mean annual extraction rate only. The solution for the corresponding heat extraction step is reduced to a dimensionless response function, which only depends on time and geometrical parameters for the borehole configuration. Simple dimensioning rules, which relate extraction rates to extraction temperatures, are obtained by superposition of step responses. Based on these fundamental response functions, the long-term thermal performance is analyzed for various borehole configurations (row, parallel rows, quadratic pattern,inclined boreholes etc.). Guide-lines for optimal borehole configuration under geometrical constraints are given.

Nomenclature

a	thermal diffusivity
B	distance between boreholes
c	heat capacity
D_i	depth of thermally insulated upper part of the borehole
g	response function for the heat extraction step, (19)
H	borehole length over which heat extraction takes place
q	heat extraction rate (W/m, borehole average)
Q	total heat extraction rate (W)
r_b	borehole radius
r_i	radial distance to borehole i
R	thermal resistances (K/(W/m))
R_b	thermal resistance between fluid and borehole wall
R_q	thermal resistance due to a heat extraction step
t	time
t_b	borehole steady-state time, (4)
t_s	steady-state extraction time, (20)
T	temperature in the ground
T_b	temperature at the borehole wall
T_f	temperature of heat carrier fluid
T_{om}	effective undisturbed ground temperature
V_f	pumping rate (m^3/s)
z	depth from the ground surface
z_i	axial coordinate along borehole i

Greek symbols

θ	borehole inclination
λ	thermal conductivity
ρ	density

Subscripts

b	borehole wall
f	fluid
i	borehole i
p	periodic
q	heat extraction step

1 INTRODUCTION

The ground may be used as heat source or sink to heat pumps. Heat is extracted from the ground in the heating mode and injected in the cooling mode. The ground heat exchanger may consist of a single borehole or a configuration of multiple boreholes. Thermal analyses and dimensioning rules for a single borehole are reported in [1]. This subsequent paper deals with the case of multiple boreholes, which influence each other thermally.

A single borehole with a depth of 80 to 150 m is sufficient for the heating demand of a Swedish one-family house. The question of thermal influence arises, when there are many, closely-spaced boreholes. This situation occurs for neighboring houses, each using a borehole, or when a large heat pump uses many boreholes as heat exchanger in the ground. Figure 1 shows a case with 8 inclined boreholes that lie in a row at the ground surface. Figure 3 in Section 6.1 concerns two boreholes, and Figure 4 sixteen boreholes in a quadratic pattern. For a system with many boreholes, it is often necessary or advantageous to let the boreholes lie close to each other at the ground surface. They are inclined outwards away from each other in order to diminish the thermal influence.

A rather common system in Sweden is to use 10 to 25 boreholes, each with a length of around 80 m, which are drilled in diverging directions from each other. The heat pump is placed close to the borehole area, often in the basement of the building.

The thermal processes inside and in the immediate vicinity of each borehole are essentially the same as for the single borehole in [1,4,2,3]. The analyses of the processes in and along the borehole in [2] and [3] are also valid for multiple boreholes. The results in [1] and [4] have to be modified due to the thermal influence. This paper deals with these modifications and with new questions and problems related to different borehole configurations. The thermal influence depends on the number, spacings, and configurations of the boreholes. An important task is to determine the optimum configuration under given restraints, for example on spacings at the ground surface and on borehole inclination. The dimensioning rules of [1] relate the lowest extraction or highest injection temperatures to heat extraction or injection rates. The modified rules for multiple boreholes, which are presented here, have been implemented on a personal computer, [5].

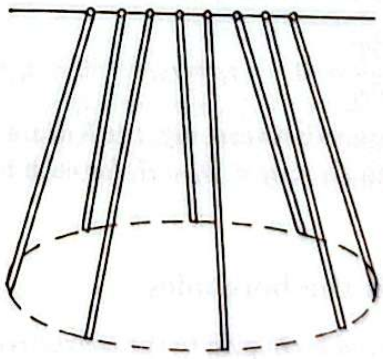

Figure 1: Eight inclined boreholes that lie in a row at the ground surface.

2 THERMAL PROBLEM

The discussion of the thermal problem with its simplifications and defining equations follows closely the previous paper [1] concerning a single borehole.

2.1 Thermal process in the ground

The temperature $T(x, y, z, t)$ in the ground outside the boreholes satisfies the heat condition equation:

$$\frac{1}{a} \cdot \frac{\partial T}{\partial t} = \frac{\partial^2 T}{\partial x^2} + \frac{\partial^2 T}{\partial y^2} + \frac{\partial^2 T}{\partial z^2} \tag{1}$$

This form of the equation presupposes that the ground is homogeneous. However, the ground is often stratified. Let in such a case λ denote the average thermal conductivity over the length of the boreholes. The error, when (1) is used with this λ (and a corresponding average heat capacity ρc), is quite small in the present applications, [1]. Eq. (1) is valid as an acceptable simplification for the stratified ground.

The climatic variations during the day and the year, including for example the effect of snow and freezing, influence only the upper few meters of the ground. It is quite sufficient in the present applications to use a constant temperature as boundary condition at the ground surface.

The undisturbed ground temperature increases with up to a few degrees from the ground surface down to the bottom of the boreholes due to the geothermal gradient. Let T_{om} denote the average undisturbed ground temperature. Experimentally, it is determined by circulation of the heat carrier fluid without heat extraction or injection. The fluid assumes after a short transient period a steady value T_{om}. The temperature T_{om} is normally with good accuracy equal to the ground temperature at the mid-depth of the borehole. It is to be used as initial ground temperature as well as boundary temperature at the ground surface. See ref. [4]:

$$T\,|_{t=0} = T_{om} \qquad T\,|_{z=0} = T_{om} \tag{2}$$

Local cylindrical coordinates are needed in the formulation of the boundary conditions at the boreholes. Let r_i and z_i be the radial and axial coordinates of borehole i. The uppermost part of the boreholes is treated as thermally insulated:

$$\frac{\partial T}{\partial r_i} = 0 \qquad r_i = r_b, \qquad 0 < z_i < D_i \tag{3}$$

The exact values of D_i for variations between, say, 1 to 5 m are not important, [1]. The conditions along the heat extraction length $D_i < z_i < D_i + H_i$ for each borehole i are discussed in the next section.

2.2 Thermal process in the boreholes

The thermal process in the ground is coupled to the convective-diffusive process in the boreholes with its heat carrier fluid, which flows down and up in channels along the borehole. The time-scales of the various local processes in the borehole are discussed in [1]. The following basic time-scale for the borehole processes is introduced:

$$t_b = \frac{5 r_b^2}{a} \tag{4}$$

We do not consider variations of the heat extraction rate on a time-scale below this limit, which is of the order of 2 hours (in Swedish applications). Transient effects associated with

the time for the fluid to circulate in the borehole are then negligible. The transient effect due to the heat capacities within the borehole may also be neglected. The thermal problem in the borehole becomes a steady-state one, which is coupled to the transient process in the ground. The convective-diffusive boundary conditions along the boreholes are detailed in [6].

To complete the thermal problem, we must specify loading conditions, which involve the inlet and outlet temperatures of the heat carrier fluid for each borehole. The fluid can flow in parallel or series in different ways between the boreholes. The hydraulic coupling and pumping rates are given. The inlet temperature to the first boreholes coupled in parallel may be a given function of time. The mixed outlet fluid temperature becomes the inlet temperature to the next group of boreholes coupled in parallel, and so on.

The heat extraction rate of borehole i is denoted $Q_i(t)$ (W):

$$Q_i(t) = \int_{D_i}^{H_i+D_i} dz_i \int_0^{2\pi} r_b d\phi_i \cdot \lambda \frac{\partial T}{\partial r_i}(r_b, \phi_i, z_i, t) dz_i \tag{5}$$

Here ϕ_i is the angle around borehole i, and T is expressed in local cylindrical coordinates. The function $Q_i(t)$ is positive for extraction, and it is negative, when heat is injected to the ground. We will in the following mostly refer to heat extraction, but all results and analyses are equally applicable to heat injection or any mixture of injection and extraction.

The extraction rates Q_i and their sum over all boreholes, $Q(t)$, are obtained as the main result from the solution. An alternative, important loading condition is to give the total heat extraction rate $Q(t)$. The inlet temperature to the first boreholes must then be chosen so that the given extraction rate is obtained.

The complete thermal problem is defined by (1-3), , the convective-diffusive equations along the boreholes, the hydraulic coupling and pumping rates, and the loading conditions. An elaborate numerical model for this problem for arbitrary borehole configurations is presented in [6]. Reference [7] is a manual for the computer model, which has been used extensively for this paper. The main idea in the model is to use one axi-symmetric solution for each borehole or symmetry group of boreholes. The total temperature field with its complex geometry is obtained by superposition of all (r_i, z_i)-solutions for all boreholes.

2.3 Average borehole temperatures

Numerical studies with the model [6,7] have shown, [8], that the thermal process from the wall of boreholes and outwards in the ground may be separated from the process inside the boreholes by considering average borehole temperatures. Let $T_b(t)$ denote the average temperature over the surface of all borehole walls, and $T_f(t)$ an average heat carrier temperature. The average heat extraction rate $q(t)$ (W/m) is equal to $Q(t)$ divided by the total borehole length. As an approximate boundary condition, the temperature at the walls of all boreholes is taken to be equal to the average $T_b(t)$:

$$T|_{r_i=r_b, z_i, t} = T_b(t) \qquad D_i < z_i < D_i + H_i \tag{6}$$

This means that a single temperature is used along the active heat extraction length of all boreholes. We start, as in the analyses in [1], with a given extraction rate and obtain the extraction temperatures $T_b(t)$ from the solution. The thermal problem in the ground is then defined by (1-3) and (6), and by the given extraction rate $Q(t)$ to the boreholes.

The discussion in [1] of the thermal process in the borehole is applicable here for each borehole. The basic equation relates the temperature drop between borehole wall and heat carrier fluid to the heat extraction rate. Here, this equation is used with the average values:

$$T_b - T_f = q \cdot R_b \tag{7}$$

The borehole thermal resistance R_b (K/(W/m)) is one of the basic parameters of the heat extraction boreholes. It should be measured in field and laboratory experiments. It is important to design the heat exchanger in the borehole so that R_b becomes as small as possible.

The borehole resistance R_b is obtained from the two-dimensional, steady-state, conductive heat flow problem between the pipes in the borehole and a circle in the ground outside the borehole, provided that there is no free water with significant natural convection in the borehole outside the pipes. An analytical solution of this case is given in [9]. The solution has been implemented on a personal computer. It is used extensively in [2], in which the borehole resistance is given and discussed for many cases of practical importance. Swedish field experiences indicate values around $R_b = 0.1$ K/(W/m) for a typical case with a plastic U-tube in a borehole.

The inlet and outlet temperatures are, in the approximation using average values,[3], given by:

$$T_{f,in} = T_f - \frac{Q(t)}{2c_f\rho_f V_f} \tag{8}$$

$$T_{f,out} = T_f + \frac{Q(t)}{2c_f\rho_f V_f} \tag{9}$$

The fluid temperature T_f becomes the mean value of the inlet and outlet fluid temperatures. The thermal resistance R_b in (7) for the two-dimensional problem perpendicular to the borehole is to be corrected by a factor that depends on the pumping rate V_f, [3]. However, the correction factor may be neglected in most applications, [1,3].

The thermal problem inside the borehole is described by the simplified equations (7-9) based on average borehole temperatures. In typical cases with all boreholes coupled in parallel, the error for extraction temperature became much less than 0.1°C, when compared to the more exact numerical solution with the model [6]. The error is larger, if the boreholes are coupled in series and there is a large temperature variation along the boreholes. The numerical model [7] should be used in those cases to check the validity of the simplified equations, which, however, have been sufficient in all the applications that we have encountered.

3 ESTIMATES OF THERMAL INFLUENCE

The detailed thermal influences between the boreholes are obtained from numerical solutions with the model [6]. However, it is of great value to have simplified estimates of the influence. We will present a few rules of thumb, which are based on analytical solutions for a line sink.

The boreholes act as line sinks and sources with a strength, $q_l(z_l,t)$, that varies along the borehole axes and with time. Let q_o (W/m) be a representative mean value of the strength of these variable line sinks. A suitable choice is to use the total extracted (or injected) heat $E(t)$ to the considered time t and take $q_o = E(t)/(t \cdot \sum H_l)$. The temperature field due to a single line sink with the strength q_o for $t > 0$ and with infinite axial extension is, [10]:

$$\Delta T = -\frac{q_o}{4\pi\lambda} E_1(\frac{r^2}{4at}) \qquad t > 0 \tag{10}$$

Here $E_1(s)$ is the exponential integral, [11]. The total temperature field is obtained as a sum of terms of the type (10). Consider in particular a borehole with N_{adj} adjacent boreholes, all at approximately the same distance B. The influence of boreholes further away is smaller and not accounted for. An estimate of the thermal influence from the surrounding boreholes is:

$$\Delta T \simeq -\frac{q_o}{2\pi\lambda} \cdot \frac{1}{2} N_{adj} \cdot E_1(\frac{B^2}{4at}) \qquad t > 0 \tag{11}$$

The reference example (26) shows that the first factor $q_o/(2\pi\lambda)$ is of the order of 1°C. A reasonable criterion for *insignificant thermal influence* is to require that the second, dimensionless factor is less than 0.1:

$$\frac{1}{2} N_{adj} \cdot E_1(\frac{B^2}{4at}) < 0.1 \tag{12}$$

The influence between the boreholes is, on the other hand, significant, if the second factor exceeds, say, 1, since the temperature drop at the boreholes is shown below to be of the order $10 \cdot q_o/(2\pi\lambda)$ (according to (18,19) and Figures 5A-J showing the g-functions). This gives the following criterion for *significant thermal influence*:

$$\frac{1}{2} N_{adj} \cdot E_1(\frac{B^2}{4at}) > 1 \tag{13}$$

Boreholes further away will increase the thermal influence so that it appears somewhat before the time given by criterion (13).

Let us consider the case $N_{adj} = 1$. From [11] we get $E_1(1) \simeq 0.2$ and $E_1(1/12) \simeq 2$. The criterion for insignificant influence of another borehole at the distance B is therefore $B^2/(4at) > 1$, or $t < (1/4) \cdot B^2/a$, while the criterion for significant influence is $B^2/(4at) < 1/12$, or $t > 3 \cdot B^2/a$. Table 1 gives the criteria (12) and (13) for a few values of N_{adj}.

N_{adj}	1	2	4	8
Insign. infl.	$t' < 1/4$	$t' < 1/6$	$t' < 1/8$	$t' < 1/10$
Sign. infl.	$t' > 3$	$t' > 1$	$t' > 1/2$	$t' > 1/4$

Table 1. The criteria (12) and (13) to assess the thermal influence, $t' = t/(B^2/a)$.

The worst case $N_{adj} = 8$ may be used for an interior borehole in a large system with boreholes in a quadratic pattern. The criteria of Table 1 involve the time-scale B^2/a $(= t/t')$. Table 2 gives a few values, which show the strong dependence on the spacing B.

B (m)	2	5	25
B^2/a	1 month	1/2 year	12 years

Table 2. Time-scale for thermal influence between boreholes, $a = 1.62 \cdot 10^{-6}$ m^2/s.

The criteria above concern the average heat extraction or injection rate. There is a superimposed variation during the annual cycle (or the cycle with any other period time). This periodic component is analysed by considering a pure sinusoidal extraction/injection: $q(t) = q_p \cdot \sin(2\pi t/t_p)$. The analytical solution for a single periodic line sink, which involves Kelvin functions, is given in [10]. The amplitude of the periodic temperature decreases with the distance r out in the ground. Figure 2 shows the ratio χ between the amplitude at the radius r and at the borehole $r = r_b$ for $r_b = 0.055$ m, $a = 0.62 \cdot 10^{-6}$ m^2/s and the period time 1 day, 1 month and 1 year. The range of the daily variations are always smaller than 1 meter, while the annual variation is quite small outside $r = 5$ m. From the attenuation of the amplitude, the following criterion for completely negligible influence of the periodic component is obtained, [8]:

$$B > 2\sqrt{at_p} \tag{14}$$

Here B is the smallest distance between two boreholes. This condition becomes $B > 0.75$ m, 4 m and 14 m for $t_p = 1$ day, 1 month and 1 year, respectively (for $a = 1.62 \cdot 10^{-6}$ m^2/s).

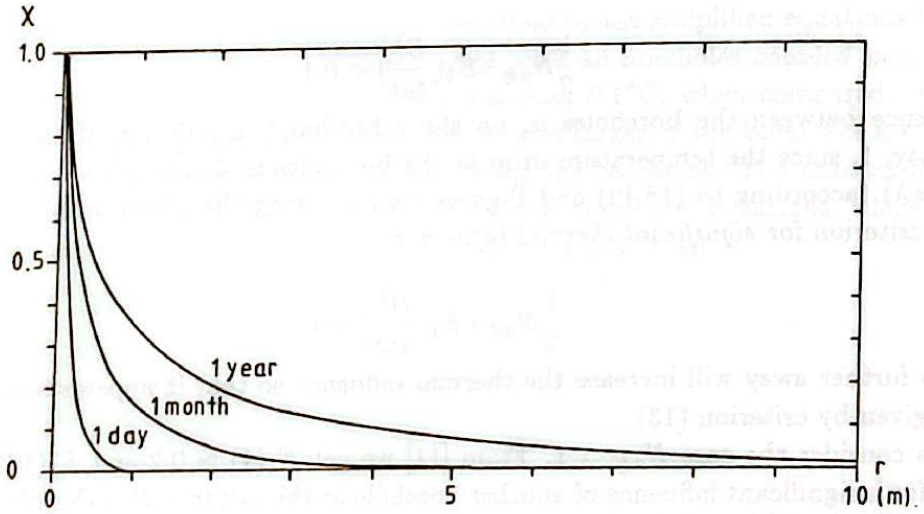

Figure 2:Relative temperature amplitude for a sinusoidal extraction/injection ($r_b = 0.055$ m, $a = 1.62 \cdot 10^{-6}$ m^2/s) for different period times t_p.

The criterion (14) is well on the safe side. The influence from surrounding boreholes, compared to the amplitude at the borehole from its own periodic extraction/injection, is less than 10%, if the following criterion is met:

$$B > 0.7\sqrt{at_p} \tag{15}$$

This criterion is based on analytical studies for an infinite number of boreholes in a quadratic pattern. This problem is approximated by a periodic line sink in a circular region with zero heat flux through the outer boundary circle, [8]. Criterion (15) is obtained by considering the amplitudes of this solution. Eq. (15) is recommended to be used instead of the stronger (14). Table 3 gives this lower limit for different period times.

t_p	1 day	1 month	1 year
$0.7\sqrt{at_p}$	0.26 m	1.4 m	5 m

Table 3. Influence range for a periodical variation, (15), $a = 1.62 \cdot 10^{-6}$ m^2/s.

It should be kept in mind that the periodic (sinusoidal) component is balanced, having equal amounts of injected and extracted heat. This results in a limited influence range, while the influence of the average component increases steadily with time according to (12,13), until three-dimensional steady-state conditions are approached. The criteria (12, 13) for the average component are based on a two-dimensional solution. They are not valid, if three-dimensional effects dominate, before the thermal influence criteria are met. The long-term influence is discussed in the next section. It is obtained from the g-functions, which are introduced in the next section. Let us only note that the thermal influence between the boreholes always is negligible, if the smallest distance B between the boreholes is larger than H. Furthermore, the influence is always small for $B > H/2$. We have the criteria:

$$\begin{aligned} &\text{Negligible influence for} && B > H \\ &\text{Small influence for} && H > B > H/2 \end{aligned} \qquad (16)$$

4 HEAT EXTRACTION STEP

The heat extraction $Q(t)$ or $q(t)$ is a given function of time. The solution for any $q(t)$ may be obtained from the solution for the heat extraction step by superposition, [1]. The basic heat extraction step is expressed with Heavyside's step function He:

$$q(t) = q_o \cdot He(t) \qquad He(t) = \begin{cases} 1 & t > 0 \\ 0 & t < 0 \end{cases} \tag{17}$$

The thermal problem is defined by (1-3), the condition (6) of a single temperature $T_b(t)$ along the borehole walls, and by the extraction step (17).

Our main interest is the borehole temperature $T_b(t)$. A straight-forward dimensional analysis shows that it may be written in the following way:

$$T_b(t) = T_{om} - q_o \cdot R_q \tag{18}$$

Here R_q (K/(W/m)), which as in [1] may be regarded as a time-dependent thermal resistance for a unit heat extraction step, is written in the following way:

$$R_q = \frac{1}{2\pi\lambda} \cdot g(t/t_s, ...) \tag{19}$$

The dimensionless step-response function g depends on the dimensionless time t/t_s with the steady-state time-scale t_s defined in [1]:

$$t_s = \frac{H^2}{9a} \tag{20}$$

Here, H denotes the borehole length or, if they differ, one of these. The g-function also depends on r_b/H, D_i/H, and on the parameters that determine the lengths H_i/H, positions x_i/H, y_i/H at the ground surface,and direction angles θ_i (inclination), φ_i (angle of rotation) of the boreholes. The dependence on D_i/H is, as in [1], negligible in the present applications. Thus, the arguments of the g-functions are :

$$t/t_s, r_b/H, ..., H_i/H, x_i/H, y_i/H, ..., \theta_i, \varphi_i, ... \tag{21}$$

The g-functions do not depend on the parameters for the heat exchanger in the boreholes. The dependence on borehole radius is simple, [1]:

$$g(t/t_s, r_b^*/H, ...) = g(t/t_s, r_b/H, ...) - ln(r_b^*/r_b) \tag{22}$$

The g-functions are in the following given for $2r_b/H = 0.001$.

The g-functions are computed with the model [6,7]. References [12,13] give the g-functions as a function of time for 226 borehole configurations. A few of these curves are shown in Figures 5A-J. Figure 5A concerns two vertical boreholes with the spacing B. There is one curve for each dimensionless spacing B/H. The dashed curve, $B = \infty$, is the g-function for a single borehole. The difference between the curves for g and the dashed curve shows the thermal influence between the boreholes. Numerically, the g-functions gives the temperature drop $T_{om} - T_b$ in °C for the extraction $q_o = 2\pi\lambda$, (18,19).

5 DIMENSIONING RULES

The dimensioning rules proposed here are the same as those for a single borehole, [1], except for necessary modifications. There is a given or prescribed heat extraction rate $Q(t) = q(t) \cdot \sum H_i$ (W) and a given lowest value $T_{f,min}$ for the temperature $T_f(t)$ of the heat carrier fluid. The dimensioning formulas give the lowest extraction temperature for any set of tentative input data. The depth of the boreholes or some other input variables are adjusted, until the prescribed $T_{f,min}$ is obtained.

The cooling mode, when heat is injected to the ground, may be the critical one in the dimensioning. Then there is a prescribed highest injection temperature $T_{f,max}$. The formulas are directly applicable by using negative values for $q(t)$.

The first dimensioning rule in [1] is based on a simplified heat extraction $q(t)$ with a constant component q_o (from the start $t = 0$) and a periodic component. There is also a superimposed heat extraction pulse with the strength q_1 and the length t_1. This pulse occurs at the time of largest periodic extraction. The formula for $T_{f,min}$ in [1] is valid, except for the constant component q_o. The steady-state resistance (R_s in (37-38) in [1]) must be replaced by the step extraction resistance $R_q(t)$. We have in accordance with (37) in [1]:

$$T_{f,min} = T_{om} - q_o \cdot R_q(t_{dim}) - q_p \cdot R_p - q_1 \cdot R'_q(t_1) - (q_o + q_p + q_1) \cdot R_b \qquad (23)$$

The periodic resistance R_p and the pulse resistance $R'_q(t)$ are given in [1]. (The three-dimensional $R_q(t_1)$ may of course be used instead of the simpler $R'_q(t_1)$, which refers to a line sink.) It is assumed that the influence between the boreholes due to the periodic component is negligible. This means that criterion (15) is satisfied with B being the smallest distance between the boreholes. In the case, when inclined boreholes lie close to each other at the ground surface, we assume that (15) is valid for at least, say, 80% of the borehole length. The time t_{dim} is given by:

$$t_{dim} = (N_{dim} - 1)t_p + t_{q,max} \simeq N_{dim} \cdot t_p \qquad (24)$$

Here the dimensioning concerns year (or period) N_{dim}, and it is assumed that the largest extraction occurs at the time $t_{q,max}$ during each period. Normally, N_{dim} lies between 5 and 25. Then it does not matter much, when $t_{q,max}$ occurs during the period, and we can simply use $t_{dim} \simeq N_{dim} \cdot t_p$.

The terms of (23) show in a very lucid way the physical character of the extraction process. The last term involving the borehole resistance R_b is determined by the design of the heat exchanger in the borehole. The periodic component, $q_p \cdot R_p$, and the extraction pulse, $q_1 \cdot R'_q(t_1)$, are the same as for the single borehole. The numerical examples in [1] are valid. These last three terms are not discussed again in this paper.

The thermal influence is determined by the constant or average component only. The magnitude of this term, $q_o \cdot g/(2\pi\lambda)$, may be modified by changing q_o or g. The extraction rates are prescribed in a given case, but the average q_o may be diminished by recharge (normally during the summer). The value of q_o becomes zero for a balanced case with the same amounts of extracted and injected heat during each cycle. The other way to influence the term $q_o \cdot R_q(t_{dim})$ is to change the g-function. The values of g decrease, when the boreholes are moved away from each other. The borehole positions at the ground surface may be fixed, while the boreholes are drilled in inclined direction away from each other. The variation of the response functions with borehole configuration is discussed in the next section.

The second dimensioning rule in [1] uses any sequence of stepwise constant values: $q(t) = q_n$, $t_n < t \leq t_{n+1}$, $n = 1, ..., N_{max}$. Formula (44) in [1] is applicable:

$$T_{f,min} = \min_{1 \le N \le N_{max}} \left\{ T_{om} - q_N \cdot R_b - \sum_{n=1}^{N} (q_n - q_{n-1}) \cdot R_q(t_{N+1} - t_n) \right\} \qquad (q_o = 0) \qquad (25)$$

Here $R_q(t)$ is the thermal resistance for the considered borehole configuration, for which the g-function has to be computed numerically.

The dimensioning rules (23) and (25) have been implemented for use on a personal computer (IBM-PC and compatible computers, MS-DOS). These interactive models, [5], are rapid and quite easy to use. Another PC-model calculates iteratively from (25) the required borehole length for a given lowest extraction temperature (or a given highest temperature in the case of dimensioning for heat injection to the ground). All the g-function of [12,13] are stored with 20 about values each.

6 THERMAL INFLUENCE AND RESPONSE FUNCTIONS

The thermal influence between boreholes has a pronounced long-term character. It is negligible during the first year, if the distance between boreholes exceeds 10 meters. The variations during the year are strongly attenuated at this distance. Only the mean extraction rate during the year is of importance for the influence. The dimensionless response functions g contain a complete information about the thermal influence. The following discussion of the thermal influence for different borehole configurations is based on these functions.

The g-functions are given over 200 borehole configurations in [12] and [13]. A few of these curves are shown in Figures 5A-J.

In the examples below we use, as in [1], the following typical Swedish data:

$$\begin{array}{lll} H = 110\,\text{m} & D = 5\,\text{m} & 2r_b = 0.11\,\text{m} \\ \lambda = 3.5\,\text{W/(mK)} & a = 1.62 \cdot 10^{-6}\,\text{m}^2/\text{s} & T_{om} = 8°\text{C} \\ q_o = 22\ \text{W/m} & R_b = 0.1\,\text{K/(W/m)} & \end{array} \tag{26}$$

This gives:

$$\begin{array}{ll} 2r_b/H = 0.001 & q_o/(2\pi\lambda) = 1.0°\text{C} \\ t_b = 2.6\,\text{hours} & t_s = 26\,\text{years} \end{array} \tag{27}$$

6.1 Two examples with 2 and 16 boreholes

Figures 3 and 4 show, for example (26), temperature fields computed with the model [6]. Figure 3 concerns two vertical boreholes with the spacing $B = 5.5$ m. The temperature along a horizontal line at the depth $z = 60$ m through the two boreholes are shown after 5 and 25 years. Note the steep gradients near the boreholes. The corresponding response function is given by the curve $B/H = 0.05$ in Figure 5A. The borehole temperature T_b is, Figure 5A and (18), 8 - 7.2 = 0.8°C after 5 years and -0.2°C after 25 years. The corresponding temperatures for a single borehole (dashed curve) are 8 - 5.8 = 2.2°C and 1.7°C, respectively.

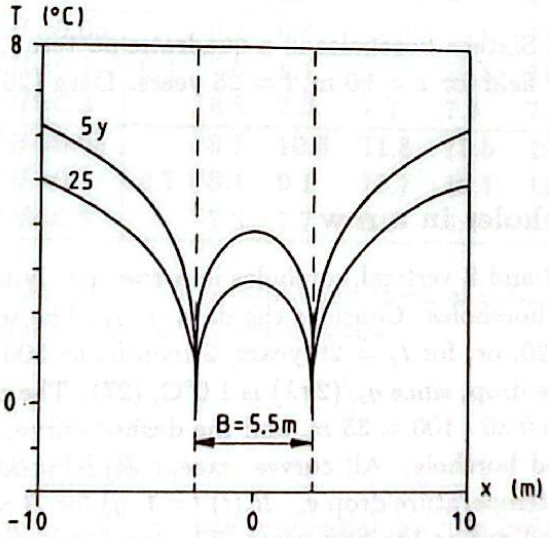

Figure 3: Two boreholes. Temperature profile at $z = 60$ m along a line through the boreholes. Data (26).

Figure 4 shows the temperature field for 16 boreholes in a quadratic pattern, 4 x 4, for z = 60 m and t = 25 years. The spacing B between the boreholes is 11 m. The thermal influence is quite strong with a colder inner region. The g-function for this case is shown by the curve B/H = 0.1 in Figure 5E. We get $g \simeq 23$ for $t/t_s = 25/26$, and hence $T_b = 8 - 1{\cdot}23 = -15°C$. The corresponding extraction temperature for the single borehole is 1.7°C. Such a large thermal influence should be unacceptable. The boreholes have to be separated more from each other, or the ground has to be recharged during each cycle.

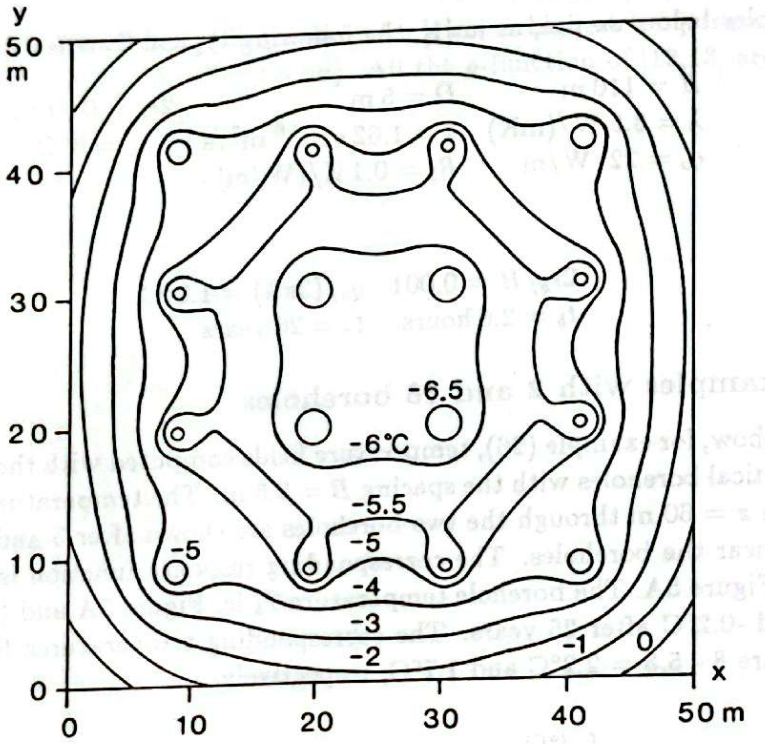

Figure 4: Sixteen boreholes in a quadratic pattern. Temperature field for z = 60 m, t = 25 years. Data (26).

6.2 Vertical boreholes in a row

Figures 5A-B concern 2 and 8 vertical boreholes in a row, i.e. lying on a straight line with the spacing B between the boreholes. Consider the data (26). The temporal range is $t/t_s = e^{-4.5}$ = 0.01 to $t/t_s = e^3 = 20$, or, for t_s = 26 years, 3 months to 500 years. The g-functions give directly the temperature drop, since $q_o/(2\pi\lambda)$ is 1.0°C, (27). The curves cover spacings from B = 0.05 · 110 = 5.5 m to 0.30 · 100 = 33 m, and the dashed curve, $B = \infty$, gives the g-function for a single, undisturbed borehole. All curves, except B/H = 0.05, coincide for the shortest time. Table 4 gives the temperature drop $q_o \cdot R_q(t)$ $(= 1 \cdot g)$ for B = 16.5 m $(B/H = 0.15)$. The thermal influence is small during the first years. The large time-scale for the thermal influence is noteworthy.

		3 months	1y	5y	25y	500y
$N_b =$	1	4.6	5.2	5.9	6.4	6.7
	2	4.6	5.3	6.3	7.3	7.8
	8	4.6	5.3	6.8	8.9	10.5

Table 4. Temperature drop $q_o \cdot R_q(t)$ $(= 1 \cdot g)$ (°C) for 1, 2 and 8 vertical boreholes, Figures 5A-B. Data (26), $B = 16.5$ m.

The temperature drops ΔT refer to the extraction rate q_o. The extraction capacity, defined as the obtained extraction rate for a unit temperature drop, becomes $q_o/\Delta T$ (W/mK). For example, Table 4 shows that the decrease of extraction capacity after 25 years for the eight boreholes compared to single boreholes is 100·(1-6.4/8.9) = 28%. Note, that we discuss only the temperature drop due to the average extraction rate. There is an added drop due to variations of the extraction rate. The decrease of extraction capacity referred to the total temperature drop will therefore give a lower value than the ones given here.

The small spacing $B = 5.5$ m $(B/H = 0.05)$ gives much larger thermal influence. For $t =$ 25 years we have, Figures 5A-B, $g = 8.2$ for $N_b = 2$ and $g = 13.5$ for $N_b = 8$, while the single borehole has $g = 6.4$. The extraction capacity of the eight boreholes decreases with 40% from the first to the twenty-fifth year.

The g-functions for vertical boreholes lying in a row are given for several N_b in [12,13]. The curves for $N_b = 4$ lie half-way between the curves for $N_b = 2$ and $N_b = 8$. Table 5 gives g-values for different times, spacings and number of boreholes.

	N_b	1	2	3	4	8	16	∞
$t = t_s/20$	B/H=0.05	5.3	6.1	6.6	6.8	7.2	7.5	7.7
	B/H=0.1		5.6	5.8	5.8	5.9	5.9	5.9
	B/H=0.3		5.3	5.3	5.3	5.3	5.3	5.3
$t = t_s$	B/H=0.05	6.4	8.2	9.6	10.8	13.6	16.1	19.7
	B/H=0.1		7.6	8.4	9.1	10.3	11.1	12.1
	B/H=0.3		6.8	7.0	7.2	7.3	7.4	7.5
$t = 20t_s$	B/H=0.05	6.7	8.7	10.3	11.8	15.5	19.3	27.4
	B/H=0.1		8.1	9.1	10.1	12.1	13.8	16.5
	B/H=0.3		7.3	7.7	8.0	8.5	8.8	9.2

Table 5. Comparison of g-values and thermal influence for vertical boreholes in a row.

6.3 Parallel rows of boreholes

Parallel rows of vertical boreholes may occur in residential districts, with one borehole for each one-family house. We will consider the case, when the spacing between the boreholes is B along and between the rows. The g-functions for a number of cases with parallel rows are given in [12,13]. Figure 5C concerns two rows with 8 boreholes each, while Figure 5B shows the corresponding curves for a single row. Note the different scales. There is a considerable increase of the g-functions, i.e. the thermal influence, when the second row is added. For example, the g-function increases from 10.3 to 14.4 for $t = t_s$, $B/H = 0.1$. One, two and four rows are compared

in Table 6. The thermal influence is small in the beginning, $t = t_s/20$, and considerable at $t = t_s$. Again, the large time-scale of the thermal influence is illustrated.

	N_b	8 x 1	8 x 2	8 x 4
$t = t_s/20$	B/H=0.05	7.2	9.5	-
	B/H=0.1	5.9	6.5	6.7
	B/H=0.3	5.3	5.3	5.3
$t = t_s$	B/H=0.05	13.6	21.0	-
	B/H=0.1	10.3	14.4	19.9
	B/H=0.3	7.3	8.2	8.9
$t = 20t_s$	B/H=0.05	15.5	24.1	-
	B/H=0.1	12.1	17.2	25.4
	B/H=0.3	8.5	10.2	12.4

Table 6. Comparison of g-functions for 1, 2 and 4 rows with 8 boreholes each.

6.4 Quadratic borehole pattern

Figures 5D-F show g-functions for a quadratic pattern of vertical boreholes. The spacing between the boreholes is B. Figures 5D,E and F concern 2 x 2 = 4, 4 x 4 = 16 and 10 x 10 = 100 boreholes, respectively. Note the different scales for the g-axis. The values of g increase strongly with the number of boreholes. The thermal influence is so strong for 100 boreholes that the case B/H = 0.05 is omitted. Table 7 gives a few values for comparison.

	N_b	2 x 2	4 x 4	10 x 10
$t = t_s/20$	B/H=0.1	6.1	6.6	6.9
	B/H=0.3	5.3	5.3	5.3
$t = t_s$	B/H=0.1	9.7	16.0	27.6
	B/H=0.3	7.4	8.6	9.5
$t = 20t_s$	B/H=0.1	10.6	18.9	38.9
	B/H=0.3	8.3	10.9	15.0

Table 7. Comparison of g-functions for 4, 16 and 100 boreholes in a quadratic pattern.

The curve $B/H = 1$ in Figure 5F shows that the thermal influence is negligible in this case even for a large system with 100 boreholes. This result and many similar ones are the basis for the criterion (16), which states that the influence is negligible for $B > H$.

6.5 Inclined boreholes

The thermal influence may be decreased considerably by deviating or inclining the boreholes away from each other. It is then possible to let the boreholes lie close to each other at the ground surface. Figures 5G-H show g-functions for 8 boreholes that lie on a circle with the radius B at the ground surface. The boreholes are inclined outwards in the circle's radial direction as shown in Figure 5G.

The curve $\theta = 0°$, i.e. vertical boreholes, in Figure 5G may be compared to the curves of Figure 5B for vertical boreholes in a row. The spacing between the boreholes in the circle of Figure 5G is $2\pi B/8 = 0.08H$. The curve for $B = 0.08H$ in Figure 5B lies around 10% below the curve 0° in Figure 5G, so there is a gain of 10% (for the long-term component, spacing $B = 0.08H$) by locating the boreholes in a row instead of a circle.

The curves of Figure 5G, concerning the larger radius $B/H = 0.1$, show that there is a considerable gain by inclining the boreholes 10°. The gain for an increase of the inclination from 20° to 30° is rather small. The initial increase of distances between the boreholes has the largest effect. The boreholes lie very close to each other at the ground surface in the case $B/H = 0.01$, Figure 5H. The curve $\theta = 0°$ is not shown. The gain, when the angle is increased from 10° to 20°, is around 20%, and another 10% is gained from 20° to 30°.

The curve $\theta = 20°$ in Figure 5H and the curve for $B/H = 0.1$ in Figure 5B lie rather close to each other. Thus, eight boreholes lying on a very small circle and with the inclination $\theta =$ 20° radially outwards experience the same thermal influence, as when the boreholes are vertical and lie in a row with the spacing $B = 0.1H$. It may be noted that the distance between the inclined boreholes at mid-depth becomes $0.14H$.

6.6 An optimal configuration

The choice of borehole configuration and the exact position of the boreholes determine the thermal influence and the heat extraction capacity. The question of optimal borehole configurations is discussed in Section 7. The problem is to determine the optimal configuration, when there are certain given constraints on the positions of the boreholes. We will here consider a particular example. The positions of the boreholes are fixed at the ground surface. They lie in a row with the spacing B. The corresponding response function for vertical boreholes is shown in Figure 5B for different spacings.

The direction of the boreholes is to be varied. Figure 5I gives the g-function for the fan-shaped configuration shown by the small drawing in the figure. All boreholes lie in the same vertical plane. The two boreholes in the middle are vertical, while the following pairs are inclined outwards 10°, 20° and 30°, respectively. Figures 5I and 5B show that this results in a considerable decrease of the g-functions, in particular for small B/H.

The thermal influence may of course be decreased further, if the boreholes are inclined away from each other in the direction perpendicular to the vertical plane of the fan configuration. The angle of inclination is limited by the capability of the drilling machine. We suppose in this example that the maximum angle of inclination is $\theta = 20°$. The bottom tip of a borehole must lie within a circle with the radius $H \cdot \sin(20°)$ around the fixed position at the ground surface. The tips of the eight boreholes must lie within an oval-shaped area. It is intuitively reasonable that the optimum configuration is obtained, when the tips lie on the periphery of this area with an equal spacing between the boreholes. This optimal configuration under the given restraints is shown by the small drawing in Figure 5J.

A comparison between the g-functions of 5B, I and J shows that the gain is considerable. For example, we have for $t = t_s$:

B/H=0.05	g=13.6	(vertical)	B/H=0.1	g=10.3	(vertical)
	g=9.6	(fan-shape)		g=8.4	(fan-shape)
	g=8.9	(optimum)		g=8.0	(optimum)

6.7 Character of g-functions

All g-functions have a similar shape as shown in Figures 5A-J. The curves have an inflection point roughly at $t = t_s$. This steady-state time $t_s = H^2/(9a)$ becomes in case (26) with its

rather deep borehole (H = 110 m) 26 years. A short borehole with H = 20 m gives the much smaller value $t_s \simeq 1$ year. The time-scale of the response functions is strongly dependent on H.

The curves in Figures 5A-J show that the steady-state condition is obtained approximately after the time $10t_s$ for a system with a few boreholes, and after $20t_s$ for a system with around 10 boreholes. Larger systems require an even longer time than $20t_s$ to attain steady-state conditions.

The g-functions and the thermal influence increase strongly with the number of boreholes, except when the boreholes lie far away from each other. Boreholes at a distance $B > H$ may be considered as independent of each other, while the influence always is small for $H > B > H/2$, (16).

6.8 Distribution of extracted heat on the boreholes

The total amount of heat from all boreholes is prescribed in the basic formulation of our problem. The distribution of this heat on the different boreholes depends on the borehole configuration. It is obtained in numerical calculations with the model [6,7].

We consider as an example 4 x 4 = 16 boreholes in a quadratic pattern of the type shown in Figure 4 and by the small drawing in Figure 5E. There are three groups of boreholes with different extraction rates: the four corner boreholes (i=1 in Figure 5E), the four inner boreholes (i=3), and the remaining eight boreholes (i=2). The data (26) are used, but we have chosen to use a constant extraction temperature.(The value of T_b does not matter, since we present relative figures only.) instead of a given total heat extraction. Table 8 shows the extracted heat during a year for the three borehole positions in per cent of the heat extraction for a corresponding single borehole. The spacing B between the boreholes is 11 and 22 m.

	Borehole position	5y	10y	25y
B=11m	i=1	63%	55%	50%
	i=2	49%	42%	38%
	i=3	33%	27%	25%
B=22m	i=1	88%	78%	68%
	i=2	82%	68%	57%
	i=3	74%	56%	44%

Table 8. Heat extraction relative to a corresponding single borehole for 4 x 4 boreholes in a quadratic pattern.

Consider as a second example the optimal configuration for eight boreholes on a line with a maximal inclination $\theta = 20°$, Figure 5J. The data (26) and a constant extraction temperature is used as in the previous example. The distance B at the ground surface between the boreholes in a row is 2.75 m. Table 9 gives the extracted heat. The borehole positions i = 1,2,3,4 are shown in Figure 5J.

Borehole position	5y	10y	25y
i=1	75%	72%	64%
i=2	74%	70%	63%
i=3	74%	71%	64%
i=4	76%	73%	67%

Table 9. Heat extraction relative to a corresponding single borehole for the optimal configuration of Figure 5J.

The extraction rates do not differ much. This is an indication that the configuration is indeed optimal.

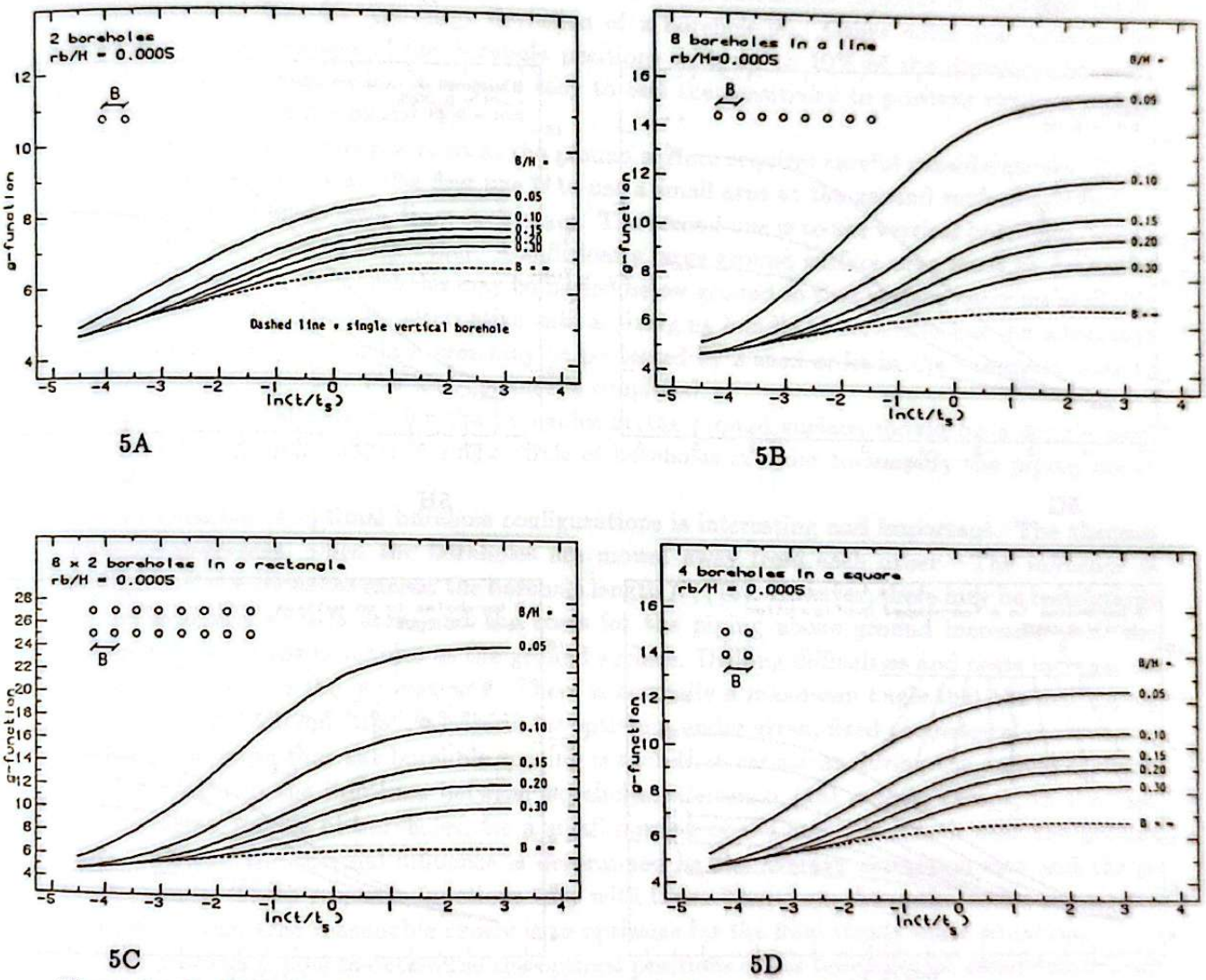

Figure 5A-D. Dimensionless response function g for different borehole configurations.

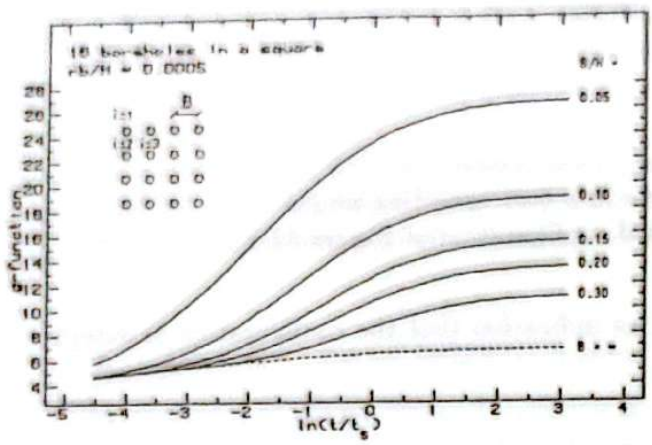

5E

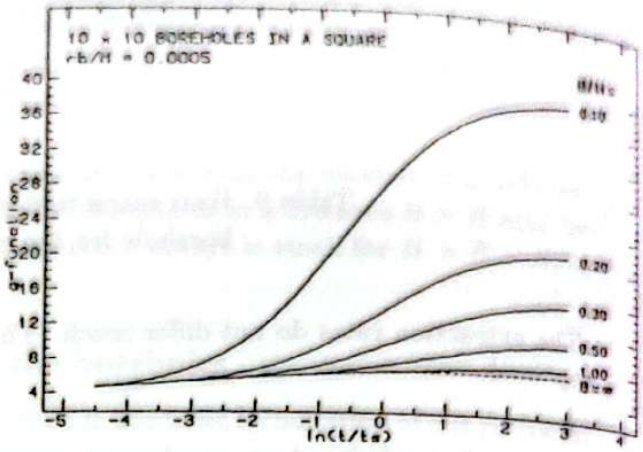

5F

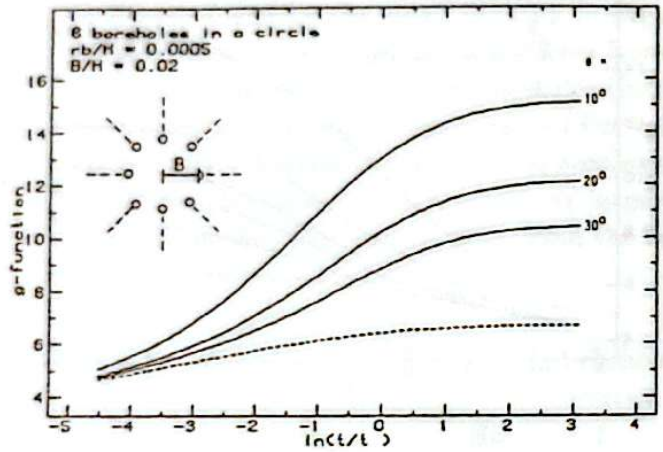

5G

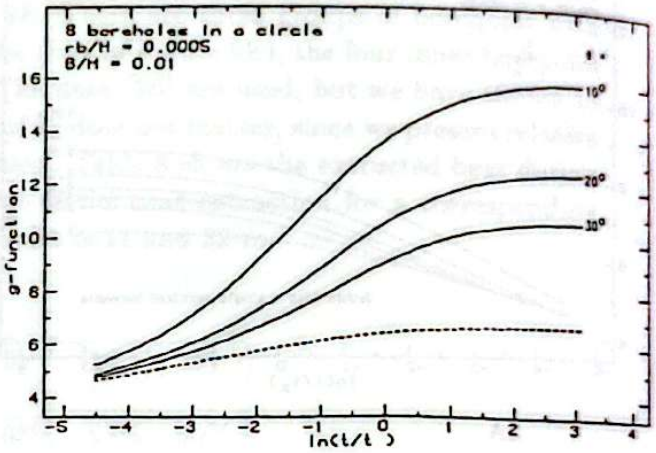

5H

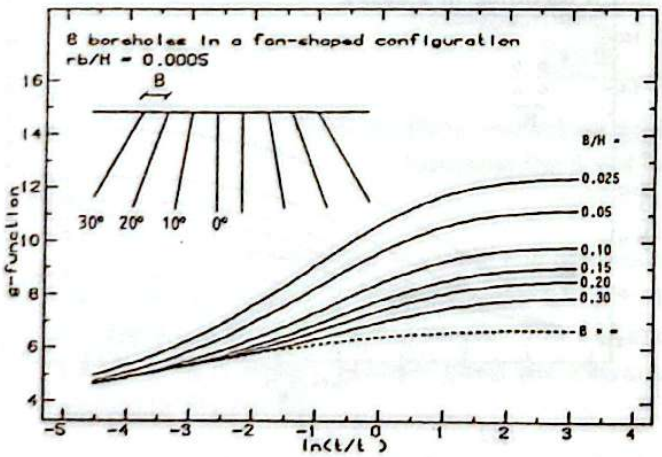

5I

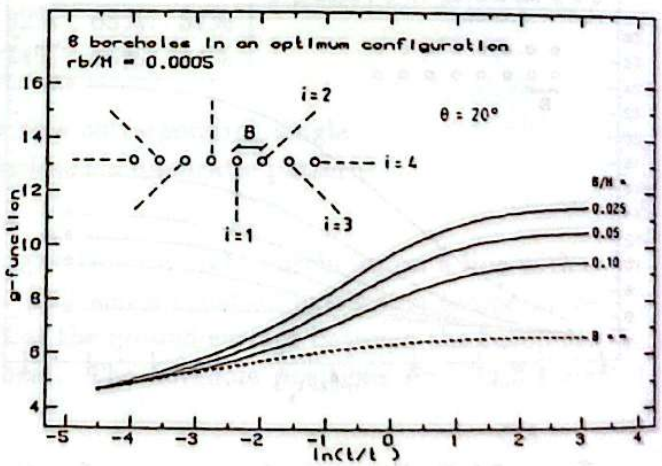

5J

Figure 5E-J. Dimensionless response function g for different borehole configurations.

7 CHOICE OF BOREHOLE CONFIGURATION

The choice of number of boreholes, configuration, and exact positions of the boreholes is quite important, as it determines the response function and the long-term performance. We will discuss the requirements on accuracy of borehole positions, the choice of borehole pattern at the ground surface, vertical versus inclined boreholes, and finally criteria for optimal borehole configuration under geometrical constraints.

Let us first note that there is a choice between a few deep boreholes and many short ones. One has to compare the g-functions in order to make a proper choice. We assume in the further discussion that the number and depth of the boreholes are given.

It is expensive to drill boreholes,in particular inclined ones, with high directional precision. Fortunately, the requirement on position accuracy is quite moderate. Consider as an example four boreholes that lie close to each other at the ground surface. They are inclined 20° outwards. The horizontal projections lie at right angles. Suppose now that we deviate one of the four borehole 45° from the radial outward direction. The heat extraction capacity is decreased about 3% in a typical case for this large deviation of a borehole,[8]. Other numerical simulations have shown that changes of the borehole positions with up to 10% of the distances between the boreholes are negligible. It is quite easy to test the sensitivity to position changes in any particular case with the model [7].

The choice of borehole positions at the ground surface requires careful considerations. There are two main alternatives. The first one is to use a small area at the ground surface and incline the boreholes outwards away from each other. The second one is to use vertical boreholes, which must lie not too close to each other. A sufficiently large ground surface area must be available. The piping between the boreholes may be buried below ground so that surface becomes available for other purposes. The first alternative with a diverging bundle of boreholes has the advantage that the small borehole surface area may be protected by a shed or lie in the basement close to the heat pump facilities. The maintenance is simplified.

The geometrical pattern for the boreholes at the ground surface should be a simple rectangular one, or, for example, a single circle of boreholes in order to simplify the piping above ground.

The question of optimal borehole configurations is interesting and important. The thermal influence decreases, when the boreholes are moved away from each other. The influence is negligible, if the distances exceed the borehole length H, (16). However, there may be restrictions on the available surface area, and the costs for the piping above ground increases with the distance between the boreholes at the ground surface. Drilling difficulties and costs increase on the other hand with the inclination θ. There is normally a maximum angle that the drilling rig can handle. We will only discuss criteria for optimum under given, fixed geometrical constraints.

We presuppose that the borehole spacing is such that variations during the annual cycle do not contribute to the influence between boreholes. Criterion (15) is met, except, in the case of a diverging bundle of boreholes, for a small portion of the borehole length near the ground surface. Then, the thermal influence is determined by the average extraction rate and the g-function only. These response functions vary with time. Therefore, the optimization must refer to a given time. One reasonable choice is to optimize for the final steady-state situation.

The problem is now to determine the optimal positions of the boreholes for steady-state heat extraction under given constraints on the positions of the boreholes. The constraints are often that the boreholes must lie within a certain fixed volume. An example is the case in Section 6.6, where this volume is determined by the straight line of borehole positions on the ground surface and a maximum angle of inclination $\theta = 20°$. The envelope of the volume is generated by straight lines between the line on the ground surface and an oval-shaped curve at the bottom of the boreholes. The optimum is to place the boreholes on the surface of constraint. They

shall be spread evenly so that the shortest distances between the boreholes become as large as possible. The optimization problem is similar to an electrostatic one, for which the electrical charges on the closed metal surface repel each other. The borehole rods 'repel' each other and lie in the optimal case as far away from each other as the constraints allow.

Consider as an example N_b boreholes with the constraints that they shall lie within a circle with the radius B at the ground surface, and that the largest angle of inclination is θ. The optimum is to distribute the boreholes evenly along the periphery of the circle and incline the boreholes with the angle θ outwards in the plane of the radial direction of the circle. The drawing in Figure 5G shows this optimum configurations for $N_b = 8$. One may perhaps think that it would be better to put one of the eight boreholes vertically in the center of the circle. A numerical calculation shows that this change increases the g-function.

References

[1] J. Claesson, P. Eskilson, Conductive Heat Extraction by a Deep Borehole. Thermal Analyses and Dimensioning Rules. Dep of Mathematical Physics and Building Physics, University of Lund, Box 118, S-221 00 Lund, Sweden, 1987.

[2] J. Claesson, G. Hellström, Thermal resistances to and between Pipes in a Composite Cylinder, Dep. of Mathematical Physics and Building Physics, University of Lund, Box 118, S-221 00 Lund, Sweden, 1987. (To be published.)

[3] J. Claesson, G. Hellström, The Effect of the Temperature Variation along the Pipes in a Heat Exchanger in the Ground, Dep. of Mathematical Physics and Building Physics, University of Lund, Box 118, S-221 00 Lund, Sweden, 1987. (To be published.)

[4] J. Claesson, P. Eskilson, Conductive Heat Extraction by a Deep Borehole. Analytical Studies. Dep. of Mathematical Physics and Building Technology, University of Lund, Box 118, S-221 00 Lund, Sweden. (Submitted to Journal of Heat and Mass Transfer)

[5] P. Eskilson, PC-programs for Dimensioning of Heat Extraction Boreholes, Dep. of Building Technology and Mathematical Physics, University of Lund, Box 118, S-221 00 Lund, Sweden, 1987.

[6] J. Claesson, P. Eskilson, Simulation Model for Thermally Interacting Heat Extraction Boreholes, Department of Mathematical Physics, University of Lund, Box 118, S-221 00 Lund, Sweden, 1987. (Accepted for publication in Journal of Numerical Heat Transfer)

[7] P. Eskilson, Superposition Borehole Model. Manual for Computer Code, Dep. of Mathematical Physics, University of Lund, Box 118, S-221 00 Lund, Sweden, 1986.

[8] J. Claesson et. al., Markvärme. En handbok om termiska analyser (Ground Heat Systems. A Handbook on Thermal Analyses), BFR-Rapport T16-T18:1985, (in Swedish, 900 pp. 460 fig.), Svensk Byggtjänst, Box 7853, S-103 99 Stockholm, Sweden, 1985.

[9] J. Bennet, J. Claesson, G. Hellström, Multipole Method to Compute the Conductive Heat Flows to and between Pipes in a Composite Cylinder, Notes on Heat Transfer 3-1987, Dep. of Building Technology and Mathematical Physics, University of Lund, Box 118, S-221 00 Lund, Sweden, 1987.

[10] H.S. Carslaw, J.C. Jaeger, Conduction of Heat in Solids. Oxford Univ. Pr., 1957. Ch. 10.4.

[11] M. Abramowitz, I. Stegun, Handbook of Mathematical Functions, National Bureau of Standards, USA, 1967.Ch. 5.

[12] P. Eskilson, Temperature Response Function g for 38 Borehole Configurations, Notes on Heat Transfer 4-1986, Dep. of Building Technology and Mathematical Physics, University of Lund, Box 118, S-221 00 Lund, Sweden, 1986.

[13] P. Eskilson, Temperature Response Function g for 12 Borehole Configurations, Notes on Heat Transfer 5-1987, Dep. of Building Technology and Mathematical Physics, University of Lund, Box 118, S-221 00 Lund, Sweden, 1987.

Simulation Model for Thermally Interacting Heat Extraction Boreholes

PER ESKILSON, JOHAN CLAESSON

Departments of Building Technology and Mathematical Physics
Lund Institute of Technology, Box 118, S-221 00, Lund, Sweden

February 1987

ABSTRACT

The proper design of heat pump systems that use deep boreholes to extract heat from the ground requires a precise model of the thermal processes in the ground. One problem is the interaction between the convective heat flow in the channels in the borehole and the conductive process in the ground. Another important problem is the thermal interaction between boreholes. A computer model for these thermal processes is presented. The three-dimensional problem with its complex geometry is by a rather intricate superposition reduced to cylindrically symmetric ones; one for each borehole or symmetry group of boreholes. Recipes for the choice of meshes are given. The accuracy of the model is shown to be very good.

Acknowledgment: The support by the Swedish Council for Building Research and the National Energy Administration is gratefully acknowledged

Typeset by AMS-TEX

NOMENCLATURE

a	thermal diffusivity
B_{min}	smallest distance between two boreholes at $z = D + H/2$
B_{max}	largest distance between two boreholes
c	heat capacity of the ground
c_f	heat capacity of the heat-carrier fluid
D	depth of thermally insulated upper part of the borehole
H	borehole length over which heat extraction takes place
q	heat extraction rate (W/m)
q_{geo}	geothermal heat flow (W/m^2)
r	radial distance
r_i	radial distance from borehole i
r_b	borehole radius
r_p	inner radius of the plastic tube
R^D_β	thermal resistance (K/(W/m)), see Figure 2 ($\beta = 1, 2, 12$)
t	time
T	temperature in the ground
T_b	temperature at the borehole wall
T_{f1}	temperature in fluid channel 1
T_i	particular solution for borehole i
T_0	average air temperature at the ground surface
T_v	one-dimensional vertical solution
V_f	pumping rate (m^3/s)
x, y	horizontal coordinates
z	vertical coordinate
z_i	axial coordinate for borehole i

Greek symbols

λ	thermal conductivity of the ground
ρ	density of the ground
ϕ_i	angle around the axis of borehole i

HEAT EXTRACTION WITH DEEP BOREHOLES

A method of extracting heat from the ground to support a heat pump for domestic heating is to use a deep borehole. The depth of the borehole is 40-150 meters. Many systems of this kind have been built in the United States and Canada, and about 5,000 are now in operation in Sweden. Multiple borehole systems can be used to support large heat pumps. In this case it is often necessary to reinject heat to the ground, normally during the summer. In systems with both air conditioning and heating, heat is injected to the ground in the cooling mode and extracted in the heating mode. The most common alternative in Sweden is to use a closed loop for the heat carrier fluid in the borehole. Figure 1 shows an example with a U-shaped plastic tube. The fluid is heated by the rock, while it flows down to the bottom of the borehole in one channel and back upwards in the second channel. The cold borehole extracts heat from the surrounding rock by pure heat conduction. Another alternative is to use the ground water in the borehole directly as heat carrier fluid with a single pipe down to the bottom.

The proper design and dimensioning of these systems require a precise knowledge of the relation between fluid temperature and heat extraction under various conditions. The local thermal processes in the borehole with the varying temperature along the borehole channels present particular complications. A further important question is the long-term 'global ' behaviour. Neighboring boreholes influence each other thermally. The question of reinjection of heat (in the summer) arises as a method to decrease the influence. A major task is to be able to calculate the complex temperature field, when several boreholes influence each other. The simulation model was developed in order to provide a tool for analysis and design of these systems. The manual for the computer program is given by [1]. Reference [2] is a general design manual for ground-coupled heat pumps. Dimensioning rules and analytical studies of a single borehole are presented in [3] and [4]. The model presented in this paper was used extensively in [5], which provides dimensioning rules for thermally interacting boreholes.

HEAT FLOW PROBLEM

Single borehole.

A single vertical borehole in an infinite homogeneous ground is shown in Figure 1. A shallow upper part of depth D is regarded as thermally insulated. The cold borehole extracts heat over the active borehole depth H from the ground by pure heat conduction.

The thermal process around the borehole is cylindrically symmetric. Local disturbances of the cylindrical symmetry due to the U-pipe in the borehole are neglected. The ground temperature satisfies the heat conduction equation:

$$\frac{1}{a}\frac{\partial T}{\partial t} = \frac{\partial^2 T}{\partial r^2} + \frac{1}{r}\frac{\partial T}{\partial r} + \frac{\partial^2 T}{\partial z^2} \tag{1}$$

The temperature at the ground surface varies during the year around the mean annual air temperature T_0. This variation will only penetrate to a depth of a few meters. The influence on the heat extraction is negligible. The temperature T_0 is therefore used as boundary condition at the ground surface:

$$T = T_0 \qquad z = 0 \tag{2}$$

Note, that all variations close to the ground surface, such as snow, air-to-ground thermal resistance, freezing, and a top-soil layer with different thermal properties, are negligible for a borehole with a depth of 100 meters.

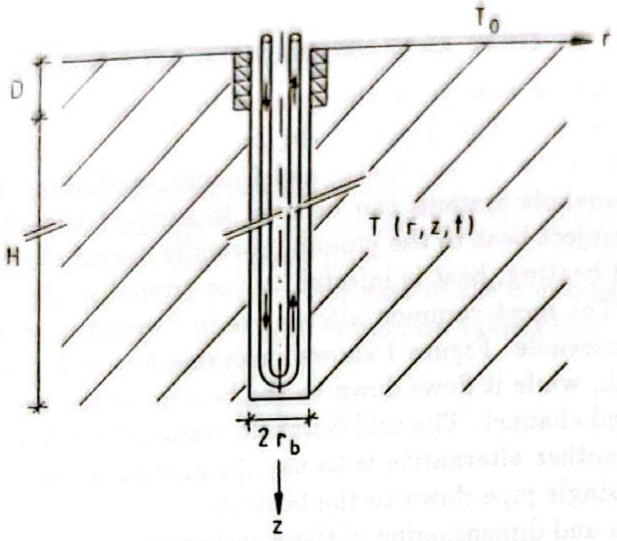

Figure 1. Heat extraction using a deep borehole.

The initial temperature in the ground increases linearly with z due to the geothermal gradient q_{geo}/λ, where q_{geo} (W/m^2) is the geothermal heat flow from below:

$$T|_{t=0} = T_0 + (q_{geo}/\lambda) \cdot z \tag{3}$$

Local processes in the borehole.

The boundary condition at the borehole wall is more complicated. The heat flux to the borehole is assumed to be zero for $0 < z < D$. Heat is extracted from the depth $z = D$ down to $z = D+H$. The local heat flow between the fluid channels and the borehole wall can for any z be described by the heat flow circuit of Figure 2. The heat flow from channel 1 to channel 2 is denoted q_{12}, while the flows from the borehole wall at temperature T_b to the channels at fluid temperatures T_{f1} and T_{f2} are q_1 and q_2, respectively. This description is based on local steady-state conditions. It is not valid on a time-scale smaller than $5r_b^2/a$, [3].

The thermal resistances R_1^D, R_2^D and R_{12}^D can be determined by laboratory experiments (D = delta circuit). The borehole outside the fluid channels may be filled with sand or another solid material in order to improve the thermal contact between the channels and the ground. In general, this borehole region has a different thermal conductivity than the surrounding ground. Approximate analytical expressions for the thermal resistances are derived in [6]. The thermal resistances R_1^D, R_2^D, and R_{12}^D are input variables to the model. The analytical expressions of [6] may be used directly in the simulation model [1].

The fluid temperatures $T_{f1}(z,t)$ and $T_{f2}(z,t)$ vary along the channels and with time. The convective heat flow along the fluid channels is balanced against the conductive heat flows between the fluid channels and the borehole wall. The conductive heat transfer along the fluid channels is very small and therefore neglected . The steady-state heat balance equations are in accordance with Figure 2:

$$\begin{aligned} \rho_f c_f V_f \frac{\partial T_{f1}}{\partial z} &= q_1 - q_{12} = (T_b - T_{f1})/R_1^D - (T_{f1} - T_{f2})/R_{12}^D \\ -\rho_f c_f V_f \frac{\partial T_{f2}}{\partial z} &= q_2 + q_{12} = (T_b - T_{f2})/R_2^D + (T_{f1} - T_{f2})/R_{12}^D \\ & \qquad D \le z \le D + H \end{aligned} \tag{4}$$

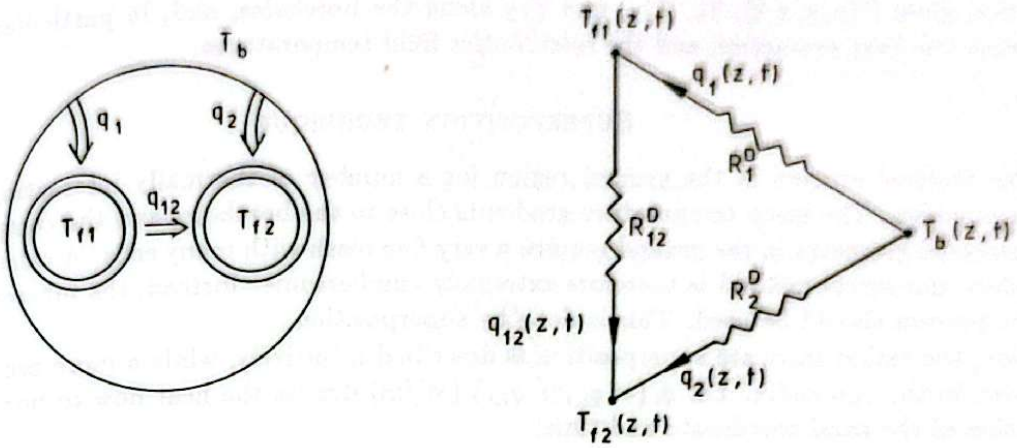

Figure 2. Cross-section of the borehole and the corresponding heat flow circuit.

Here V_f (m^3_{fluid}/s) is the pumping rate or flow rate in the pipes. The value of V_f is positive, when the flow in channel 1 is in the positive z-direction. The steady-state description with a thermal resistance circuit is not valid for variations on a time-scale below $5r_b^2/a$. The time for the fluid to circulate through the borehole is $\pi r_p^2 \cdot 2H/V_f$. Transients on this time-scale are not accounted for in (4). Eqs. (4) can only describe input variations of fluid temperature and pumping rate on a time-scale larger than these limits. We have the following limit t_b below which the model cannot simulate input variations:

$$t_b = 5r_b^2/a + \pi r_p^2 \cdot 2H/V_f \tag{5}$$

This time is characteristically around 2-3 hours in the present applications. More rapid variations would require a more detailed local analysis in the borehole.

Thermally interacting boreholes.

We will now consider the general case with a number of thermally interacting boreholes. They may be vertical or inclined in arbitrary directions. There is no longer any cylindrical symmetry. The temperature satisfies the heat conduction equation outside the boreholes:

$$\frac{1}{a}\frac{\partial T}{\partial t} = \frac{\partial^2 T}{\partial x^2} + \frac{\partial^2 T}{\partial y^2} + \frac{\partial^2 T}{\partial z^2} \tag{6}$$

The boundary condition at the ground surface and the initial temperature in the ground are given by (2) and (3). At the boreholes, the heat balance equation (4) is still valid. The vertical coordinate z is replaced by the local axial coordinate z_i along borehole i with heat extraction in the interval $0 < z_i < H_i$. The temperatures along the the fluid channels, $T_{f1,i}$ and $T_{f2,i}$, and the temperature $T_{b,i}$ at each borehole wall are functions of z_i and t.

The inlet temperatures of the different boreholes depend on the hydraulic coupling between these. A simple case is to couple the boreholes in series. The inlet temperature to the first borehole is given. The outlet temperature of the first borehole becomes the inlet temperature to the second borehole, and so on.

The thermal problem to be solved is defined by (6), (2), (3), and (4). The heat balance (4) is to be satisfied for each borehole i along its axial coordinate z_i for $0 < z_i < H_i$. The pumping rate

and the hydraulic coupling are given. A basic case for the loading conditions is a given inlet fluid temperature as a function of time. Another possibility is to prescribe the heat extraction rate. The solution gives $T(x,y,z,t)$, T_b, T_{f1}, and T_{f2} along the boreholes, and, in particular, the relation between the heat extraction and the inlet/outlet fluid temperatures.

SUPERPOSITION TECHNIQUE

The thermal process in the ground region for a number of thermally interacting boreholes is quite complex. The steep temperature gradients close to the boreholes and the complicated three-dimensional geometry in the ground require a very fine mesh with many cells. A calculation using a standard numerical method is therefore extremely cumbersome. Instead, the inherent symmetries of the process should be used. This is done by superposition.

Here, the rather intricate superposition is described intuitively, while a more precise discussion is given in the Appendix. Let q_i $(= q_{1,i} + q_{2,i})$ (W/m) denote the heat flow to borehole i. It is a function of the axial coordinate and time:

$$q_i = q_i(z_i, t) \qquad 0 < z_i < H_i\,, \quad t > 0 \tag{7}$$

Let us now consider the particular thermal process with the heat extraction $q_i(z_i,t)$ of borehole i alone, while there is no heat extraction from any of the other boreholes $(q_j = 0, j \neq i)$, which are replaced by undisturbed ground. The ground is assumed to be infinite in all directions (the effect of the ground surface is allowed for by mirror boreholes as described below). The initial ground temperature is zero. The solution of this particular thermal process is denoted T_i. The process is cylindrically symmetric around the borehole:

$$T_i = T_i(r_i, z_i, t) \tag{8}$$

Here r_i is the radial distance to the borehole i, Figure 3.

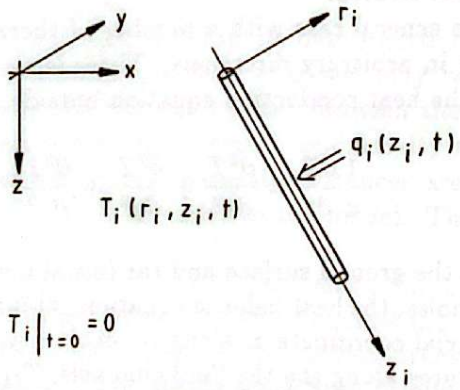

Figure 3. Particular thermal process $T_i(r_i, z_i, t)$ due to the heat extraction q_i of borehole i alone in an infinite surrounding.

The solution T_i, with its infinite region of definition, will give a varying temperature at the ground surface z=0. In order to get zero temperature at z=0 we use mirror technique. A mirror borehole is imagined to lie above the ground surface, see Figure 4. The heat extraction is -q_i and

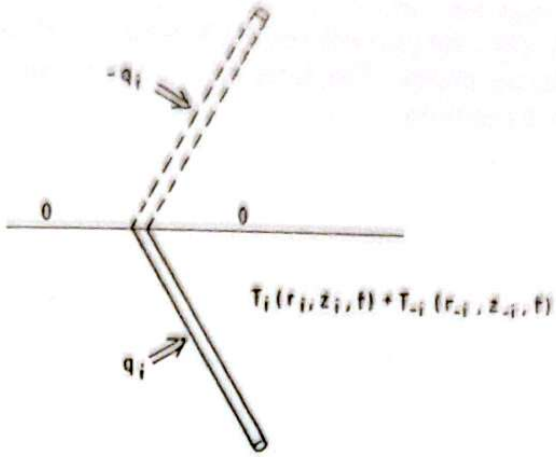

Figure 4. Mirror borehole to satisfy the boundary condition of zero temperature at the ground surface.

the associated temperature field is denoted T_{-i}. The sum $T_{-i} + T_i$ is zero for z=0 due to antisymmetry. The two solutions are the same except for the sign, but they have different positions or coordinates:

$$T_{-i}(r_{-i}, z_{-i}, t) = -T_i(r_i, z_i, t) \tag{9}$$

The principle of superposition can be applied to an arbitrary number of boreholes. A system with N boreholes requires superposition of 2N solutions. The mirror boreholes are not needed for the case of vertical boreholes. The zero surface temperature can then be satisfied in each solution directly without destroying the cylindrical symmetry. Superposition of N solutions is then required.

The ground surface temperature and the initial temperature are given by (2) and (3). Let $T_v(z)$ be the one-dimensional undisturbed ground temperature (3):

$$T_v(z) = T_0 + (q_{geo}/\lambda) \cdot z \tag{10}$$

Finally, the temperature in the ground is given by a superposition of the particular solutions above:

$$T(x, y, z, t) = T_v(z) + \sum_{\substack{i=-N \\ (i \neq 0)}}^{N} T_i(r_i, z_i, t) \tag{11}$$

The temperature at the wall of borehole i is:

$$T_{b,i}(z_i, t) = T_v|_{z_i} + T_i(r_b, z_i, t) + \sum_{j \neq i} T_j|_{r_i = 0, z_i} \tag{12}$$

The fluid temperatures are determined by using this expression for the borehole temperature T_b in (4).

The boreholes are often located in a regular pattern with certain symmetries. Boreholes belonging to the same symmetry group with the same inlet temperature and pumping flow will give the same solution T_i. Consider an example with six graded boreholes according to Figure 5. All

boreholes are coupled in parallel with the same inlet temperature. The four corner boreholes and their mirror boreholes are located symmetrically. Hence, they all have the same solution. This is also the case for the two (+ two) middle boreholes. There are two solutions to be computed, one for each symmetry group. The total solution is obtained by superposition of the computed solutions in the 8+4 positions.

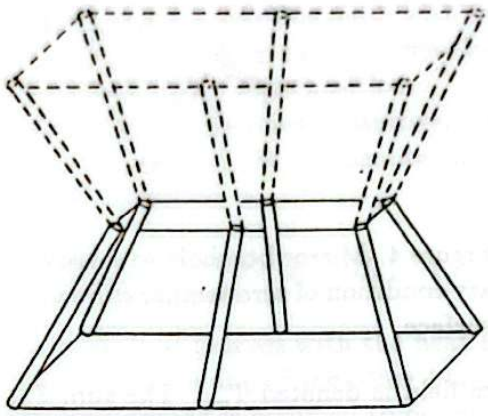

Figure 5. Six graded boreholes and the corresponding mirror boreholes.

TEMPERATURES OF THE HEAT CARRIER FLUID

The temperature along the fluid channels satisfies the two coupled linear differential equations (4). The solution may be derived using Laplace transforms in a straight-forward way. The final expressions are:

$$\begin{aligned} T_{f1}(z_i,t) &= T_{f1}(0,t)f_1(z_i) + T_{f2}(0,t)f_2(z_i) + \int_0^{z_i} T_{b,i}(\varsigma,t)f_4(z_i-\varsigma)d\varsigma \\ T_{f2}(z_i,t) &= -T_{f1}(0,t)f_2(z_i) + T_{f2}(0,t)f_3(z_i) - \int_0^{z_i} T_{b,i}(\varsigma,t)f_5(z_i-\varsigma)d\varsigma \\ & \qquad 0 \le z_i \le H_i \end{aligned} \tag{13}$$

The functions f_1 , f_2 , ...f_5 are given by the expressions:

$$\begin{aligned} f_1(z) &= e^{\beta z}\cdot(cosh(\gamma z) - \delta sinh(\gamma z)) \\ f_2(z) &= e^{\beta z}\frac{\beta_{12}}{\gamma} sinh(\gamma z) \\ f_3(z) &= e^{\beta z}\cdot(cosh(\gamma z) + \delta sinh(\gamma z)) \\ f_4(z) &= e^{\beta z}\cdot\left(\beta_1 cosh(\gamma z) - (\delta\beta_1 + \frac{\beta_2\beta_{12}}{\gamma})\cdot sinh(\gamma z)\right) \\ f_5(z) &= e^{\beta z}\cdot\left(\beta_2 cosh(\gamma z) + (\delta\beta_2 + \frac{\beta_1\beta_{12}}{\gamma})\cdot sinh(\gamma z)\right) \end{aligned} \tag{14}$$

$$\beta_1 = 1/(R_1^D \rho_f c_f V_f) \qquad \beta_2 = 1/(R_2^D \rho_f c_f V_f) \qquad \beta_{12} = 1/(R_{12}^D \rho_f c_f V_f)$$
$$\beta = \frac{\beta_2 - \beta_1}{2} \qquad \gamma = \sqrt{(\beta_1 + \beta_2)^2/4 + \beta_{12}(\beta_1 + \beta_2)} \qquad \delta = \frac{1}{\gamma}\left(\beta_{12} + \frac{\beta_1 + \beta_2}{2}\right) \tag{15}$$

The temperature $T_{b,i}$ in the integrals is given by (12). The inlet temperature $T_{fin}(t) = T_{f1}(0,t)$ is a given function of time. The two fluid channels are connected at the bottom:

$$T_{f1}(H_i,t) = T_{f2}(H_i,t) \tag{16}$$

Eqs. (13) and (16) determine the outlet temperature $T_{fout}(t) = T_{f2}(0,t)$:

$$T_{fout}(t) = \frac{f_1(H_i) + f_2(H_i)}{f_3(H_i) - f_2(H_i)} T_{fin}(t) + \int_0^{H_i} \frac{T_b(\varsigma,t)[f_4(H_i - \varsigma) + f_5(H_i - \varsigma)]}{f_3(H_i) - f_2(H_i)}\, d\varsigma \tag{17}$$

COUPLING BETWEEN THE SOLUTIONS T_i

The formulation of the thermal problem after the superposition is somewhat intricate. The total temperature is given by the sum (11). The vertical solution $T_v(z)$ is defined by (10). The mirror solutions T_{-i} are directly obtained from T_i according to (9). The solution $T_i(r_i, z_i, t)$ associated with the heat extraction of borehole i alone satisfies the heat conduction equation (1) in an infinite surrounding with $z = z_i$ and $r = r_i$. Its initial temperature is zero.

The heat flux q_i is obtained from the sum of the two equations (4):

$$q_i(z_i,t) = (T_{b,i} - T_{f1,i})/R_1^D + (T_{b,i} - T_{f2,i})/R_2^D \tag{18}$$

However, this heat flux is also obtained from the solution T_i:

$$q_i(z_i,t) = 2\pi r_b \lambda \left.\frac{\partial T_i}{\partial r_i}\right|_{r_i = r_b} \tag{19}$$

Note, that the other solutions T_j $(j \neq i)$ do not contribute to q_i in the right-hand side of (19). Eqs. (18) and (19) give:

$$(T_{b,i} - T_{f1,i})/R_1^D + (T_{b,i} - T_{f2,i})/R_2^D = 2\pi r_b \lambda \left.\frac{\partial T_i}{\partial r_i}\right|_{r_i = r_b} \qquad 0 < z_i < H_i \tag{20}$$

The temperatures $T_{f1,i}$ and $T_{f2,i}$ are determined by $T_{b,i}$ and Eqs. (13-17), while $T_{b,i}$ is obtained from (12). The above equation expresses the coupling between the solution T_i and the other solutions.

NUMERICAL SOLUTION TECHNIQUE

Each solution $T_i(r_i, z_i, t)$ corresponds to one (r,z)-problem. These solutions $(i = 1, \ldots N)$ are calculated simultaneously. Each problem uses an expanding rectangular mesh in the (r_i, z_i)-plane with the temperature node in the middle of the cell. The cell widths are small close to the borehole and expand outwards in the ground. The heat flows from the last cells in the outward radial and the upward and downward axial directions are zero. This boundary condition is also used in the

radial direction below and above the borehole at $r_i = r_b$, $z_i < 0$ and $z_i > H_i$. Explicit forward differences are used. The maximum time-step is smaller than or equal to the stability time-step, which is determined by the smallest cell.

The borehole temperature $T_{b,i}(z_i, t)$ is given by (12) as a sum of all the different solutions. Quite a lot of interpolation work between the coordinate systems r_j, z_j and r_i, z_i is required. This is described in [1]. The temperatures T_{f1} and T_{f2} along the borehole channels are calculated by using $T_{b,i}$ in the two equations of (13) and in (17). The temperature $T_{b,i}(\zeta_i, t)$ is in the discrete approximation piece-wise constant for each cell. The heat flux q_i is obtained from the left-hand side of (20), when $T_{f1,i}$ and $T_{f2,i}$ are known.

The simulation model has a number of options for the loading conditions. The basic case is a given inlet fluid temperature. Another possibility is to prescribe the total heat extraction rate. The program determines the required inlet temperature. A complete discussion of the different types of loading conditions is given in [1].

RULES FOR THE CHOICE OF MESH

The proper choice of mesh depends strongly on the specific problem to be solved. A recipe based upon a detailed numerical study of different meshes will be presented in this section, [7]. A measure of the radial penetration depth after the time t for a heat extraction pulse is:

$$r_p = \sqrt{at} \tag{21}$$

In the case of a single borehole, the radial size of the smallest cell is recommended to be:

$$\Delta r_{min} = \min(\sqrt{at_{min}}, H/5) \tag{22}$$

Here t_{min} is the shortest time interval between a change in the loading condition and a print-out time. The following cell widths, starting from the borehole, are recommended:

$$\Delta r = 3 \times \Delta r_{min}, 2\Delta r_{min}, 4\Delta r_{min}, \cdots \tag{23}$$

The cells are extended to the radial distance $r_{max} = 3\sqrt{at_{max}}$, where t_{max} is the time for which the process is simulated.

For systems with many boreholes, there should be at least three cells between two neighboring boreholes. The choice of Δr_{min} then becomes:

$$\Delta r_{min} = \min\left(\sqrt{at_{min}}, H/5, B_{min}/3\right) \tag{24}$$

For vertical boreholes B_{min} is taken to be the smallest distance between two neighbouring boreholes. For graded boreholes B_{min} is taken to be the smallest horizontal distance at the middepth of the boreholes. The mesh division (23) is recommended for systems with up to, say, 8 boreholes. For larger systems it is advisable to use a finer mesh, where all the cells in (23) have been divided in two:

$$\Delta r = 6 \times 0.5\Delta r_{min}, 2 \times \Delta r_{min}, 2 \times 2\Delta r_{min}, \ldots \tag{25}$$

The mesh is expanded so that the midpoint of the last cell in the radial direction is located at $r_{max} \geq \max(3\sqrt{at_{max}}, B_{max})$, where B_{max} is the largest radial distance between two boreholes.

The axial mesh is generated automatically with a parameter n_z. The borehole length, $0 < z_i < H_i$, is divided into $2 \cdot n_z$ cells in an expanding mesh. The parameter n_z is normally given values

between 3 and 6, with the higher value beeing on the safe side. The size of the first cell at the top and at the bottom of the borehole is:

$$\Delta z_{min} = \frac{H_i}{2} \frac{\sqrt{2}-1}{(\sqrt{2})^{n_z}-1} \tag{26}$$

The cell widths expand with the factor $\sqrt{2}$ to the middle of the borehole. The first cell above and below the borehole has the width Δz_{min}. The following cells above and below expand with the factor 2. There are $4 \cdot n_z + 8$ cells in the axial direction, including two boundary cells.

The accuracy of the numerical solution has been very good in all our tests . The temperature decrease at the borehole wall has been calculated for a single borehole with the meshes (23) and (25), with $n_z = 6$ [7]. Relative differences were less than 1%. Tests against line source solutions [8] for systems with up to 120 boreholes gave errors below 2%, when the rules above were followed.

COMPUTER CODE

The computer code [1] is written in FORTRAN 77. The size of the source code is 3600 lines or 134 kbytes. It is implemented on a NORD 570, which uses a word length of 32 bits (4 bytes). The executable code requires 36 kbytes for the information bank and 134 kbytes for the data bank in the basic version, which can handle a case with up to 3 symmetry groups with 8 boreholes each ($N = 3 \times 8 = 24$). The size of the data bank increases rapidly with the number of boreholes. A simulation of a large heat store in Luleå, Sweden, required 30 symmetry groups, 30 x 4 boreholes, and 2500 kbytes of data storage [9].

Computer time strongly depends on the number of boreholes. A case with one single borehole and constant heat extraction needs only a few CPU-seconds to perform a simulation of 1000 years on a NORD 570 or SPERRY 1100/80. A simulation of an annual cycle for the heat store in Luleå takes almost 30 minutes when time-steps of one day are used.

Input to the model are the thermal properties of the ground, the borehole geometry, and data for the heat collector in the borehole. The coupling between the fluid channels of the different boreholes can be arranged in many ways. There is a choice between coupling in series, in parallel, or a hybrid of these two. Consider a system with the inlet temperature T_{fin}. The inlet flow is divided into a number of different channels. Each channel consists of a number of symmetry groups coupled in series. The boreholes in each separate symmetry group are coupled in parallel. The outlet temperatures from all the channels are mixed and used as inlet temperature for a new group of channels. The procedure can be repeated for an arbitrary number of groups. The mixed outlet temperature from the last group is the outlet temperature of the system. Another possibility of the simulation model is that the boreholes are coupled in separate hydraulic systems, each with an independently given inlet temperature or average heat extraction rate.

Output from the model is the heat extraction rate, the injected and extracted energy, the extracted energy of each separate borehole, the overall average value of the varying temperature along the borehole walls , and finally the inlet, outlet, and bottom temperatures of each borehole. Temperature fields may be obtained in horizontal and vertical planes.

EXAMPLES

We will give two examples in order to illustrate the use of the model. The first example concerns the long-term heat extraction from a single borehole. The gradual approach to steady-state conditions is to be studied. In the second example a configuration with six graded boreholes is simulated for 25 years. The loading conditions are given by monthly average values. A number of systems of this size have been installed in Sweden, two of which are described in [10] and [11].

Long-term heat extraction with a single borehole.

Consider a single vertical borehole in a homogeneous ground with the following typical Swedish data:

$$H = 110\,\text{m} \qquad D = 5\,\text{m} \qquad r_b = 0.055\,\text{m} \qquad \lambda = 3.5\,\text{W/m}\cdot\text{K} \qquad \rho c = 2.16\cdot 10^6\,\text{J/m}^3\cdot\text{K}$$

The boundary temperature at the ground surface, T_0, is 7.0 °C and the geothermal heat flow, q_{geo}, is 0.072 W/m^2. The fluid enters the borehole through two pipes and returns through a single pipe. The two downward channels are identical. They are in the numerical model considered as one channel after due correction of the thermal resistances R_1^D, R_2^D, and R_{12}^D [6]. The inner and outer radii of the plastic tube are 0.0176 m and 0.0200 m respectively. The thermal conductivity of the plastic is 0.43 W/m·K. The three channels are located in a triangle with equal sides. The distance from the center of the borehole to the center of any of the channels is 0.033 m.

In this example, we will consider long-term effects only. Therefore, the heat extraction rate is constant. It is equal to 3300 W, i.e. 30 W/m. The pumping rate is 0.001 m^3/s.

The radial mesh is determined by (22) and (23) with t_{min} equal to 5 years. The mesh is extended to the distance 1040 m > 678 m = r_{max}:

$$\Delta r = 16, 16, 16, 32, 64, 128, 256, 512\,\text{m}$$

The axial mesh is determined by n_z=3. The smallest cell width is equal to 12.5 meter, (26). The fluid temperature T_{fin} after 5, 25, 100, and 1000 years becomes -1.5, -2.3, -2.6 and -2.7 °C, repectively.

The simulation took 6.7 CPU-seconds on a NORD-570. The stability time-step was 1 year.The same calculation, using a much finer mesh with $\Delta r_{min} = 2\,\text{m}$ and $n_z = 6$, took 444 CPU-seconds and had a stability time-step of 9 days. The maximum temperature difference between the two cases was 0.05 °C

System with six boreholes.

Consider the system with six boreholes shown in Figure 5. The distance at the ground surface between two neighbouring boreholes is 5 meters. The boreholes are inclined 30° outwards.

The data for the boreholes and the ground are the same as in the previous example. The heat extraction and the pumping rate during each annual cycle are given as monthly average values in Table 1.

month	1	2	3	4	5	6	7	8	9	10	11	12
q (W/m)	16	23	31	38	41	39	33	26	17	0	0	0
V_f ($10^{-3}\cdot$m^3/s)	3.0	3.6	4.5	4.8	4.8	4.5	3.6	3.0	2.4	0	0	0

Table 1: Heat extraction and pumping rate for the example with 6 boreholes.

The radial cell widths are determined by (24) and (23) with t_{min} equal to 1 month. The time t_{max} is equal to 25 years, and the mesh is extended to the distance 130 m > 105 m = r_{max}:

$$\Delta r = 2, 2, 2, 4, 8, 16, 32, 64\,\text{m}$$

The axial mesh is determined by n_z=6. The smallest cell height becomes 3.2 m, (26).

The coldest inlet temperature during year 1, 5, 10 and 25 becomes -2.7, -3.9, -4.5 and -5.3°C, respectively.

The simulation required 40 CPU-seconds on a NORD 570. The simulation was also performed for the finer mesh (25). This simulation took 2.5 CPU-minutes. The maximum temperature difference between the two cases was less than 0.15 °C.

APPENDIX. DETAILED DISCUSSION OF THE SUPERPOSITION

The superposition of cylindrically symmetric solutions involves a few approximations, which require a detailed discussion. Let T' be the solution of our thermal problem in a particular case with heat extraction and perhaps reinjection of heat during certain periods. Let q_i' (W/m^2) be the heat flux to the wall of borehole i. The flux varies with the axial coordinate z_i but also with the angle ϕ_i around the borehole:

$$q_i' = q_i'(\phi_i, z_i, t) \qquad \text{at} \quad S_{b,i} \tag{A.1}$$

Here $S_{b,i}$ denotes the surface of borehole i through which heat extraction takes place:

$$S_{b,i}: \quad r_i = r_b, \quad 0 \le \phi_i \le 2\pi, \quad 0 \le z_i \le H_i \tag{A.2}$$

The exact temperature field in the ground is determined by these heat fluxes at the boundary surfaces $S_{b,i}$, $i = \pm 1, \ldots \pm N$.

Let T_i' be the solution for the case with the heat flux q_i' at $S_{b,i}$ and zero heat flux at the surfaces of the other boreholes (and the mirror boreholes). The boundary conditions for T_i' are then:

$$\lambda \frac{\partial T_i'}{\partial r_i} = q_i'(\phi_i, z_i, t) \qquad \text{at} \quad S_{b,i} \tag{A.3}$$

$$\lambda \frac{\partial T_i'}{\partial r_j} = 0 \qquad \text{at} \quad S_{b,j} \qquad j \neq i \tag{A.4}$$

Let T_v' be the solution for the vertical part. It satisfies (3) at t=0. The heat flux is zero through the surfaces of all boreholes:

$$\lambda \frac{\partial T_v'}{\partial r_j} = 0 \qquad \text{at } S_{b,j} \qquad j = \pm 1, \ldots \pm N \tag{A.5}$$

The exact temperature T' in the ground is by superposition:

$$T'(x, y, z, t) = T_v'(x, y, z, t) + \sum_{\substack{i=-N \\ (i \neq 0)}}^{N} T_i'(r_i, \phi_i, z_i, t) \tag{A.6}$$

In the model T_i' is approximated by the cylindrically symmetric $T_i(r_i, z_i, t)$ and T_v' by $T_v(z)$, Eq. (10).

As a first approximation we neglect the influence of the other boreholes (including the mirror boreholes) on T_i'. Let T_i'' be this solution with the boundary condition (A.3) in an infinite, homogeneous surrounding. The other boreholes with the zero-flux boundary condition (A.4) are replaced by undisturbed ground. The temperature field T_i'' is determined by the heat flux $q_i'(\phi_i, z_i, t)$ only.

In order to assess the error in this approximation we consider the behaviour of T_i'' near another (removed) borehole j. We retain only first-order terms in an expansion near the axis of borehole j:

$$T_i'' \simeq T_i''|_{r_j=0} + K \cdot x_j + K_z \cdot z_j \tag{A.7}$$

Here K_z is the derivative of T_i'' in the axial direction z_j. The x_j-axis is chosen to point in the direction of the gradient of T_i'' in the plane perpendicular to the axis of borehole j, and K is the magnitude of this gradient. The solution T_i' satisfies (A.4) ,while the term $\vec{K} \cdot \vec{x}_j$ in T_i'' gives a heat flux through the boundary $r_j = r_b$ of borehole j. It is simple to introduce a correction term T_{corr} so that (A.4) is satisfied, if we consider K to be constant. We have, using the solution $cos(\phi_j)/r_j$ of $\nabla^2 T = 0$ in polar coordinates:

$$K x_j + T_{corr} = K r_j cos(\phi_j) + A \cdot \frac{cos(\phi_j)}{r_j}$$

$$\frac{\partial}{\partial r_j}(K x_j + T_{corr})\Big|_{r_j = r_b} = K cos(\phi_j) - A \cdot \frac{cos(\phi_j)}{r_b^2} = 0 \tag{A.8}$$

or

$$T_{corr} = K r_b^2 \cdot \frac{cos(\phi_j)}{r_j} \tag{A.9}$$

This expression gives the order of magnitude of the difference between T_i' and T_i''. We need an assessement of the gradient K.

Consider for q_i' a Fourier expansion in ϕ_i:

$$q_i'(\phi_i, z_i, t) = \frac{1}{2\pi r_b}\{q_0(z_i, t) + q_1(z_i, t) \cdot cos(\phi_i) + ...\} \tag{A.10}$$

Let q_0 be a representative average of $q_0(z_i, t)$. The temperature corresponding to a constant q_0 is $q_0/(2\pi\lambda) \cdot ln(r_i)$. The derivative gives an estimate of K:

$$K \simeq \frac{q_0}{2\pi\lambda} \cdot \frac{1}{r_i} = \frac{q_0}{2\pi\lambda} \cdot \frac{1}{B_{ij}} \tag{A.11}$$

Here B_{ij} is the distance between borehole i and borehole j. The next term in (A.10) gives a gradient of the order $q_1 r_b/(2\pi\lambda B_{ij}^2)$. It is therefore at least a factor r_b/B_{ij} less than (A.11).

From (A.9) and (A.11) we get the following estimate of the error at borehole j:

$$T_i' - T_i'' \simeq \frac{q_0}{2\pi\lambda} \cdot \frac{r_b}{B_{ij}} cos(\phi_j) \qquad \text{at borehole j} \tag{A.12}$$

An estimate of the error at borehole i from the effect of borehole j is obtained by putting $r_j = B_{ij}$ in (A.9):

$$T_i' - T_i'' \simeq \frac{q_0}{2\pi\lambda} \cdot \left(\frac{r_b}{B_{ij}}\right)^2 \qquad \text{at borehole i} \tag{A.13}$$

The difference between T_v and T_v' is that T_v' satisfies the zero-flux condition (A.5) at the boreholes. The analysis above is directly applicable with K equal to the gradient of T_v perpendicular to the borehole axis. We have from (10):

$$K = \frac{q_{geo}}{\lambda} \cdot sin(\theta_j) \tag{A.14}$$

Here θ_j is the angle between the axis of borehole j and the vertical z-axis. This gradient is characteristically at least a factor 10 smaller than (A.11). The error involved in the vertical solution is therefore less important than the effect of the influence between the pipes.

With the two approximations above there is only one remaining cause for deviations from the cylindrical symmetry of the solutions for each borehole alone. This is the asymmetry due to the pipes in the borehole. The temperature field caused by this second term of (A.10) is of the type $cos(\phi_i)/r_i$, if q_1 is taken to be constant. The change ΔT of the temperature field due to this term is:

$$\Delta T \simeq \frac{1}{2\pi r_b} \cdot q_1 \cdot \frac{cos(\phi_i)}{r_i} \cdot \frac{-r_b^2}{\lambda} = -\frac{q_1}{2\pi\lambda} \cdot \frac{r_b}{r_i} cos(\phi_i) \tag{A.15}$$

The order of magnitude of the effect of the ϕ_i-dependent part at another borehole j is obtained by putting r_i equal to B_{ij}. We have:

$$\Delta T \simeq \frac{q_1}{2\pi\lambda} \cdot \frac{r_b}{B_{ij}} \tag{A.16}$$

The amplitude q_1 (and terms of higher order) in (A.10) is judged to be characteristically at least 10 times smaller than q_0 in practical cases.

Let us summarize these estimates of the error, when rotationally symmetric solutions are used for each borehole. The largest error in the temperature at a borehole is from (A.12):

$$\Delta T \simeq \frac{q_0}{2\pi\lambda} \cdot \frac{r_b}{B_{ij}} \tag{A.17}$$

The average value around the borehole of the error (A.12) is zero. The error in temperature levels in predictions of heat fluxes $q_i(z_i, t)$ is therefore of the order (A.13) or (A.16):

$$(\Delta T)_{heat\,flux} = \max\left(\frac{q_0}{2\pi\lambda} \cdot \left(\frac{r_b}{B_{ij}}\right)^2, \frac{q_1}{2\pi\lambda} \cdot \frac{r_b}{B_{ij}}\right) \tag{A.17}$$

Let us consider a numerical example. The following data may be representative for heat extraction borehole:

$$\frac{q_0}{2\pi\lambda} \simeq 1\,^\circ\mathrm{C} \qquad r_b \simeq 0.06\,\mathrm{m} \qquad q_1 \simeq \frac{q_0}{20}$$
$$B_{ij} \simeq 6\,\mathrm{m} \tag{A.18}$$

Then we have:

$$\Delta T \simeq 1 \cdot \frac{1}{100} = 0.01\,^\circ\mathrm{C}$$

$$(\Delta T)_{heat\,flux} = \max\left(1 \cdot \left(\frac{1}{100}\right)^2, \frac{1}{20} \cdot \frac{1}{100}\right) = 5 \cdot 10^{-4}\,^\circ\mathrm{C}$$

This example shows that the errors involved in the presented model are negligible.

REFERENCES

1. P. Eskilson, Superposition Borehole Model. Manual for Computer Code, Dep. of Mathematical Physics, University of Lund, Box 118, S-221 00 Lund, Sweden, 1986.

2. J.E. Bose, J.D. Parker, F.C. McQuiston, Design/Data Manual for Closed-Loop Ground-Coupled Heat Pump Systems, ASHREA, 1791 Tullie Circle, NE, Atlanta, GA 30329, USA, 1985.

3. J. Claesson, P. Eskilson, Conductive Heat Extraction by a Deep Borehole. Analytical Studies. Dep. of Mathematical Physics and Building Technology, University of Lund, Box 118, S-221 00 Lund, Sweden, 1986. (Submitted to Journal of Heat and Mass Transfer)

4. J. Claesson, P. Eskilson, Conductive Heat Extraction by a Deep Borehole. Thermal Analyses and Dimensioning Rules, Dep. of Mathematical Physics, University of Lund, Box 118, S-221 00 Lund, Sweden, 1987.

5. P. Eskilson, J. Claesson, Conductive Heat Extraction by Thermally Interacting Deep Boreholes. Dep. of Mathematical Physics, University of Lund, Box 118, S-221 00 Lund, Sweden, 1987.

6. J. Claesson, G. Hellström, Thermal Resistances to and between Pipes in a Composite Cylinder, Dep. of Mathematical Physics, University of Lund, Box 118, S-221 00 Lund, Sweden, 1987. (To be published.)

7. P. Eskilson, Numerical Study of Radial and Vertical Mesh Division for a Single Heat Extraction Borehole, Notes on Heat Transfer 2-1986, Dep. of Mathematical Physics, University of Lund, Box 118, S-221 00 Lund, Sweden, 1986.

8. P. Eskilson, Numerical Study of the Radial Mesh for Two Systems with 16 and 120 Boreholes, Notes on Heat Transfer 3-1986, Dep. of Building Technology and Matematical Physics, University of Lund, Box 118, S-221 00 Lund, Sweden, 1986.

9. B. Nordell, T. Sehlberg, T. Åbyhammar, System Design for Borehole Heat Stores, General Aspects and Operational Experience from the Store at Luleå, Sweden. Proceedings of Enerstock 85, Toronto, September, 1985.

10. Bergvärme med solvärmeåterladdning för radhusområde i Vällingby (Heat Extraction from Rock with Solar Heat Reinjection for Houses in Vällingby), Swedish State Power Board, Technical report 1983:3.

11. Bergvärme för grupphus i Vallentuna (Heat Extraction from Rock to Support a House in Vallentuna), Swedish State Power Board, Technical report 1983:7.

Notes on Heat Transfer 8-1987

PC-programs for Dimensioning of Heat Extraction Boreholes

Per Eskilson
Departments of Building Technology and Mathematical Physics
Lund Institute of Technology
Box 118, S-221 00 Lund, Sweden

June 1987

CODEN:LUTVDG/(TVBH-7099)/1-19/(1987)

Contents

1 Introduction 1

2 Description of the programs 1

3 Files on the disks 2

4 How to use the programs 2
- 4.1 Run program from a floppy disk . . . 2
- 4.2 Run program from a hard disk . . . 2
- 4.3 Using the programs . . . 2

5 Program TFSING 4
- 5.1 Input Data . . . 4
- 5.2 An example . . . 5

6 Program TFMULT 6
- 6.1 Input Data . . . 6
- 6.2 Save and restore input data . . . 7
- 6.3 An example . . . 7
- 6.4 Choice of g-function . . . 8

7 Program TFSTEP 10
- 7.1 Input Data . . . 10
- 7.2 Save and restore input data . . . 10
- 7.3 An example . . . 11

8 Program DIM 12
- 8.1 Iteration procedure . . . 12
- 8.2 Input Data . . . 12
  - 8.2.1 Alternatives for the time t_{dim} . . . 13
  - 8.2.2 Restrictions on the temperature $T_{f,out}$ . . . 13
- 8.3 Save and restore input data . . . 13
- 8.4 An example . . . 14

9 Program INOUT 15
- 9.1 Input Data . . . 15
- 9.2 An example . . . 15

10 Program QSURF 16
- 10.1 Input Data . . . 16
- 10.2 An example . . . 16

11 Program QTOTSURF 17
- 11.1 An example . . . 17

12 Program GRWATER 18
- 12.1 An example . . . 18

References 19

1 Introduction

An extensive thermal analysis of heat extraction boreholes is presented in [1,2,3]. In these reports different formulas for various important particular processes, and for the thermal dimensioning for single and multiple borehole systems, are presented. These formulas have been adapted to small PC-programs described in this manual. The theory and the PC-programs can also be used for the case with heat injection to the ground, and for combinations of injection and extraction.

The programs run under MS-DOS on IBM-PC and compatible computers. The source code is written in TURBO-PASCAL (Version 3.0). The input is given interactively in a spreadsheet format. The file `README.DOC` may include important information about changes in the programs described in this manual. Be sure to read this file before you use the programs.

2 Description of the programs

There are eight different programs on the disks. The programs TFSING, TFMULT, TFSTEP, and DIM are used for dimensioning, while INOUT, QSURF, QTOTSURF, and GRWATER concern particular thermal processes. A brief description of the programs are given below:

TFSING Calculates the lowest or highest fluid temperature (mean value of the inlet and outlet temperatures) for a single borehole. The heat extraction rate $q(t)$ (W/m) is given by one constant average component, one periodic component, and one superimposed pulse.

TFMULT Calculates the lowest or highest fluid temperature for a multiple borehole system (or a single borehole). The heat extraction rate is of the same type as for the program TFSING.

TFSTEP Calculates the fluid temperature for a single borehole or a multiple borehole system at an arbitrary time. The heat extraction rate $q(t)$ (W/m) is given by 12 steps or less with arbitrary lengths. The 12 steps are repeated cyclically after the period time t_p (normally 1 year).

DIM Calculates by iteration the required active borehole length H for a single borehole or a multiple borehole system when the outlet fluid temperature is prescribed at a certain time, or when the lowest or highest temperature during the year (or any other period) is prescribed. The total heat extraction rate $Q(t)$ (W) is given by twelve steps or less. The twelve steps may be repeated cyclically.

INOUT Calculates simply the inlet and outlet temperatures when the mean fluid temperature is given. The program INOUT is useful when the mean fluid temperature has been calculated by either of the programs TFSING, TFMULT, and TFSTEP.

QSURF Calculates the heat flow through the ground surface q_{surf} (W/m^2) at the radius r from the centre of a single borehole.

QTOTSURF Calculates the total heat flow through the ground surface Q_{surf} (W) for a single borehole.

GRWATER Calculates the steady-state temperature at the borehole wall for a single borehole, when the heat extraction is influenced by groundwater filtration.

3 Files on the disks

The executable code of the program lies on the root directory of the two disks. Some of the programs on disk 1 require additional data files, which lie on the directory `\borehole\gfunc`. The two disks contain the following programs:

Disk 1

`README.DOC`	Updates this manual to the current version of the programs.
`TFMULT.COM`	Lowest (or highest) fluid temperature for a system with multiple boreholes.
`TFSTEP.COM`	Fluid temperature $T_f(t_{print})$ at the time t_{print}.
`DIM.COM`	Required borehole length for a prescribed lowest outlet temperature.

Disk 2

`TFSING.COM`	Lowest (or highest) fluid temperature for a single borehole.
`INOUT.COM`	Inlet and outlet temperature.
`QSURF.COM`	Heat flow q_{surf} (W/m^2) through the ground surface.
`QTOTSURF.COM`	Total heat flow Q_{surf} (W) through the ground surface.
`GRWATER.COM`	Steady-state temperature decrease allowing for groundwater filtration.

4 How to use the programs

4.1 Run program from a floppy disk

To run the programs, insert the disk 1 or 2 into a drive, make that drive the default drive, and type the program name.

4.2 Run program from a hard disk

To install the *entire* package with programs onto the hard disk, insert the disk into drive A and type `a:install`. The installation program will create a directory `c:\borehole` and one subdirectory `c:\borehole\gfunc`. The programs will be copied from the two disks to the directory `c:\borehole`. The g-functions (which are explained below) are copied to the subdirectory `c:\borehole\gfunc`.

To run a program make `c:\borehole` the default directory and type the program name.

4.3 Using the programs

Start the program according to the instructions given above. A spreadsheet menu is displayed on the screen. The input parameters are given values of a basic example. The corresponding results are shown. Enter your input data. Use the cursor keys ↑, ↓, Home, and End to move. The results are obtained by pressing the Enter key. These results are always in accordance with the displayed input parameter values. If an input value is out of the allowed range, the program will give an error message and the results are not displayed. Correct this by changing the erroneous value and press Enter once more. Press the ESC key to leave the program.

All input data are given in SI-Units. However, the input of time values may be facilitated by using special characters to represent common time units, i.e. years, months (=1/12 year), days, hours, and seconds. An example is 25y6m12d6h200s which represents 25 years 6 months

12 days 6 hours and 200 seconds. Any of the time units may be left out. However, the order must be in decreasing time units, e.g. the number of years must preceed the number of days.

5 Program TFSING

The program TFSING (Fluid temperature T_f, single borehole) calculates the lowest fluid temperature $T_{f,min}$ (or highest $T_{f,max}$, when heat is injected) for a single borehole, when the heat extraction rate is given by one average component q_0, one periodic component with the amplitude q_p and the period time t_p (= 1 year normally), and one superimposed pulse q_1 with the duration t_1. The three extraction components (q_0, q_p, q_1) are positive (any of them may also be zero), when heat is extracted, and negative when heat is injected to the ground. Heat is extracted over the depth H [1].

In Eq. (1) given below, the extraction case is considered. The temperature T_f is the mean value of the inlet and outlet temperature to the borehole. The minimum value of T_f is denoted $T_{f,min}$ and is given by Eq.(37) in [2] as:

$$T_{f,min} = T_{om} - q_0 \cdot R_s - q_p \cdot R_p - q_1 \cdot R_q(t_1) - (q_0 + q_p + q_1) \cdot R_b \qquad (1)$$

The explicit expressions for R_s, R_p, and $R_q \simeq R'_q$ are given by Eqs. (6.4), (8.4), and (5.3) in [1]. The borehole thermal resistance R_b is discussed in [2]. The effective undisturbed ground temperature T_{om} is discussed in detail in [2]. Equation (1) is based on the assumption that the end of the extraction pulse and the maximum of the periodic heat extraction occurs roughly at the same time. The discussion given above is valid also for the case of heat injection. The temperature $T_{f,min}$ is then replaced by the maximum fluid temperature $T_{f,max}$.

5.1 Input Data

H	Active borehole length, (m)
r_b	Borehole radius, (m)
λ	Thermal conductivity of the ground, (W/(mK))
C	Volumetric heat capacity of the ground, (J/(m^{3}K))
T_{om}	Effective undisturbed ground temperature, (°C)
R_b	Thermal resistance between the fluid channels and the borehole wall, (K/(W/m))
t_p	Period time for periodic heat extraction component
t_1	Duration of heat extraction pulse
q_0	Average heat extraction rate, (W/m)
q_p	Amplitude of the periodic heat extraction component, (W/m)
q_1	Heat extraction rate for superimposed pulse, (W/m)

The time t_1 must be greater than $5r_b^2/a$ [2], where a is the thermal diffusivity ($a = \lambda/C$).

Combinations of positive and negative values on the three extraction rates q_1, q_2, and q_3 are not allowed.

[1] The total borehole depth is $H + D$, where D is the thermally insulated upper part, and H is the active part over which heat is extracted. The depth D may for example be the depth of the ground water table, or the depth of an insulated casing. The depth D is of secondary importance in our applications

5.2 An example

When the program is started, the following sample case will be displayed on the screen:

```
Program TFSING : Lowest/highest fluid temperature for a single borehole

     Active borehole length, H      110.0_____  (m)
     Borehole radius, rb            0.055       (m)
     Thermal conductivity, lambda   3.5         (W/(mK))
     Volumetric heat capacity, C    2160000.    (J/(m3K))
     Undist. ground temp, Tom       8.0         (°C)
     Borehole therm. res., Rb       0.1         (K/(W/m))
     Period time, tp                1y
     Duration for pulse, t1         1m
     Average heat extraction, q0    20.0        (W/m)
     Periodic heat extraction, qp   15.0        (W/m)
     Extraction rate for pulse, q1  10.0        (W/m)

                    Thermal resistances (K/(W/m))
Steady-state, Rs = 0.314   Periodic, Rp = 0.188   Pulse, Rq(t1) = 0.183

              Lowest fluid temperature Tf,min =   -7.44  °C

Use cursor keys ↓ ↑  Home End to move      Enter Run  ESC Quit
```

6 Program TFMULT

The program TFMULT (Fluid temperature T_f, multiple boreholes) calculates the lowest fluid temperature $T_{f,min}$ (or highest $T_{f,max}$ when heat is injected) for the case with multiple thermally interacting boreholes. The heat extraction rate is given by one constant component q_0 until the time t_{dim}, one periodic component with the amplitude q_p and the period time t_p, and one superimposed pulse q_1 with the duration t_1. The average component q_0 starts at the time zero and continues until the time t_{dim}, which is the dimensioning time [3].

The three extraction components (q_0, q_p, q_1) are all positive (any of them may also be zero) when heat is extracted, and negative when heat is injected to the ground.

In Eq. (1) given below, the extraction case is considered. The temperature T_f is the mean value of the inlet and outlet temperature to the borehole. The minimum value of T_f is denoted $T_{f,min}$, and it is given by the first dimensioning rule in [3] as:

$$\begin{aligned} T_{f,min} &= T_{om} - q_0 \cdot R_q(t_{dim}) - q_p \cdot R_p - q_1 \cdot R_q(t_1) - (q_0 + q_p + q_1) \cdot R_b \\ &\quad (t_{dim} \geq 5r_b^2/a, \quad t_1 \geq 5r_b^2/a) \end{aligned} \tag{2}$$

The thermal resistance $R_q(t)$ can be calculated only if the temperature response function for the particular borehole configuration is known. The temperature response function is given by a so-called g-function. The g-function depends on the relative spacing B/H. Here B is the spacing at the ground surface between two neighbouring boreholes, and H is the active borehole length. See footnote[1] at page 4.

In the case of graded boreholes the g-functions also depend on the tilt angle θ relative to the vertical. Note that when H is changed in the input, the value of B is changed too, since B/H is constant for each particular g-function. The borehole thermal resistance R_b, and the effective undisturbed ground temperature T_{om} are discussed in [2]. The discussion given above is valid also for the case of heat injection. The temperature $T_{f,min}$ is then replaced bu the maximum fluid temperature $T_{f,max}$.

Eq. (2) is based on the assumption that the end of the extraction pulse and the maximum of the periodic heat extraction occurs at the time t_{dim}. The exact value of t_{dim} during the period is not important after more than, say, three period times ($t_{dim} \geq 3t_p$). Normal values for t_{dim}, when t_p is equal to one year, are 5 to 25 years.

6.1 Input Data

H	Active borehole length, (m) (See footnote[1], page 4.)
r_b	Borehole radius, (m)
λ	Thermal conductivity of the ground, (W/(mK))
C	Volumetric heat capacity of the ground, (J/(m^{3}K))
T_{om}	Effective undisturbed ground temperature, (°C)
R_b	Thermal resistance between the fluid channels and the borehole wall, (K/(W/m))
t_{dim}	Duration of the dimensioning period
t_p	Period time for periodic heat extraction component
t_1	Duration of heat extraction pulse
q_0	Average heat extraction rate, (W/m)
q_p	Amplitude of the periodic heat extraction component, (W/m)
q_1	Heat extraction rate for superimposed pulse, (W/m)

The times t_1 and t_p must both be larger than $5r_b^2/a$, $(a = \lambda/C)$.

Combinations of positive and negative values on the three extraction rates q_0, q_p, and q_1 are not allowed.

6.2 Save and restore input data

To save the input data on a file, press **F1** and enter the filename. The data will be stored on the file `filename.dat`. The extension `.dat` is added automatically.

To restore input data from a file, press **F2** and enter the filename. The data will then be restored from the file `filename.dat`.

6.3 An example

When the program is started, the following sample case will be displayed on the screen:

```
Program TFMULT : Lowest/highest fluid temperature for a multiple borehole system

        Name of g-function
        Active borehole length, H        110.0_____ (m)
        Borehole radius, rb              0.055      (m)
        Thermal conductivity, lambda     3.5        (W/(mK))
        Volumetric heat capacity, C      2160000.   (J/(m3K))
        Undist. ground temp, Tom         8.0        (°C)
        Borehole therm. res., Rb         0.1        (K/(W/m))
        Duration of dim. period, tdim    25y
        Period time, tp                  1y
        Pulse time, t1                   1m
        Average heat extraction, q0      20.0       (W/m)
        Periodic heat extraction, qp     15.0       (W/m)
        Extraction rate for pulse, q1    10.0       (W/m)

                        Thermal resistances (K/(W/m))
   Average, Rq(t) = 0.291   Periodic, Rp = 0.188   Pulse, Rq(t1) = 0.183

              Lowest fluid temperature Tf,min =   -6.98 °C

F1 Save  F2 Read              g-function F3 List  F4 Read    Enter Run  Esc Quit
```

6.4 Choice of g-function

In the present version of the program, g-functions for 50 different borehole configurations can be chosen. For each configuration there is also a choice of g-functions for different B/H (and θ). These g-functions have been calculated with use of the large simulation model Superposition Borehole Model [6,7]. Figures of these configurations and curves of the g-functions are shown in [4] and [5]. Each borehole configuration has an identification number (1-50), defined in the list of g-functions. Press F3 key. The following list below will then be displayed.

A configuration is chosen by pressing the F4 key, and then entering the identification number of the configuration. After this the program will prompt for a choice of the B/H-value, or in the case of graded boreholes, for a choice of the tilt angle θ. Only the given parameter values for B/H and θ are used. There is no interpolation for values in between.

The parameter values of the different g-functions are given on files in the directory \borehole \gfunc of disk 1. The first line on each g-file contains a text string, which is displayed when the program uses that particular g-function. The second line contains the number of boreholes N_b, and the relative spacing B/H between the boreholes. The third line contains the number of parameter values N_{par} for the g-function. The following N_{par} lines contain each a $ln(t/t_s)$-value and a value of the g-function. There is linear interpolation between the points.

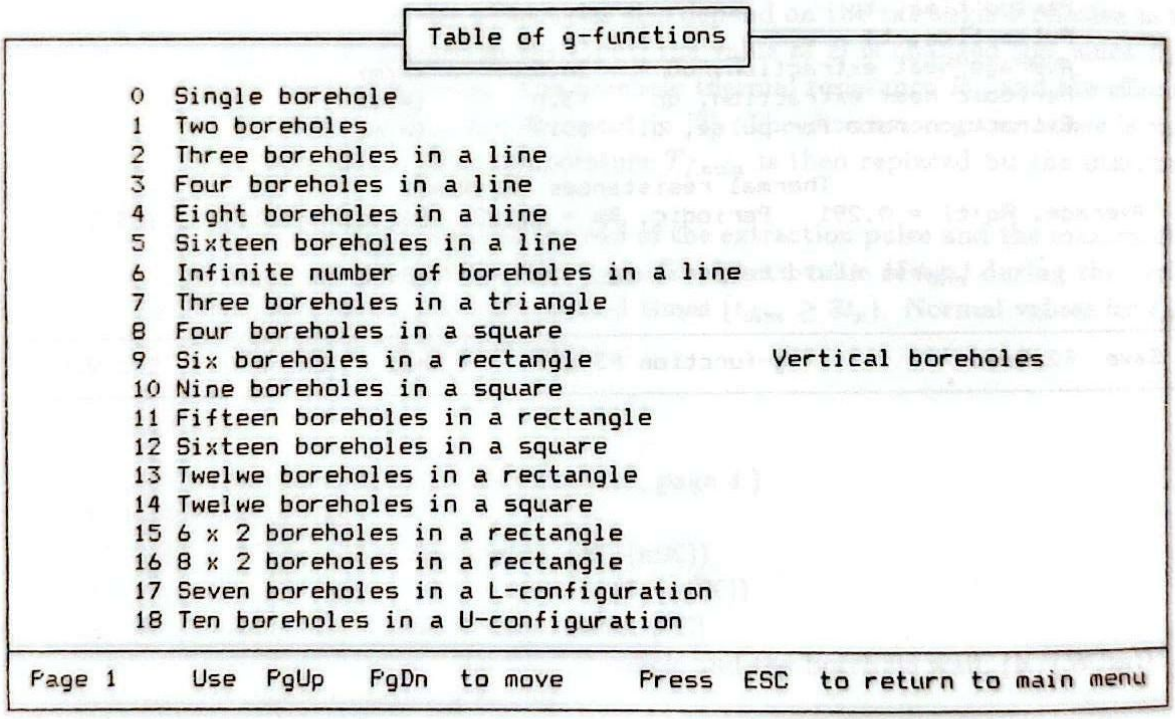

Table of g-functions

```
19 Two boreholes, B/H=0.1
20 Two boreholes, B/H=0.05
21 Four boreholes in a line, B/H=0.1
22 Four boreholes in a line, B/H=0.05
23 Six boreholes in a line, B/H=0.1
24 Six boreholes in a line, B/H=0.05
25 Four boreholes in a square, B/H=0.1
26 Four boreholes in a square, B/H=0.01
27 Six boreholes in a circle, B/H=0.1
28 Six boreholes in a circle, B/H=0.01      Graded boreholes
29 Eight boreholes in a circle, B/H=0.1
30 Eight boreholes in a circle, B/H=0.01
31 4 + 1 boreholes in a circle, B/H=0.1
32 4 + 1 boreholes in a circle, B/H=0.01
33 6 + 1 boreholes in a circle, B/H=0.1
34 6 + 1 boreholes in a circle, B/H=0.01
35 8 + 1 boreholes in a circle, B/H=0.1
36 8 + 1 boreholes in a circle, B/H=0.01
```

Page 2 Use PgUp PgDn to move Press ESC to return to main menu

Table of g-functions

```
37 Eight boreholes in a fan-shaped configuration
38 Eight boreholes in an optimum configuration
39 Six boreholes in a line
40 Eight boreholes in a line
41 Ten boreholes in a line
42 6 x 2  (=12) boreholes in a rectangle
43 8 x 2  (=16) boreholes in a rectangle
44 10 x 2 (=20) boreholes in a rectangle
45 6 x 3  (=18) boreholes in a rectangle
46 8 x 4  (=32) boreholes in a rectangle   Vertical boreholes
47 10 x 5 (=50) boreholes in a rectangle   (except 37 and 38)
48 6 x 6  (=36) boreholes in a square
49 8 x 8  (=64) boreholes in a square
50 10 x 10 (=100) boreholes in a square
51 External g-function, given by user
```

Page 3 Use PgUp PgDn to move Press ESC to return to main menu

7 Program TFSTEP

The program TFSTEP calculates the fluid temperature T_f at a time t_{print} for the case with multiple, thermally interacting boreholes. The heat extraction is given by a maximum of 12 consequtive steps q_n (n=1,2,...,12). The step n (n <12) has a duration $t_n < t \leq t_{n+1}$. The last step (n=12) is valid during the intervall $t_{12} < t \leq t_p$. The program ignores steps starting at a time $t_n \geq t_{print}$.

After the time t_p the values $q_1 ... q_{12}$ are repeated cyclically with the period time t_p. The total number of steps N used in the calculation is determined by the condition $t_N < t_{print} \leq t_{N+1}$.

The fluid temperature T_f is the mean value between the inlet and outlet temperature. The expression for T_f is given in [3] as:

$$T_f(t_{print}) = T_{om} - \sum_{n=1}^{N} (q_n - q_{n-1}) \cdot R_q(t_{print} - t_n) - q_N \cdot R_b \qquad (3)$$

$$t_{print} > t_N + 5r_b^2/a$$

The thermal resistance $R_q(t)$ can be calculated only if the temperature response function for the particular borehole configuration is known. The temperature response function is given by a so-called g-function. The g-function depends on the relative spacing B/H. Here B is the spacing at the ground surface between two neighbouring boreholes. In the case of graded boreholes the g-functions also depend on the tilt angle θ relative to the vertical. Note that when H is changed in the input, the value of B is changed too since B/H is constant for each particular g-function. The choice of g-function is explained in section 6.4.

The borehole thermal resistance R_b and the effective undisturbed ground temperature T_{om} are discussed in [2].

7.1 Input Data

H	Active borehole length, (m) (See footnote[1], page 4)
r_b	Borehole radius, (m)
λ	Thermal conductivity of the ground, (W/(mK))
C	Volumetric heat capacity of the ground, (J/(m^{3}K))
T_{om}	Effective undisturbed ground temperature, (°C)
R_b	Thermal resistance between the fluid channels and the borehole wall, (K/(W/m))
t_p	Period time for cyclical repetition (and end time for step 12)
t_{print}	Print-out time for results.
t_n	Start time for heat extraction step q_n (n =1,2,..., 12)
q_n	Heat extraction rate in the intervall $t_n < t \leq t_{n+1}$, (n=1,2,...,12), (W/m)

The time t_{print} must satisfy the condition $t_{print} > t_N + 5r_b^2/a$ [2]. All times t_n, for $n = 1...N$, must satisfy the condition $t_n \leq t_{n+1}$. All times t_n (n=1...12) must be smaller than t_p.

To illustrate the different time conditions consider an example with two pulses (N=2). We have then the restriction: $t_1 \leq t_2 + 5r_b^2/a \leq t_{print} \leq t_3$. The times $t_4 ... t_{12}$ may be given any values ($< t_p$), since they are not used.

Note that when heat is injected to the ground the sign of the heat extraction rate q_n is negative.

7.2 Save and restore input data

To save the input data on a file, press F1 and enter the filename. The data will then be stored on the file `filename.dat`. The extension `.dat` is added automatically.

To restore input data from a file, press F2 and enter the filename. The data will then be restored from the file **filename.dat**.

7.3 An example

When the program is started, the following sample case will be displayed on the screen:

```
Program TFSTEP : Fluid temperature Tf (°C) for a step-wisely varying
heat extraction (with maximum 12 steps with periodic repetition)

Name of g-function                                   tn         | qn (W/m)
                                                     -----------+---------
Active borehole length, H      110.0_____  (m)                  |
Borehole radius, rb            0.055       (m)          0m      |16.0
Thermal conductivity, lambda   3.5         (W/(mK))     1m      |23.0
Volumetric heat capacity, C    2160000.    (J/(m3K))    2m      |31.0
Undist. ground temp, Tom       8.0         (°C)         3m      |38.0
Borehole therm. resist., Rb    0.1         (K/(W/m))    4m      |41.0
Period time, tp                1y                       5m      |39.0
Print-out time, tprint         5m                       6m      |33.0
                                                        7m      |26.0
                                                        8m      |17.0
                                                        9m      |0
                                                        10m     |0
                                                        11m     |0

Distance between the boreholes,     B =     0.00  m
Average fluid temperature,         Tf =   -4.709 °C

F1 Save  F2 Read        g-function: F3 List  F4 Read     Enter Run  Esc Quit
```

8 Program DIM

The program DIM (Dimensioning) calculates the required active borehole length H for the case with multiple, thermally interacting boreholes, when the lowest or highest outlet temperature from the boreholes , $T_{f,out}$, is given as input. The heat extraction is given by a maximum of 12 consequtive steps Q_n (n=1,2,...,12). Note that Q_n (W) is the total heat extraction rate from all the boreholes, $Q_n = q_n \cdot H \cdot N_b$, where N_b is the number of boreholes (assuming equal length). Each step Q_n has a duration $t_n < t \leq t_{n+1}$. The last step Q_{12} is valid during the intervall $t_{12} < t < t_p$, where t_p is the end time for pulse 12. After the time t_p the values $Q_1 ... Q_{12}$ are repeated cyclically with the period time t_p. Note that $t_n \leq t_{n+1}$ and $t_{12} \leq t_p$ [2]. All boreholes are coupled in parallel with the total pumping rate V_f (m^3/s).

The active borehole length H is calculated by an iterative procedure, see below. The iteration procedure stops when the calculated outlet temperature differs with less than $0.01°C$ from the prescribed value. The iteration procedure fails when H decreases below $100 \cdot r_b$. The equations, on which the thermal analyses are based on, are not valid for $H < 100 r_b$. The program will then display an error message.

The program DIM requires a temperature response function g for the borehole configuration (compare with program TFSTEP). To choose a particular g-function see section 6.4.

8.1 Iteration procedure

An inital trial value of $H^{\nu=0}$ (=110 m) is automatically set by the program. The average fluid temperature is then calculated according to Eq. (3), with $t_{dim} = t_{print}$. The outlet temperature becomes $T_{f,out} = T_f + Q_i/(2C_f V_f)$ [2]. The outlet temperature temperature is used to calculate a new trial borehole length $H^{\nu+1}$ according to:

$$H^{\nu+1} = \frac{T_{f,out}^{trial,\nu} - T_{om}}{T_{f,out} - T_{om}} \cdot H^{\nu} \tag{4}$$

The order of iteration is denoted ν. The iteration procedure stops when $|T_{f,out}^{trial,\nu} - T_{f,out}| <$ 0.01 °C, or when $H^{\nu+1}$ decreases below $100 \cdot r_b$ (see above).

8.2 Input Data

r_b	Borehole radius, (m)
λ	Thermal conductivity of the ground, (W/(mK))
C	Volumetric heat capacity of the ground, ($J/(m^3K)$)
T_{om}	Effective undisturbed ground temperature, (°C)
R_b	Thermal resistance between the fluid channels and the borehole wall, (K/(W/m))
C_f	Volumetric heat capacity of the fluid, ($J/(m^3K)$)
V_f	Pumping rate of the fluid, (m^3/s)
$T_{f,out}$	Prescribed outlet temperature of the heat-carrier fluid
t_p	Period time for cyclical repetition (and end time for step 12)
t_{dim}	Duration of the dimensioning period
t_n	Start time for heat extraction step q_n (n =1,2,..., 12)
Q_n	Heat extraction rate during $t_n < t \leq t_{n+1}$, (n=1,2,...,12), (W/(mK))

The lowest lowest outlet temperature is calulated when $T_{f,out}$ is given a value lower than T_{om}, and the highest oulet temperature is calculated when $T_{f,out}$ is higher than T_{om}. Note that when heat is injected to the ground the sign of the heat extraction rate q_n is negative.

[2] For cases with less than 12 steps, see chapter 7. The parameters t_{print} and t_{dim} are used in exactly the same way, with the same restrictions.

8.2.1 Alternatives for the time t_{dim}

The time t_{dim} may be chosen in two alternative ways:

1. *The time t_{dim} is not a multiple of t_p:* [3] In this case the program considers $T_{f,out}$ as the outlet temperature at the time t_{dim} and calculates the required borehole length H at this paricular time. The time t_{dim} occurs during pulse N with the heat extraction Q_N [4]. The time t_{dim} must satisfy the condition $t_{dim} > t_N + 5r_b^2/a$. Otherwise, an error message will be displayed.

2. *The time t_{dim} is a multiple of t_p:* In this case the program consider the temperature $T_{f,out}$ as the lowest (or highest) outlet temperature during the whole dimensioning period until the time t_{dim}. The required H is calculated. The lowest (or highest) temperature always occurs at the end of one of the twelve pulses during the last cycle. The times t_n must satisfy the conditions $t_n > t_{n-1} + 5r_b^2/a$, for n=1,...N, and $t_p > t_{12} + 5r_b^2/a$. Otherwise, an error message will be displayed.

8.2.2 Restrictions on the temperature $T_{f,out}$

The prescribed outlet temperature $T_{f,out}$ must be within a certain range in order to give physically meaningful results. If the value of $T_{f,out}$ lies outside the allowed range, then the iterative procedure will not converge, the calculation will be interrupted, and an error message will be displayed. Typically the error is caused by a too low value of V_f or by a too high value of $T_{f,out}$ in the case of heat extraction, or a too low value of $T_{f,out}$ in the case of heat injection. The restrictions on $T_{f,out}$ for the two alternatives for t_{dim} are:

1. The time t_{dim} is *not* a multiple of t_p:

   - $Q_N > 0$, *i.e. dimensioning for an extraction pulse N:* The temperature $T_{f,out}$ must satisfy the condition $T_{f,out} < T_{om} - Q_N/(2C_fV_f)$.
   - $Q_N < 0$, *i.e. dimensioning for an injection pulse N:* The temperature $T_{f,out}$ must satisfy the condition $T_{f,out} > T_{om} - Q_N/(2C_fV_f)$.

2. The time t_{dim} is a multiple of t_p:

   - $max_{1\le n\le 12}[Q_n] > 0$ *and dimensioning for heat extraction:* The temperature $T_{f,out}$ must satisfy the condition $T_{f,out} < \min_{1\le n\le 12}[T_{om} - Q_n/(2C_fV_f)]$.
   - $min_{1\le n\le 12}[Q_n] < 0$ *and dimensioning for heat injection:* The temperature $T_{f,out}$ must satisfy the condition $T_{f,out} > \max_{1\le n\le 12}[T_{om} - Q_n/(2C_fV_f)]$.

8.3 Save and restore input data

To save the input data on a file, press F1 and enter the filename. The data will then be stored on the file `filename.dat`. The extension `.dat` is added automatically.

To restore input data from a file, press F2 and enter the filename. The data will then be restored from the file `filename.dat`.

[3] The time t_{dim} may in this case be any time except a multiple of t_p

[4] The parameter N is defined by the condition $t_N < t_{dim} \le t_{N+1}$.

8.4 An example

When the program is started, the following sample case will be displayed on the screen:

```
Program DIM : Required borehole depth H for one by the user chosen lowest
outlet temperature Tf,out (°C)

Name of g-function

                                                        tn      | Qn (W)
Borehole radius, rb              0.055_____   (m)
Thermal conductivity, lambda     3.5          (W/(mK))   0m      | 1760.0
Volumetric heat capacity, C      2160000.     (J/(m3K))  1m      | 2530.0
Undist. ground temp, Tom         8.0          (°C)       2m      | 3410.0
Borehole therm. resist., Rb      0.1          (K/(W/m))  3m      | 4180.0
Vol. fluid heat cap., Cf         4200000.     (J/(m3K))  4m      | 4510.0
Pumping rate, Vf                 0.0005       (m3/s)     5m      | 4290.0
Outlet temperature, Tf,out       -4.4         (°C)       6m      | 3630.0
Period time, tp                  1y                      7m      | 2860.0
Dimensioning time, tdim          5m                      8m      | 1870.0
                                                         9m      | 0.
                                                         10m     | 0.
Inlet fluid temperature,      Tf,in =    -6.55 °C       11m     | 0.
Distance between boreholes,       B =     0.00 m
Required active borehole depth,   H =   103.71 m
Tf,in and Tf,out are the inlet and outlet temperature at the time tdim

F1 Save  F2 Read          g-function: F3 List  F4 Read    Enter Run  Esc Quit
```

9 Program INOUT

The program INOUT calculates simply the inlet temperature $T_{f,in}$ and the outlet temperature $T_{f,out}$ according to (35) in [2], when the average value T_f between the inlet and outlet temperature is known:

$$T_{f,in} = T_f + \frac{Q}{2C_f V_f} \qquad T_{f,out} = T_f - \frac{Q}{2C_f V_f} \tag{5}$$

The pumping rate V_f always is positive. The temperature T_f is obtained by any of the programs TFSING, TFMULT, TFSTEP.

The total heat extraction rate is equal to $Q = q \cdot N_b H$, where q is the heat extraction rate per meter borehole, and N_b the number of boreholes (with equal length). The heat extraction rate q is in the program TFSING and TFMULT equal to $q_0 + q_p + q_1$, and in the program TFSTEP q is equal to q_N.

9.1 Input Data

T_f Average fluid temperature, (°C)
C_f Volumetric heat capacity of the fluid, $(C_f = \rho_f c_f)$, J/(m³K)
V_f Pumping rate, m³/s
Q Total heat extraction rate $Q = q \cdot N_b H$, at the considered time, (W)

9.2 An example

When the program is started, the following sample case will be displayed on the screen:

```
INOUT :  Inlet temperature Tf,in (°C) and outlet temperature Tf,out (°C)

     Average fluid temperature, Tf  -2.0_____  (°C)
     Volumetric heat capacity, Cf   4200000.  (J/(m3K))
     Pumping rate of the fluid, Vf  0.001      (m3/s)
     Heat extraction rate, Q        2200.0     (W)

        Inlet  fluid temperature Tf,in  =   -2.262 °C
        Outlet fluid temperature Tf,out =   -1.738 °C

Use cursor keys ↑ ↓  Home End to move     Enter Run  ESC Quit
```

10 Program QSURF

The program QSURF calculates the heat flow q_{surf} (W/m^2) through the the ground surface at the radius r from the centre of a single borehole. The expression for q_{surf} is given by formula (11.1) in [1]:

$$q_{surf}(r,t) = \frac{q_1}{2\pi}\left[\frac{1}{\sqrt{r^2+D^2}}erfc\left(\frac{\sqrt{r^2+D^2}}{\sqrt{4at}}\right) - \frac{1}{\sqrt{r^2+(D+H)^2}}erfc\left(\frac{\sqrt{r^2+(D+H)^2}}{\sqrt{4at}}\right)\right] \quad (6)$$

The heat flow q_{surf} is the thermal disturbance at the ground surface due to a constant heat extraction q_1 from a single vertical borehole.

10.1 Input Data

H	Active borehole length, (m)
D	Depth of thermally insulated upper part of the borehole, (m)
a	Thermal diffusivity, $a = \lambda/\rho c$, (m^2/s)
r	Radial distance from the center of the borehole, (m)
q_1	Heat extraction rate, (W/m)
t	Time

10.2 An example

When the program is started, the following sample case will be displayed on the screen:

```
Program QSURF : Heat flow, qsurf (W/m²), through the ground surface

   Active borehole length      (H)   110.0_____ m
   Insulated borehole length   (D)   5.0        m
   Thermal diffusivity         (a)   1.62E-6    m²/s
   Radial distance             (r)   25.0       m
   Heat extraction rate        (q1)  22.0       W/m
   Time                        (t)   10y

   Heat flow through the ground surface, qsurf =  0.05838  W/m²

Use cursor keys ↑ ↓  Home End to move     Enter Run  ESC Quit
```

11 Program QTOTSURF

The program QTOTSURF calculates the total heat flow Q_{surf} (W) through the ground surface for a single borehole according to formula (11.5) in [1].

$$Q_{surf}(t) = q_1\sqrt{4at}\left\{ierfc(\frac{D}{\sqrt{4at}}) - ierfc(\frac{D+H}{\sqrt{4at}})\right\} \quad (7)$$

The heat flow Q_{surf} is compared with the total heat extraction rate $q_1 \cdot H$ (W) from the borehole. The heat flow Q_{surf} approaches $q_1 \cdot H$, when t tends to infinity. At steady-state all the extracted heat comes from the ground surface.

H	Active borehole length, (m)
D	Depth of thermally insulated upper part of the borehole, (m)
a	Thermal diffusivity, $a = \lambda/C$, (m^2/s)
q_1	Heat extraction rate, (W/m)
t	Time

11.1 An example

When the program is started, the following sample case will be displayed on the screen:

```
Program QTOTSURF : Total heat flow, Qsurf (W), through ground surface

        Active borehole length      (H)   110.0_____ m
        Insulated borehole length   (D)   5.0        m
        Thermal diffusivity         (a)   1.62E-6    m²/s
        Heat extraction rate        (q1)  22.0       W/m
        Time                        (t)   10y

        Total heat flow through the ground surface,  Qsurf =   457.89 W
        Total heat extraction rate,                  q1*H  =  2420.00 W

                                                Qsurf/(q1*H) =    0.189

Use cursor keys ↑ ↓  Home End to move     Enter Run  ESC Quit
```

12 Program GRWATER

The program GRWATER calculates the steady-state temperature deviation (from the undisturbed level T_{om}) at the borehole wall for a single borehole, when the heat extraction is influenced by groundwater filtration. The ground is treated as a homogeneous porous medium. The borehole temperature is then according to formula (11.5) in [1]:

$$T_{sw,b} = -q_0 \cdot R_{sw} \qquad (8)$$

The thermal resistance R_{sw} is in the program compared with the normal steady-state thermal resistance R_s without groundwater filtration. A condition for validity of Eq. (7) is: $\lambda/(5C_wKI) > r_b$ [1].

H	Active borehole length, (m)
r_b	Borehole radius, (m)
λ	Thermal conductivity of the ground, (W/(mK))
C_w	Volumetric heat capacity of the groundwater, $C_w = \rho c_w$, (J/(m^{3}K))
K	Hydraulic conductivity, (m/s)
I	Gradient of the groundwater table , (m/m)
q_0	Heat extraction rate, (W/m)

12.1 An example

When the program is started, the following sample case will be displayed on the screen:

```
Program GRWATER : Temperature increase at the borehole at steady-state for
the case without and the case with groundwater filtration

   Active borehole length      (H)   110.0_____  m
   Borehole radius             (rb)  0.055       m
   Thermal conductivity  (lambda)    3.5         W/(mK)
   Volumetric heat capacity  (Cw)    4.2E6       J/(m3K)
   Hydraulic conductivity      (K)   1.0E-6      m/s
   Gradient of water table     (I)   0.0151515   m/m
   Heat extraction rate        (q)   22.0        W/m


   Thermal resistances (K/(W/m))    Rs  0.314     Rsw   0.308

   Borehole temperature (°C)       Ts,b -6.911   Tsw,b  -6.786

   Influence of groundwater filtration, 100*(Rs-Rsw)/Rs (%)    1.80

Use cursor keys ¦ ¦  Home End to move     Enter Run  ESC Quit
```

References

[1] J. Claesson, P. Eskilson, Conductive Heat Extraction by a Deep Borehole. Analytical Studies. Dep. of Mathematical Physics and Building Technology, University of Lund, Box 118, S-221 00 Lund, Sweden, 1986. (Submitted to Journal of Heat and Mass Transfer)

[2] J. Claesson, P. Eskilson, Conductive Heat Extraction by a Deep Borehole. Thermal Analyses and Dimensioning Rules, Dep. of Mathematical Physics, University of Lund, Box 118, S-221 00 Lund, Sweden, 1987.

[3] P. Eskilson, J. Claesson, Conductive Heat Extraction by Thermally Interacting Deep Boreholes. Dep. of Mathematical Physics, University of Lund, Box 118, S-221 00 Lund, Sweden, 1987.

[4] P. Eskilson, Temperature Response Function g for 38 Borehole Configurations, Notes on Heat Transfer 4-1986, Dep. of Mathematical Physics and Building Technology, University of Lund, Box 118, S-221 00 Lund, Sweden, 1986.

[5] P. Eskilson, Temperature Response Function g for 12 Borehole Configurations, Notes on Heat Transfer 5-1987, Dep. of Mathematical Physics and Building Technology, University of Lund, Box 118, S-221 00 Lund, Sweden, 1987.

[6] J. Claesson, P. Eskilson, Simulation Model for Thermally Interacting Heat Extraction Boreholes, Dep. of Mathematical Physics, University of Lund, Box 118, S-221 00 Lund, Sweden, 1987.

[7] P. Eskilson, Superposition Borehole Model. Manual for Computer Code, Dep. of Mathematical Physics, University of Lund, Box 118, S-221 00 Lund, Sweden, 1986.

Notes on Heat Transfer 9-1987

Response Test for a Heat Store with 25 Boreholes

Per Eskilson, Göran Hellström
Departments of Building Technology and Mathematical Physics,
Lund Institute of Technology, Box 118, S-221 00 Lund, Sweden

Bengt Wånggren
Monitoring Centre for Energy Research,
Royal Institute of Technology,
S-100 44 Stockholm, Sweden

June 1987

CODEN:LUTVDG/(TVBH-7100)/1-21/(1987)

Response Test for a Heat Store with 25 Boreholes

Per Eskilson, Göran Hellström
Departments of Building Technology and Mathematical Physics
Lund Institute of Technology, Box 118, S-221 00 Lund, Sweden

Bengt Wånggren
Monitoring Centre for Energy Research, Royal Institute of Technology
S-100 44 Stockholm, Sweden

June 1987

Summary

A response test was performed for a heat store with 25 boreholes. Heat was injected at a constant rate of about 100 kW during a few days (with two interruptions). The inlet and outlet temperatures of the heat-carrier fluid were measured for the whole system of 25 boreholes coupled in parallel, and for three separate boreholes.

The meaurements give the effective average thermal conductivity and the thermal resistance R_b between the fluid and the borehole wall. The mathematical analysis of this response test method is presented.

The effective thermal conductivity became 4.5, 3.8, and 3.2 W/mK for three different time intervals. The difference may be due to transient effects of the temperature variation along the borehole or convective heat transfer with warmer water flowing out in cracks near the borehole. This should be analyzed further. The measured value of R_b was 0.1 K/(W/m). This is in accordance with theoretical estimates of R_b that are based on conductive heat transfer in the borehole.

Contents

1 **Introduction** 1

2 **Data for the heat store** 1

3 **Field experiment** 1
- 3.1 Sensors 1
- 3.2 Datacollection 2
- 3.3 Computer preparation and presentation 2
- 3.4 Log-book for the experiment 2

4 **Theoretical analysis** 6
- 4.1 Theoretical background for the thermal analysis 6
- 4.2 Calculation of the thermal conductivity 7
- 4.3 Thermal resistance between the fluid channels and the borehole wall 9
- 4.4 Theoretical estimation of the thermal resistance between the fluid channels and the borehole wall 10

References 12

Appendix. T_f **versus** τ_n 13

1 Introduction

The measurements on the heat store Höstvetet, Stockholm, were made by the Monitoring Centre for Energy Research (MCE), Royal Institute of Technology (KTH), at the request of the Project Group for Energy Economizing in Buildings (EHUB), KTH. The experiment is included in a large project named The Stockholm Project. The planning of the experiment was made by Johan Claesson, Lund Institute of Technology (LTH), and Bengt Wånggren, MCE. The measurements were performed by MCE. The theoretical analysis of the results was made by Per Eskilson and Göran Hellström, LTH.

2 Data for the heat store

The heat store consists of 25 boreholes. See Figure 1. Each borehole has the depth H=80 m, and the radius r_b=0.0575 m. The heat collector in each borehole consists of two plastic tubes, connected at the bottom (U-tube). All 25 boreholes are coupled in parallel with equal pumping rate, Figure 1 *right*. The heat-carrier fluid is a glycol-water mixture.

3 Field experiment

The injection or extraction of heat to the store is normally made by the use of two heat pumps. These were not used in the experiment, since we did not believe that the heat pumps right after the installation would work constantly during the experiment. (This doubt was later shown to be correct). A large number of starts and stops would have made the analysis very hard or impossible. The electric boiler (the back-up for the heat-pumps) could not be used because it was needed to heat the inhabited house to which the borehole belonged. In addition to this we were not allowed to let the hot heat-carrier fluid pass through the heat pumps to the store. Instead we had to install a separate electrical boiler of 90 kW. The boiler was used to inject heat to the store with the help of the existing heat exchanger, without letting the heat-carrier fluid pass through the heat pumps. However, even for this simple system there were a few interuptions, but these disturbances did not affect the possibility to evaluate the experiment analytically.

The inlet temperature $T_{f,in}$ (°C), the outlet temperature $T_{f,out}$ (°C), and the pumping rate V_f (m^3/h) were measured and plotted versus time for three separate boreholes (enumerated 11, 31, and 55 in Figure 1 *right*), and for the total mixed fluid flow from all 25 boreholes.

The heat flows were then calculated from the temperature difference, $T_{f,in} - T_{f,out}$, and the pumping rate, V_f. A 26th borehole was used to measure the ground temperature at six different depths: 1, 16, 32, 48, 64, and 80m. See Figure 1. This borehole was not used for heat injection. It was filled with sand after the installation of the thermoelements. The temperature of the groundwater was mesured at three levels in one of the injection boreholes (number 33).

3.1 Sensors

The pumping flow in each borehole was ajusted to be equal for all boreholes by a check valve. The pumping rate was measured by a calibrated mechanical water meter, with an error of less than 2 % in our specific cases. The water meter gave pulses to a counter.

The temperatures were measured with platinum resistance sensors, Pt-100, which via a multiplexer (scanner) were connected to a precision multimeter. The temperature sensors were connected for 4-wire resistance measurements. The temperature sensors for the determination of the heat injection rate were chosen as pairs and calibrated. The 'pairing' implies that two temperature sensors with almost the same performance were chosen. The error in

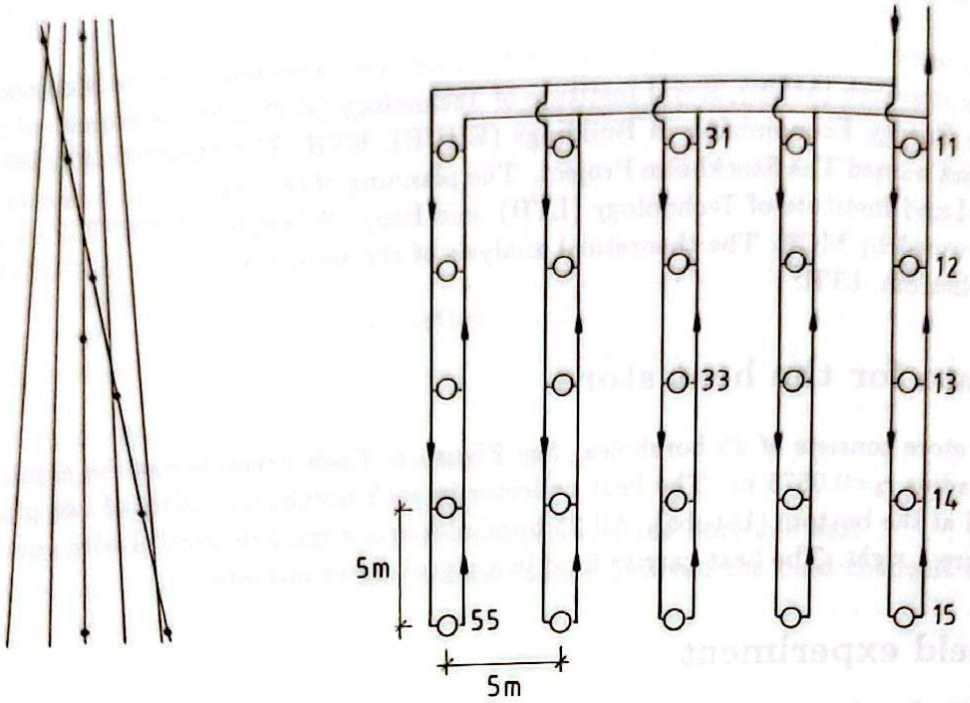

Figure 1: *Left*: Vertical cross-section of the heat store. The measuring points in the diagonal borehole, and in one of the extraction boreholes, are marked with dots. *Right*: Borehole geometry at the ground surface showing the coupling in parallel.

the temperature-difference measurements was estimated to be less than 0.05 °C, which with a temperature-difference of 4 °C gave a relative error of less than 1.2 %.

3.2 Datacollection

The measurements were carried out by a computerized measurement station for which the most important components were a micro-computer, a precision multimeter, a pulse counter, and a multiplexer. The instuments were inter-connected with a GPIB-bus, Fig 4.

The measurements were made at intervals of five minutes. The measured values were converted to suitable units and stored on magnetic casettes. The storage was performed either at each measurement (intensive measurement) or once per hour (normal measurement). Hence, the measured data were available with values each five minute or each hour.

3.3 Computer preparation and presentation

The data from the casette were transferred to a mini-computer at the MCE for preparation and presentation. The heat flows, which in the measuring computer were calculated for water, were recalculated for the water-glycol mixture. Then the figures shown in the reference [6] were drawn.

3.4 Log-book for the experiment

860110 The measurements on the undisturbed ground started at 11.00. No circulation of the heat-carrier fluid. Measurment each five minute. Calibration of the temperature sensors used for heat flow measurements in the ice-water.

860117 Circulation of the heat carrier fluid is started.

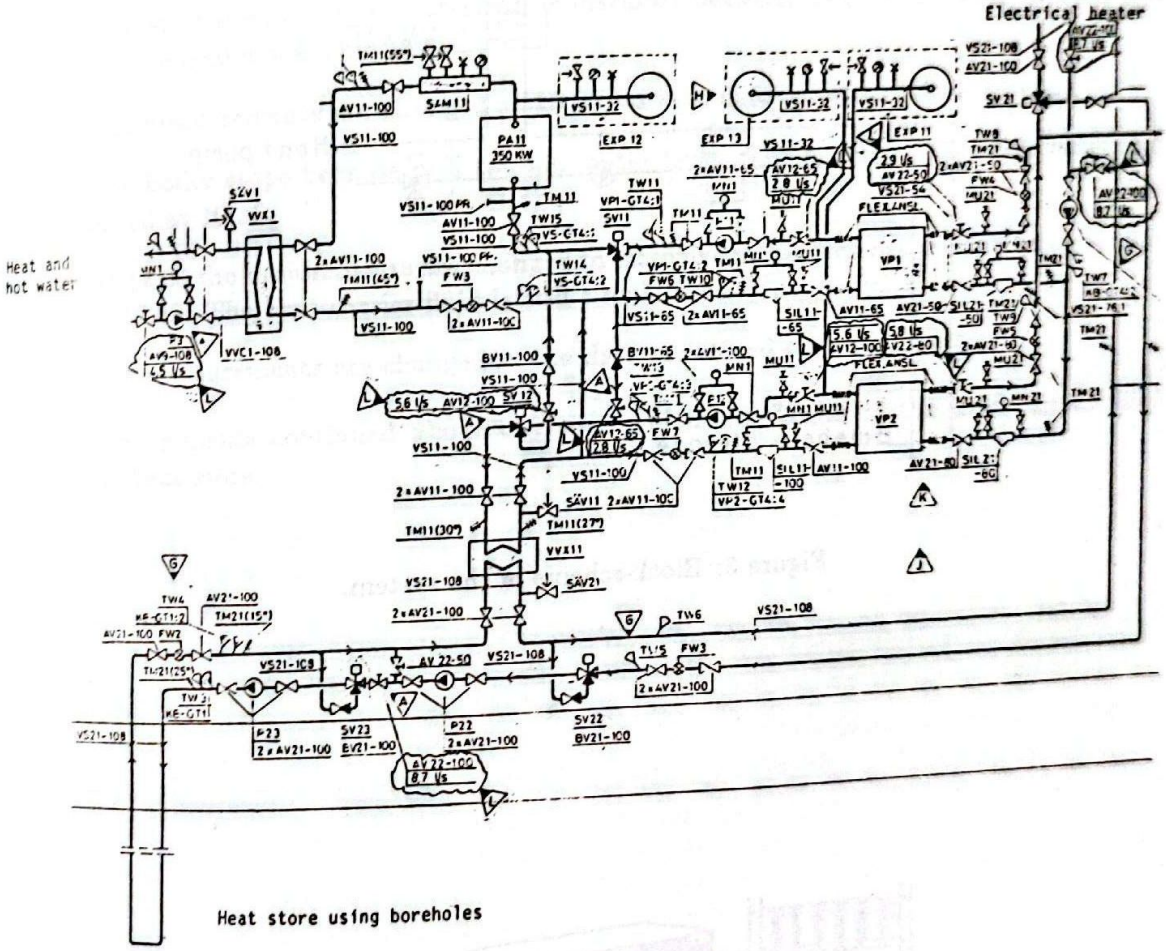

Figure 2: Fluid flow paths for the heat store.

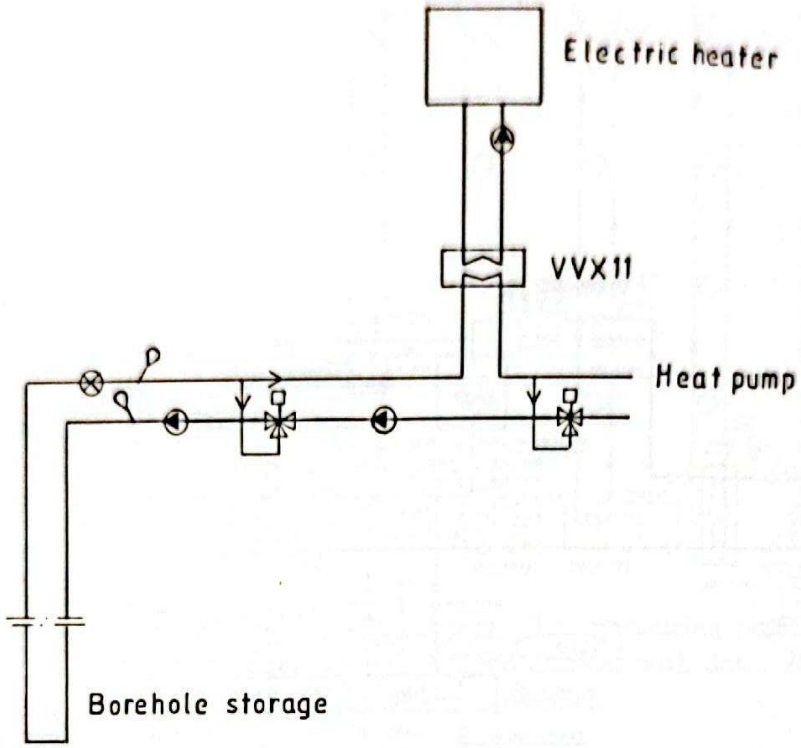

Figure 3: Block-scheme of the system.

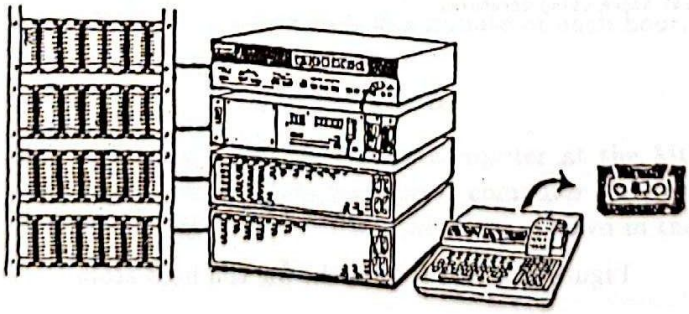

Figure 4: Equipment for collection of data.

860118 The water meters are blocked by plastic sawdust from the pipes. The pumping rate is close to zero. The water meter for the total pumping rate is replaced by a filter. All water meters are rinsed.

860120 The filter is removed and the water meter is reinstalled.

860122 The electric boiler starts at 10.00. Just before the start the measurements are changed so that the values are stored each five minute. After the start, the emergency protection to the boiler is found to be broken. However, we succeeded to start the boiler by making a by-pass connection that circumvents this protection. The heater is operating at 10.50. An operational emergency protection is installed between 14.08 and 14.38. During this period the heater was shut down.

860123 The measurements are changed at 10.00, so that data are stored once an hour.

860125 The boiler stops because of a too low water level. The boiler is filled with water and restarted at 10.35.

860126 At 12.00 the mesurements are changed to intensive measurements and the boiler is shut down 12.30. The heat-carrier fluid is still circulating.

860127 The measurements are changed so the data are stored once per hour.

The measurements continued about one week, with circulation of the heat carrier fluid through the heat store.

4 Theoretical analysis

The theory upon which the responce test method is based is described in [1,2,4]. The thermal conductivity is determined by plotting the outlet temperature $T_{f,out}$ versus the dimensionless time-parameter τ, defined by (2) or (6). One temperature curve is plotted for each of four different time intervals, when the heat injection is practically constant, for borehole 11, 31 and 55, and for the whole system with all 25 boreholes. The sixteen curves are straight lines. The slopes of these lines give independent determinations of the thermal conductivity.

The undisturbed ground temperature was measured at six levels in the measuring borehole (nr.26) before any heat was injected. See figure A.6.1 in [6]. The average value over five of the six levels (excluding the temperature at 1m) gave the effective undisturbed ground temperature T_{om}= 7.5°C. With this temperature known, and with the thermal conductivity given by the temperature curves ($T_{f,out}$ versus τ), the thermal resistance between the fluid and the borehole wall R_b (K/(W/m)) is determined. Each point on the temperature curves gives one value for R_b.

4.1 Theoretical background for the thermal analysis

The thermal process around a borehole is with a very good approximation radial during the response test. It is assumed that the heat injection is constant per unit borehole length. With these assumptions each borehole can be approximated with a continuous line source. It should be noted that there is no influence between the boreholes during the responce test with a duration of a few days [4].

Consider the case when the heat injection is a step with the constant value q_1 (W/m) starting at t=0. The continuous line-source gives the following temperature increase of the average fluid temperature $T_f(t)$ relative to undisturbed temperature T_{om} [1,2]:

$$T_f(t) - T_{om} = \frac{q_1}{4\pi\lambda}\left[ln(\frac{4at}{r_b^2}) - \gamma\right] + q_1 \cdot R_b = \frac{q_1}{4\pi\lambda}\tau(t) + q_1\left\{R_b + \frac{1}{4\pi\lambda}\left[ln(\frac{4a}{r_b^2}) - \gamma\right]\right\}$$
$$\left(\gamma = 0.5772, \quad t \geq 5r_b^2/a \right) \qquad (1)$$

The temperature $T_f(t)$ is equal to the average value between the inlet and outlet temperature ($T_f(t) = \frac{1}{2}(T_{f,in}(t) + T_{f,out}(t))$). The time restriction for formula (1), $t \geq 5r_b^2/a$, ensures that the capacity of the volume of the borehole can be neglected in the line-source approximation [1]. The thermal conductivity and diffusivity of the ground are λ (W/(mK)) and a (m^2/s). The temperature (1) is a linear function of the parameter $\tau(t)$, defined from (1) as:

$$\tau(t) = ln(t) \qquad (2)$$

When the temperature T_f is plotted versus $\tau(t)$, the slope ϕ of the line gives the thermal conductivity λ as:

$$\lambda = \frac{q_1}{4\pi\phi} \qquad (3)$$

A more general case is when the heat injection rate is given by step-wise constant values:

$$q(t) = \begin{cases} q_1 & t_1 < t < t_2 \quad (t_1 = 0) \\ q_2 & t_2 < t < t_3 \\ \cdot & \\ \cdot & \\ \cdot & \\ q_N & t_N < t < t_{N+1} \end{cases} \qquad (4)$$

Superposition gives the temperature increase at the borehole wall as a sum of the contributions from each step n [1,2]:

$$T_f(t) - T_{om} = \sum_{n=1}^{N} \frac{q_n - q_{n-1}}{4\pi\lambda} ln(t - t_n) + q_N \left[R_b + \frac{1}{4\pi\lambda} \left(ln(\frac{4a}{r_b^2}) - \gamma \right) \right] =$$

$$= \frac{q_{ref}}{4\pi\lambda} \tau_N(t) + q_N \left[R_b + \frac{1}{4\pi\lambda} \left(ln(\frac{4a}{r_b^2}) - \gamma \right) \right] \quad t_N + 5r_b^2/a < t < t_{N+1}, \quad q_0 = 0 \quad (5)$$

The dimensionless parameter τ_N is from (5) given by:

$$\tau_N(t) = \sum_{n=1}^{N} \frac{q_n - q_{n-1}}{q_{ref}} ln(t - t_n) \qquad t_N + 5r_b^2/a < t < t_{N+1} \qquad (6)$$

The expression (6) for τ_N changes for every step change in the heat injection rate. The temperature (5) is a linear function of τ_N in the time interval $t_N + 5r_b^2/a \leq t \leq t_{N+1}$. The slope of the line, ϕ, gives the thermal conductivity as:

$$\lambda = \frac{q_{ref}}{4\pi\phi} \qquad (7)$$

The reference heat injection q_{ref} can be chosen arbitrarily ($q_{ref} \neq 0$). It is introduced for convenience in order to obtain the dimensionless time parameter τ_n. The parameter q_{ref} cancels, when (6) is inserted in (5).

4.2 Calculation of the thermal conductivity

In the field experiment the heat injection is approximately constant, except for two periods when it is zero. See Figure 5. The curve of the heat injection rate is the same for all boreholes, since they are coupled in parallel. However, the levels q_{ref} and q_6 differ somewhat for the different boreholes. The times $t_1, t_2, ..., t_6$, and the heat injection rates are given in Table 1 and Table 2 respectively.

The reference level q_{ref} for the heat injection is chosen to the value during step 1. For step n=1, 3, 5, and 6 (6=recovery period), expression (6) then becomes:

$$\begin{aligned}
&\text{step 1:} \quad \tau_1(t) = ln(t) \\
&\text{step 3:} \quad \tau_3(t) = ln(t) - ln(t - t_2) + ln(t - t_3) \\
&\text{step 5:} \quad \tau_5(t) = ln(t) - ln(t - t_2) + ln(t - t_3) - ln(t - t_4) + ln(t - t_5) \\
&\text{step 6:} \quad \tau_6(t) = ln(t) - ln(t - t_2) + ln(t - t_3) - ln(t - t_4) + ln(t - t_5) - \frac{q_6}{q_{ref}} ln(t - t_6)
\end{aligned} \qquad (8)$$

Step 2 and 4 without heat injection are not used, since the water circulation was stopped or uncertain. The outlet temperature $T_{f,out}$ is plotted versus τ_n during step n=1,3,5 and 6, for borehole 11, 31, 55, and for all the boreholes in parallel. The sixteen curves are given by Figs. a-p in the Appendix. The temperature points in the figures are taken from the measured temperatures given in Figs. A.2.1 to A.5.5 in [6].

Note that the slope of the outlet temperature is identical with that of the inlet temperature since the heat injection rate is constant ($q \cdot H = C_f V_f (T_{f,in} - T_{f,out})$) for each of the 16 cases. It is therefore possible to use the outlet temperature instead of the avarage temperature $T_f = \frac{1}{2}(T_{f,in} + T_{f,out})$ to determine λ. The temperature T_f lies between 1.3 and 1.5°C higher than the outlet temperature.

The slope of each curve gives an independent determination of the thermal conductivity. The obtained values are given in Table 3.

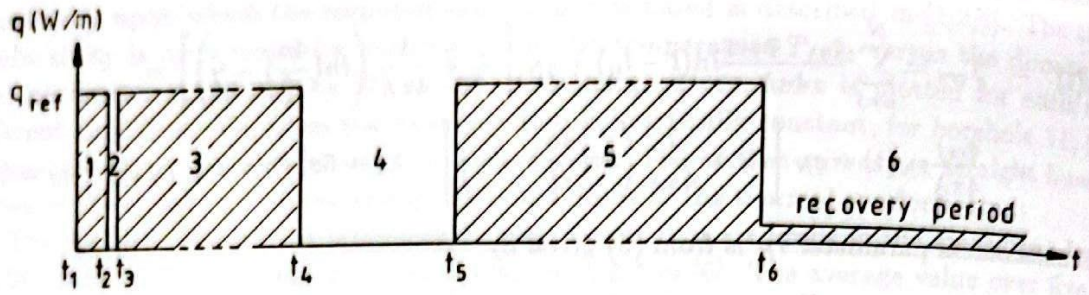

Figure 5: Heat injection function for borehole 11, 31, 55, and all 25 boreholes in parallel (All four cases have the same shape on q(t)).

Notation	Date-Hours.Min	Time from start
t_1	860122-10.00	00h 00min
t_2	860122-14.08	03h 18min
t_3	860122-14.38	03h 48min
t_4	860124-11.00	48h 10min
t_5	860125-10.00	71h 10min
t_6	860126-12.30	97h 40min

Table 1: The times $t_1 - t_6$ of figure 5.

Step :	1	2	3	4	5	6
Borehole 11	47.00.	0	47.00	0	47.00	2.75
Borehole 31	45.00.	0	45.00	0	45.00	2.57
Borehole 55	46.25.	0	46.25	0	46.25	2.67
Total	46.25.	0	46.25	0	46.25	2.23

Table 2: Heat injection rate $q(t)$ (W/m) for the different boreholes and for the total heat store

Borehole	Step 1	Step 3	Step 5	Step 6
Borehole 11	(3.00)	4.57	3.86	3.27
Borehole 31	(2.93)	4.47	3.68	3.30
Borehole 55	(2.75)	4.46	3.65	3.08
Total	(2.85)	4.33	3.69	3.27

Table 3: The obtained thermal conductivity λ for the 16 different cases of the response test

Borehole	Step 1	Step 3	Step 5
Borehole 11	(0.145)	0.100	0.088
Borehole 31	(0.151)	0.109	0.095
Borehole 55	(0.156)	0.111	0.098
All boreholes	(0.142)	0.105	0.091

Table 4: Thermal resistance R_b determined from the response test.

The values of step 1 in Tab. 3 are given within brackets, since they do not satisfy the time criterion of Eq. (5). These values cannot be used. They are included in this report only to show the importance of the time criterion.

Step number 3 gives very high values for the thermal conductivity. Step 5 shows much lower values. During the recovery period (step 6) we obtain even lower values on λ than for step 3 and 5. There are two possible explanations of the decreasing value of λ:

- Transient effects connected with the temperature variation along the boreholes.
- Convective heat flow in the rock caused by the sharp temperature gradients close to the fluid channels. The heat is transported with the groundwater through cracks a few tenths of a meter out in the rock. This process becomes less important when the temperature gradient decreases with time.

In this study we do not penetrate deeper into these problems. They need to be further investigated.

The best estimation of the thermal conductivity ought to be the average value of the values of step 5 and 6. Step 5 give too high values due to the assumed convective transport of heat out in the ground, while step 6 (recovery period) gives lower values. The average over all the values during step 5 and 6 become:

$$\bar{\lambda} = 3.5\,\mathrm{W/(mK)} \tag{9}$$

This is a reasonable value for granite.

4.3 Thermal resistance between the fluid channels and the borehole wall

All variables and parameters of equation (5) except R_b are now known. The temperature T_f is the average value between the inlet temperature $T_{f,in}$ and the outlet temperature $T_{f,out}$, which are measured functions of time, see Figs. A.2.1-A.5.5 in [6]. The thermal conductivity λ during the different steps is given by Table 3.

The thermal resistance R_b is calculated with (5) for some different times during heat injection step 1, 3, and 5. The average value of R_b for each step is given in Table 4 for borehole 11, 31, 55, and all 25 boreholes.

The values of step 1, given within brackets, are not correct, since the time criterion in (5) is not satisfied. They cannot be used. Furthermore, it is not possible to calculate R_b with (5) during the recovery period, since there is (almost) no heat injection during this period. The average value of R_b during step 3 and 5 becomes approximately 0.1 K/(W/m):

$$\overline{R_b} = 0.1\ \mathrm{K/(W/m)} \tag{10}$$

Angle	0 mm	1 mm	2 mm
180	0.093	0.120	0.127
135	0.115	0.123	0.131
90	0.126	0.134	0.142
45.3	0.132		

Table 5: Estimated thermal resistance R_b (K/(W/m)) based on theoretical methods.

4.4 Theoretical estimation of the thermal resistance between the fluid channels and the borehole wall

Each borehole is fitted with two plastic pipes connected at the bottom of the borehole (U-tube). The heat transfer from the heat carrier fluid to the surrounding rock depends on the location of the pipes in the borehole, the properties of the fluid, and the flow rate in the pipes. There is a heat exchange between the two pipes and between the pipes and the surrounding rock.

The heat transfer capacity of the heat exchanger in the borehole is given by the thermal resistance R_b between the bulk fluid in the two pipes and the borehole wall. This thermal resistance consists of three parts, namely

- Heat transfer resistance between the bulk fluid in a pipe and the inner wall of the pipe.
- Thermal resistance of the material between the inner and the outer wall of the pipe.
- Heat transfer resistance between the outer wall of the pipes and the borehole wall.

The plastic pipes are made of medium-density polyethylene (PEM, PN6) with an outer diameter of 0.032 m and a wall thickness of 0.0021 m. The thermal conductivity of the plastic material is 0.36 W/mK at 20 °C. The thermal resistance between the inner and the outer wall of the pipe becomes 0.062 K/(W/m) according to [3].

The pumping flow rate per borehole is about $3.33 \cdot 10^{-4}$ m^3/s (1.2 m^3/h). The density of the fluid (ordinary water) is about 1000 kg/m^3. The viscosity is $1.1 \cdot 10^{-3}$ kg/ms at 15 °C. This gives a Reynold's number of 13,900, which means that the flow is turbulent in the pipe. The thermal conductivity of the fluid is 0.59 W/mK at 15 °C. The heat transfer resistance between the bulk fluid in the pipe and the inner wall of the pipe at this value of the Reynold's number is then 0.006 K/(W/m).

The total thermal resistance R_p between the bulk fluid and the outer wall of a plastic pipe becomes 0.068 K/(W/m).

The heat transfer resistance between the outer wall of the pipes and the borehole wall is more difficult to quantify. There may be both conductive and convective heat transport through the fluid that fills the borehole outside the pipes. The main uncertainty is if the convective part gives any significant contribution in this case. Experiences from heat extraction by deep boreholes indicate that the convective part is negligable at fluid temperatures around 0 °C. We will assume that this is true also for this case, where the temperatures may reach 15 °C. The thermal resistance R_b may then be obtained from an analytical solution for the *conductive* heat flow between the fluid channels and the borehole wall [5].

Figure 6 shows a horizontal cross-section through the borehole and the two plastic pipes. The distance from the plastic pipe to the borehole wall is denoted d. The angle α between the pipes is defined by Figure 6. The diameter of the borehole is 0.115 m.

The theoretical estimations of the thermal resistance R_b are given in Table 5. The angle between the pipes may vary from 45 ° to 180 °. The angle 45.3 ° and a distance of 0 mm between the pipe and the borehole wall represents the case were the plastic pipes lie together at the borehole wall.

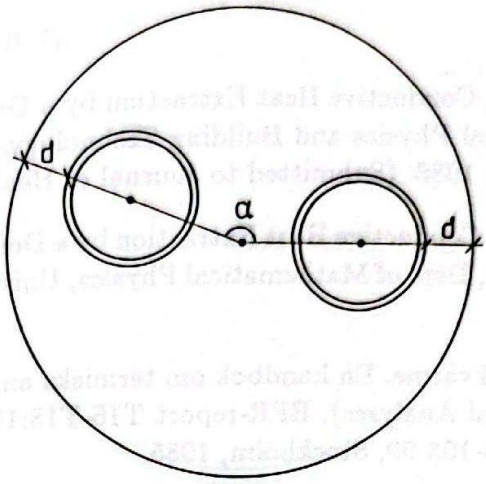

Figure 6: Horizontal cross-section through the borehole and the two plastic pipes.

The lowest thermal resistance is obtained when the pipes are in contact with the borehole wall and at an angle 180°. There are no arrangements to keep the pipes in this optimum position. However, the plastic pipes are believed to be close to the borehole wall for most part of the borehole depth. It is reasonable to assume an average distance of 1-2 mm between the pipes and the borehole wall with its irregularities.

The thermal resistance R_b is 0.266 for the worst possible case where the two tubes lies together in the center of the borehole. The range of possible values is 0.09-0.27 K/(W/m). Judging by the values presented in Table 5 one may expect R_b to be about 0.12-0.13. Given the uncertainty of the evaluation, this is in accordance with value of R_b equal 0.1 K/(W/m).

References

[1] J. Claesson, P. Eskilson, Conductive Heat Extraction by a Deep Borehole. Analytical Studies. Dep. of Mathematical Physics and Building Technology, University of Lund, Box 118, S-221 00 Lund, Sweden, 1986. (Submitted to Journal of Heat and Mass Transfer)

[2] J. Claesson, P. Eskilson, Conductive Heat Extraction by a Deep Borehole. Thermal Analyses and Dimensioning Rules, Dep. of Mathematical Physics, University of Lund, Box 118, S-221 00 Lund, Sweden, 1987.

[3] J. Claesson et. al. , Markvärme. En handbok om termiska analyser (Ground Heat Systems. A Handbook on Thermal Analyses), BFR-report T16-T18:1985, (900pp., 460 fig.), Svensk Byggtjänst, Box 7853, S-103 99, Stockholm, 1985.

[4] J. Claesson, P. Eskilson, Conductive Heat Extraction by Thermally Interacting Deep Boreholes. Dep. of Mathematical Physics, University of Lund, Box 118, S-221 00 Lund, Sweden, 1987.

[5] J. Bennet, J. Claesson, G. Hellström, Multiple Method to Compute the Conductive Heat Transfer to and between Pipes in a Composite Cylinder. Notes on Heat Transfer 3-1987, Dep. of Building Technology and Mathematical Physics, Lund Institute of Technology, S-221 00 Lund, Sweden, 1987.

[6] P. Eskilson, Göran Hellström, *Bengt Wånggren*, Response Test for a Heat Store with 25 Boreholes. Measured Data, Notes on Heat Transfer 9.1-1987, Departments of Building Technology and Mathematical Physics, Lund Institute of Technology, Box 118, S-221 00 Lund, Sweden, and *Monitoring Centre for Energy Research, Royal Institute of Technology, S-100 44 Stockholm, Sweden, 1987.*

Appendix. T_f versus τ_n

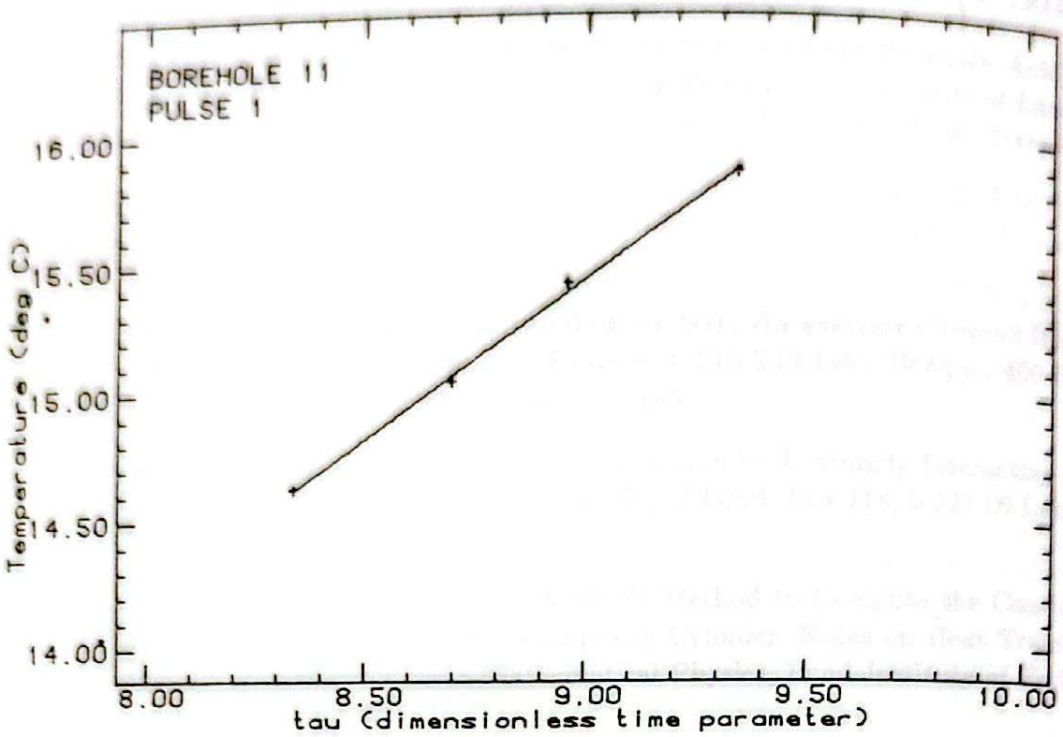

Figur a

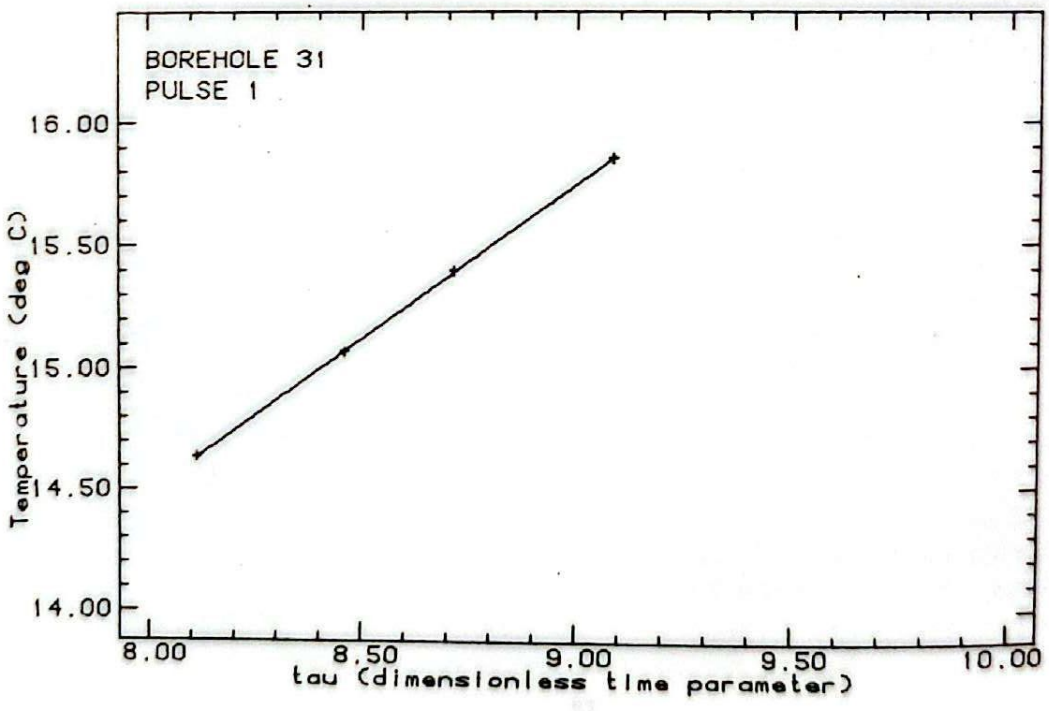

Figur b

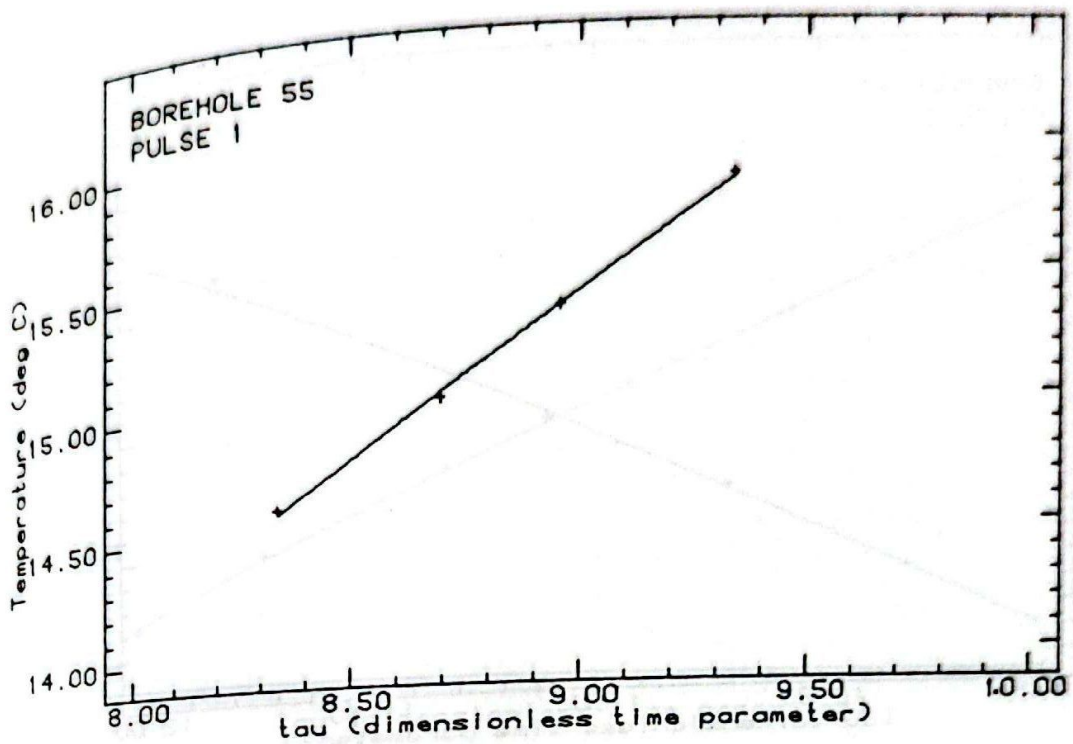

Figur c

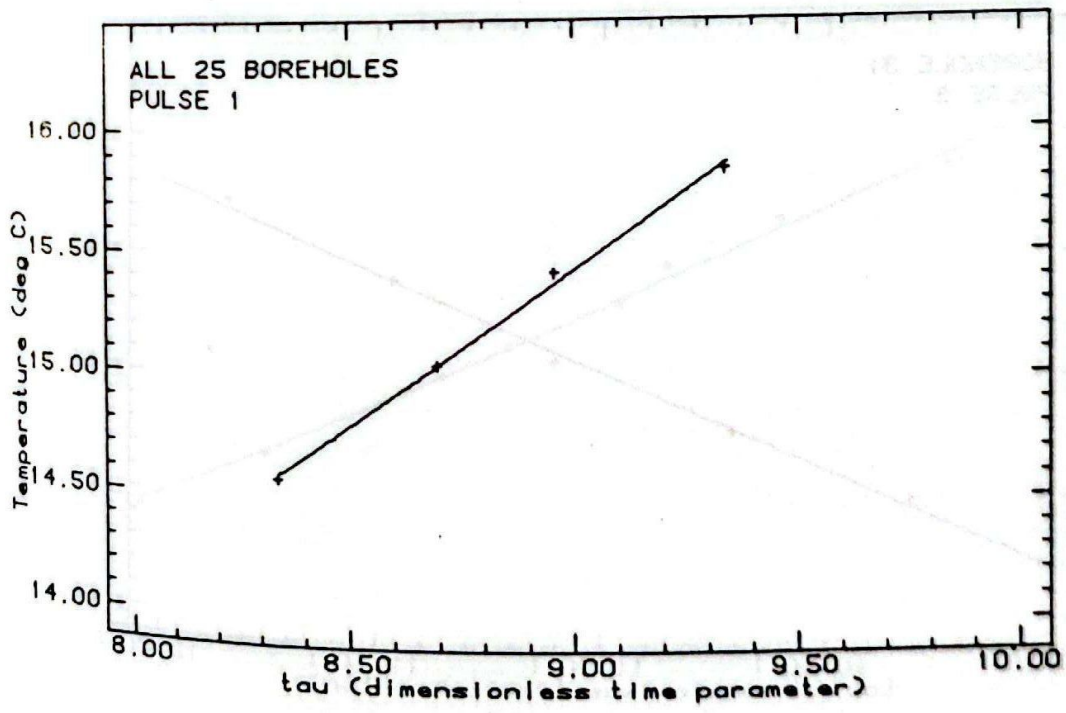

Figur d

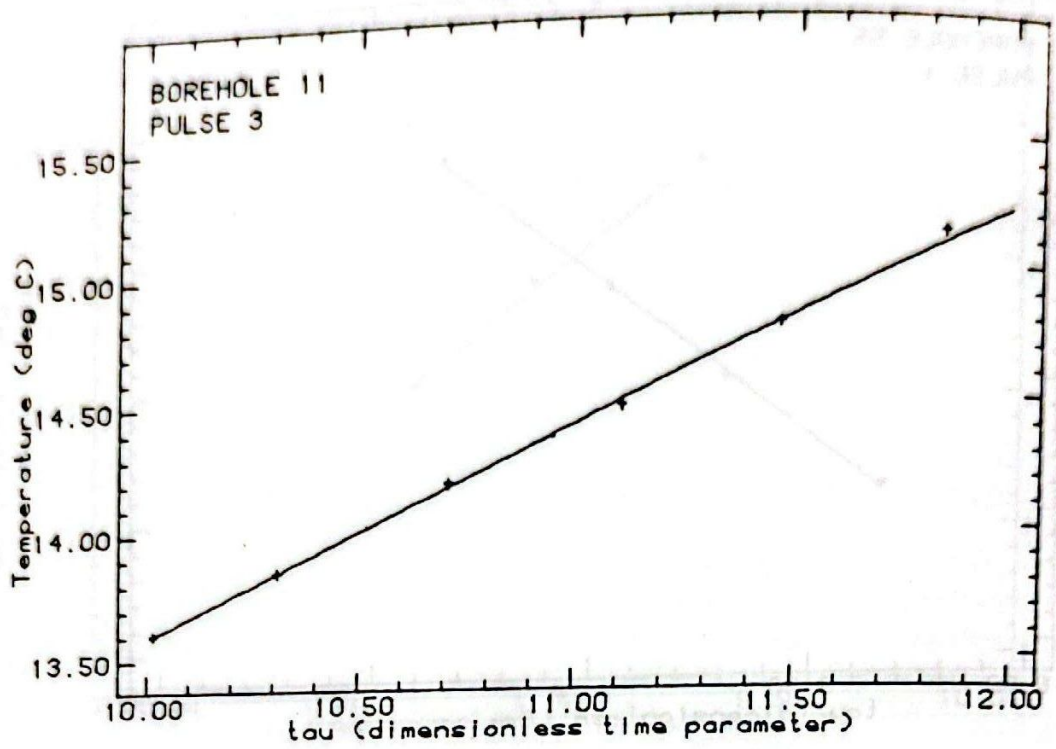

Figur e

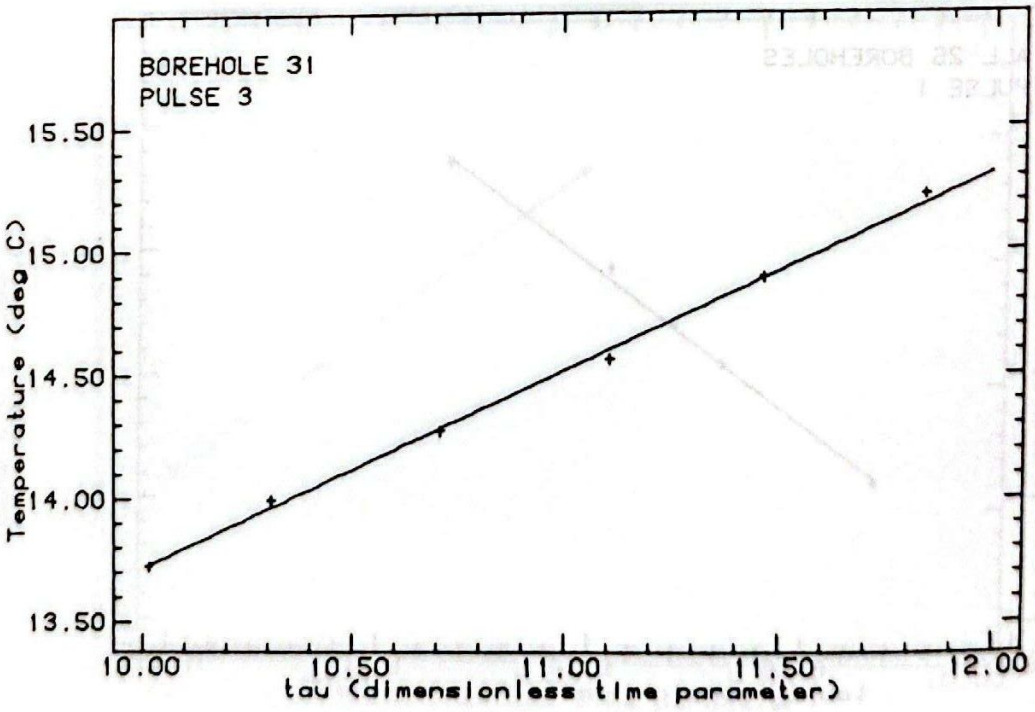

Figur f

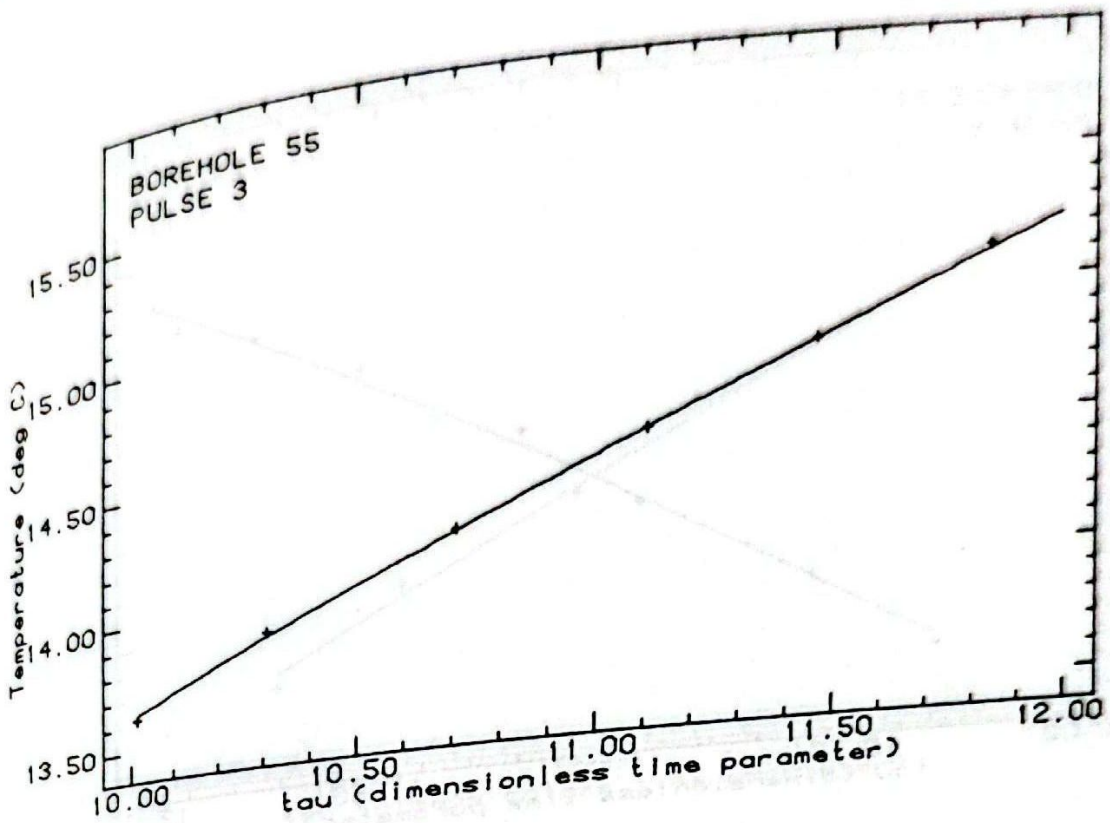

Figur g

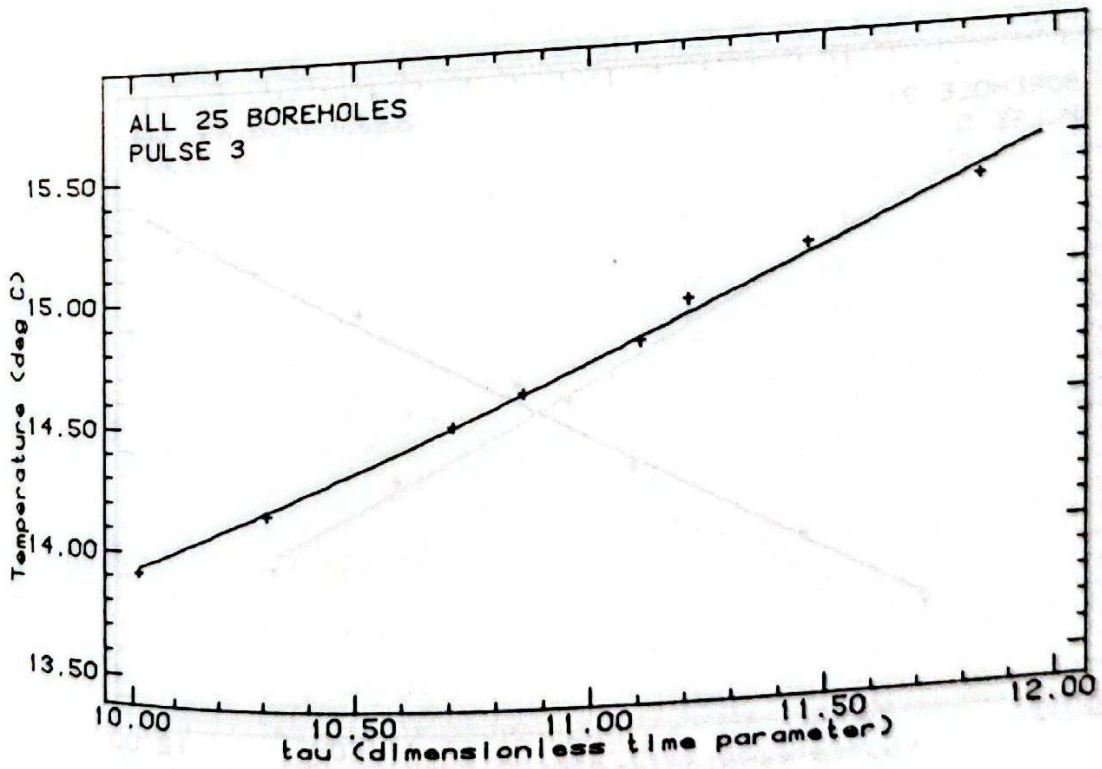

Figur h

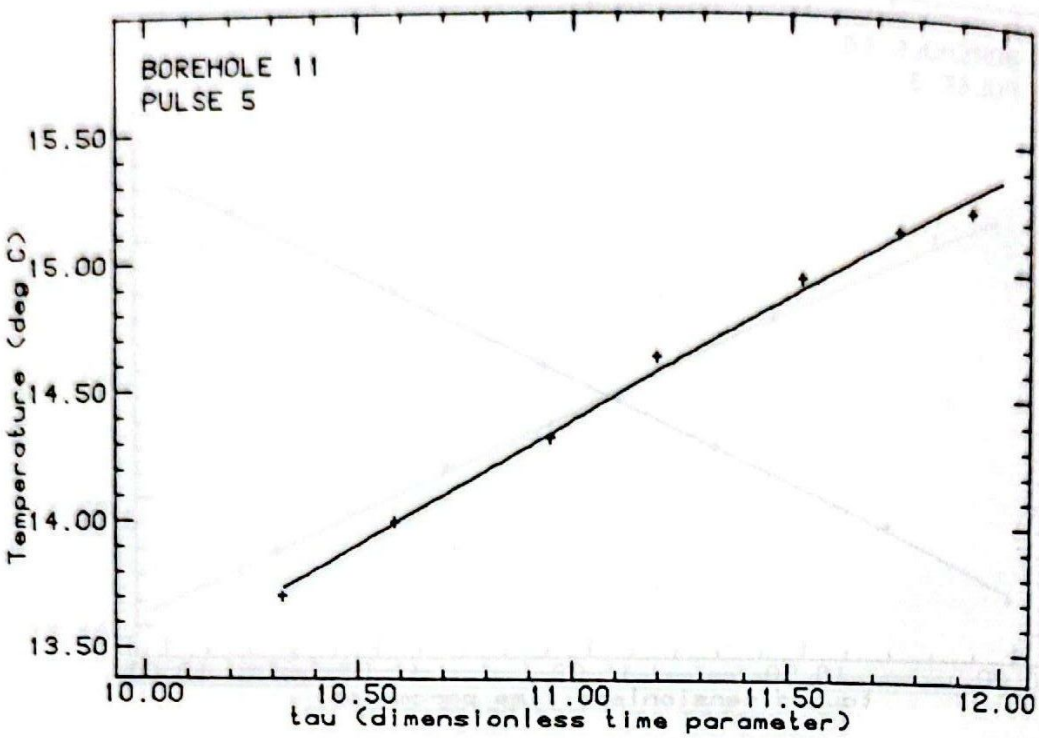

Figur i

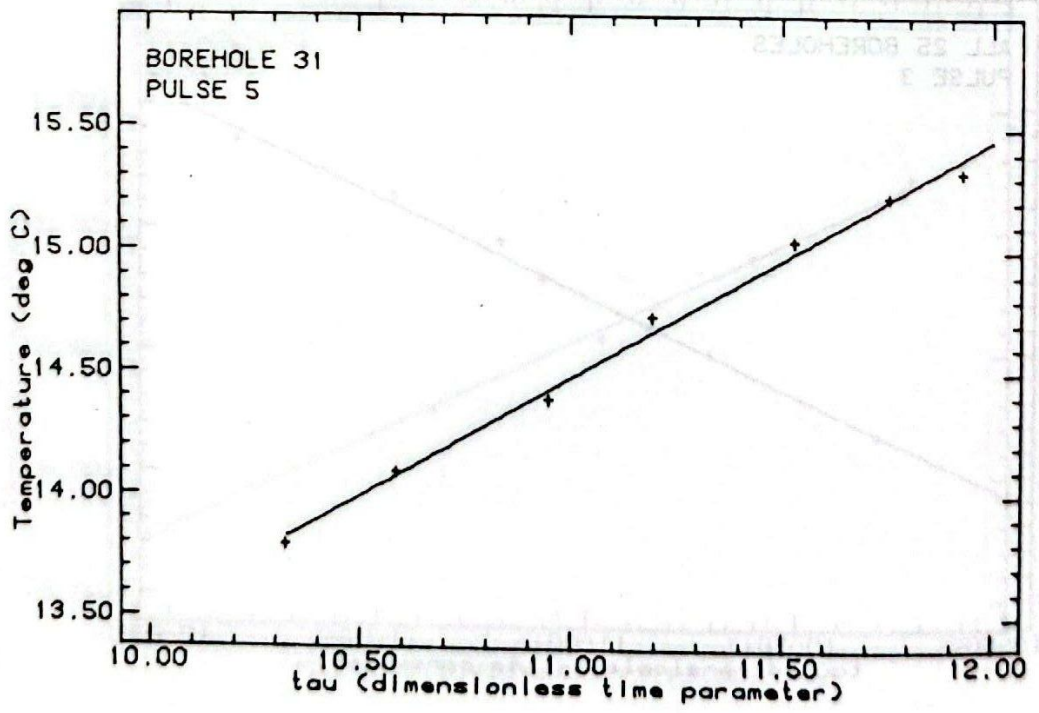

Figur j

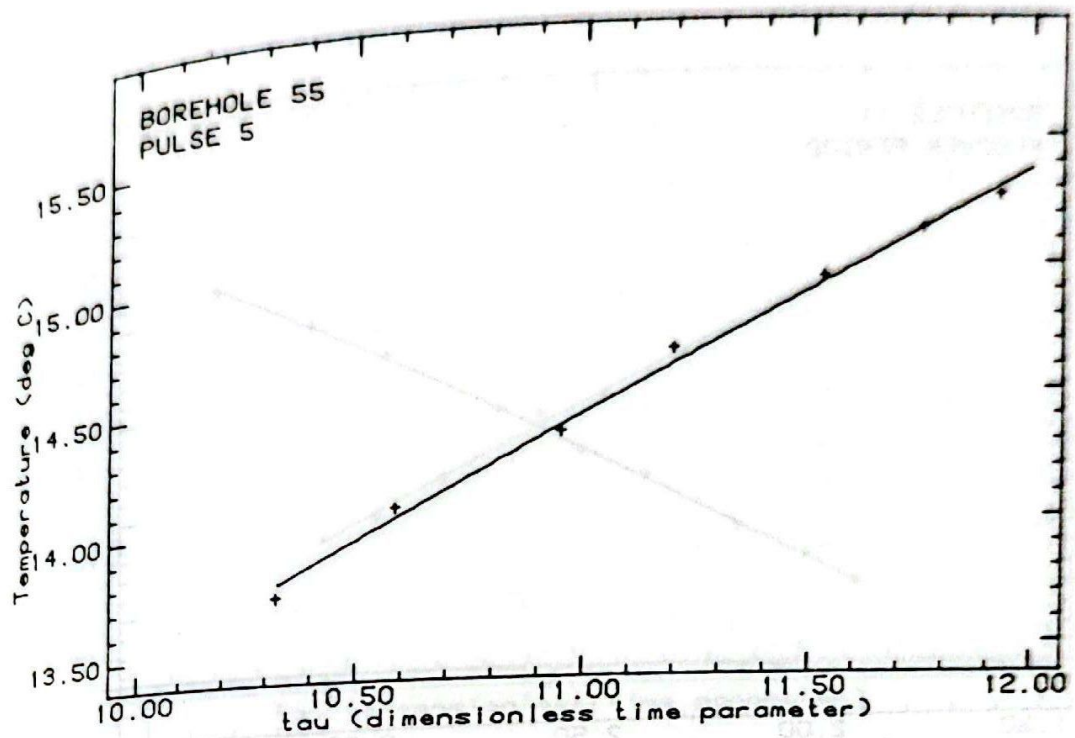

Figur k

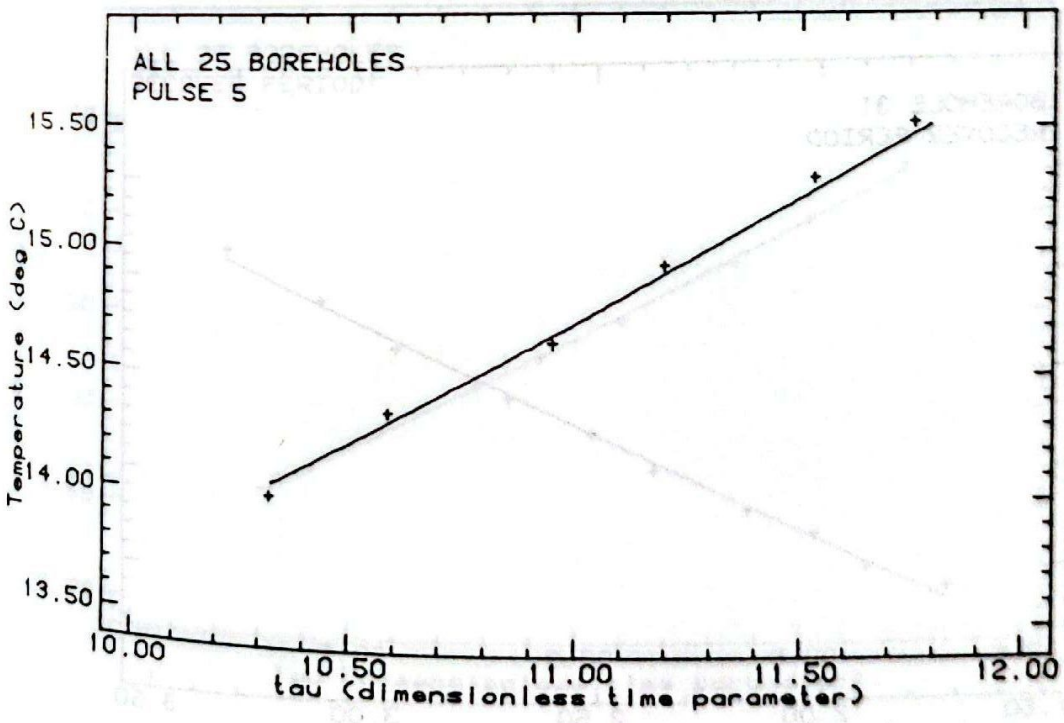

Figur 1

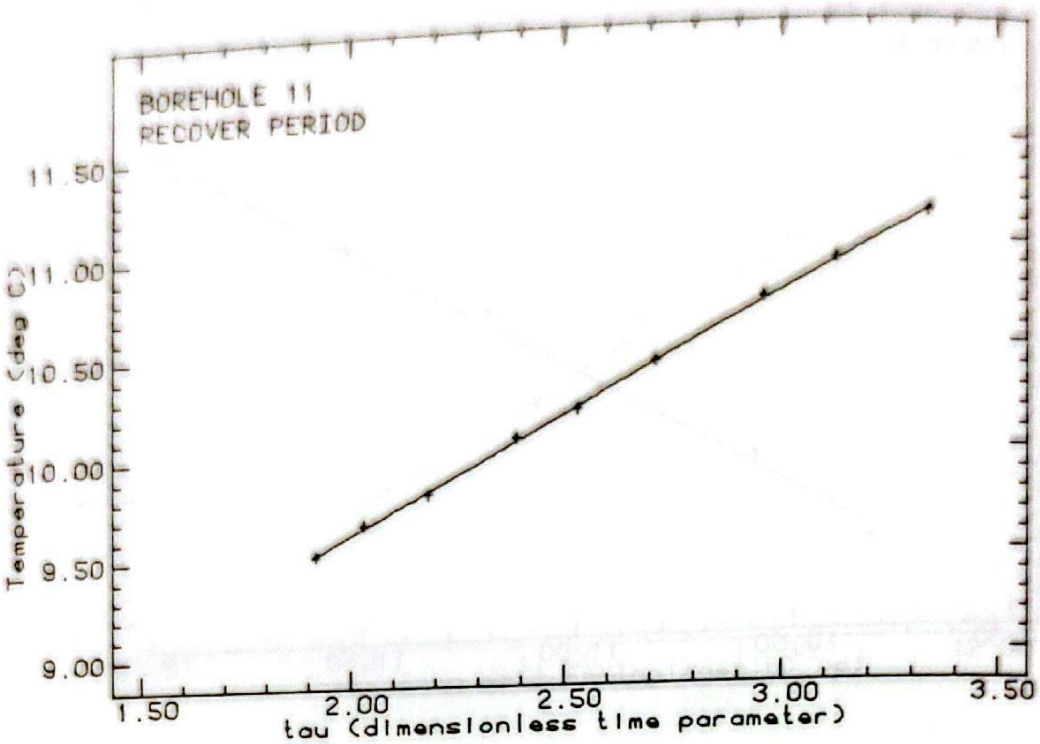

Figur m

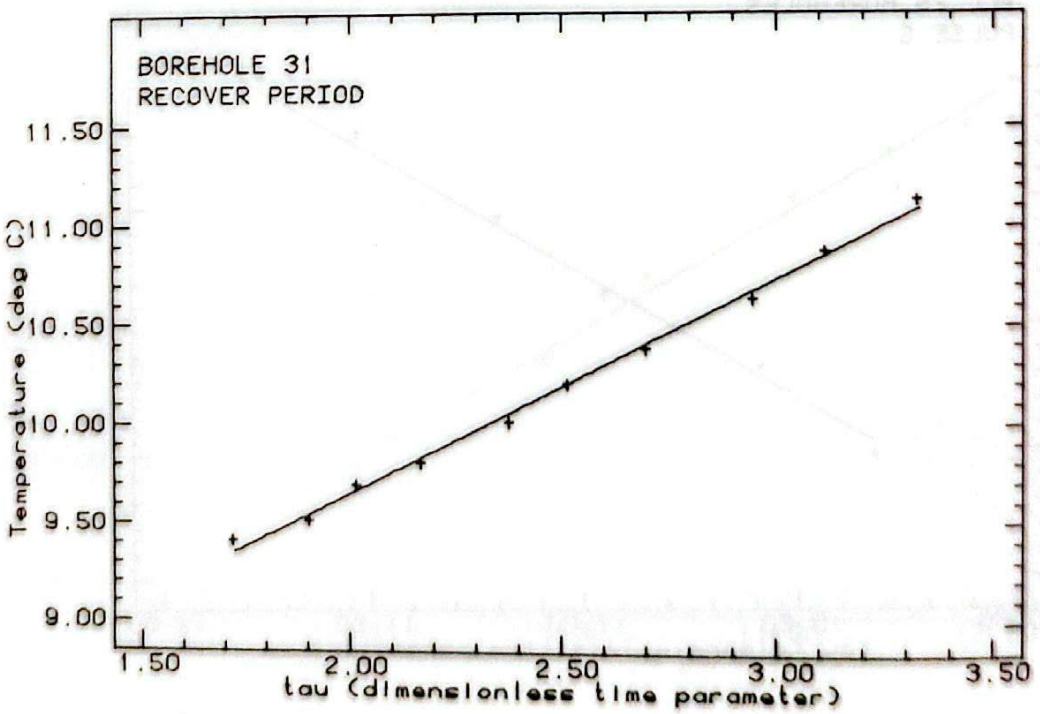

Figur n

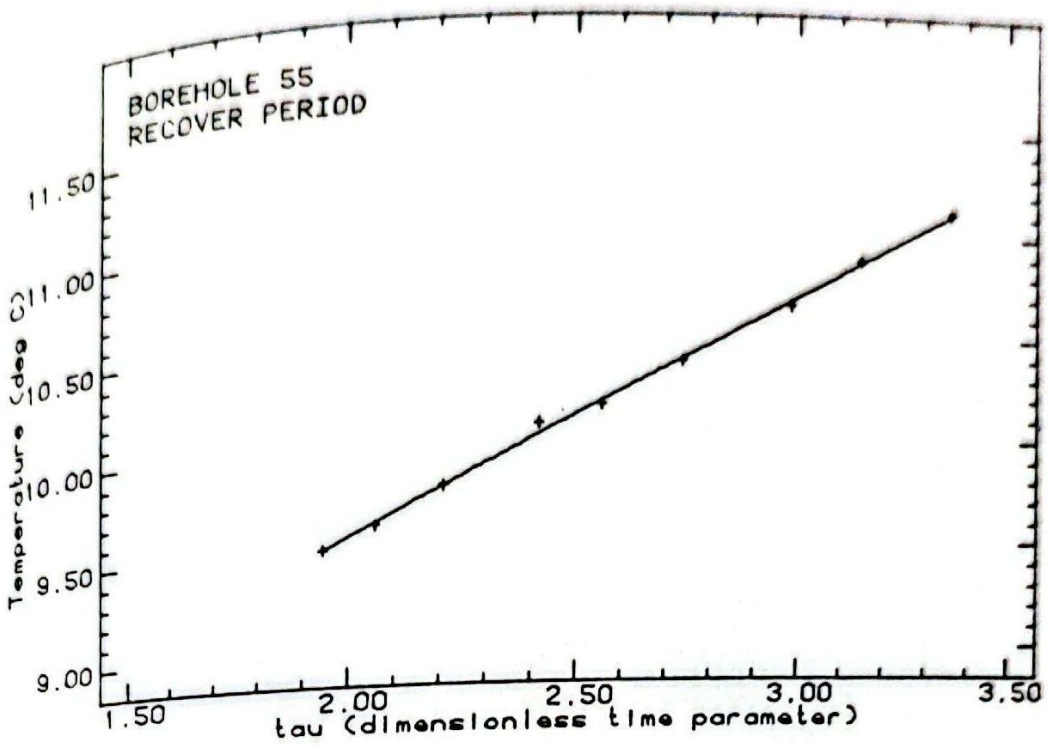

Figur o

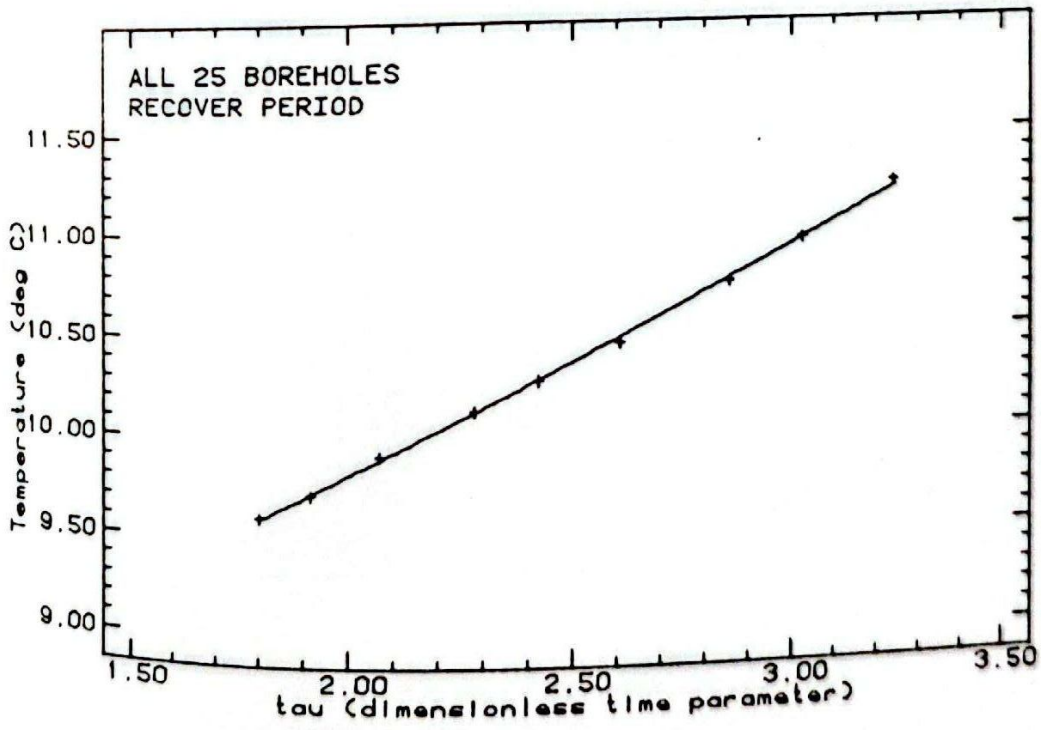

Figur p

Notes on Heat Transfer 2-1986

Numerical Study of Radial and Vertical Mesh Division for a Single Heat Extraction Borehole

Per Eskilson

October 1986

Departments of Building Technology
and Mathematical Physics
University of Lund
Box 118
S-221 00 Lund, Sweden

Contents

		page
1	Introduction	1
2	Penetration radius r_p	2
3	Radial process	3
3.1	Three equally sized cells: $\Delta r = r_p$	5
3.2	Three equally sized cells: $\Delta r = 2r_p$	6
3.3	Six equally sized cells: $\Delta r = r_p/2$	7
3.4	Expanding mesh with seven cells	8
3.5	Expanding meshes with ten to fourteen cells	9
3.6	Monthly step-wise variation of the heat injection rate	14
3.6.1	Periodic pulse-train	14
3.6.2	Sinusoidal heat injection	15
3.6.3	Example with typical monthly loading conditions	16
3.7	Conclusions	17
4	Three-dimensional radial-axial process	20
4.1	Comparison of meshes for the first 25 years	22
4.2	Comparison of meshes for very long times	25
5	Rules for the choice of mesh	28

1 Introduction

The thermal process for a single heat extraction borehole is calculated numerically with finite difference technique in [1,2]. Cylindrically symmetric coordinates are used. The ground is divided into a number of cells in a radial-axial mesh. See Figure 1.1. Each cell is shaped like an annulus, i.e. a circle ring with rectangular cross-section. The specific choice of mesh determines the numerical accuracy of the solution. Small cells give a short stability time-step and good numerical accuracy. The disadvantage using small cells is that the small time-steps give long execution times on the computers. It is therefore advisable not to use smaller cells than necessary for the specific problem to be solved.

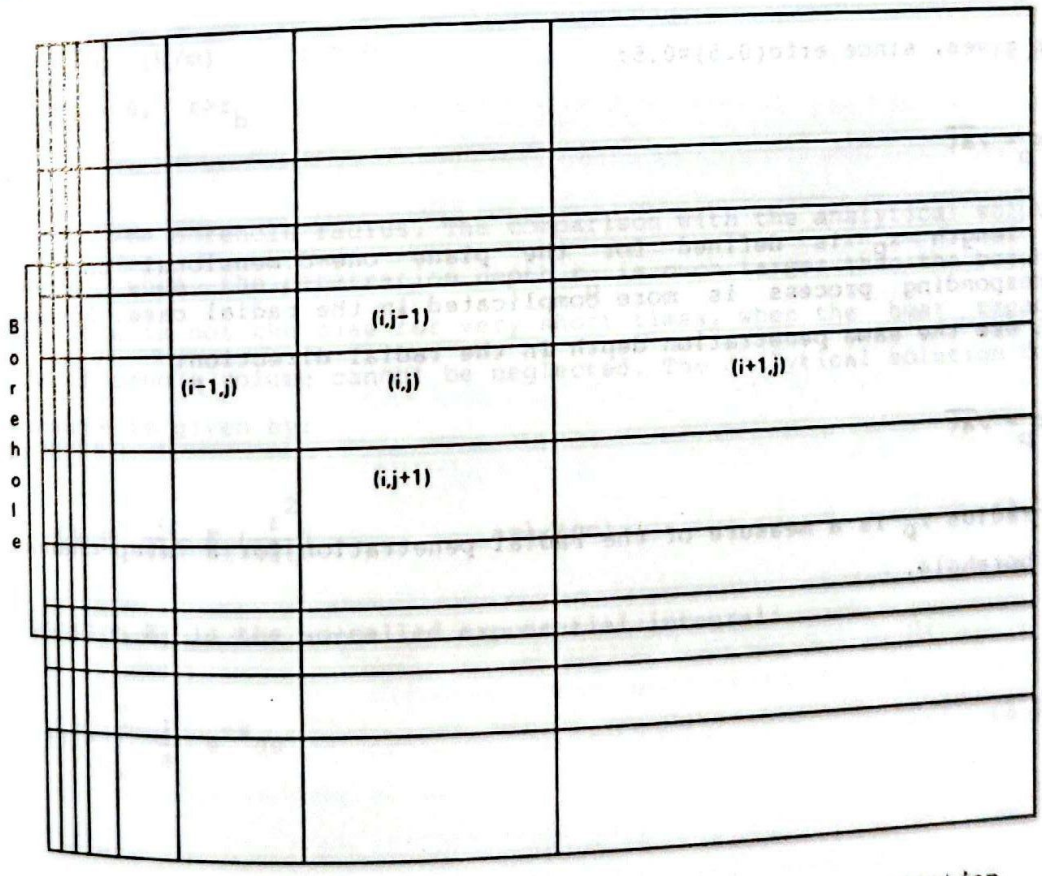

Figure 1.1 Two-dimensional radial-axial mesh for a heat extraction borehole in the ground.

2 Penetration radius r_p

Consider the following semi-infinite one-dimensional process ($x > 0$). The temperature is zero for all x at t=0. The boundary temperature at x=0 makes a step at the start time t=0:

$$T(0,t) = 1,\ t > 0 \qquad T(x,0)=0,\ x > 0 \tag{2.1}$$

The temperature solution for $x \geq 0$ and $t \geq 0$ is given by the so-called error function:

$$T(x,t)= \operatorname{erfc}(x/(2\sqrt{at})) \tag{2.2}$$

The penetration depth $x = x_p$ is defined as the depth for which the temperature (2.2) equals half the value at the boundary x=0:

$$\operatorname{erfc}(x_p/(2\sqrt{at})) = 0.50 \tag{2.3}$$

This gives, since $\operatorname{erfc}(0.5)\approx 0.5$:

$$x_p = \sqrt{at} \tag{2.4}$$

The length x_p is defined for the plane one-dimensional case. The corresponding process is more complicated in the radial case. Anyhow, we will use the same penetration depth in the radial direction:

$$r_p = \sqrt{at} \tag{2.5}$$

The radius r_p is a measure of the radial penetration for a step-change at the borehole.

3 Radial process

The thermal process around a borehole is three-dimensional in the (r,z)-plane of Figure 1.1. The heat extraction disturbs the temperature field in the region close to the borehole. The penetration depth of this disturbance (2.5) is small compared to the borehole depth during quite a long time from the start of the heat extraction. During this period the axial heat flows are small compared to the radial heat flows. A radial solution is then valid. The radial approximation is valid with very high accuracy for times when r_p in (2.5) is less than H/10, but can be used until r_p is equal to H/3, i.e. for $t < H^2/(9a)$.

We will in this chapter make a number of simulations with different choices of mesh in the radial direction. The numerically calculated temperatures are compared with the analytical solution for a line source. The considered examples concern a constant heat injection rate q from a borehole starting at t=0. The initial temperature in the ground is zero:

$$q(t) = q \quad (W/m) \qquad t > 0$$
$$T(r,0) = 0, \quad r>r_b \qquad (3.0.1)$$

Here r_b is the borehole radius. The comparison with the analytical solution is valid when the penetration depth r_p is much larger than the borehole radius. This is not the case for very short times, when the heat capacity of the borehole volume cannot be neglected. The analytical solution for a line source is given by:

$$T(r,t) = \frac{q}{4\pi\lambda} E_1\left(\frac{r^2}{4at}\right) \qquad a=\lambda/(\rho c) \qquad (3.0.2)$$

The function E_1 is the so-called exponential integral:

$$E_1(x) = \int_x^\infty \frac{1}{s} e^{-s} ds \qquad (3.0.3)$$

The differences between the numerical and analytical solutions will in the following sections, if nothing else is stated, be given as relative errors. The analytically calculated borehole temperature is then used as a reference level:

$$\text{Relative error} = \frac{\text{(Numerical temp.) - (Analytical temp.)}}{\text{(Analytical borehole temp.)}} \qquad (3.0.4)$$

The temperature at the cell boundary between the two nodal points of cell i-1 and i is calculated with logarithmic interpolation according to:

$$T_{i-1/2} = T_{i-1} + (T_i - T_{i-1}) \cdot \frac{\ln(r_{i-1/2}/r_{i-1})}{\ln(r_i/r_{i-1})} \qquad (3.0.5)$$

The index i-1/2 indicates the boundary between the two cells at the radial distance $r_{i-1/2} = r_{i-1} + \Delta r_{i-1}/2$, where r_{i-1} and Δr_{i-1} are the midpoint and the cell width of cell i-1. The logarithmic interpolation is strictly valid only for steady-state conditions. It gives less precise values if the thermal process is strongly transient.

In the considered examples the thermal conductivity and the thermal diffusivity of the ground are chosen to standard values for granite:

$$\lambda = 3.5 \text{ W/mK} \qquad a = 1.62 \cdot 10^{-6} \text{ m}^2/\text{s} \qquad (3.0.6)$$

The borehole radius r_b and the heat flow q from the borehole are:

$$r_b = 0.055 \text{ m} \qquad q = 10 \text{ W/m}, \quad t > 0 \qquad (3.0.7)$$

In the sections 3.1 and 3.2 calculations are made by using three equally sized cells in the radial direction. These cells have the widths r_p and $2r_p$ respectively. Three time-steps with the length $t_{pr}/3$ are used to calculate the temperatures in the nodal points and at the borehole wall at the print-out time t_{pr}. Similar calculations are made in section 3.3 with six eqally sized cells with the time-step approximately equal to the stability time-step. An expanding mesh with nine cells is used in section 3.4. Calculations for four meshes with 10 - 14 cells are made in section 3.5. A case with a step-wise variation of the heat extraction is studied in section 3.6.

3.1 Three equally sized cells: $\Delta r = r_p$

The calculations concern a time period $0 < t < t_{pr}$. The results are printed at t_{pr}. The ground is divided into three equally sized cells. Each cell has the width $\Delta r_p = r_p = \sqrt{a t_{pr}}$. See Figure 3.1. Four different simulations with t_{pr} = 1 day, 1 month, 10 years, and 1000 years are made. The stability time-steps Δt_{stab} become 9 hours, 12 days, 4.5 years, and 480 years respectively. The used time-steps are chosen to $t_{pr}/3$. This means that three time-steps are used.

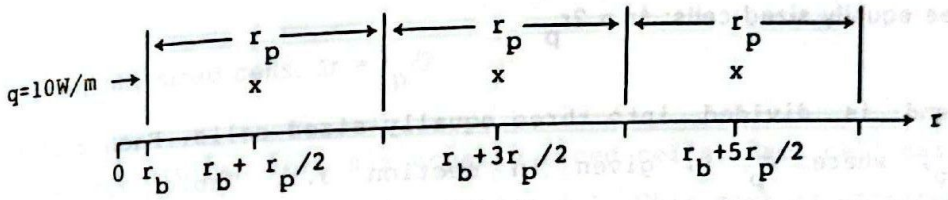

Figure 3.1 Three cells with the width r_p

Table 3.1 gives the temperatures at the borehole wall, at the radial distance $r_p = \sqrt{a t_{pr}}$, and at the midpoints of the three cells. The comparison with the analytical solution shows good agreement for all three cells at all times. The relative error, defined by (3.0.4), is smaller than 0.5 %. The temperature at the borehole wall shows the same good agreement for all times except when t_{pr} is equal to 1 day. The line-source solution is then not valid. It can be noted that the temperature at the radial distance r_p between cell one and two shows somewhat less agreement than the nodal temperatures. This temperature is calculated with the interpolation formula (3.0.5).

The right boundary of cell 3 is treated as thermally insulated in the numerical calculation. The temperature gradient here is so small that the heat flow can be neglected. The relative error for this cell is less than 0.2 %.

			Temparatures (°C)				
t_{pr}	r_p (m)	solu-tion	r_b	r_p	cell 1	cell 2	cell 3
1 day	0.374	num anal	1.072 1.055	0.254 0.237	0.399 0.404	0.089 0.088	0.019 0.016
1 month	2.06	num anal	1.844 1.832	0.257 0.237	0.488 0.489	0.105 0.107	0.016 0.020
10 year	22.6	num anal	2.928 2.921	0.255 0.237	0.505 0.512	0.107 0.111	0.016 0.021
1000 year	226	num anal	3.975 3.968	0.250 0.237	0.496 0.514	0.105 0.111	0.019 0.021

Table 3.1 Comparison between numerical and analytical solution for the mesh of Figure 3.1.

3.2 Three equally sized cells: $\Delta r = 2r_p$

The ground is divided into three equally sized cells. Each cell has the width $2r_p$, where r_p is given in section 3.1. Table 3.2 gives the temperature at the borehole wall and in the midpoints of the three cells for four different simulations with t_{pr} = 1 day, 1 month, 10 years and 1000 years. The stability time-steps become 37 hours, 52 days, 19 years, and 1900 years respectively. The used time-steps is chosen to $t_{pr}/3$ for all four simulations.

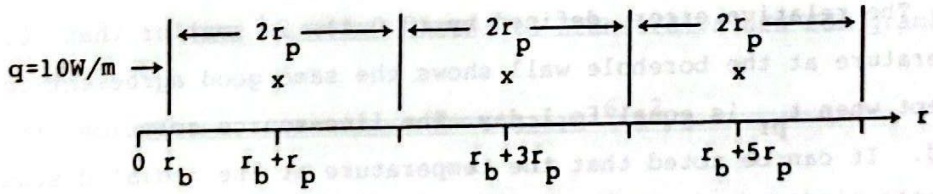

Figure 3.2 Three cells with the width $2r_p$.

The agreement is still not too bad. The relative error of the borehole temperature and in the nodal points is less than 1.5 % for all times exept when t_{pr} is 1 day. The line-source approximation is not valid at this time. The widths of the cells are chosen to twice the size of the penetration depth $2r_p$ at the print-out time t_{pr}. These cell widths are too large to give good resolution. The heat capacity of each cell and the flow resistances are too large to respond properly to a step pulse with the duration t_{pr}.

t_{pr}	r_p (m)	solution	Temperatures (°C) r_b	cell 1	cell 2	cell 3
1 day	0.374	num	1.106	0.170	0.002	0
		anal	1.055	0.190	0.006	0
1 month	2.06	num	1.851	0.193	0.010	0
		anal	1.832	0.228	0.008	0
10 year	22.6	num	2.933	0.195	0.010	0
		anal	2.921	0.237	0.008	0
1000 year	226	num	3.979	0.195	0.010	0
		anal	3.968	0.237	0.008	0

Table 3.2 Comparison between numerical and analytical solution for the mesh in Figure 3.2.

3.3 Six equally sized cells: $\Delta r = r_p/2$

The ground is divided into six equally sized cells. Each cell has the width $0.5r_p$, where r_p is given in section 3.1. This mesh is obtained from the mesh in section 3.1 by division of the cells into two halves. See Figure 3.3.

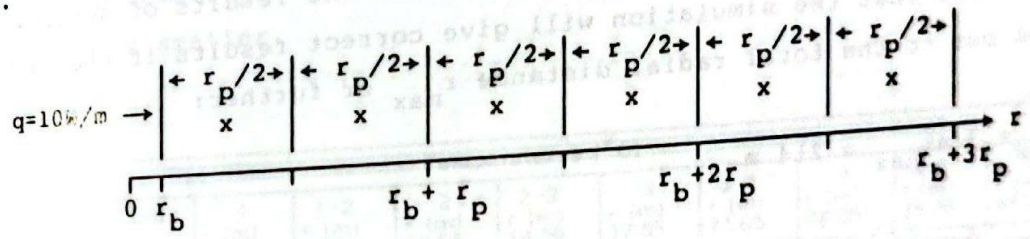

Figure 3.3 Six cells with the width $r_p/2$.

Table 3.3 gives the temperature at the borehole wall and at the nodal points of the cells for four different simulations with t_{pr} = 1 day, 1 month, 10 years and 1000 years. The stability time-steps Δt_{stab} become 2 hours, 3 days, 1.1 years and 118 years respectively. The used time-step is chosen to $0.99 \cdot \Delta t_{stab}$.

The agreement between numerically and analytically calculated temperatures is extremely good except for t_{pr}=1 day. The line-source approximation is not valid at this time. The relative error for all other values of t_{pr} is less than 0.2 % and normally around 0.1 %.

			Temperatures (°C)						
t_{pr}	r_p (m)	solu-tion	r_b	cell 1	cell 2	cell 3	cell 4	cell 5	cell 6
1 day	0.374	num anal	1.073 1.056	0.622 0.612	0.284 0.273	0.135 0.131	0.062 0.059	0.027 0.025	0.013 0.011
1 year	2.06	num anal	1.834 1.832	0.771 0.769	0.332 0.330	0.157 0.157	0.072 0.072	0.031 0.031	0.016 0.013
10 years	22.6	num anal	2.923 2.921	0.812 0.812	0.344 0.342	0.162 0.163	0.073 0.076	0.032 0.033	0.015 0.013
1000 years	226	num anal	3.970 3.968	0.812 0.816	0.344 0.343	0.163 0.163	0.074 0.075	0.032 0.033	0.015 0.014

Table 3.3 Comparison between numerical and analytical solution for the radial mesh of Figure 3.3.

3.4 Expanding mesh with seven cells

We will now use the results of section 3.1 to choose a suitable mesh for a simulation with many print-out times. The first print-out time is after one year. The calculation ends at t_{max}= 100 years. The results of section 3.1 - 3.3 indicate that the simulation will give correct results if the last cell reaches out to the total radial distance r_{max} or further:

$$r_{max} = 3\sqrt{at}_{max} = 214 \text{ m} \qquad (3.4.1)$$

Let t_{pr1} denote the first, i.e. the smallest, print-out time, which is equal to 1 year. The smallest cell width is in accordance with section 3.1 chosen to:

$$\Delta r_{min} = \sqrt{at}_{pr1} = 7 \text{ m} \qquad (3.4.2)$$

The three first cell widths have the size Δr_{min}. The following cells are expanding with the factor two. Seven cells are used. The right boundary of the last cell lies at r=231 m > r_{max}:

$$\Delta r = 7, 7, 7, 14, 28, 56, 112 \text{ meters} \qquad (3.4.3)$$

The stability time-step is equal to 5 months. The used time-step is $t_{pr1}/3$=4 months. Table 3.4 gives the numerically and analytically calculated results after 1, 10 and 100 years. The temperatures are given at the borehole wall, in the midpoints of cell 1 to 6, and at the boundary

between these cells. The temperatures at the cell walls are calculated with logarithmic interpolation formula (3.0.5).

The results show a maximum relative error of approximately 0.5 % except in one case. The temperature between cell 1 and 2 (r=7.055 m) has an error of roughly 1 % after one year. The interpolation formula (3.0.5) does not give a correct result at the radial distance $r_p=\sqrt{at}=7$ meters at t= 1 year. The error of the interpolation formula can be estimated, if the analytical values at the midpoints of cell 1 and 2 are used to calculate the temperature at the boundary between the cells. The interpolated temperature is compared with the exact analytical value at the boundary. The error is then 0.5%.

One could object that the same error should appear at a larger radius $r=\sqrt{at}=22$ meters at t=10 years, and $r=\sqrt{at}=71$ meters at t=100 years. This is also true. The absolute error at the radial distance 21.05 meters is roughly 0.015°C year 10 and 0.019°C at the radial distance 63.05 meters at year 100. However, the borehole temperature has increased, so the relative error becomes smaller.

		Temperatures (°C)											
time (year)	mesh	r_b(m) 0.055	1 r (m) 3.555	1-2 r (m) 7.055	2 r (m) 10.55	2-3 r (m) 14.05	3 r (m) 17.55	3-4 r (m) 21.05	4 r (m) 28.05	4-5 r (m) 35.05	5 r (m) 49.05	5-6 r (m) 63.05	6 r (m) 91.05
1	(3.4.3)	2.407	0.511	0.260	0.112	0.059	0.018	0.011	0	0	0	0	0
	anal	2.397	0.516	0.241	0.115	0.053	0.023	0.009	0	0	0	0	0
10	(3.4.3)	2.930	1.034	0.730	0.551	0.433	0.342	0.275	0.171	0.117	0.035	0.022	0.002
	anal	2.921	1.025	0.718	0.541	0.421	0.329	0.260	0.165	0.103	0.038	0.013	0.001
100	(3.4.3)	3.458	1.562	1.251	1.069	0.940	0.840	0.759	0.631	0.536	0.392	0.299	0.162
	anal	3.444	1.548	1.236	1.053	0.925	0.823	0.741	0.615	0.522	0.380	0.280	0.157

Table 3.4 Comparison between numerical and analytical solution for the radial mesh defined by (3.4.3).

3.5 Expanding meshes with ten to fourteen cells

The results in section 3.4 concerned an expanding mesh with the smallest cell widths $\Delta r_{min}=\sqrt{at_{prl}}$. We will now try to improve the numerical accuracy by using more and finer cells.

Consider a mesh with six cells of 3.5 meter followed by an expanding mesh of the same type as in (3.4.3). The cell widths become:

$$\Delta r = 3.5,\ 3.5,\ 3.5,\ 3.5,\ 3.5,\ 3.5,\ 7,\ 14,\ 28,\ 56,\ 112 \text{ m} \qquad (3.5.1)$$

The stability time-step Δt_{stab} is equal to 37 days. The chosen time-step is $0.99 \cdot \Delta t_{stab}$. Table 3.5 gives the results for the first four cells, and at the cell walls between these cells after 1, 10, and 100 years. The agreement with the analytical solution is very good after one year. The relative error is 0.05 % at the borehole wall and in the nodal points, and 0.25 % at the cell walls. The penetration depth r_p after one year is 7 meters. The temperature variation is then relatively large in the region around r=7 meters. The six cells of 3.5 meter ($r_p/2 \approx 3.5$ m) give very high resolution in the region $0.055 \leq r \leq 12.3$ meters. Hence, this mesh is particulary good for a simulation where high resolution is important after one year. The mesh (3.5.1) does not give any improved resolution at t=10 or 100 years. The cells followed by the six 3.5 meter cells expand to fast to give good numerical accuracy at these times.

		Temperatures (^{0}C)							
time (year)	mesh	r_b(m) 0.055	1 r (m) 1.805	1-2 r (m) 3.555	2 r (m) 5.305	2-3 r (m) 7.055	3 r (m) 8.055	3-4 r (m) 10.55	4 r (m) 12.30
1	(3.5.1)	2.398	0.811	0.521	0.349	0.247	0.167	0.118	0.077
	anal	2.397	0.812	0.516	0.348	0.241	0.168	0.115	0.078
10	(3.5.1)	2.927	1.339	1.033	0.852	0.726	0.628	0.550	0.484
	anal	2.921	1.333	1.025	0.844	0.719	0.619	0.541	0.475
100	(3.5.1)	3.457	1.870	1.562	1.380	1.250	1.150	1.068	0.998
	anal	3.444	1.857	1.549	1.367	1.237	1.136	1.053	0.984

Table 3.5 Comparison between numerical and analytical solution for the radial mesh given by (3.5.1).

Consider now a second mesh with the cell widths:

$$\Delta r = 7,\ 7,\ 7,\ 7,\ 7,\ 7,\ 14,\ 28,\ 56,\ 112 \text{ meters} \qquad (3.5.2)$$

The stability time step for this mesh is 5 months. The chosen time-step is 4 months ($t_{pr1}/3$=4 months). Table 3.6 gives the results for the nodal points of cell 2 to 5, and at the cell walls between these cells after 1, 10, and 100 years. The agreement with the analytical solution is very good after ten years. The relative error is 0.05 % at the borehole wall, 0.1 % for the nodal points, and 0.15 % at the cell walls. The penetration depth

is 22 meters after ten years. The temperature variation is relatively large in the region around r=22 meters. The six 7 meter cells ($r_p/3 \approx 7$ m) give a very high resolution after ten years in the region $10.55 \leq r \leq 31.55$ meters. Hence, this mesh is particulary good for a simulation where high resolution is important after ten years. The mesh (3.5.2) does not give especially high resolution after one or hundred years. The first cells are too large to give good accuracy after one year, and the cells followed by the six cells of 7 meters are expanding to fast to give good accuracy after 100 years.

		Temperatures (^{0}C)							
time (year)	mesh	r_b(m) 0.055	2 r (m) 10.55	2-3 r (m) 14.05	3 r (m) 17.55	3-4 r (m) 21.05	4 r (m) 24.55	4-5 r (m) 28.05	5 r (m) 31.55
1	(3.5.2)	2.407	0.112	0.059	0.018	0.008	0	0	0
	anal	2.397	0.115	0.053	0.023	0.009	0.004	0.001	0.241
10	(3.5.2)	2.920	0.542	0.424	0.332	0.265	0.209	0.168	0.132
	anal	2.921	0.541	0.421	0.330	0.260	0.209	0.165	0.131
100	(3.5.2)	3.455	1.065	0.936	0.836	0.755	0.686	0.628	0.577
	anal	3.444	1.053	0.925	0.824	0.741	0.675	0.615	0.565

Table 3.6 Comparison between numerical and analytical solution for the radial mesh given by 3.5.2.

Consider now a third mesh with the following cell widths:

$$\Delta r = 7,\ 14,\ 28,\ 28,\ 28,\ 28,\ 28,\ 28,\ 56,\ 112 \text{ meters} \qquad (3.5.3)$$

The stability time-step and the used time-step are the same as for mesh (3.5.2). Table 3.7 gives the results in the nodal points of cell 3 - 6, and at the cell walls between these cells after 1, 10 and 100 years. The agreement with the analytical solution is very good after hundred years. The relative error is 0.03 % at the borehole wall, 0.12 % for the nodal temperatures, and 0.06 % at the cell walls between the nodal points. The penetration depth is 71 meters after hundred years. The temperature variation is relatively large in the region around r=71 meters. The six 28 meter cells ($r_p/2.5 \approx 28$ m) give very high resolution after 100 years in the region $35 \leq r \leq 119$ meters. Hence, this mesh is particulary good for a simulation where high resolution is important after hundred years. The mesh (3.5.3) uses too large cells to give good accuracy after one and ten years.

Note that the CPU-time demand for the calculation with the meshes (3.5.2-3) is almost the same as for the the mesh (3.4.3). The smallest cell widths are the same for these three meshes. This implies the same stability time-step. However, the meshes (3.5.2-3) give an improvement only at one specific time each.

		Temperatures (^{0}C)							
time (year)	mesh	r_b(m) 0.055	3 r (m) 35.05	3-4 r (m) 49.05	4 r (m) 63.05	4-5 r (m) 77.05	5 r (m) 91.05	5-6 r (m) 105.1	6 r (m) 119.1
1	(3.5.3)	2.451	0	0	0	0	0	0	0
	anal	2.397	0	0	0	0	0	0	0
10	(3.5.3)	2.938	0.095	0.048	0.013	0.007	0.002	0.001	0
	anal	2.921	0.103	0.038	0.013	0.004	0.001	0	0
100	(3.5.3)	3.443	0.517	0.381	0.280	0.212	0.156	0.118	0.085
	anal	3.444	0.521	0.380	0.280	0.211	0.157	0.117	0.086

Table 3.7 Comparison between numerical and analytical solution for the radial mesh (3.5.3).

The three examples above have printouts between $t_{prl} \leq t \leq t_{max}$. They show that it is possible to obtain very good numerical accuracy in the whole region $r_b \leq r \leq 1.5r_p$ at any specific printout time by using six cells with a width between say $r_p/3$ and $r_p/2$, where r_p is the penetration depth at the printout.

We shall now look at a mesh such that all cells in the region out to $r= 1.5r_p$ have cell widths equal to or less than $r_p/2$ for all printouts times in the time intervall $t_{prl} \leq t \leq t_{max}$. The smallest cell width becomes $\Delta r_{min}=0.5\sqrt{at_{prl}}$ where t_{prl} is the first print-out time. Such a mesh ought to give high resolution at all times.

Consider the case when t_{prl} is equal to 1 year. A mesh that satisfies the conditions above is obtained by dividing all cells in mesh (3.4.3) into two halves:

$$\Delta r = 3.5, 3.5, 3.5, 3.5, 3.5, 3.5, 7, 7, 14, 14, 28, 28, 56, 56 \quad (3.5.4)$$

The stability time-step and the used time-step are the same as for mesh (3.5.1). The results of the numerical and the analytical solutions for cell 1 - 12, and for the boundary between these cells are given by Table 3.8. The agreement is good at all times. The relative error of the borehole temperature is always less than 0.1 %. The corresponding error of the ground temperaures is 0.25 %. Hence, the relative error has been reduced

from 0.5 % to 0.25 % by using the mesh (3.5.4) instead of mesh (3.4.3). The cost of this improvement is a shorter stability time-step and the use of twice as many cells. The CPU-time is increased with a factor four.

time (year)	mesh	Temperatures (^{0}C)							
		r_b(m) 0.055	1 r (m) 1.805	1-2 r (m) 3.555	2 r (m) 5.305	2-3 r (m) 7.055	3 r (m) 8.805	3-4 r (m) 10.55	4 r (m) 12.30
1	(3.5.4)	2.398	0.811	0.521	0.349	0.247	0.167	0.118	0.077
	anal	2.397	0.811	0.516	0.348	0.241	0.168	0.118	0.078
10	(3.5.4)	2.923	1.336	1.030	0.849	0.722	0.624	0.546	0.480
	anal	2.921	1.333	1.025	0.844	0.719	0.619	0.541	0.475
100	(3.5.4)	3.447	1.861	1.553	1.371	1.241	1.141	1.059	0.990
	anal	3.444	1.857	1.549	1.367	1.237	1.136	1.053	0.984

time (year)	solu-tion	Temperatures (^{0}C)							
		4-5 r (m) 14.05	5 r (m) 15.80	5-6 r (m) 17.55	6 r (m) 19.30	6-7 r (m) 21.05	7 r (m) 24.55	7-8 r (m) 28.05	8 r (m) 31.55
1	(3.5.4)	0.054	0.033	0.023	0.013	0.009	0.002	0.001	0
	anal	0.053	0.035	0.023	0.015	0.009	0.004	0.001	0
10	(3.5.4)	0.425	0.376	0.335	0.298	0.266	0.210	0.169	0.133
	anal	0.421	0.373	0.330	0.292	0.260	0.209	0.165	0.131
100	(3.5.4)	0.930	0.877	0.830	0.787	0.749	0.680	0.622	0.571
	anal	0.925	0.873	0.824	0.780	0.741	0.675	0.615	0.565

time (year)	mesh	Temperatures (^{0}C)							
		8-9 r (m) 35.05	9 r (m) 42.05	9-10 r (m) 49.05	10 r (m) 56.05	10-11 r (m) 63.05	11 r (m) 77.05	11-12 r (m) 91.05	12 r (m) 105.1
1	(3.5.4)	0	0	0	0	0	0	0	0
	anal	0	0	0	0	0	0	0	0
10	(3.5.4)	0.107	0.061	0.040	0.022	0.015	0.003	0.002	0
	anal	0.103	0.063	0.038	0.021	0.013	0.004	0.001	0
100	(3.5.4)	0.525	0.448	0.385	0.332	0.288	0.213	0.162	0.119
	anal	0.522	0.443	0.380	0.326	0.280	0.211	0.157	0.117

Table 3.8 Comparison between numerical and analytical solution for the radial mesh given by 3.5.4.

3.6 Monthly step-wise variation of the heat injection rate

We will now study three different meshes for a step-wise variation of the injection rate. The step length is chosen to t_{step}=1 month. The print-outs are given at the end of each step. The duration of the process is t_{max}=5 years.

The first two meshes, (3.6.1) and (3.6.2), expand in the same way as the meshes (3.4.3) and (3.5.4). The smallest cells for the latter meshes were equal to the penetration depth (=7m) and half the penetration depth (=3.5m) at the first print-out time t_{pr1}=1 year. The corresponding meshes here have the smallest cell widths 2 and 1 meters, which are equal to the penetration depth and half the penetration depth at the time t_{step}=1 month. A third and still finer mesh, (3.6.3), is also used. This mesh is the same as mesh (3.6.2), but with the three first cells divided into two halves. The three meshes are extended out to the radial distance 68 m $\geq$ 48 m (r_{max} = $3\sqrt{at_{max}}$=3·16 = 48 meters).:

$$\Delta r = 2,\ 2,\ 2,\ 4,\ 8,\ 16,\ 32 \text{ m} \qquad (3.6.1)$$

$$\Delta r = 1,\ 1,\ 1,\ 1,\ 1,\ 1,\ 2,\ 2,\ 4,\ 4,\ 8,\ 8,\ 16,\ 16 \text{ m} \qquad (3.6.2)$$

$$\Delta r = 0.5,\ 0.5,\ 0.5,\ 0.5,\ 0.5,\ 0.5,\ 1.,\ 1.,\ 1.,\ 2,\ 2,\ 4,\ 4,\ 8,\ 8,\ 16,\ 16 \text{ m} \qquad (3.6.3)$$

The used time-step is equal to $0.99 \cdot \Delta t_{stab}$, where Δt_{stab} is equal to 12 days, 2.83 days and 16 hours for the three meshes.

3.6.1 Periodic pulse-train

Consider the case when the heat flow at the borehole wall is a pulse train with the values +10, -10, +10, ... W/m for month 1, 2, 3, and so on. This periodic heat injection has the average value zero over the time 2 months. Table 3.9 gives the results for the meshes (3.6.1-3) after 5 months, 6 months, 49 months, and 50 months. The reference level for the relative errors is equal to the peak to peak value of the borehole temperature. This temperature is approximately 3.47 ^{0}C for all four print-out times. The maximum relative error of the borehole temperature is 0.4 % for mesh (3.6.1), 0.1 % for mesh (3.6.2), and 0.05 % for mesh (3.6.3). The maximum

error of the temperature in the ground is 1 %, 0.5 %, and 0.5 % for the three meshes respectively. This error occurs for all three meshes at the radial distance 2.055 meters at the time 49 months. For all other radial distances and times the errors are much less. Note that the penetration depth for a step pulse with the length one month is equal to 2 meters.

		Temperatures (^{0}C)					
time	mesh	r (m) 0.055	r (m) 1.055	r (m) 2.055	r (m) 3.055	r (m) 5.055	r (m) 10.055
5 months	(3.6.1)	1.775	0.432	0.206	0.072	0.001	0.007
	(3.6.2)	1.756	0.437	0.184	0.075	0.011	0.009
	(3.6.3)	1.754	0.432	0.181	0.074	0.013	0.009
	anal	1.752	0.427	0.173	0.068	0.014	0.010
6 months	(3.6.1)	-1.733	-0.389	-0.166	-0.033	0.032	0.017
	(3.6.2)	-1.714	-0.396	-0.144	-0.037	0.032	0.016
	(3.6.3)	-1.712	-0.391	-0.141	-0.036	0.019	0.015
	anal	-1.711	-0.387	-0.133	-0.030	0.018	0.015
49 months	(3.6.1)	1.754	0.411	0.187	0.053	-0.014	-0.003
	(3.6.2)	1.735	0.417	0.165	0.057	-0.003	0.000
	(3.6.3)	1.733	0.412	0.161	0.056	-0.002	-0.001
	anal	1.732	0.406	0.146	0.053	-0.005	0.001
50 months	(3.6.1)	-1.749	-0.406	-0.182	-0.049	0.019	0.008
	(3.6.2)	-1.731	-0.412	-0.160	-0.052	0.008	0.007
	(3.6.3)	-1.729	-0.407	-0.157	-0.051	0.007	0.006
	anal	-1.727	-0.401	-0.141	-0.048	0.009	0.005

Table 3.9 Numerical results for the meshes (3.6.1-3) when the heat flow at the borehole is changing between +10 and -10 W/m at the end of each month.

3.6.2 Sinusoidal heat injection

The heat injection is given by an approximation of a sine function with the amplitude 10 W/m and the period time one year. The sine function is approximated by twelve steps of one month. The size of the steps is determined by the value of the sine-function in the middle of each period, $10 \cdot \sin((2n-1) \cdot \pi/12)$, n= 1,2, ... 12:

Month:	1	2	3	4	5	6
q (W/m)	2.59	7.08	9.66	9.66	7.08	2.59
Month:	7	8	9	10	11	12
q (W/m)	-2.59	-7.08	-9.66	-9.66	-7.08	-2.59

Table 3.10 shows the results after 4 months, 10 months, 4 years and 4 months, and 4 years and 10 months. The reference level for the calculations of the relative errors is chosen as the peak to peak value of the borehole

temperature during the year (3.88 and 3.82 °C for year 1 and 5 respectively). The relative error of the borehole temperature is less than 0.15 % for mesh (3.6.1), and less than 0.05% for the meshes (3.6.2) and (3.6.3). The largest error outside the borehole occurs at the radial distance r=3.055 m. This error is equal to 0.5 % for all three meshes at the time 4 years and 4 months. At all other radial distances the error is smaller than 0.4 % for mesh (3.6.1), and 0.2 % for the meshes (3.6.2-3).

		Temperatures (°C)						
time	mesh	r (m) 0.055	r (m) 1.055	r (m) 2.055	r (m) 3.055	r (m) 5.055	r (m) 7.055	r (m) 10.055
4 months	(3.6.1)	2.009	0.711	0.443	0.283	0.126	0.057	0.018
	(3.6.2)	2.005	0.714	0.435	0.283	0.123	0.049	0.014
	(3.6.3)	2.006	0.714	0.435	0.283	0.123	0.050	0.014
	anal	2.004	0.709	0.432	0.278	0.121	0.050	0.012
10 months	(3.6.1)	-1.876	-0.578	-0.316	-0.160	-0.019	0.029	0.037
	(3.6.2)	-1.873	-0.584	-0.309	-0.162	-0.019	0.035	0.039
	(3.6.3)	-1.875	-0.584	-0.309	-0.162	-0.019	0.035	0.039
	anal	-1.873	-0.580	-0.306	-0.157	-0.019	0.033	0.040
4 years 4 months	(3.6.1)	1.927	0.630	0.366	0.209	0.065	0.012	-0.005
	(3.6.2)	1.924	0.634	0.358	0.211	0.064	0.005	-0.007
	(3.6.3)	1.925	0.634	0.358	0.211	0.064	0.003	-0.006
	anal	1.923	0.632	0.354	0.194	0.063	0.000	-0.014
4 years 10 months	(3.6.1)	-1.910	-0.612	-0.349	-0.192	-0.048	0.005	0.021
	(3.6.2)	-1.907	-0.617	-0.342	-0.194	-0.048	0.011	0.023
	(3.6.3)	-1.908	-0.617	-0.341	-0.194	-0.048	0.011	0.022
	anal	-1.907	-0.615	-0.342	-0.178	-0.046	0.015	0.029

Table 3.10 Numerically calulated temperatures for a sinusoidal heat injection with the meshes 3.6.1-3.

3.6.3 Example with typical monthly loading conditions

Consider a case when the annual heat injection rate is given by 12 monthly values which may be monthly average values for a practical case:

Month:	1	2	3	4	5	6
q (W/m)	16	23	31	38	41	39
Month:	7	8	9	10	11	12
q (W/m)	33	26	17	0	0	0

Table 3.11 shows the results for mesh (3.6.1) and (3.6.2) at the borehole radius r_b, and at eleven different radial distances. Mesh (3.6.3) is not considered in this comparison. The different radial distances are located in the mid-points and at the cell walls of cell 1 to 6 in mesh (3.6.1). These radial distances corresponds also to the cell walls between cell 1 to

12 in mesh (3.6.2). The printout times are 5 months, 1 year, 4 years and 5 months, and 5 years. The reference level, which is used for calculation of the relative errors, is equal to the largest borehole temperature during the year. These temperatures are 8.63°C and 9.67°C for year 1 and 5 respectively. The comparison with the analytical solution gives the maximum relative error 0.7 % for mesh (3.6.1), and 0.6 % for mesh (3.6.2) at the radial distance r=3.055 m for the time 4 years and 5 months. The relative error of the borehole temperature is less than 0.4 % and 0.1 % for the two meshes respectively.

		Temperatures (°C)											
ime	mesh	r (m) 0.055	r (m) 1.055	r (m) 2.055	r (m) 3.055	r (m) 4.055	r (m) 5.055	r (m) 6.055	r (m) 8.055	r (m) 10.05	r (m) 14.05	r (m) 18.05	r (m) 26.05
months	(3.6.1)	8.654	3.147	2.001	1.320	0.932	0.630	0.459	0.188	0.119	0.015	0.009	0
	(3.6.2)	8.634	3.153	1.967	1.316	0.901	0.621	0.430	0.203	0.097	0.019	0.004	0
	anal	8.629	3.136	1.953	1.298	0.883	0.611	0.419	0.194	0.088	0.016	0.002	0
year	(3.6.1)	0.915	0.915	0.868	0.840	0.771	0.717	0.638	0.513	0.368	0.149	0.092	0.008
	(3.6.2)	0.904	0.892	0.864	0.822	0.767	0.703	0.632	0.488	0.353	0.163	0.069	0.009
	anal	0.898	0.889	0.856	0.824	0.764	0.695	0.620	0.483	0.348	0.155	0.059	0.006
years months	(3.6.1)	9.704	4.197	3.031	2.338	1.919	1.593	1.380	1.044	0.865	0.594	0.424	0.174
	(3.6.2)	9.674	4.188	2.991	2.321	1.882	1.573	1.347	1.039	0.842	0.580	0.402	0.186
	anal	9.670	4.175	2.987	2.276	1.864	1.568	1.329	1.020	0.823	0.562	0.395	0.176
years	(3.6.1)	1.673	1.673	1.616	1.583	1.499	1.434	1.335	1.179	0.975	0.668	0.480	0.206
	(3.6.2)	1.658	1.643	1.610	1.559	1.493	1.415	1.328	1.142	0.959	0.660	0.453	0.216
	anal	1.650	1.641	1.601	1.581	1.487	1.421	1.318	1.140	0.968	0.647	0.442	0.204

Table 3.11 Comparison between numerical and analytical solution for the example in section 3.6.3.

The general conclusion of the examples in section 3.6.1 - 3.6.3 concerning variations on monthly basis is that mesh (3.6.1) ought to give the required numerical accuracy in most applications. Mesh (3.6.2) can be used when it necessary to have extremely good precision. Mesh (3.6.3) does not give any improved resolution compared with mesh (3.6.2). It should therefore never be used.

3.7 Conclusions

Consider a simulation starting at t=0 and with a duration $t=t_{max}$. The conclusion from section 3.1 - 3.3 is that the radial mesh must reach out to at least the radial distance r_{max} defined by:

$$r_{max} = 3\sqrt{at}_{max} \leq \Sigma \Delta r_i \qquad (3.7.1)$$

Here Δr_i is the width of cell i. The smallest cell widths are detemined by a time t_{min} according to:

$$\Delta r_{min} = \sqrt{at}_{min} \qquad (3.7.2)$$

The radial cell widths are:

$$\Delta r = \Delta r_{min}, \Delta r_{min}, \Delta r_{min}, 2\Delta r_{min}, 4\Delta r_{min}, 8\Delta r_{min} \quad \ldots \qquad (3.7.3)$$

The choice of t_{min} in different cases is discussed below. In section 3.1 to 3.5 the heat injection is constant during the whole simulation $0 \leq t \leq t_{max}$. The time t_{min} is then equal to the first print-out time. See Figure 3.4a. In section 3.6 the heat injection is given by a function with step-wise variation. Each step has the length of one month. The print-out times lie at the end of each step as in Figure 3.4b. The time t_{min} is in this case equal to one month.

Consider now the general case when the injection is a step-wisely varying function with different step lengths. The print-out times may lie at any times as in Figure 3.4c. Consider a specific print-out time t_{pr}. The difference between the time t_{pr} and the time for the last step in boundary heat flow t_{step} before t_{pr} is denoted Δt_{pr}:

$$\Delta t_{pr} = t_{pr} - t_{step} \qquad (3.7.4)$$

The time t_{min} is in general defined as the smallest value of Δt_{pr} for all the different print-out times:

$$t_{min} = \min(\Delta t_{pr1}, \Delta t_{pr2}, \ldots, \Delta t_{pr,n}) \qquad (3.7.5)$$

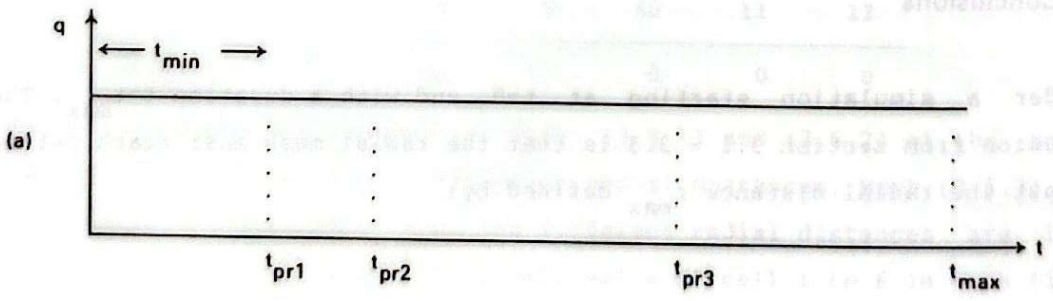

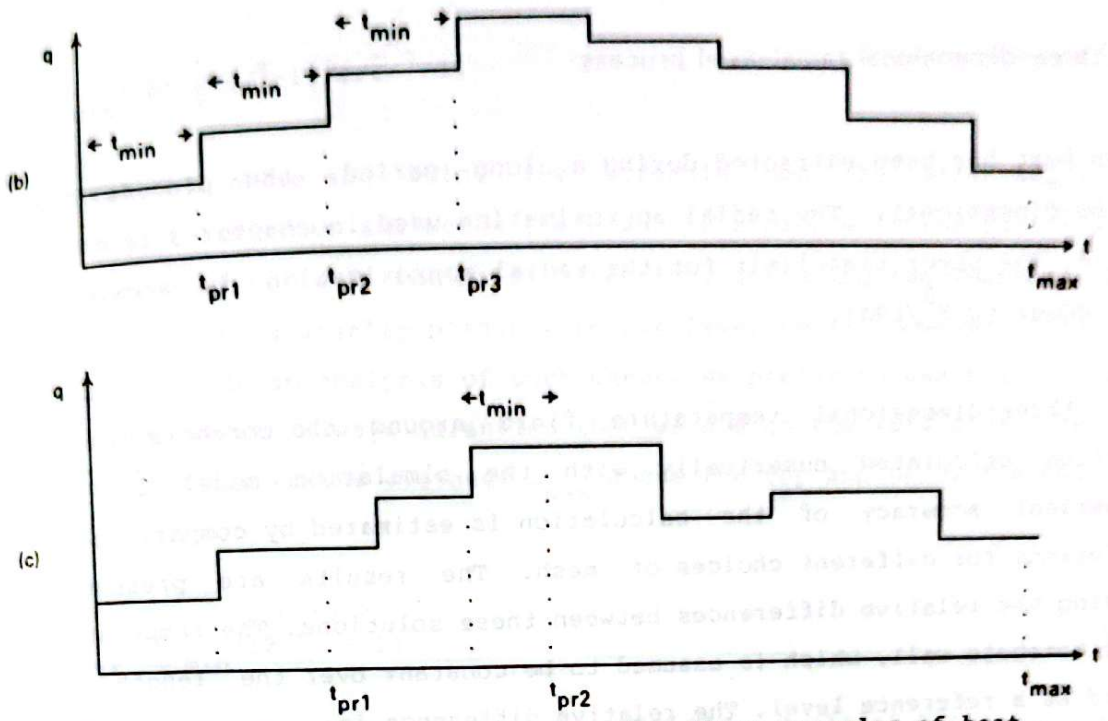

Figure 3.4a-c *Choice of the time t_{min} for three examples of heat extraction functions and print-outs.*

The heat injection may vary with steps shorter than t_{min} during a period with no print-outs. But the recipe (3.7.5) for the choice of t_{min} is still valid. A new time-step in the numerical simulation is always started for every new heat injection step. The total heat injection is then always correct. According to (3.7.5) there are no print-outs before a time period t_{min} after any step in the boundary heat flow. The rapid variations will therefore not influence the solution at the print-out times.

The choice of cell widths is obtained from the analysis of cases when the boundary condition at the borehole wall is given by a step-wise variation of the heat-flow q(t) (W/m). The situation is somewhat different when the boundary condition is a step-wise variation of the temperature at the borehole wall. In this case the injected energy is dependent on the numerical accuracy. The error in the injected heat may be large if the cell widths close to the borehole are too large to give good resolution. The recipe may be used also in this latter case. The accuracy is judged to be of the same order as in the cases of given injection rates.

4 Three-dimensional radial-axial process

When heat has been extracted during a long period, the process becomes three-dimensional. The radial approximation used in chapter 3 is no longer valid. The upper time limit for the radial approximation is according to [3] equal to $H^2/(9a)$.

The three-dimensional temperature field around the borehole is in this section calculated numerically with the simulation model [1,2]. The numerical accuracy of the calculation is estimated by comparison of the solutions for different choices of mesh. The results are presented by giving the relative differences between these solutions. The temperature at the borehole wall, which is assumed to be constant over the length H, is used as a reference level. The relative difference is:

$$\text{Relative difference} = \frac{\text{(Numerical temp. 1)} - \text{(Numerical temp. 2)}}{\text{(Borehole temp.)}} \qquad (4.1)$$

The numerical calculations are made with typical Swedish data for the ground and the borehole. The data for the ground are given by (3.0.6). The radius of the borehole is r_b. The upper part of the borehole is thermally insulated down to the depth D. Heat is extracted over the length H. The total borehole length is D+H. The data for the borehole are:

$$r_b = 0.055 \text{ m} \qquad D = 5 \text{ m} \qquad H = 110 \text{ m} \qquad (4.2)$$

The heat injection is constant with an average value of q=10 W/m for $t \geq 0$.

The mesh division in the axial direction is generated automatically by the parameter n_z. The number of cells along half of the length H is equal to n_z. The cells are expanding with the factor $\sqrt{2}$ from the top and the bottom of the borehole to the middle of the borehole. The smallest cell width becomes:

$$\Delta z_{min} = H \cdot \frac{1}{2} (\sqrt{2}-1)/(\sqrt{2}^{n_z}-1) \qquad (4.3)$$

The first cell above and below the borehole has the size Δz_{min}. The following cells above and below the borehole expand with the factor 2. The total number of cells in the axial direction, including two boundary cells, is $4 \cdot n_z + 8$. It is usually possible to use fewer cells. However, this study does not include an analysis of such cases. We prefer to use the automatic generation which always garanties that we are on the safe side. The axial mesh reaches out to the distance z_{max} above the top and below the bottom of the borehole:

$$z_{max} = \Delta z_{min} \cdot (2^{n_z+3} - 1) \qquad (4.5)$$

The axial mesh has the total size $H+2z_{max}$. The values on Δz_{min} and Δz_{max} become for n_z = 3, 4, 5 and 6:

$n_z=3$	$\Delta z_{min} = H/8.8$	$\Delta z_{max} = H \cdot 7.1$
$n_z=4$	$\Delta z_{min} = H/14.5$	$\Delta z_{max} = H \cdot 8.8$
$n_z=5$	$\Delta z_{min} = H/22.5$	$\Delta z_{max} = H \cdot 11.3$
$n_z=6$	$\Delta z_{min} = H/33.8$	$\Delta z_{max} = H \cdot 15.1$

(4.4)

In Figure 1.1 a mesh with $n_z=3$ is shown. The figure does not cover the whole mesh far above and below the borehole. The number of cells is therefore less than $4 \cdot 3+8=20$. The complete sequence of cell widhts Δz_j becomes for $n_z=3$ and H=110:

$$\Delta z = 399, 199, 100, 50, 25, 12, \underline{12, 18, 25, 25, 18, 12}, 12, 25, 50, 100, 199, 399 \text{ m} \qquad (4.6)$$

The cell widths along the borehole are underlined. A comparison between five different meshes is made for the times 1 and 5 years. A similar comparison with three of the meshes is made at year 25. The results are given in section 4.1. A comparison between three different meshes at large times, when the solution is approaching steady-state, is given in section 4.2.

4.1 Comparison of meshes during the first 25 years

Consider the process during 25 years: t_{max}=25 years. A comparison between five different meshes is made at two print-out times after 1 and 5 years. A third comparison between three of these meshes is made at the print-out time 25 years.

The five different meshes are given by the radial cell widths and by the parameter n_z for the automatic mesh generation in the axial direction:

1. Δr = 14, 14, 14, 28, 56, 112 m n_z= 4 (4.1.1)
2. Δr = 7 ,7, 7, 14, 28, 56, 112 m n_z= 4 (4.1.2)
3. Δr = 3.5, 3.5, 3.5, 3.5, 3.5, 3.5, 7, 7, 14, 14, 28 , 28, 56, 56 m n_z= 5 (4.1.3)
4. Δr = 0.25, 0.25, 0.25, 0.25, 0.25, 0.25, 0.5, 0.5, 0.5, 1, 1, 2, 2, 4, 4, 8, 8, 16, 16 m n_z= 6 (4.1.4)
5. Δr = 0.25, 0.25, 0.25, 0.25, 0.25, 0.25, 0.5, 0.5, 0.5, 1, 1, 2, 2, 4, 4, 8, 8, 16, 16 m n_z=14 (4.1.5)

The value of n_z determines the smallest cell widths in the axial direction to 7.6, 7.6, 4.9, 3.2 and 0.18 meters respectively. The axial cell widths for n_z=4 are:

$$\Delta z = 486, 243, 122, 61, 30, 15, 7.6, \underline{7.6, 11, 15, 21, 21, 15, 11, 7.6}, 7.6, 15, 30, 61, 122, 243, 486 \quad (4.1.6)$$

The cell widths along the borehole are underlined. The stability time-steps for the five meshes are 5.5 months,3 months, 27 days, 3.9 hours, and 1.7 hours respectively. The stability time-step of mesh (4.1.5) is 2400 times smaller than for mesh (4.1.1). The number of cells in these two meshes are 1116 and 132 respectively.

Table 4.1 shows the temperatures after one year at the radial distances r = 0.055, 5.5, 11 and 22 meters for three depths z = 5, 60 and 115 meters. These depths lies at the top, middle, and bottom of the borehole respectively. The value for r=0.055 m is the borehole temperature, which is same over the borehole length. The relative differences between the solutions of the different meshes are largest at the top (z=5 m) and at the bottom (z=115 m) of the borehole for the radius 5.5 meters. The maximum

relative difference is 1 %. The big cells in the first and second mesh cannot describe the local three-dimensional process here. However, the local disturbances at the top and the bottom of the borehole can be neglected if we are concerned about the total heat extraction over the whole borehole depth D ≤ z ≤ D+H.

Mesh (4.1.1) gives a difference relative to mesh (4.1.5) of less than 1% for all distances r and depths z. The three 14 meter cells in mesh (4.1.1) are to large to give very high resolution at the time 1 year. This result was expected since the smallest cell widths did not follow the rule (3.7.2) for t_{min}=1 year. If the rule (3.7.2) is followed, mesh (4.1.1) cannot be used during the period 0 < t ≤ 4 years.

time = 1 year		Temperatures (^{0}C)			
z-coord	mesh	r=0.055 m	r= 5.5 m	r= 11 m	r= 22 m
5 m	(4.1.1)	2.390	0.138	0.050	0.004
	(4.1.2)	2.376	0.141	0.040	0.004
	(4.1.3)	2.360	0.157	0.051	0.005
	(4.1.4)	2.371	0.148	0.042	0.008
	(4.1.5)	2.362	0.156	0.044	0.003
60 m	(4.1.1)		0.317	0.125	0.009
	(4.1.2)		0.343	0.103	0.011
	(4.1.3)	-"-	0.337	0.114	0.013
	(4.1.4)		0.335	0.105	0.008
	(4.1.5)		0.334	0.105	0.008
115 m	(4.1.1)		0.160	0.063	0.005
	(4.1.2)		0.176	0.052	0.005
	(4.1.3)	-"-	0.178	0.060	0.007
	(4.1.4)		0.180	0.056	0.004
	(4.1.5)		0.184	0.057	0.004

Table 4.1 Comparison between numerical calculations with five different choices of mesh according to (4.1.1-5) after one year.

Table 4.2 gives the results after 5 years. Mesh (4.1.1) does not show very good agreement at any depth. The three 14 meter cells in the radial direction seems too large to describe steep gradients close to the borehole. The agreement for mesh (4.1.2) is good at the middle at the borehole. This part is representative for most of the borehole length. This mesh is therefore fine enough to use, except for calculation of the temperature in the vincinity of the top and bottom of the borehole. In this case one of the meshes (4.1.3 - 5) shall be used.

The two meshes (4.1.4) and (4.1.5) have the same radial mesh division. The parameter n_z for the axial mesh generation is 6 and 14 respectively. The smallest cell widths in the axial direction are 3.2 and 0.18 meters (H/600≈0.18 m). The local process in the vicinity of the top and the bottom of the borehole is more correctly described with mesh (4.1.5). However, the relative difference between the calculated borehole temperature for mesh (4.1.4) and (4.1.5) is less than 0.4 % at both year 1 and year 5.

time = 5 years		Temperatures (^{0}C)			
z-coord	mesh	r=0.055 m	r= 5.5 m	r= 11 m	r= 22 m
5 m	(4.1.1) (4.1.2) (4.1.3) (4.1.4) (4.1.5)	2.685 2.692 2.690 2.682 2.671	0.225 0.231 0.257 0.242 0.253	0.111 0.109 0.124 0.112 0.114	0.031 0.035 0.036 0.032 0.033
60 m	(4.1.1) (4.1.2) (4.1.3) (4.1.4) (4.1.5)	-"-	0.639 0.664 0.668 0.659 0.657	0.368 0.374 0.382 0.372 0.371	0.126 0.141 0.139 0.133 0.133
115 m	(4.1.1) (4.1.2) (4.1.3) (4.1.4) (4.1.5)	-"-	0.339 0.358 0.367 0.366 0.372	0.194 0.208 0.207 0.202 0.204	0.066 0.075 0.074 0.072 0.072

Table 4.2 Comparison between numerical calculations with five different choices of mesh according to (4.1.1-5) after 5 years.

Table 4.3 shows the results for the meshes (4.1.1-3) after 25 years. The results are now given for two more radial distances, r= 55 and 110 meters. The relative differences between mesh (4.1.1) and (4.1.3) is 0.2 % at the borehole wall, 1 % at the top of the borehole (z=5m), and 0.7 % at the middle of the borehole (z=60m). The corresponding disagreements between mesh (4.1.2) and (4.1.3) are 0.15 %, 1 % and 0.3 %. The difference of the calculated borehole temperature is less than 0.3% for all three meshes.

time = 25 years		Temperatures (^{0}C)					
z-coord (m)	mesh	r= 0.055m	r= 5.5 m	r= 11 m	r= 22 m	r= 55 m	r= 110 m
5	(4.1.1) (4.1.2) (4.1.3)	2.933 2.931 2.927	0.281 0.284 0.313	0.156 0.154 0.070	0.066 0.070 0.169	0.011 0.012 0.013	0.001 0.001 0.001
60	(4.1.1) (4.1.2) (4.1.3)	-"-	0.928 0.939 0.944	0.638 0.644 0.651	0.359 0.367 0.371	0.080 0.088 0.094	0.007 0.010 0.011
115	(4.1.1) (4.1.2) (4.1.3)	-"-	0.532 0.543 0.552	0.371 0.376 0.382	0.215 0.220 0.222	0.052 0.057 0.060	0.005 0.007 0.007

Table 4.3 Comparison between numerical calculations with three different choices of mesh according to (4.1.1-3) at the time t=25 years.

4.2 Comparison of meshes for very long times

A comparison between three meshes is made for the print-out times 237 and 947 years. A third simulation with two of the meshes is made for the print-out time 3789 years. These three times refer to the penteration depths r_p=H, r_p=2H and r_p=4H respectively (H=110 m). These penetration depths are equal to or greater than the borehole length H. The mesh division in the radial and axial directions is therefore no longer determined by the penetration depth at a certain print-out time, but by the length of the borehole. The three different meshes are given by the radial cell widths and by the parameter n_z. The smallest cells in the radial direction are chosen to H/5, H/10, and H/22:

1. Δr = 22, 22, 22, 44, 88, 176, 352, 704 m $\quad n_z = 2$ (4.2.1)
2. Δr = 11, 11, 11, 22, 44, 88, 176, 352, 704 m $\quad n_z = 3$ (4.2.2)
3. Δr = 5, 5, 5, 10, 20, 40, 60, 100, 200, 400 m $\quad n_z = 4$ (4.2.3)

Temperatures are given for the radial distances r = 0.055, 5.5, 11, 22, 55 and 110 meters at the three depths z = 5, 60 and 115 meters. These depths lie at the top, middle, and bottom of the borehole. Table 4.4 gives the results after 237 years. The agreement between mesh (4.2.2) and (4.2.3) is overall good. The maximum relative difference is 0.7 % at the bottom of the borehole (r=5.5 m, z=115 m) and 0.5 % at half the borehole depth. The relative difference between the borehole temperatures is less than 0.2 %. Mesh (4.2.1) gives less good results at the top and at the bottom of the borehole. The maximum relative difference to mesh (4.2.3) is 1.5 %. The

relative difference of the borehole temperature is 1 %.
Table 4.5 gives the temperatures at the time 947 years. The differences between the results with the different meshes are almost exactly the same as after 237 years. However, all temperatures have increased slightly towards the steady-state values.

Table 4.6 gives the results for the meshes (4.2.1) and (4.2.2) after 3789 years. The relative difference from the time 947 years is less than 0.1 % for all radial distances and all depths. The maximum relative difference from the time 237 years is 0.1 % for z=5 meters, 0.3 % for z=60 meters, and 0.5 % for z=115 meters. The conclusion from the comparison between the tables 4.4 - 4.6 is that the relative difference from the steady-state value is less than 1 % at the time 237 years (r_p=H) for all radial distances and all depths in the region $r_b < r < H$, $D < z < D+H$. The steady-state condition is almost attained after 237 years, i.e. when r_p=H.

time = 237 years		Temperatures (^{0}C)					
z-coord (m)	mesh	r= 0.055m	r= 5.5 m	r= 11 m	r= 22 m	r= 55 m	r= 110 m
5	(4.2.1) (4.2.2) (4.2.3)	3.086 3.058 3.053	0.323 0.289 0.310	0.172 0.177 0.176	0.095 0.084 0.085	0.024 0.024 0.024	0.007 0.007 0.006
60	(4.2.1) (4.2.2) (4.2.3)	-"-	1.062 1.084 1.072	0.759 0.792 0.778	0.493 0.509 0.496	0.186 0.200 0.195	0.060 0.063 0.060
115	(4.2.1) (4.2.2) (4.2.3)	-"-	0.670 0.676 0.684	0.512 0.516 0.518	0.361 0.359 0.357	0.172 0.171 0.168	0.067 0.067 0.063

Table 4.4 Comparison between numerical calculations for three different meshes (4.2.1-3) after 237 years.

time = 947 years		Temperatures (^{0}C)					
z-coord (m)	mesh	r= 0.055m	r= 5.5 m	r= 11 m	r= 22 m	r= 55 m	r= 110 m
5	(4.2.1) (4.2.2) (4.2.3)	3.095 3.067 3.062	0.324 0.290 0.311	0.173 0.178 0.177	0.096 0.084 0.085	0.024 0.025 0.025	0.007 0.007 0.007
60	(4.2.1) (4.2.2) (4.2.3)	-"-	1.071 1.094 1.086	0.769 0.802 0.792	0.502 0.518 0.505	0.193 0.209 0.200	0.067 0.071 0.077
115	(4.2.1) (4.2.2) (4.2.3)	-"-	0.685 0.691 0.700	0.528 0.532 0.533	0.377 0.375 0.373	0.188 0.209 0.183	0.081 0.071 0.077

Table 4.5 Comparison between numerical calculations for three different meshes (4.2.1-3) after 947 years.

time =3789 years		Temperatures (^{0}C)					
z-coord (m)	mesh	r= 0.055m	r= 5.5 m	r= 11 m	r= 22 m	r= 55 m	r= 110 m
5	(4.2.1) (4.2.2)	3.097 3.069	0.324 0.290	0.173 0.178	0.096 0.085	0.024 0.025	0.007 0.008
60	(4.2.1) (4.2.2)	-"-	1.073 1.095	0.770 0.803	0.503 0.519	0.197 0.210	0.070 0.073
115	(4.2.1) (4.2.2)	-"-	0.687 0.693	0.530 0.534	0.379 0.377	0.190 0.189	0.083 0.083

Table 4.6 Numerically calculated temperatures for the meshes (4.2.1-2) after 3789 years.

The temperature solution in the ground due to short-time variations of the boundary conditions is not sensitive to the choice of the axial mesh. The quick variations have a very short penetration depth out in the ground. Since the borehole normally have a length of 100-150 meters, the axial heat flows are negligible compared with radial heat flows. Short-time variations can therefore be treated by a pure radial solution.

The local three-dimensional process in the vicinity of the top and the bottom of the borehole can be neglected with respect to the total heat extraction over the borehole depth, $D \leq z \leq D+H$. It is normally unnecessary to use cell widths smaller than $\Delta z_{min}=H/10$ in the axial direction. The choice of n_z shall therefore be between 3 and 6 except when the local effects at the top and the bottom shall be studied. Normally used values are 5 and 6.

5 Rules for the choice of mesh

The results of chapter 3 and 4 can now be summarized to obtain rules for a suitable choice of mesh. According to section 3.1-3 the size of three smallest cells in the radial direction must have the size less than or equal to $\Delta r_{min}=\min(\sqrt{at_{min}},H/5)$. The upper limit H/5 is included to avoid problems with the axial effects at large times. The time t_{min} is defined by (3.7.5) as the smallest time period between a step in the boundary heat flow at the borehole wall and a printout time. The expanding mesh (3.4.3) satisfies this condition. The generalization of mesh (3.4.3) gives the following choice of cell widths in the radial direction:

$$\Delta r = \Delta r_{min},\Delta r_{min},\Delta r_{min},2\Delta r_{min},4\Delta r_{min},8\Delta r_{min} \quad . \; . \; . \qquad (5.1)$$

The cell widths keep expanding out to the total radial distance $r_{max}=3\sqrt{at_{max}}$, where t_{max} is equal to the end time of the simulation.

The numerical accuracy of mesh (5.1) may be insufficient in some cases when it is necessary to calculate the temperatures in the ground with very good precision. It is in these cases advisable to use a mesh where all the cell widths in (5.1) have been divided into two parts. Such a mesh is given by (3.5.4). A simulation with the latter mesh increaces the CPU-time between four and eight times.

The axial mesh is determined by the parameter n_z according to chapter 4. The number of cells along half of the length H is equal to n_z. The cells are expanding with the factor $\sqrt{2}$ from the top and the bottom of the borehole to the middle of the borehole. The smallest cells at the top and the bottom of the borehole have the size:

$$\Delta z_{min} = H\cdot \frac{1}{2}\,(\sqrt{2}-1)/(\sqrt{2}^{n_z}-1) \qquad (5.2)$$

The first cell above and below the borehole has the size Δz_{min}. The following cells above and below the borehole expand with the factor 2. The axial mesh reaches out the distance z_{max} above the top and below the bottom of the borehole:

$$z_{max} = \Delta z_{min} \cdot (2^{n_z+3} - 1) \qquad (5.3)$$

The axial mesh has the total size $H+2z_{max}$. The total number of cells in the axial direction, including two boundary cells, is equal to $4 \cdot n_z + 8$.

The value of n_z shall lie between 3 and 6 in normal situations. The lower value is used when t_{max} is large (t_{max} > 100 years, when 100 < H < 150 meters). For very long simulations, i.e. close to steady-state condition ($t > H^2/a$) it is possible to choose a radial mesh with the smallest cells equal to H/5 and n_z equal to 2. The local effects in the vicinity of the top and the bottom of the borehole can be studied by choosing a very fine radial mesh and n_z equal to 14, see section 4.1. The smallest cell width has then a size that is less than 0.2 % of the total borehole length.

For the examples considered in this study the relative error defined by (3.0.4) is less than 1 % for mesh (5.1). The corresponding error for the finer mesh with twice as many cells is 0.5 %. These errors are calculated for a pure radial solution without any axial disturbances. The transient three-dimensional radial-axial process can not be calculated analytically. The error must therefore be estimated by comparing the solution for different choices of mesh. The relative difference defined by (4.1) between the different solutions is according to chapter 4 less than 1 % if the rules above are followed.

References

1. J. Claesson, P. Eskilson, Simulation Model for Thermally Interacting Heat Extraction Boreholes, Dep. of Mathematical Physics, University of Lund, Box 118, S-221 00 Lund, Sweden, 1987. (Submitted to Journal of Numerical Heat Transfer)

2. P. Eskilson, Superposition Borehole Model. Manual for Computer Code, Dep. of Mathematical Physics, University of Lund, Box 118, S-221 00 Lund, Sweden, 1986.

3. J. Claesson, P. Eskilson, Conductive Heat Extraction by a Deep Borehole. Thermal Analyses and Dimensioning Rules, Dep. of Mathematical Physics, University of Lund, Box 118, S-221 00 Lund, Sweden, 1987.

Notes on Heat Transfer 3-1986

Numerical Study of the Radial Mesh for Two Systems with 16 and 120 Boreholes

Per Eskilson

October 1986

Departments of Building Technology
and Mathematical Physics
University of Lund
Box 118
S-221 00 Lund, Sweden

TABLE OF CONTENTS

Section		Page
1	Introduction	1
2	Analytical expression for the borehole temperature	2
3	Simulation for a configuration with 4 x 4 boreholes	2
4	Simulation for a configuration with 12 x 10 boreholes	4

1 Introduction

The Superposition Borehole Model, described in [1,2], has been developed to simulate the thermal performance for a system with many heat extraction boreholes placed in any pattern. The model uses finite differences for the numerical calculation of the temperature solution. The accuracy of the numerical solution with respect to different choices of the radial mesh is analysed here for two different borehole configurations with 16 and 120 boreholes respectively.

The computer model allows for five different types of loading conditions for the heat extraction from the boreholes. We will in this study only consider the simplest possible type, when the heat extraction rate q (W/m) at the borehole wall is constant per unit length of the borehole.

With given q each borehole is essentially a continuous finite line source. Each such finite line source solution is calulated numerically with finite differences in axial symmetric coordinates, i.e. the (r,z)-plane. The temperature in the ground is given by superposition of the line source solutions from each of the boreholes [1]. There is no simple analytical solution to the continuous finite line source.

The thermal problem may be simplified by neglecting the vertical (axial) heat transfer process. The finite length of the borehole is then not considered. In this case each borehole may be represented by an infinite continuous line source, for which there is a simple analytical solution.

The temperature in the ground can in this case be calculated by superposition of either the numerically or analytically calculated line source solutions. We will in section 3 and 4 compare the numerical and analytical temperature solution at the borehole wall for two configurations with 16 and 120 boreholes respectively. The numerical solution is for each configuration calculated for three different choices of the radial mesh.

2 Analytical expression for the borehole temperature

Consider a number of infinite continuous line sources in an homogeneous medium. Each line source represents a borehole. The borehole temperature T_{bi} at the radial distance r_b outside line source i is given by the contribution from the own source i and the contributions from all other sources $j \neq i$:

$$T_{b,i}(t) = \frac{q}{4\pi\lambda} E_1(r_b^2/(4at)) + \sum_{j \neq i} \frac{q}{4\pi\lambda} E_1(r_{ij}^2/(4at)) \qquad (2.1)$$

The exponential integral E_1 is given in [3]. The distance between the borehole i and j is r_{ij}. The variation of r_{ij} around the radius r_b is neglected.

3 Simulation for a configuration with 4 x 4 boreholes

Consider the configuration with 4 x 4 boreholes in Figure 1. The distance B between two neighbouring boreholes is 10 meters. The thermal conductivity λ, the thermal diffusivity a, and the radius of the borehole r_b, are:

$$\lambda = 3.5 \text{ W/mK} \qquad a = 1.62 \cdot 10^{-6} \text{ m}^2/\text{s} \qquad r_b = 0.055 \text{ m} \qquad (3.1)$$

In the numerical calculation the borehole length H and the depth D of the upper insulated part are set to 100,000 and 500 meters. The borehole temperature is calcuated at half the borehole depth. In this region of the borehole the axial effects can be neglected. The accuracy of the numerical solution can then be estimated by comparison with the analytical solution (2.1).

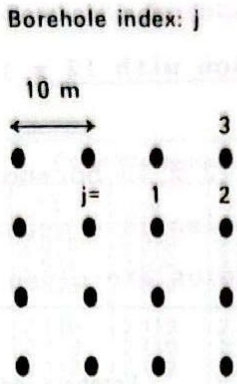

Figure 1. Sixteen boreholes in a square. The distance B between two neighbouring holes is 10 meters.

Three different radial meshes are used to calculate the borehole temperatures numerically. The meshes are given by the radial cell widths:

$$\Delta r = 7, 7, 7, 14, 28, 56, 112, 224, 448 \text{ m} \quad (3.2)$$

$$\Delta r = 3.5, 3.5, 3.5, 3.5, 3.5, 3.5, 7, 7, 14, 14, 28, 28, 56, 56, 112, 112, 224, 224 \text{ m} \quad (3.3)$$

$$\Delta r = 1.75, 1.75, 1.75, 1.75, 1.75, 1.75, 3.5, 3.5, 3.5, 7, 7, 14, 14, 28, 28, 56, 56, 112, 112, 224, 224 \text{ m} \quad (3.4)$$

Table 1 gives the borehole temperatures for borehole 1, 2, and 3 in Figure 1 after 1, 10, and 100 years. The maximum error of the borehole temperatures compared to the analytical solution is 3 %, 0.7% ,and 0.7 % for the three meshes respectively. The size of the smallest cells in mesh (3.2) is 7 meters. These cell widths are almost as large as the distance B (=10m). This results in less numerical accuracy.

Borehole temperature (^{0}C)				
	mesh	j=1	j=2	j=3
1 year	(3.2)	3.229	2.972	2.773
	(3.3)	3.192	2.948	2.756
	(3.4)	3.197	2.952	2.761
	anal	3.174	2.936	2.748
10 years	(3.2)	8.726	7.583	6.659
	(3.3)	8.603	7.457	6.529
	(3.4)	8.601	7.456	6.529
	anal	8.552	7.409	6.486
100 years	(3.2)	16.695	15.281	14.099
	(3.3)	16.538	15.124	13.942
	(3.4)	16.538	15.124	13.941
	anal	16.475	15.062	13.880

Table 1. Numerical and analytical borehole temperatures for the configuration in Figure 1.

4 Simulation for a configuration with 12 x 10 boreholes

Consider the system with with 12 x 10 boreholes in Figure 2. The distance B between two neighbouring boreholes is 4 meters. The thermal properties of the ground and the borehole radius are given by (3.1).

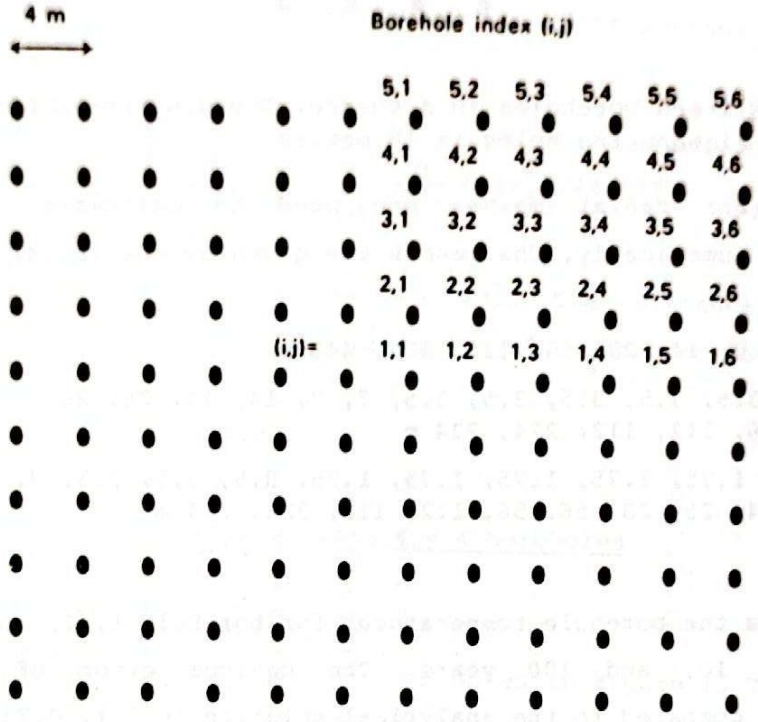

Figure 2 120 boreholes in a rectangle. The distance B between two neighbouring holes is 4 m.

Two different radial meshes are used to calculate the borehole temperatures. The meshes are given by the radial cell widths:

$$\Delta r = 1, 1, 1, 2, 2, 4, 4, 8, 8, 16, 16, 32, 32, 64, 64, 128, 128 \text{ m} \quad (4.1)$$

$$\Delta r = 1, 1, 1, 2, 2, 2, 3, 3, 3, 5, 5, 5, 5, 5, 5, 5, 5, 5, 5, 1000 \text{ m} \quad (4.2)$$

Tables 2a-c give the borehole temperatures after 1 month, 6 months, and 5 years for borehole (i,j)=(1,1) to borehole (i,j)=(5,6). The mesh (4.1) gives a maximum error compared to the analytical result of 0.4 %, 2 % ,and 2 % for the three different times respectively. The corresponding errors for the calculations with mesh (4.2) are 0.3%, 1.4%, and 0.3%. The

precision for mesh (4.2) is remarkably good at 5 years. At this time there is a very large influence between the boreholes.

t= 1 months		Borehole temperature					
	mesh	j=1	j=2	j=3	j=4	j=5	j=6
i=5	(4.1)	2.036	2.036	2.036	2.036	2.034	1.964
	(4.2)	2.034	2.034	2.034	2.034	2.032	1.964
	anal	2.029	2.029	2.029	2.029	2.028	1.959
i=4	(4.1)	2.119	2.119	2.119	2.119	2.117	2.034
	(4.2)	2.119	2.119	2.119	2.119	2.116	2.032
	anal	2.112	2.112	2.112	2.112	2.110	2.028
i=3	(4.1)	2.121	2.121	2.121	2.121	2.119	2.036
	(4.2)	2.121	2.121	2.121	2.121	2.119	2.034
	anal	2.114	2.114	2.114	2.114	2.112	2.028
i=2	(4.1)	2.121	2.121	2.121	2.121	2.119	2.036
	(4.2)	2.121	2.121	2.121	2.121	2.119	2.034
	anal	2.114	2.114	2.114	2.114	2.110	2.028
i=1	(4.1)	2.121	2.121	2.121	2.121	2.119	2.036
	(4.2)	2.121	2.121	2.121	2.121	2.119	2.034
	anal	2.114	2.114	2.114	2.114	2.112	2.029

t= 6 months		Borehole temperature (^{0}C)					
	mesh	j=1	j=2	j=3	j=4	j=5	j=6
i=5	(4.1)	4.608	4.603	4.585	4.518	4.290	3.657
	(4.2)	4.580	4.577	4.560	4.492	4.268	3.640
	anal	4.533	4.530	4.516	4.454	4.236	3.614
i=4	(4.1)	5.544	5.538	5.514	5.427	5.123	4.290
	(4.2)	5.512	5.507	5.486	5.396	5.096	4.268
	anal	5.458	5.449	5.431	5.348	5.058	4.237
i=3	(4.1)	5.900	5.892	5.865	5.764	5.426	4.518
	(4.2)	5.861	5.856	5.831	5.730	5.396	4.492
	anal	5.790	5.786	5.765	5.672	5.348	4.454
i=2	(4.1)	6.007	5.999	5.969	5.864	5.513	4.584
	(4.2)	5.968	5.963	5.862	5.831	5.486	4.560
	anal	5.888	5.884	5.862	5.765	5.431	4.451
i=1	(4.1)	6.035	6.027	5.997	5.890	5.536	4.601
	(4.2)	5.994	5.988	5.962	5.855	5.560	4.576
	anal	5.910	5.906	5.884	5.785	5.449	4.530

t= 5 years		Borehole temperature (^{0}C)					
	mesh	j=1	j=2	j=3	j=4	j=5	j=6
i=5	(4.1)	23.89	23.44	22.52	21.06	18.96	16.11
	(4.2)	23.53	23.08	22.18	20.71	18.63	15.73
	anal	23.48	23.03	22.11	20.65	18.58	15.75
i=4	(4.1)	28.18	27.66	26.58	24.85	22.33	18.86
	(4.2)	27.83	27.31	26.22	24.50	22.00	18.54
	anal	27.78	27.25	26.16	24.44	21.95	18.49
i=3	(4.1)	31.22	30.64	29.43	27.49	24.67	20.79
	(4.2)	30.88	30.30	29.08	27.14	24.34	20.47
	anal	30.83	30.24	29.02	27.08	24.28	20.42
i=2	(4.1)	33.17	32.54	31.29	29.17	26.14	22.02
	(4.2)	32.84	32.21	30.90	28.82	25.81	21.70
	anal	32.78	32.15	30.84	28.76	25.76	21.64
i=1	(4.1)	34.11	33.46	31.13	29.98	26.86	22.61
	(4.2)	33.78	33.14	31.78	29.63	26.53	22.30
	anal	33.72	33.08	31.72	29.57	26.47	22.25

Table 2a-c Numerical and analytical borehole temperatures for the configuration in Figure 2 after 1 month, 6 months, and 5 years.

A simulation was made to calculate the error for a very bad choice of mesh. Mesh (3.2) was used for the 12x10 borehole system in Figure 2. The thickness of the first cell close to the borehole is 7 meters in mesh (3.2). This distance shall be compared with the the distance between two neighbouring boreholes, which is 4 meters. The interpolation of the influence temperature in the simulation model ought to be very bad. However, the results show an error of the borehole temperatures which is less than 5 % after both 6 months and 5 years. The simulation model is suprisingly unsensitive to the choice of mesh.

References

1. Claesson J., Eskilson P., Numerical Model for Thermally Interacting Heat Extraction Boreholes, Department of Mathematical Physics, University of Lund Box 118 S-221 00 Lund, Sweden, 1987. Submitted to Journal of Numerical Heat Transfer.

2. P. Eskilson, Superposition Borehole Model. Manual for Computer Code, Dep. of Mathematical Physics, University of Lund, Box 118, 221 00 Lund, Sweden, 1986.

3. Claesson J., Eftring B., Eskilson P., Hellström G., Markvärme. En handbok om termiska analyser. (Ground Heat Systems. A Handbook on Thermal Analyses.), BFR-rapport T16-T18:1985. (Swedish Council for Building Research)

Notes on Heat Transfer 4-1986

Temperature Response Function g for 38 Borehole Configurations.

Per Eskilson

August 1986

Departments of Mathematical Physics
and Building Technology
University of Lund
Box 118
S-221 00 Lund, Sweden

Temperature Response Function g for 38 Borehole Configurations

The curves on the following pages give the temperature response function g, which is described in [1], for 38 different borehole configurations. Each g-function is given as a function of $\ln(t/t_s)$, where t is the time and $t_s=H^2/(9a)$ (H=active borehole depth, a=thermal diffusivity). The figures 1 to 18 show g-functions for vertical boreholes, and figures 19 to 38 for graded boreholes. In each figure curves are given for different values on the relative distance B/H between the boreholes (Figures 1-18, 37-38), or for different angle θ of graded boreholes (Figures 19-36).

The curves are calculated numerically with the simulation model described in [2,3] for the case when the ratio between the borehole radius and the borehole length is $r_b/H=0.0005$. For any other radius the simple relation between two radii in [1] is valid with very high accuracy.

Note that the g-function gives directly the temperature drop in °C at the borehole wall for the heat extraction rate $q=2\pi\lambda$ (W/m).

References:

1. J. Claesson, P. Eskilson, Conductive Heat Extraction by Thermally Interacting Deep Boreholes. Dep. of Mathematical Physics, University of Lund, Box 118, S-221 00 Lund, Sweden, 1987.

2. J. Claesson, P. Eskilson, Simulation Model for Thermally Interacting Heat Extraction Boreholes, Department of Mathematical Physics, University of Lund Box 118 S-221 00 Lund, Sweden, 1987. Submitted to Journal of Numerical Heat Transfer.

3. P. Eskilson, Superposition Borehole Model. Manual for Computer Code, Dep. of Mathematical Physics, University of Lund, Box 118, S-221 00 Lund, Sweden, 1986.

Figure 1-18: Vertical boreholes with the spacing B at the ground surface.

Figure 19-24: Graded borholes located on a line at the ground surface. The spacing between two neighbouring boreholes is B. The boreholes are graded an angle θ according to the dashed lines in the figures (θ=10, 20, 30^0).

Figure 25-30: Graded boreholes located on a circle at the ground surface. The radius of the circle is B. The boreholes are graded between 0 - 30^0.

Figure 31-36: Graded boreholes located on a circle at the ground surface. In the middle of the circle a vertical borehole is placed. The tilt angle of the boreholes in the circle varies between 0-30^0.

Figure 37 Eight boreholes in a fan-shaped configuration. The configuration is shown in the figure in a vertical cross-section.

Figure 38 Eight boreholes located on a line at the ground surface and graded outwards 20^0 in the directions indicated in the figure.

The dashed line gives the g-function for a single vertical borehole.

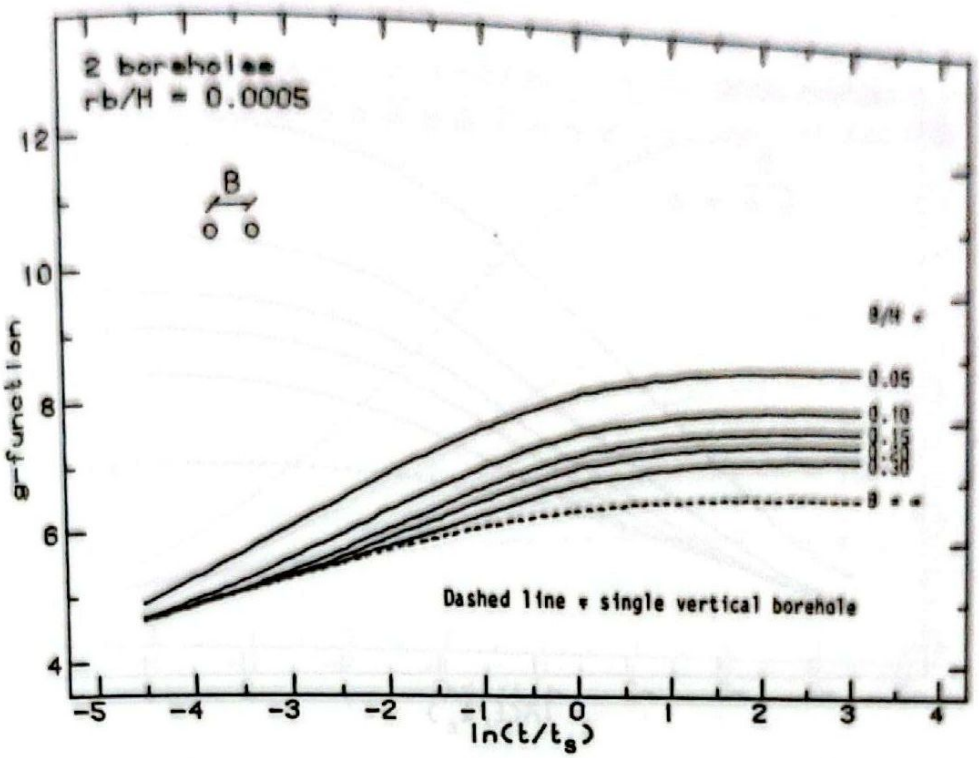

Figure 1

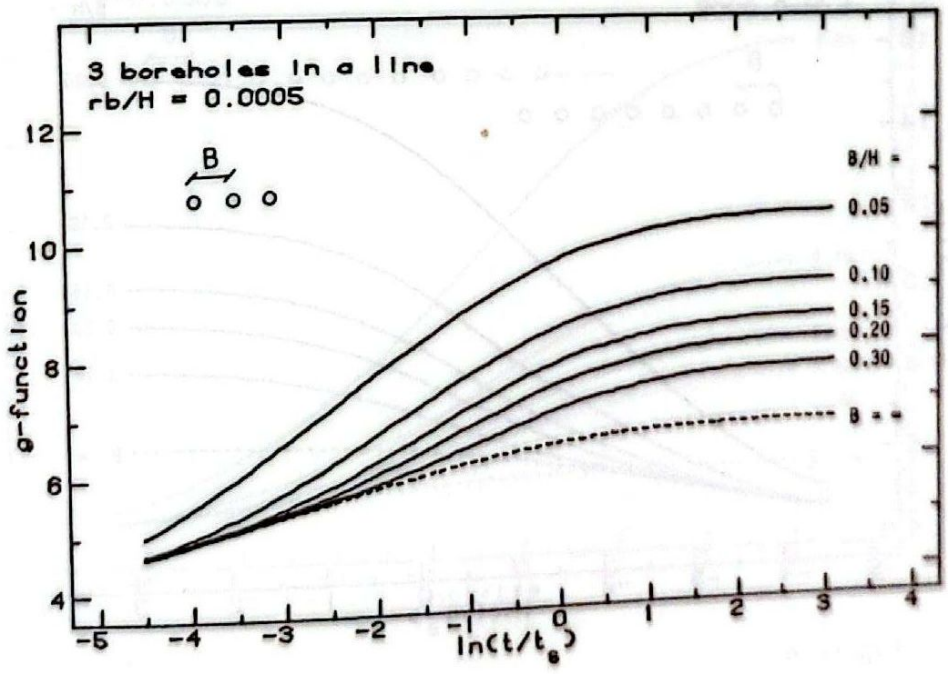

Figure 2

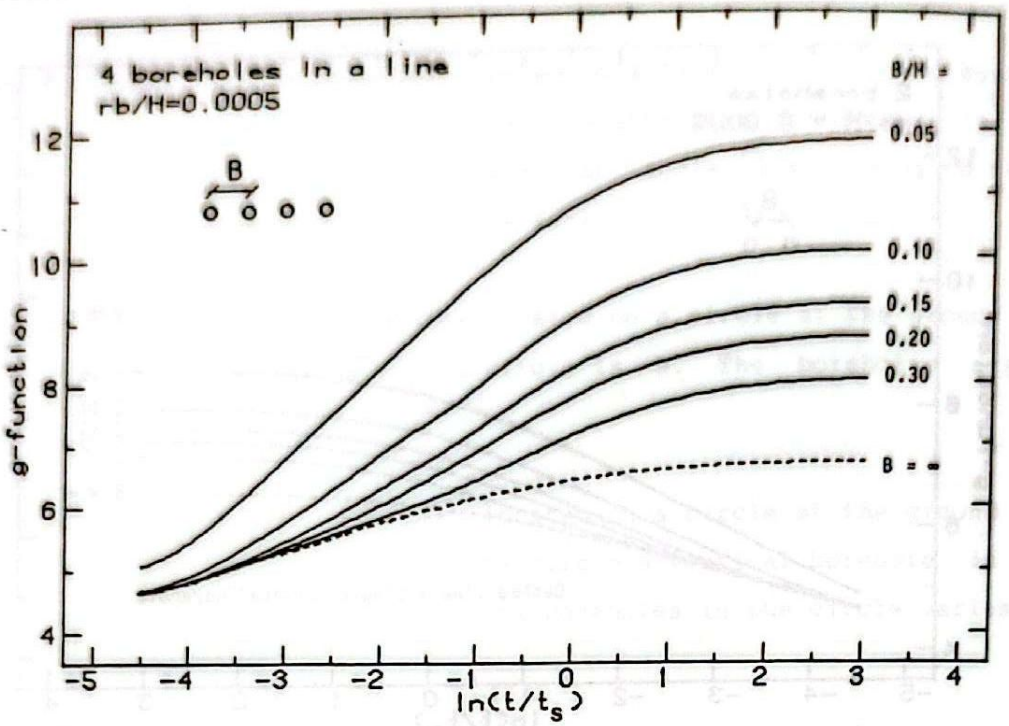

Figure 3

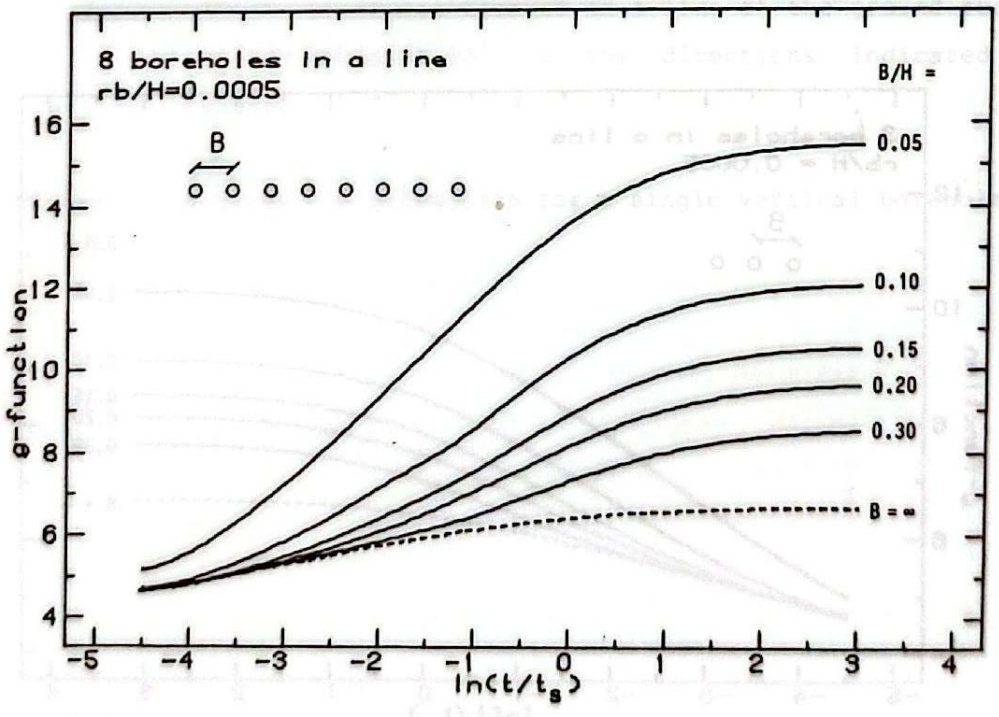

Figure 4

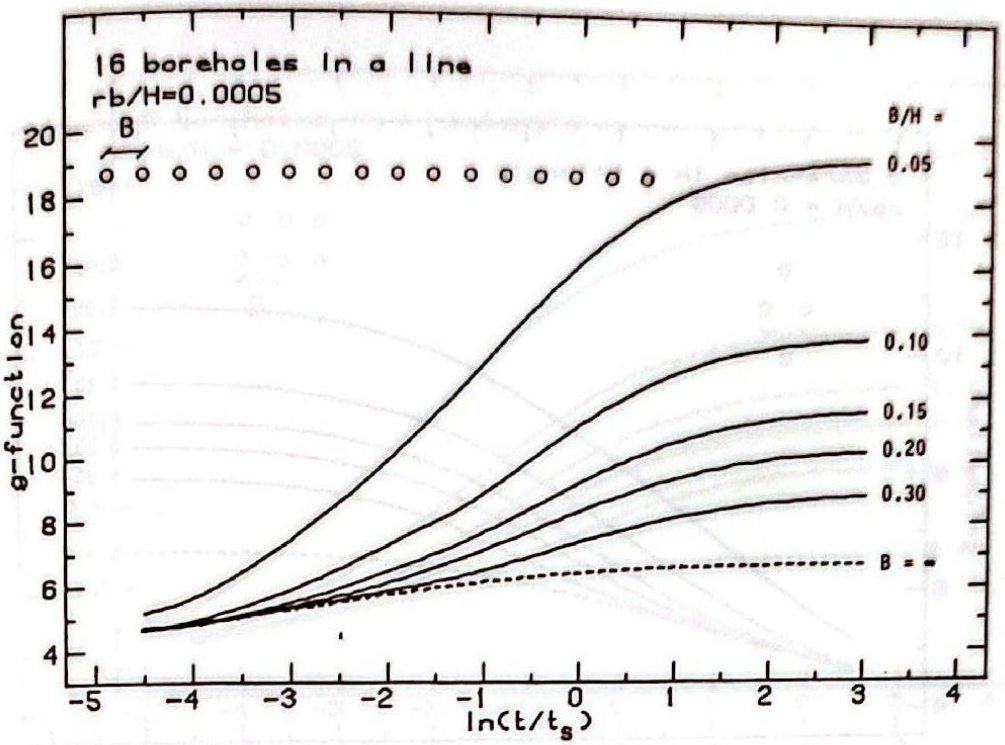

Figure 5

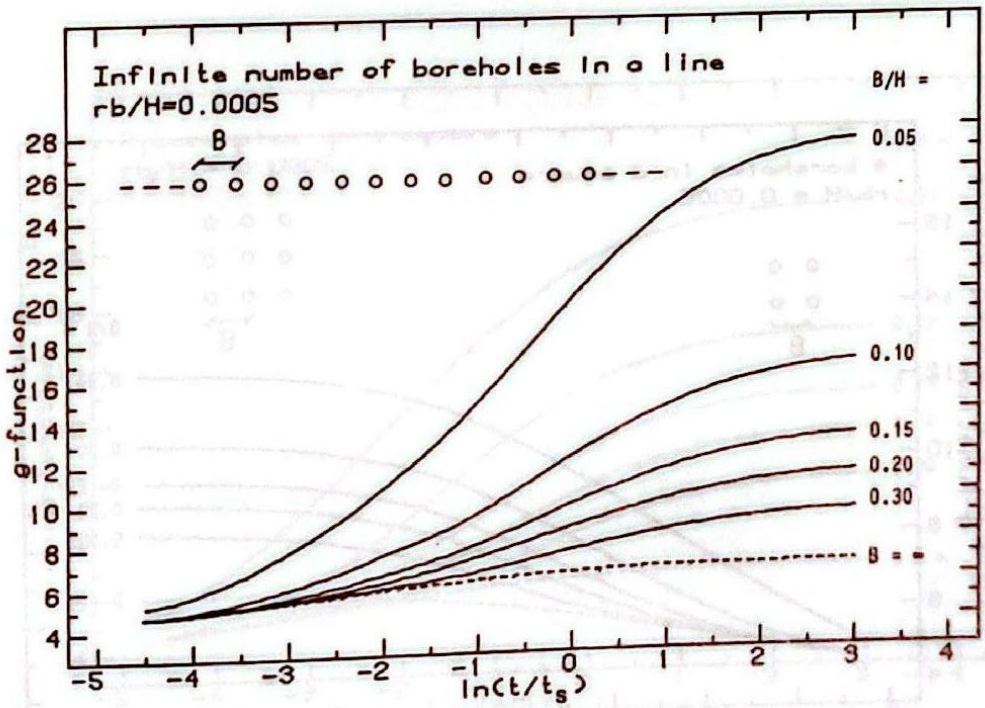

Figure 6

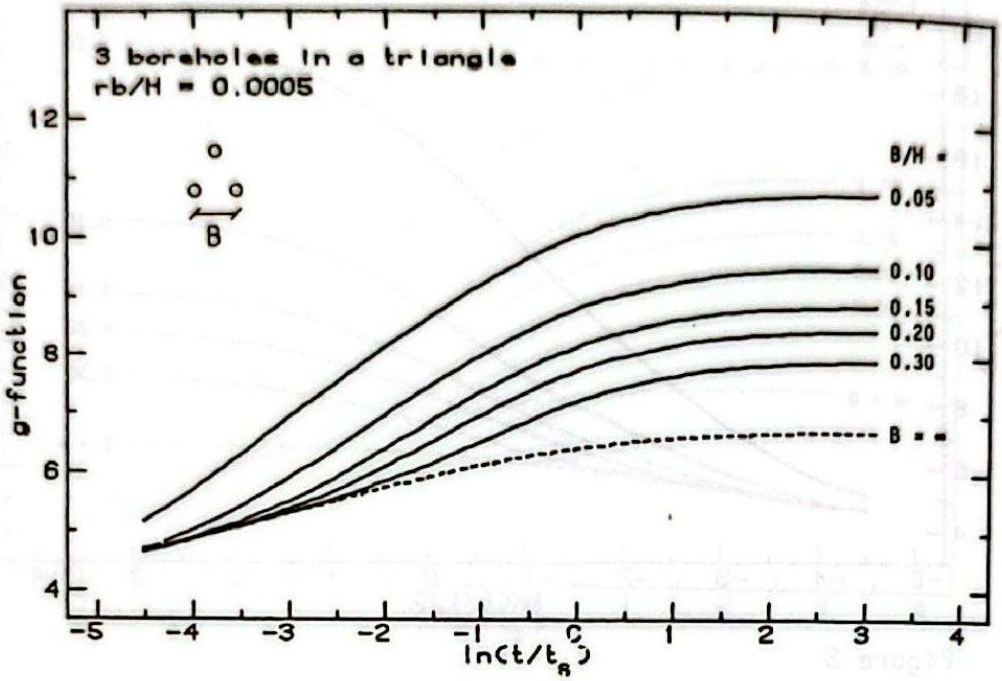

Figure 7

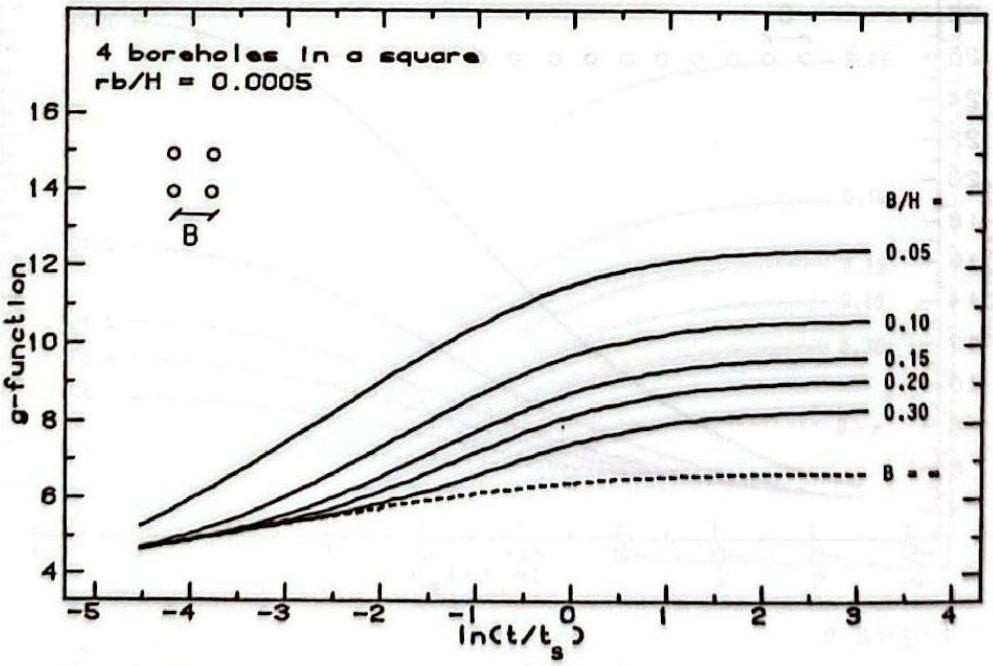

Figure 8

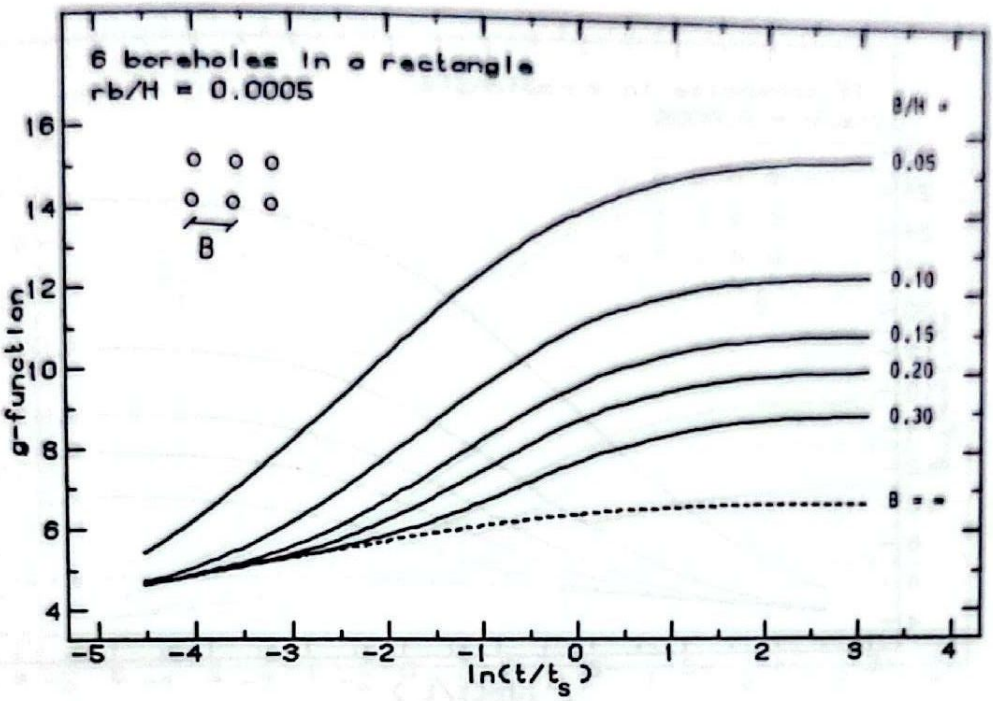

Figure 9

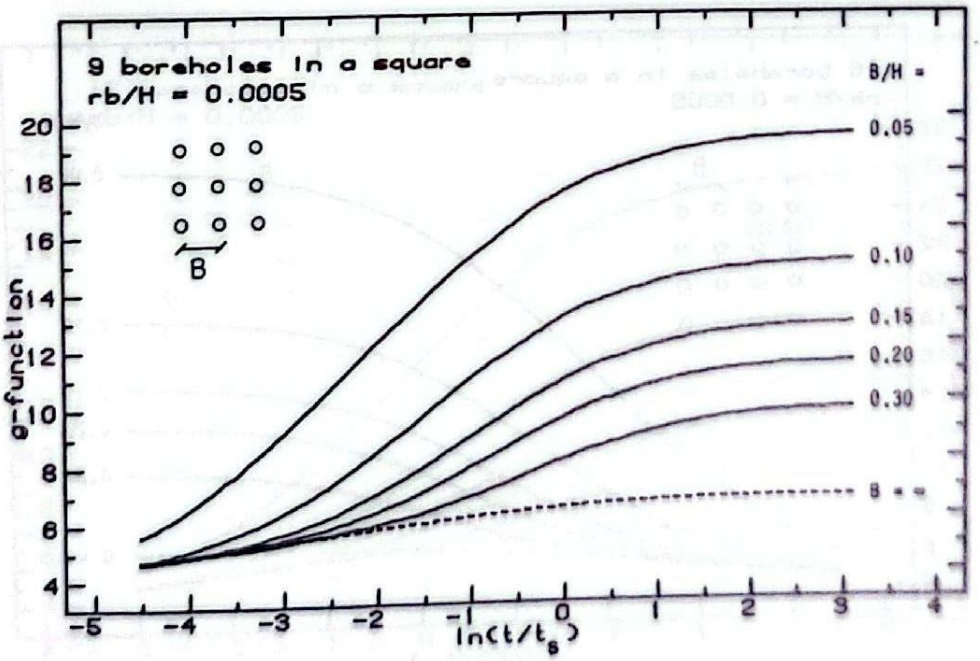

Figure 10

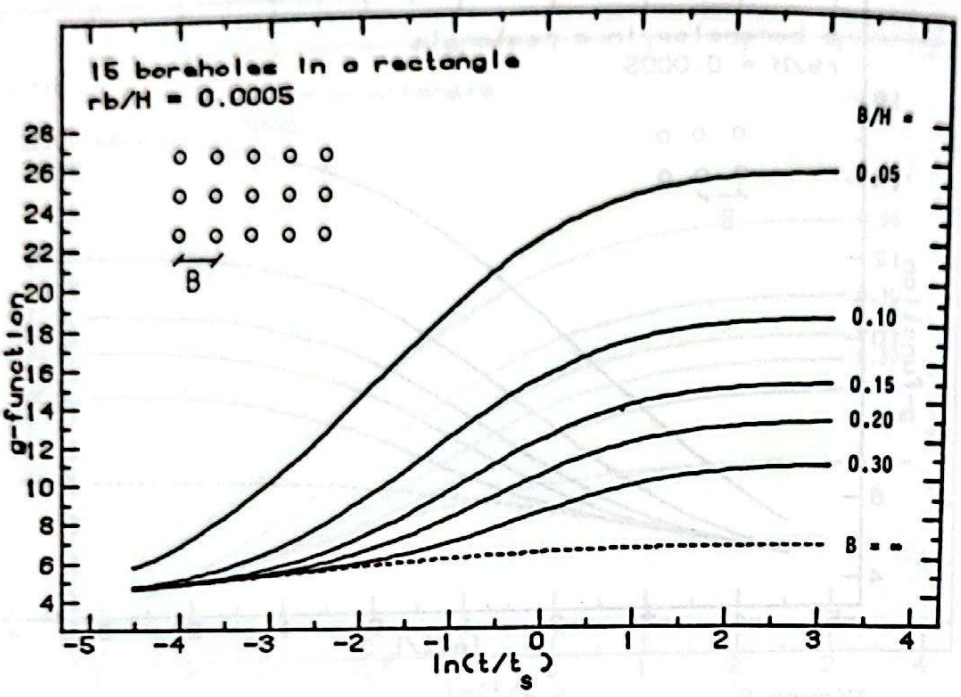

Figure 11

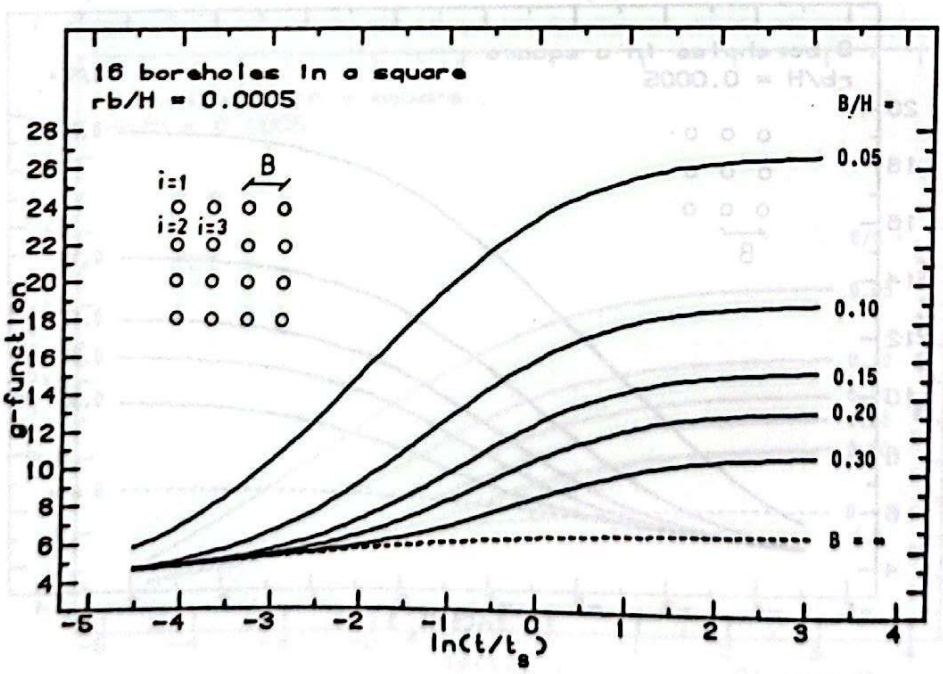

Figure 12

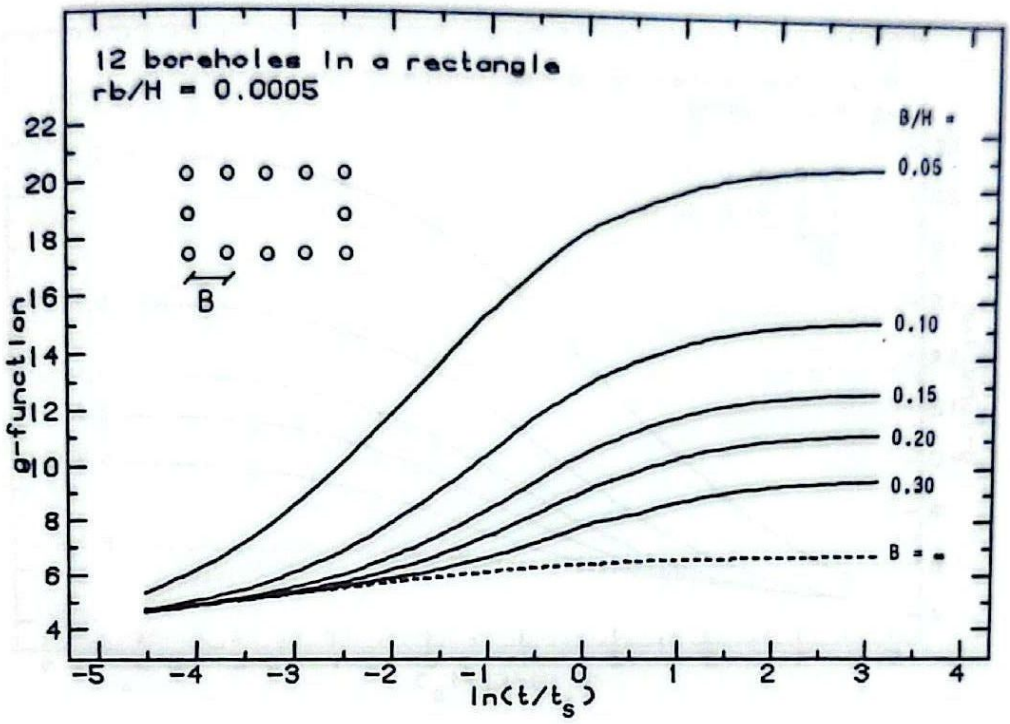

Figure 13

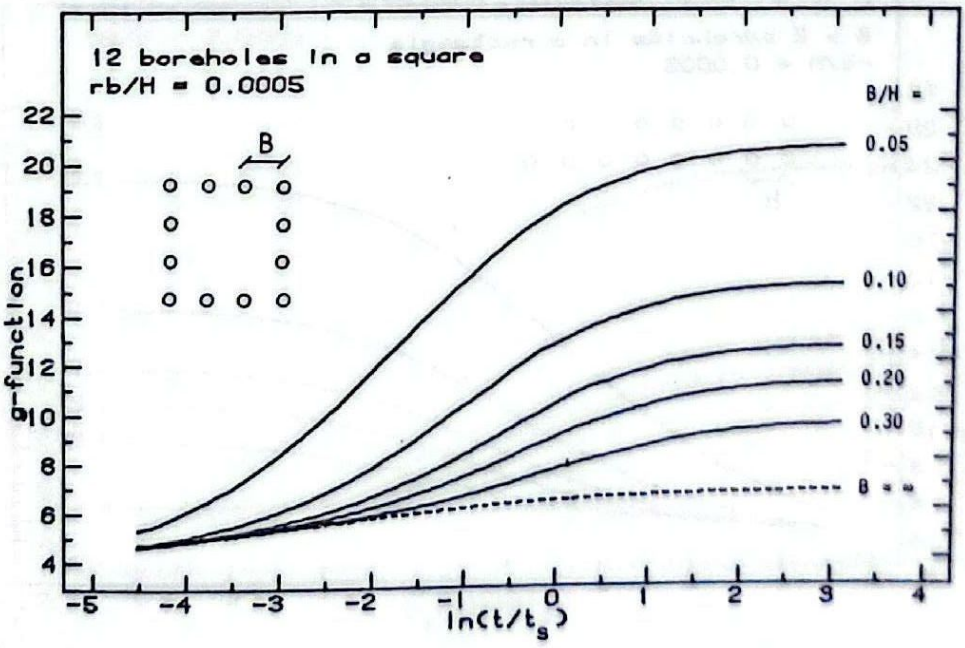

Figure 14

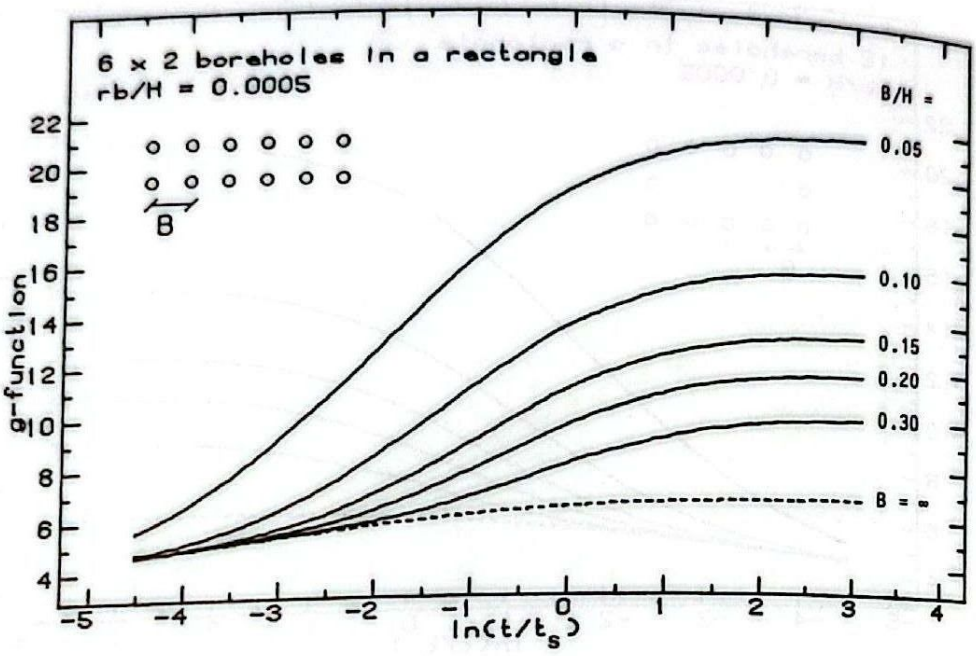

Figure 15

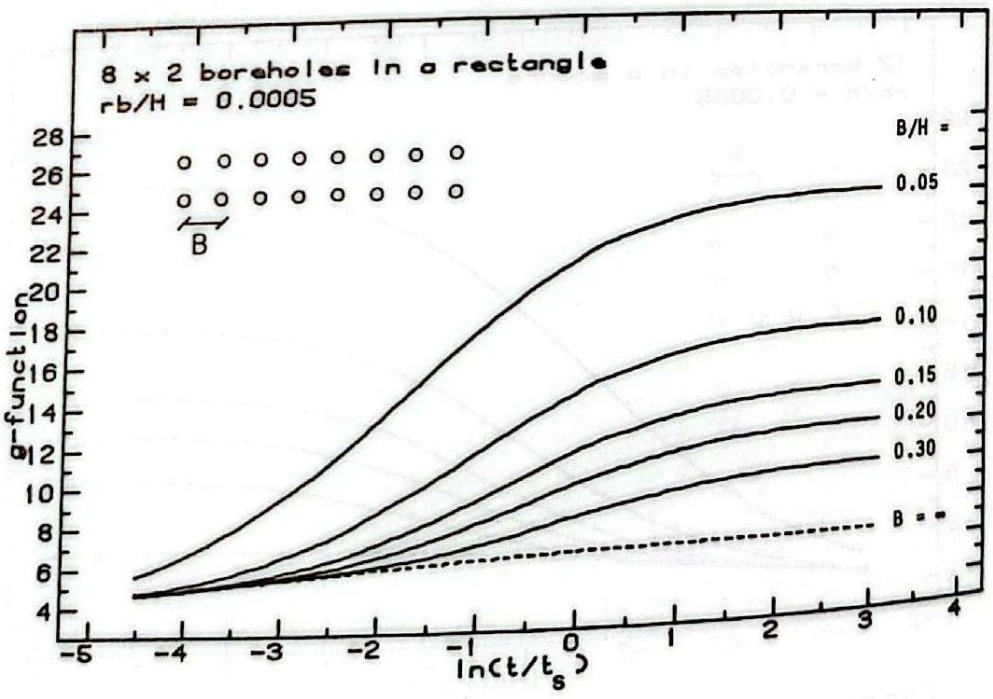

Figure 16

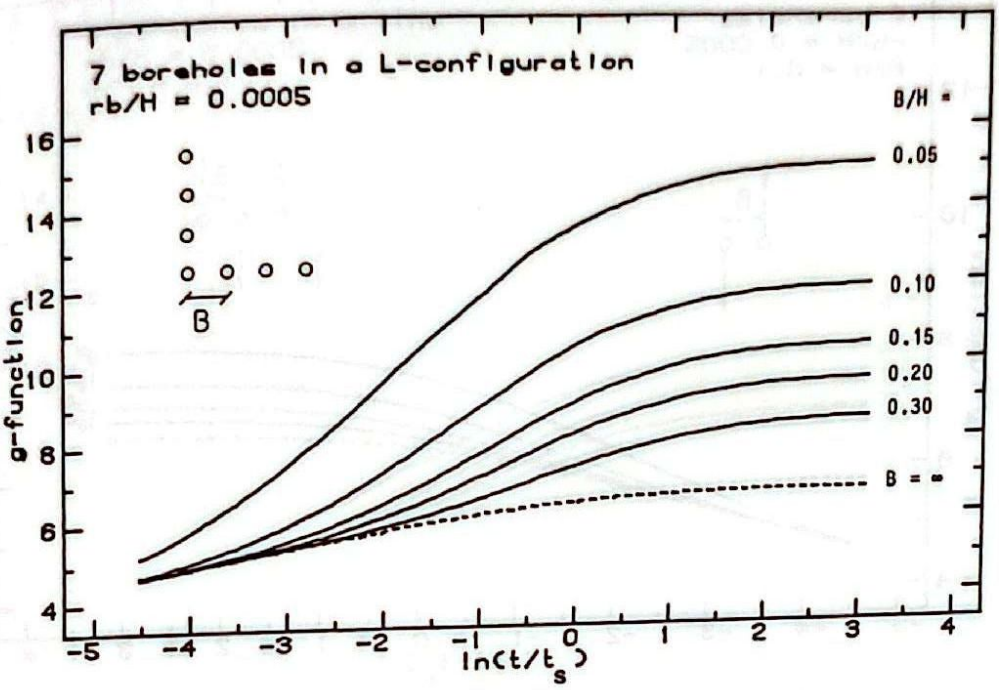

Figure 17

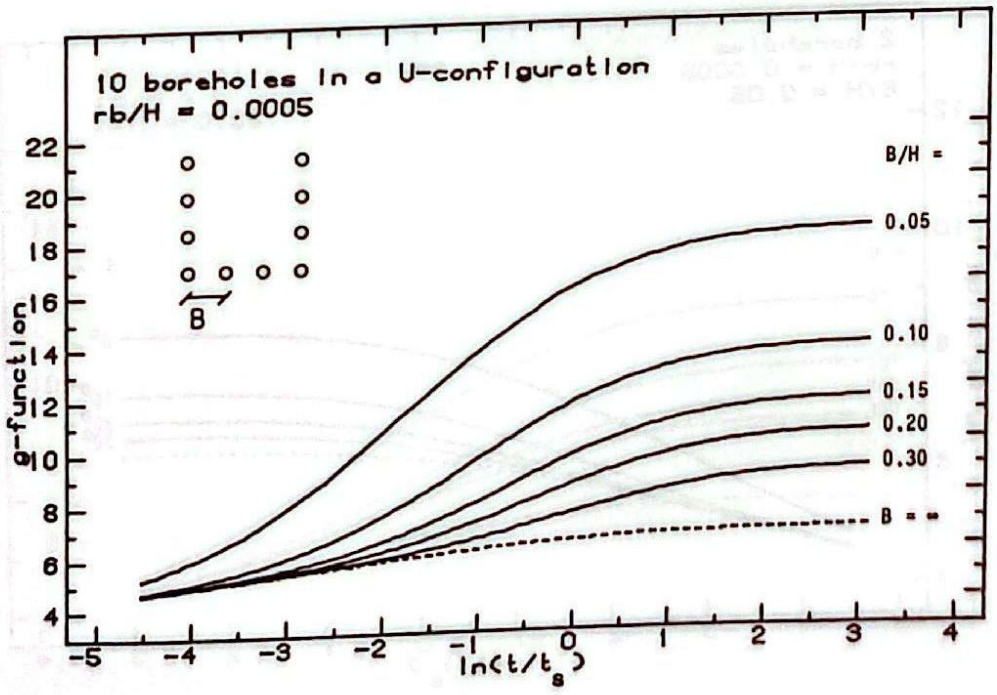

Figure 18

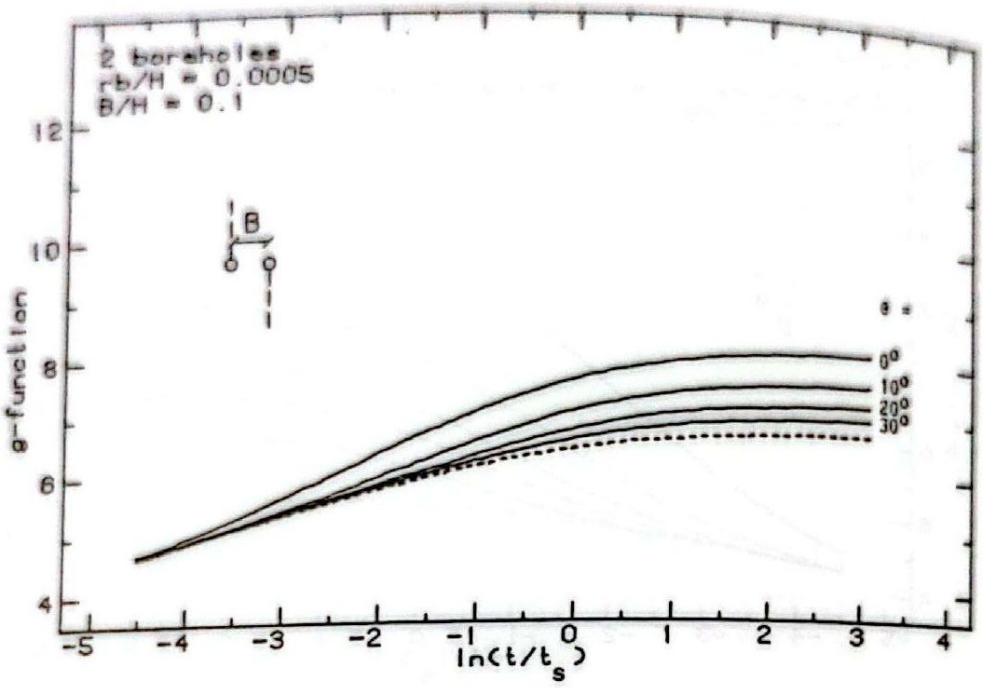

Figure 19

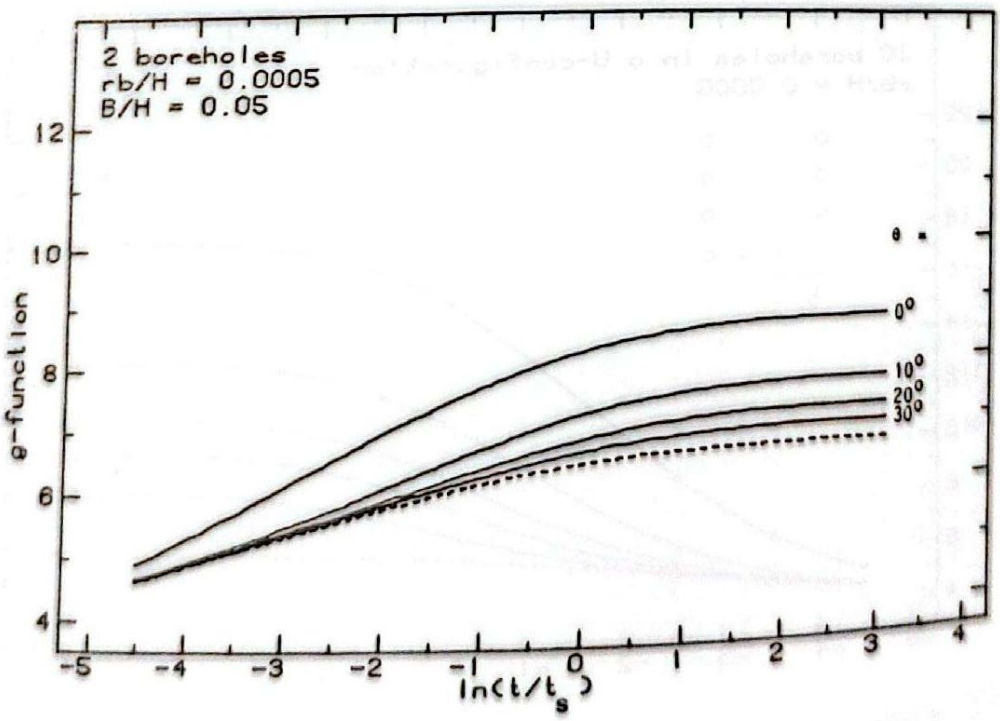

Figure 20

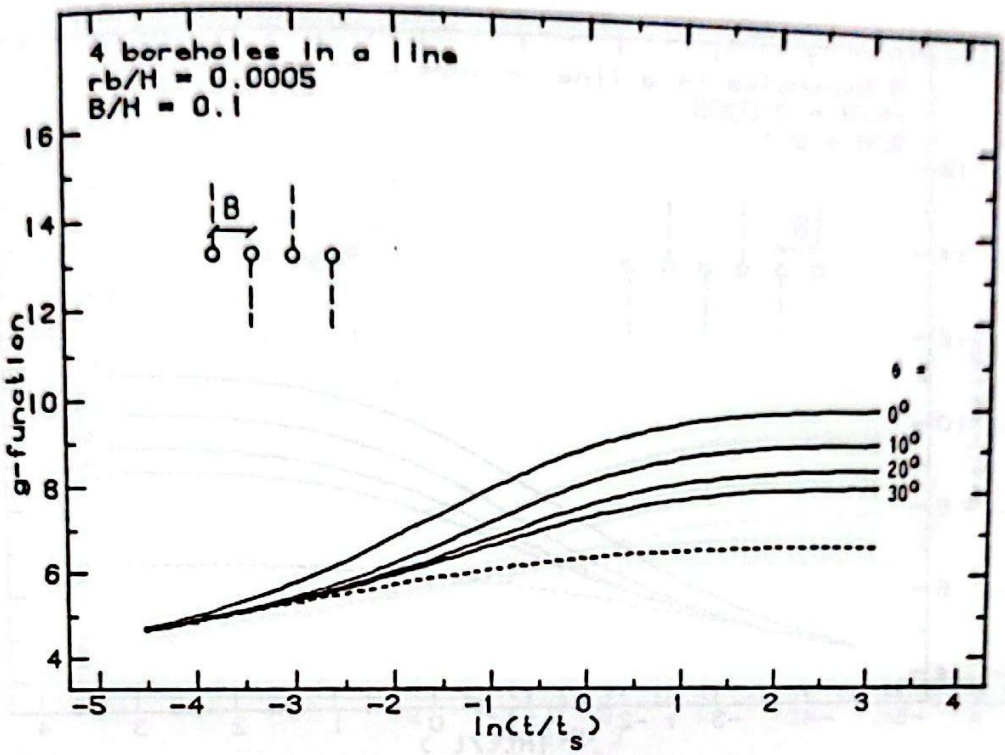

Figure 21

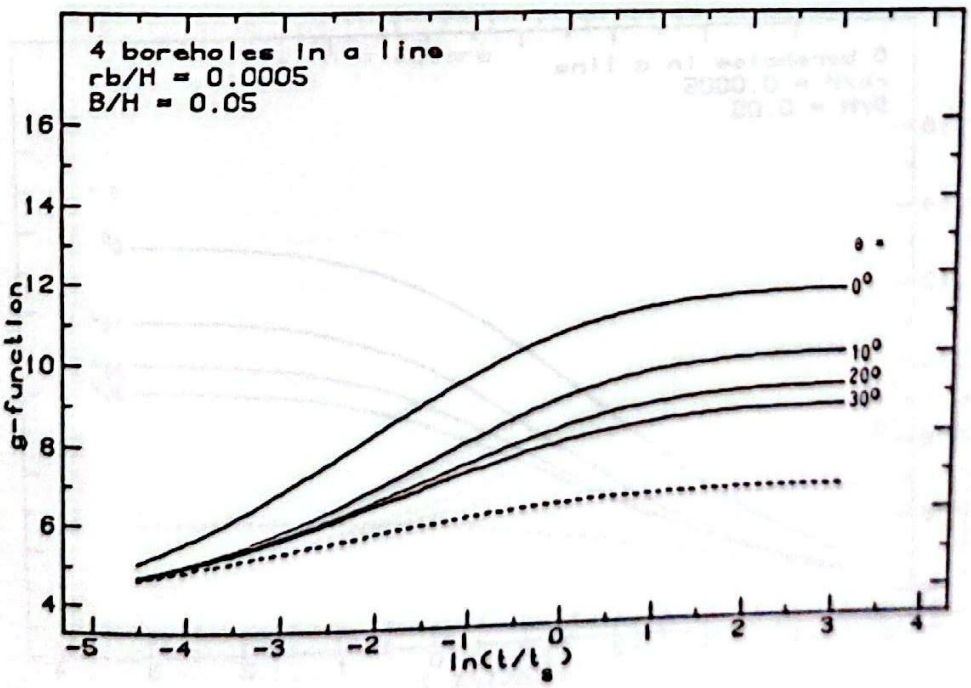

Figure 22

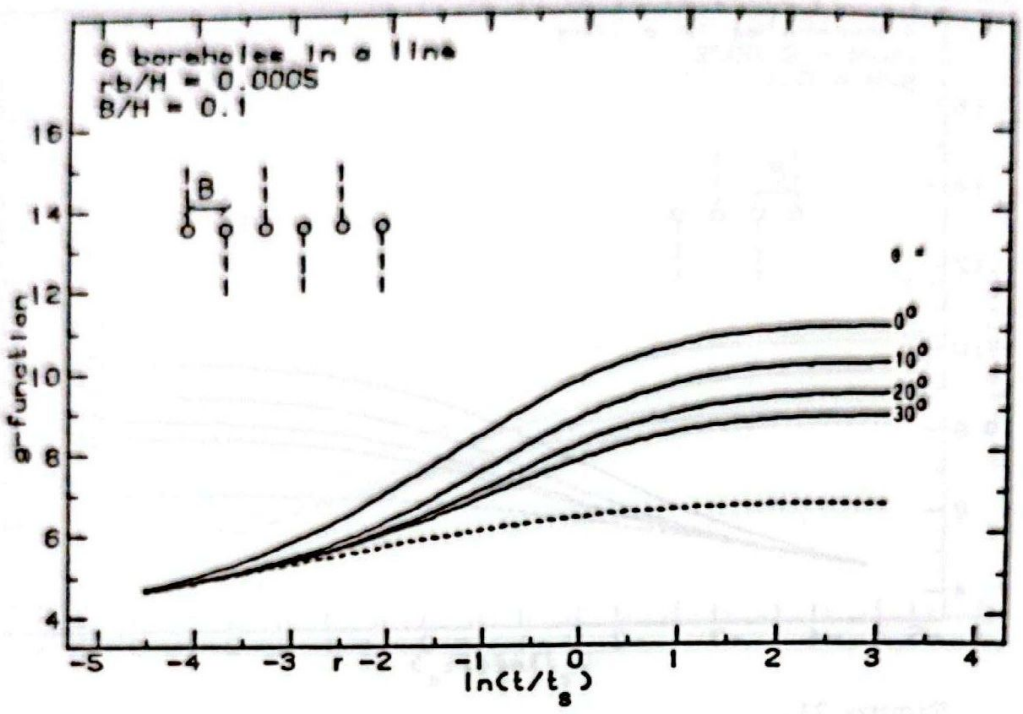

Figure 23

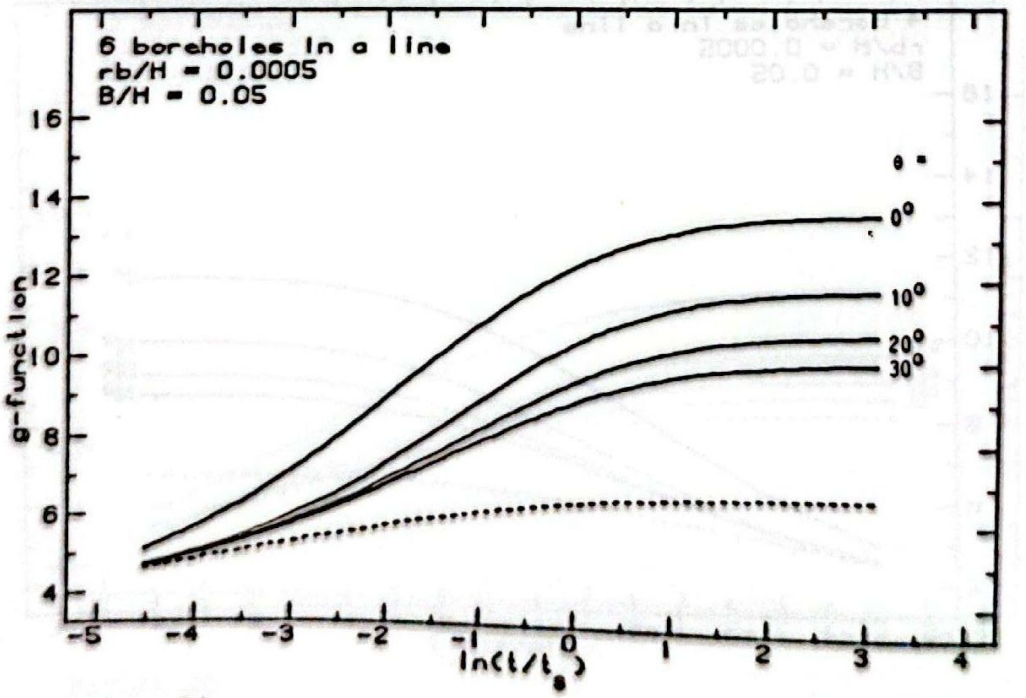

Figure 24

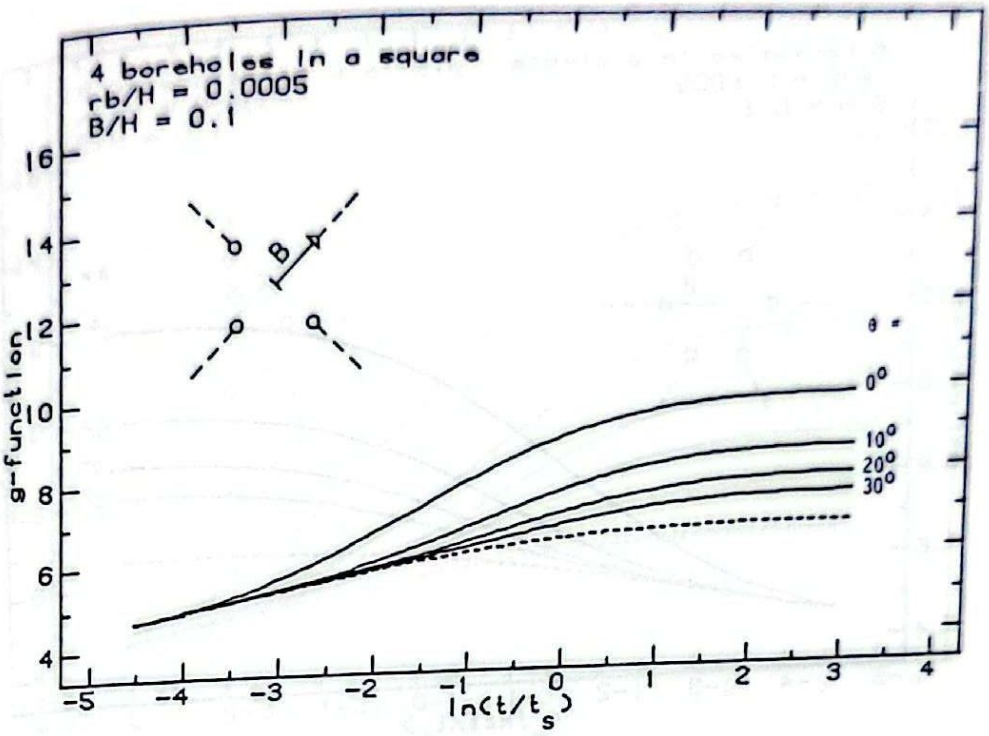

Figure 25

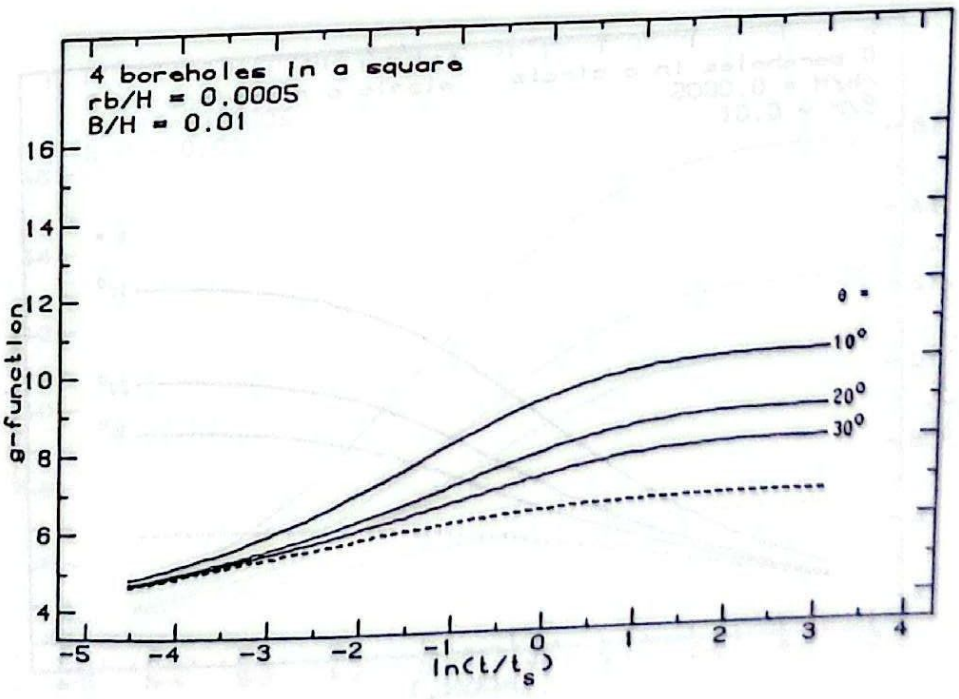

Figure 26

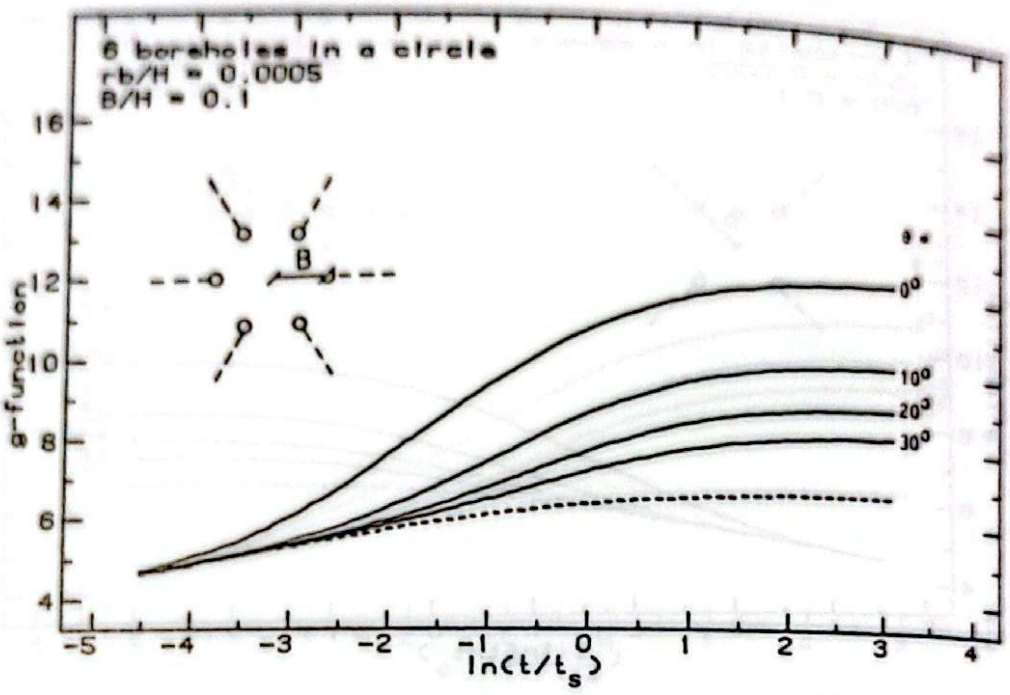

Figure 27

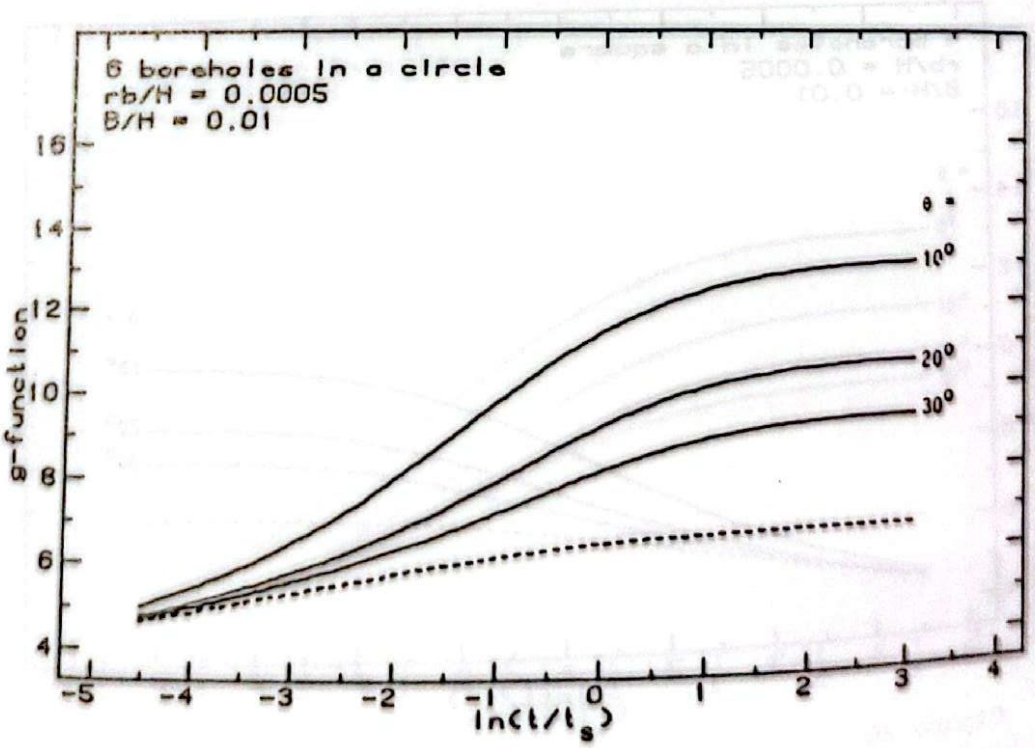

Figure 28

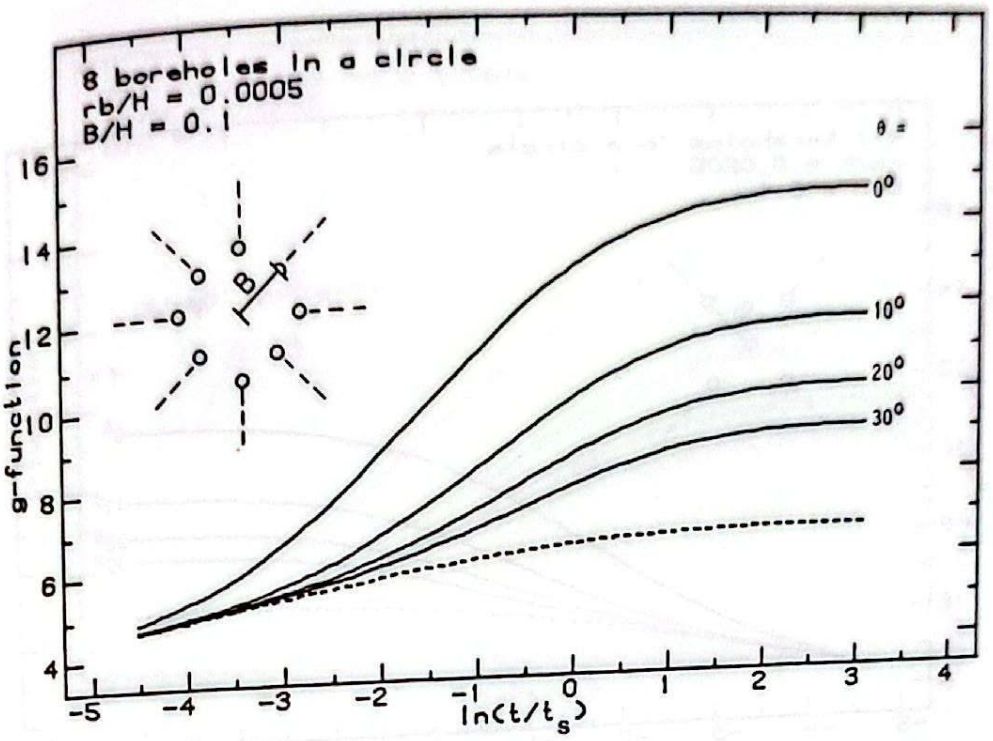

Figure 29

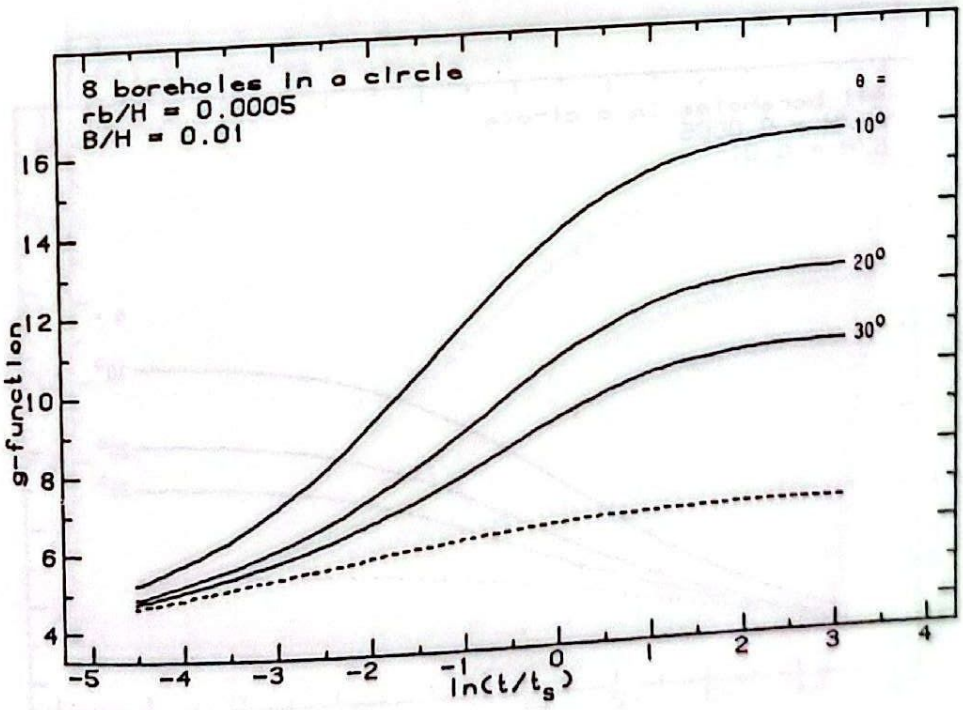

Figure 30

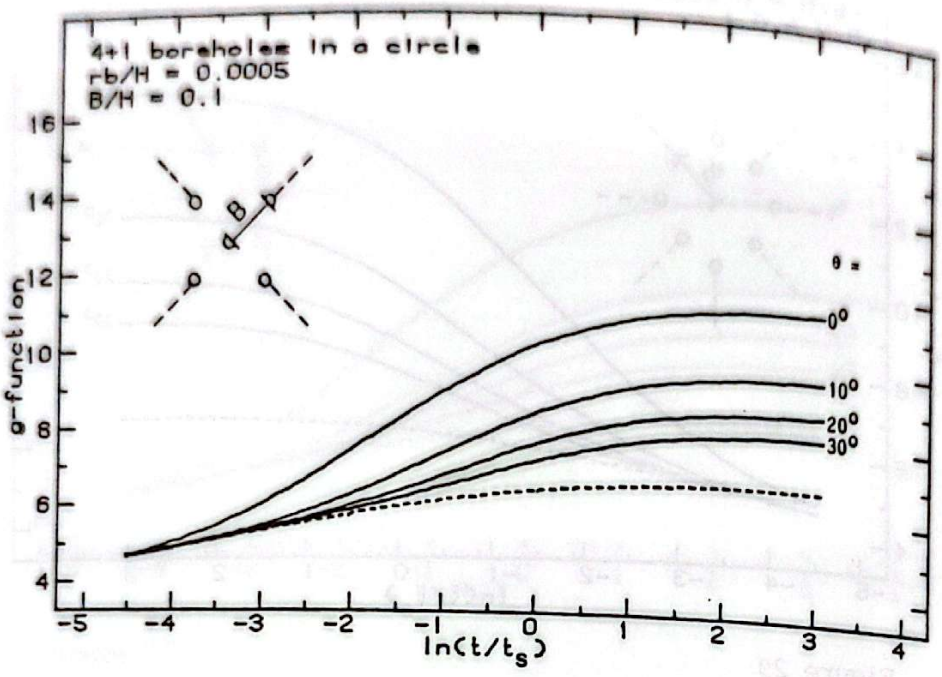

Figure 31

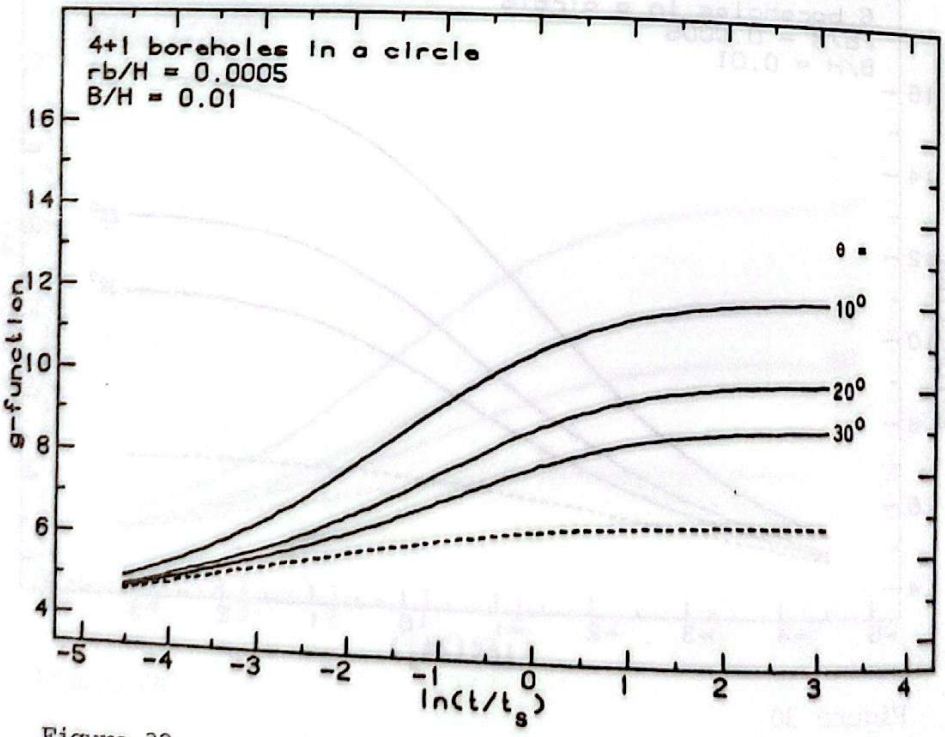

Figure 32

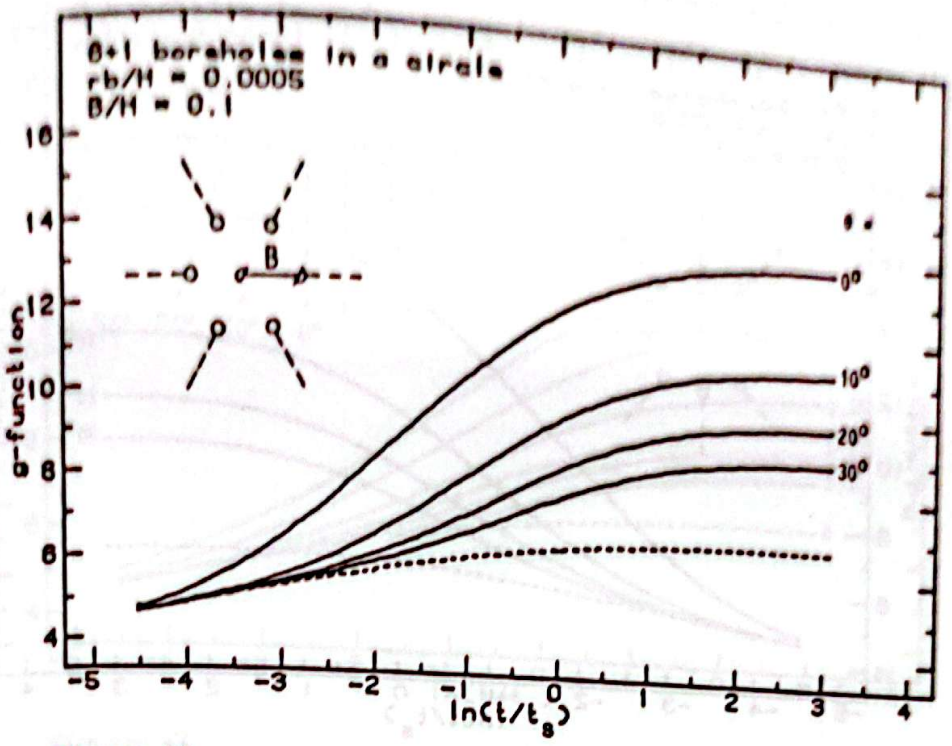

Figure 33

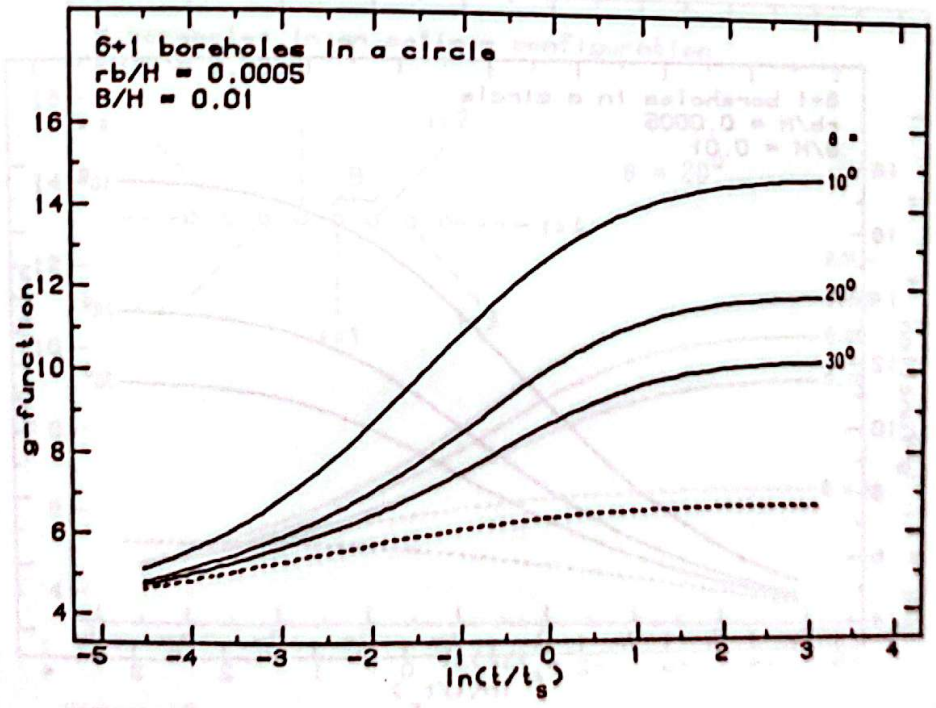

Figure 34

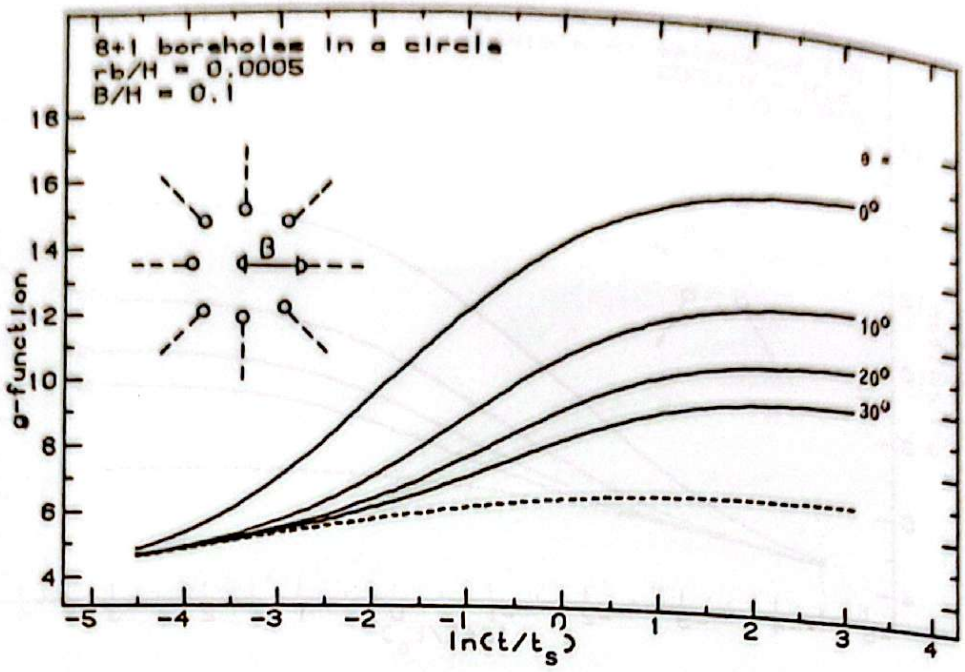

Figure 35

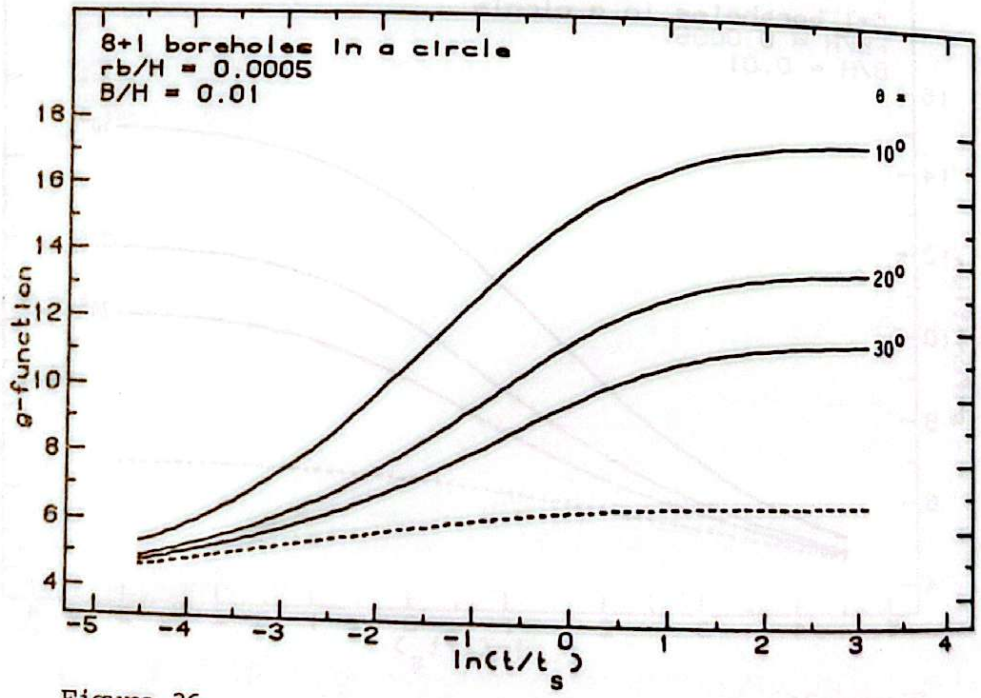

Figure 36

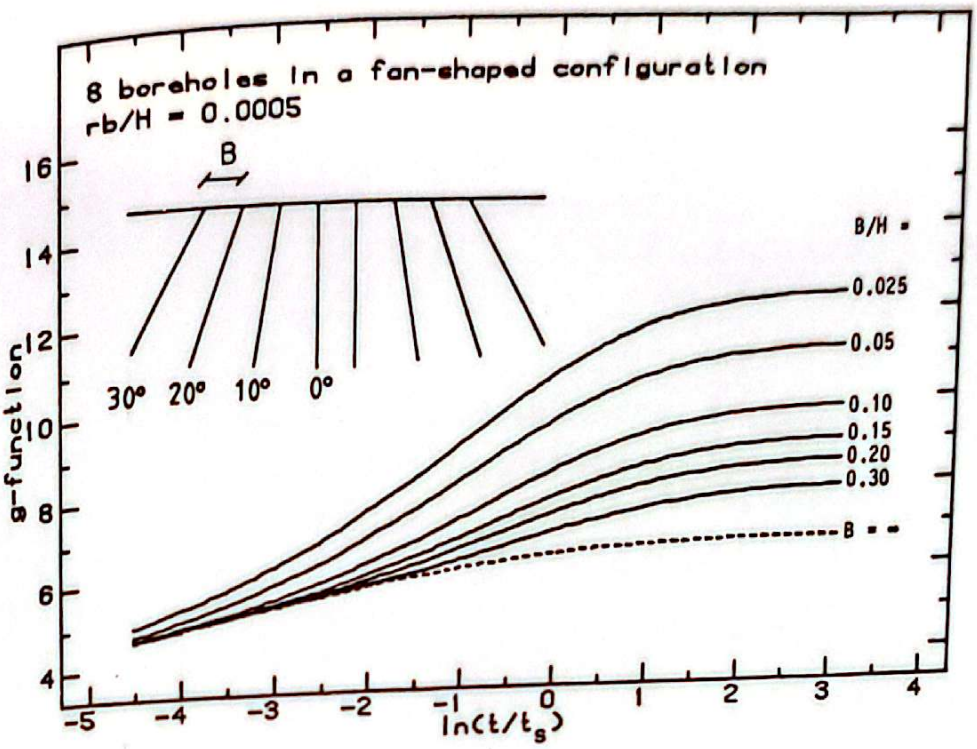

Figure 37

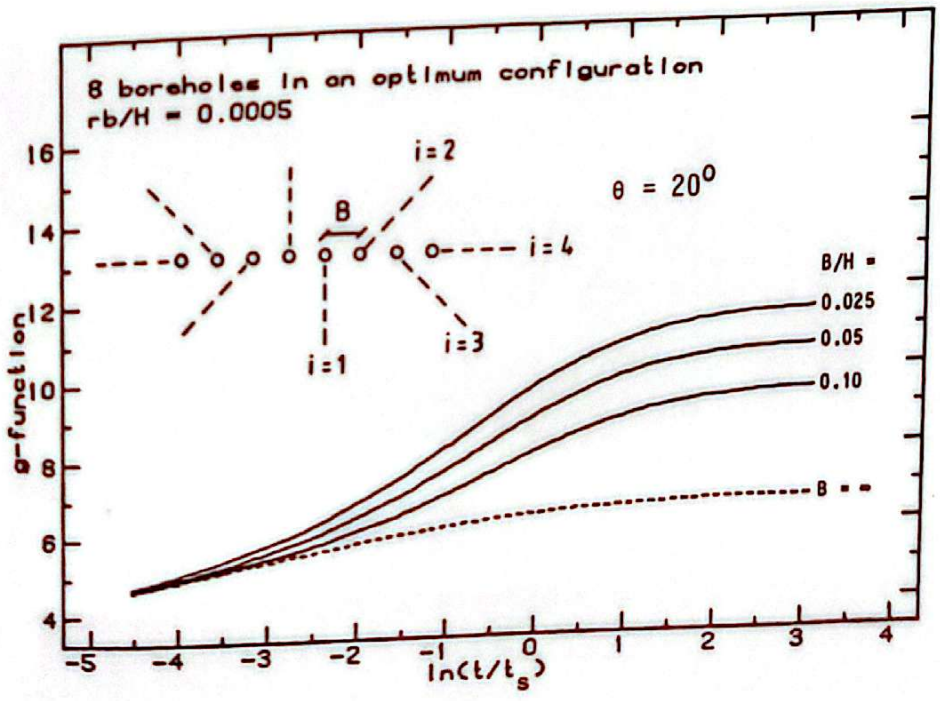

Figure 38

Notes on Heat Transfer 5-1987

Temperature Response Function g for 12 Borehole Configurations.

Per Eskilson

January 1987

Departments of Mathematical Physics
and Building Technology
University of Lund
Box 118
S-221 00 Lund, Sweden

CODEN : LUTVDG/(TVBH-7095)/1-8/(1987)

Temperature Response Function g for 12 Borehole Configurations

The curves on the following pages give the temperature response function g, described in [1], for 12 different configurations with vertical boreholes. Each g-function is given as a function of $\ln(t/t_s)$, where t is the time and $t_s=H^2/(9a)$ (H=active borehole depth, a=thermal diffusivity). Figures 1-3 concern boreholes on a line with equal spacing B (m). Figures 4-12 concern boreholes located in a regular rectangular pattern with equal spacing in the x- and y-direction. For each configuration there is a family of curves with varying value on the relative spacing B/H between the boreholes.

The curves are calculated numerically with the simulation model described in [2,3] for the case when the ratio between the borehole radius and the borehole length is $r_b/H=0.0005$. For any other radius the simple relation between two borehole radii in [1] is valid with very high accuracy.

Note that the g-function gives directly the temperature drop in °C at the borehole wall for the heat extraction rate $q=2\pi\lambda$ (W/m).

References:

1. J. Claesson, P. Eskilson, Conductive Heat Extraction by Thermally Interacting Deep Boreholes. Dep. of Mathematical Physics, University of Lund, Box 118, S-221 00 Lund, Sweden, 1987.

2. J. Claesson, P. Eskilson, Simulation Model for Thermally Interacting Heat Extraction Boreholes, Department of Mathematical Physics, University of Lund Box 118 S-221 00 Lund, Sweden, 1987. Submitted to Journal of Numerical Heat Transfer.

3. P. Eskilson, Superposition Borehole Model. Manual for Computer Code, Dep. of Mathematical Physics, University of Lund, Box 118, 221 00 Lund, Sweden, 1986.

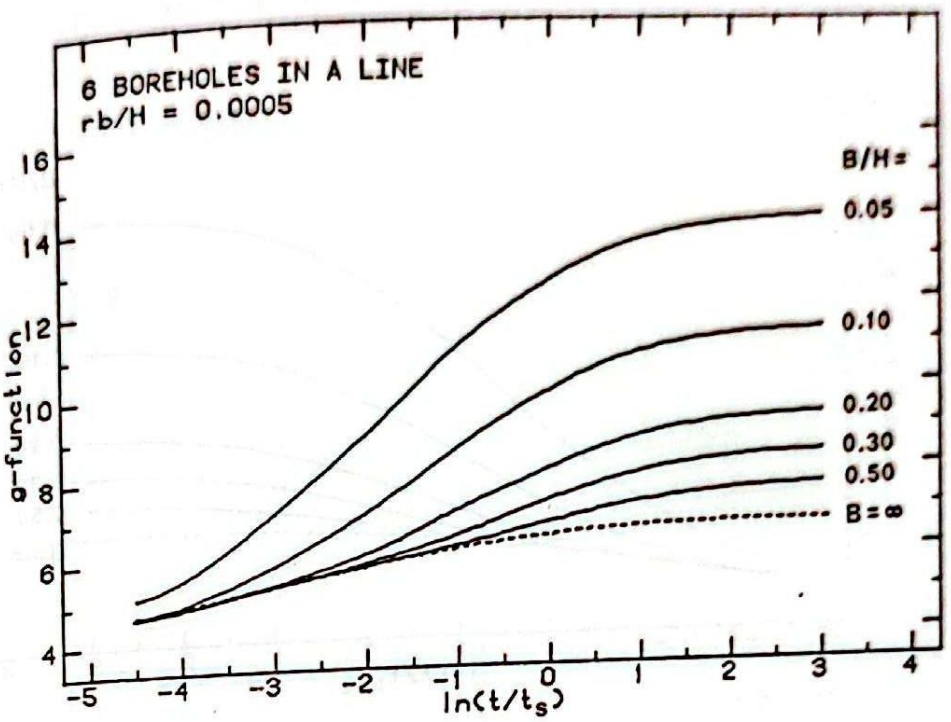

Figure 1

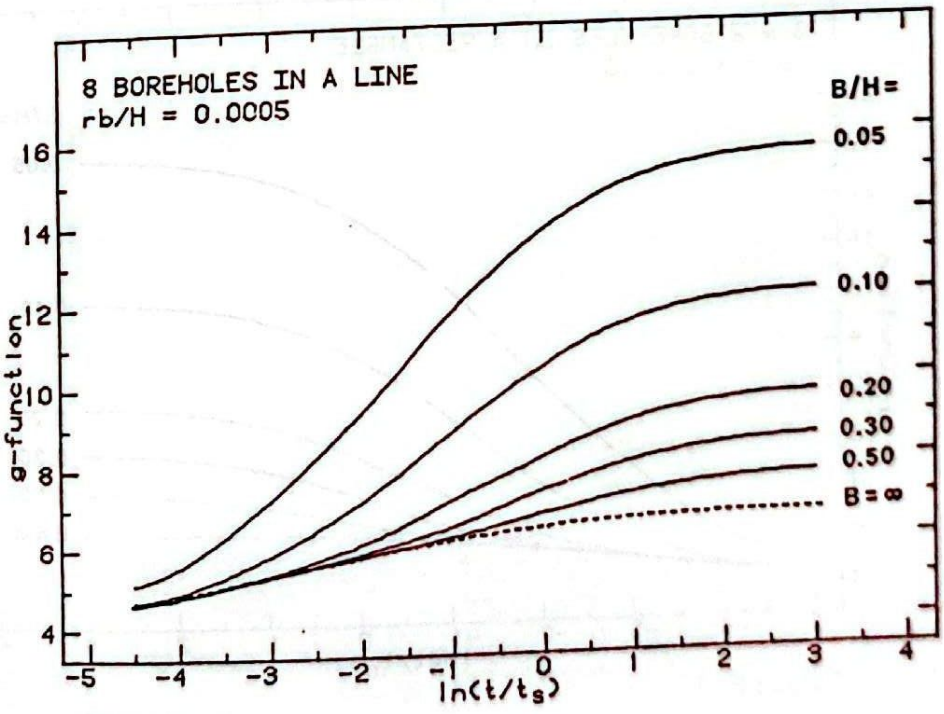

Figure 2

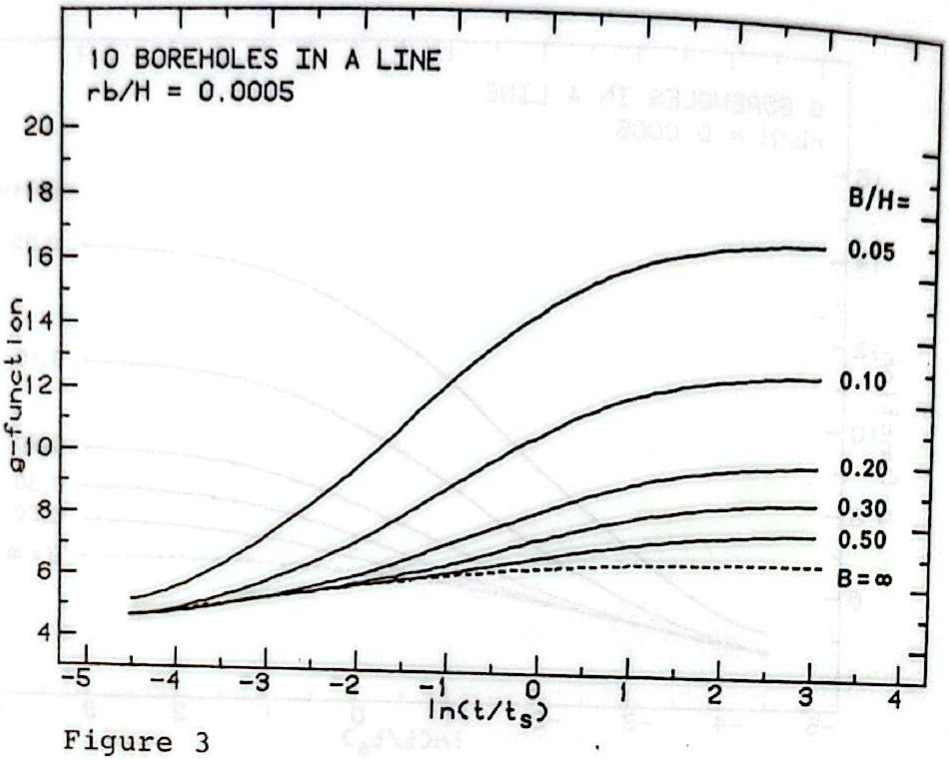

Figure 3

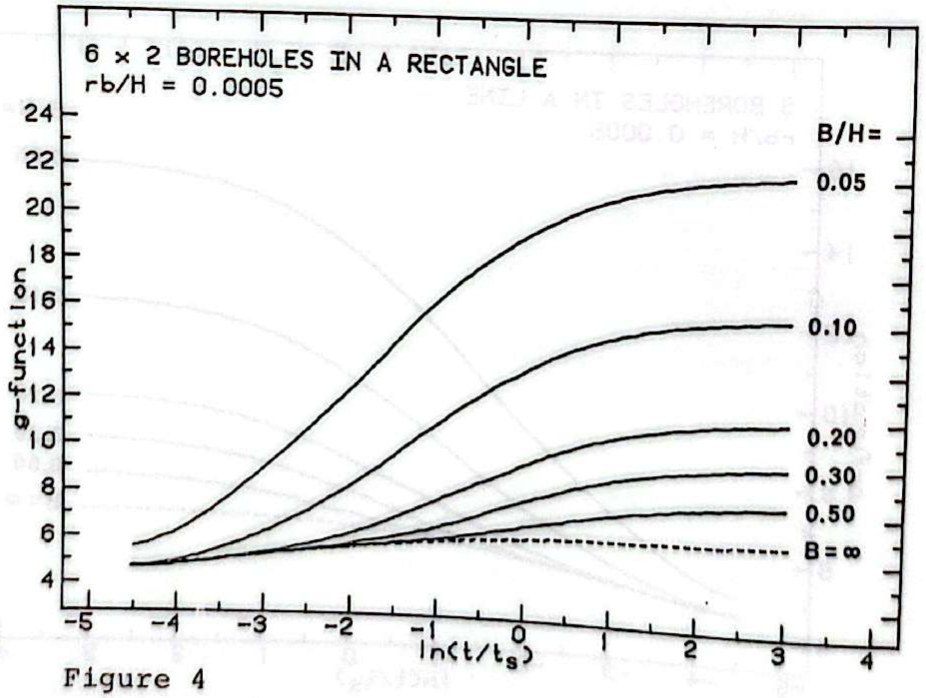

Figure 4

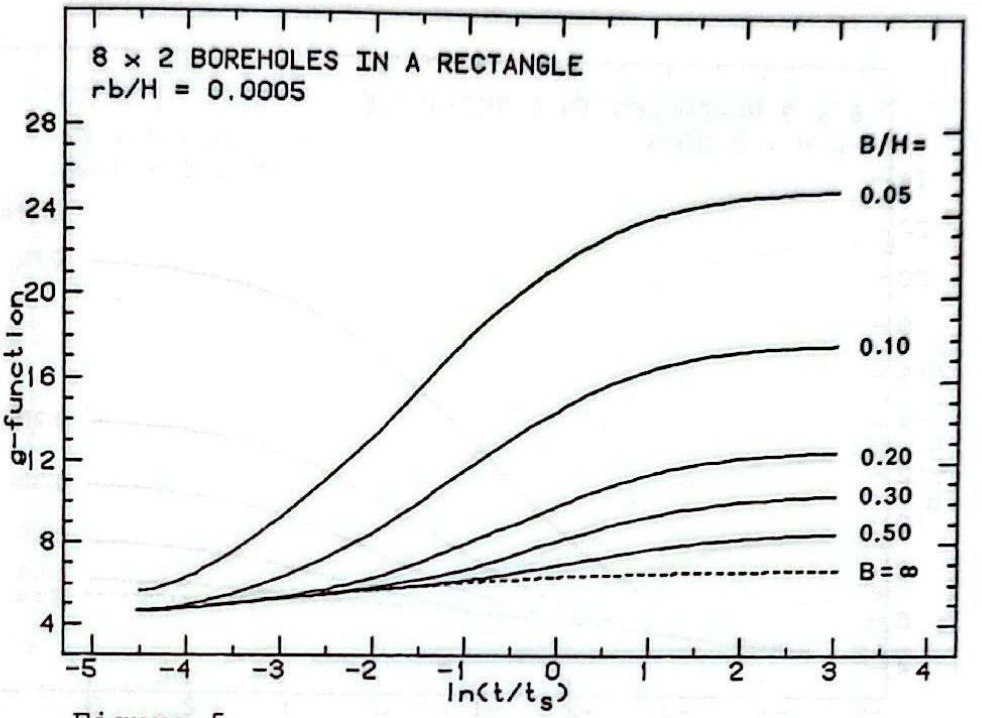

Figure 5

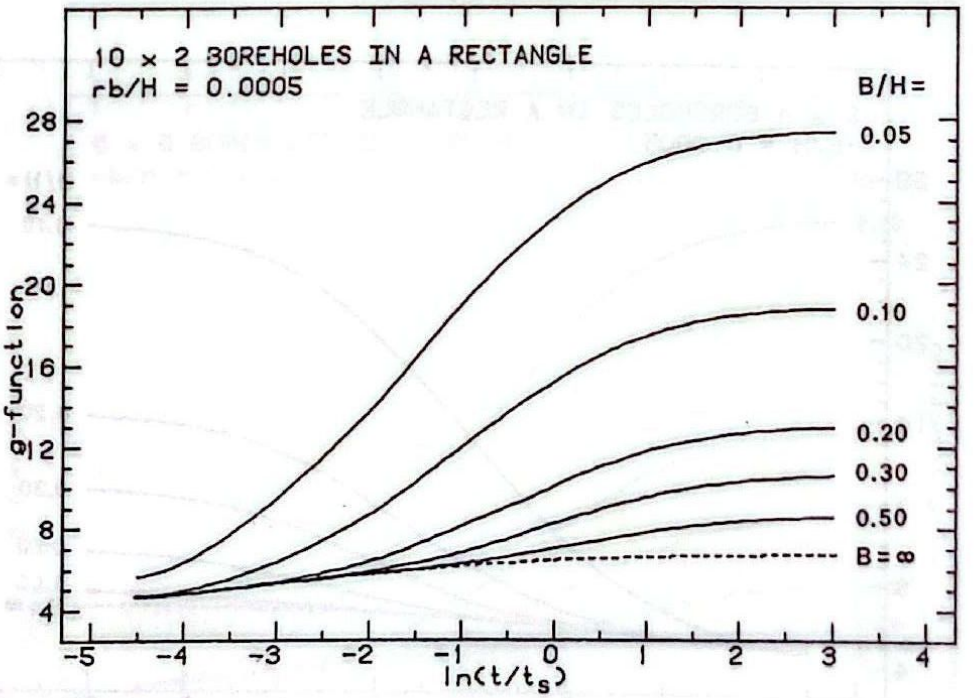

Figure 6

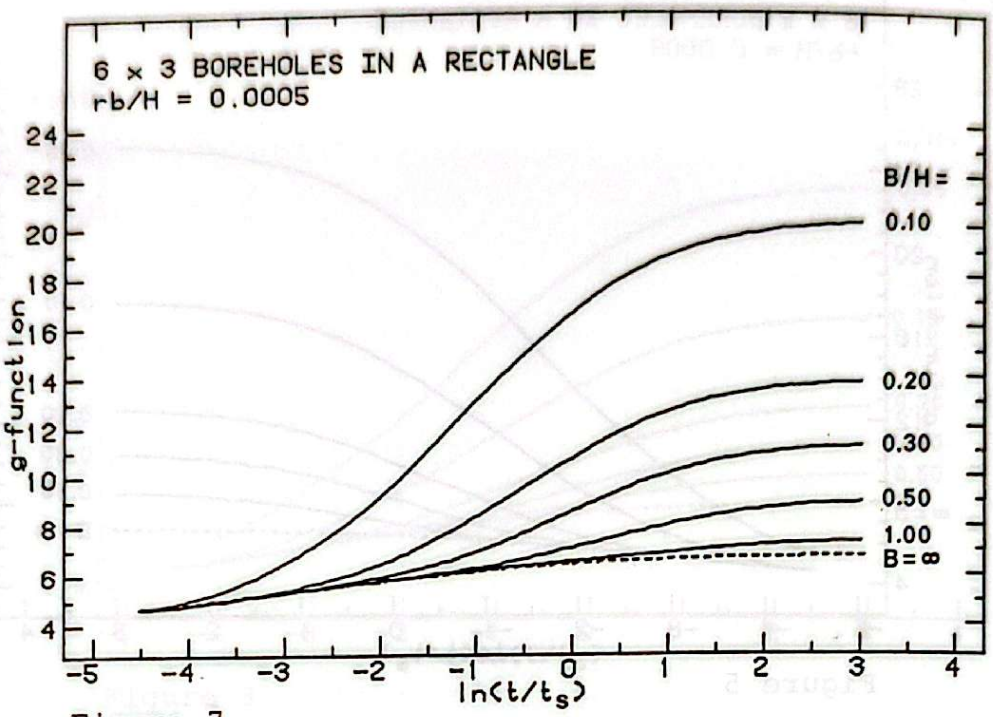

Figure 7

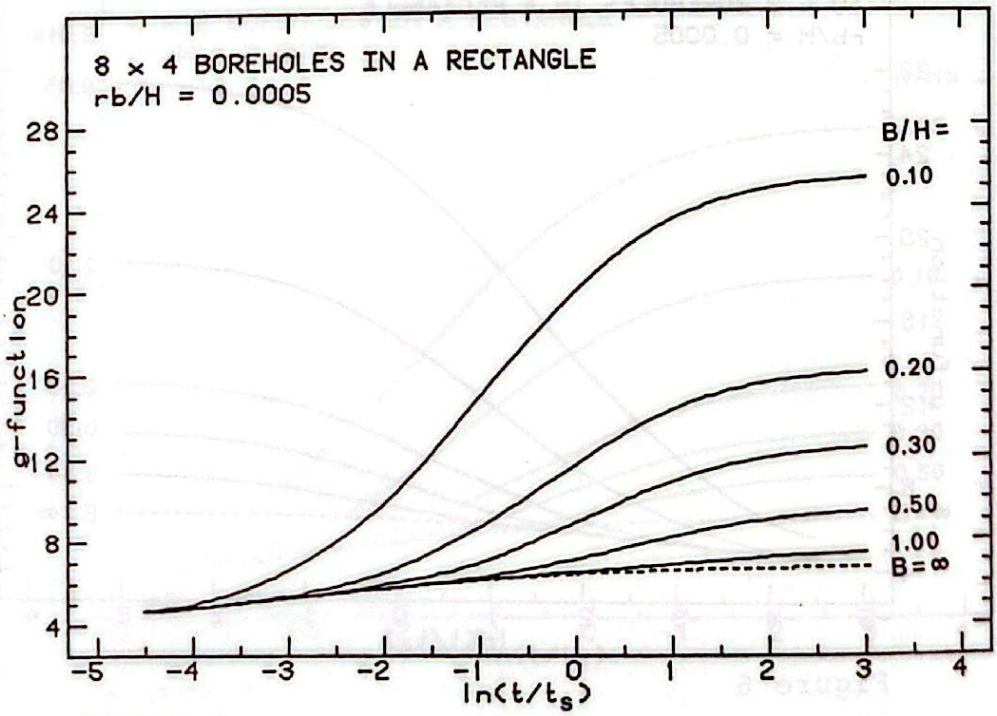

Figure 8

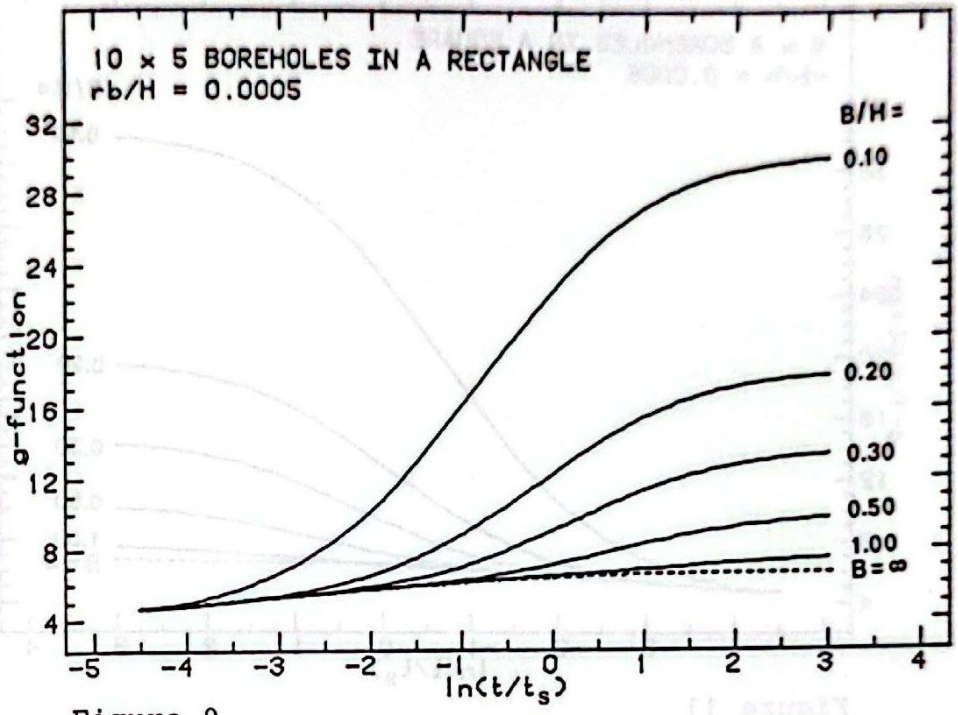

Figure 9

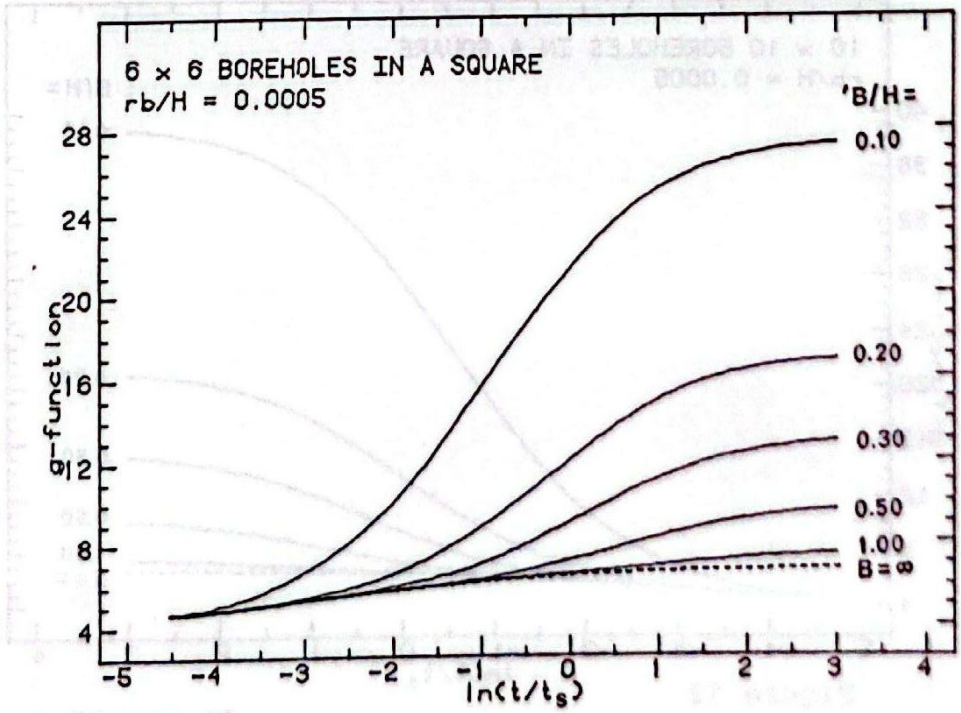

Figure 10

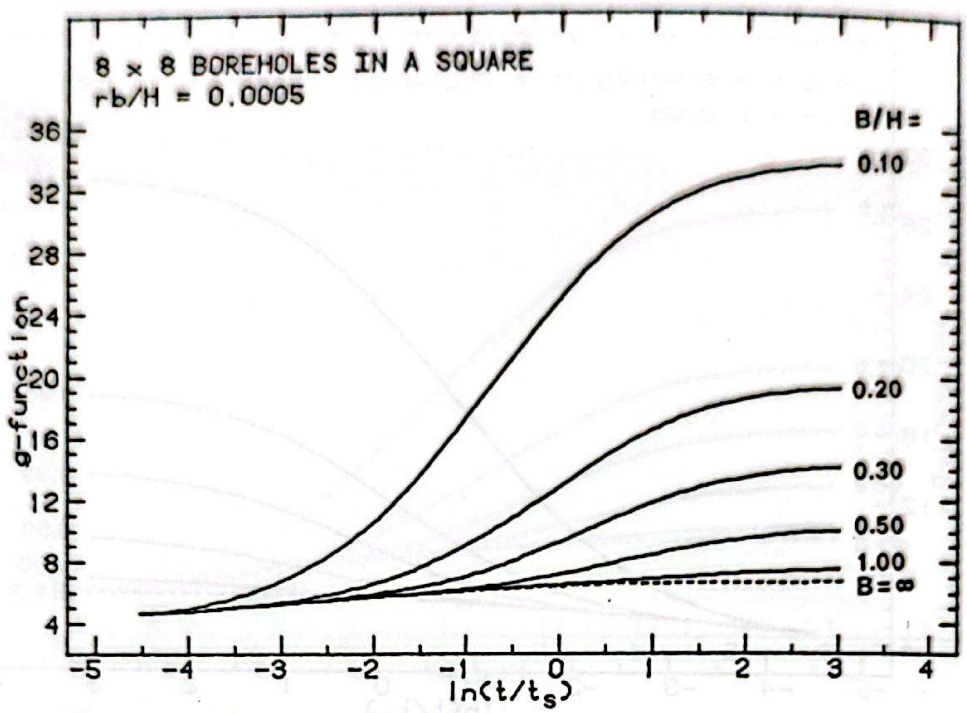

Figure 11

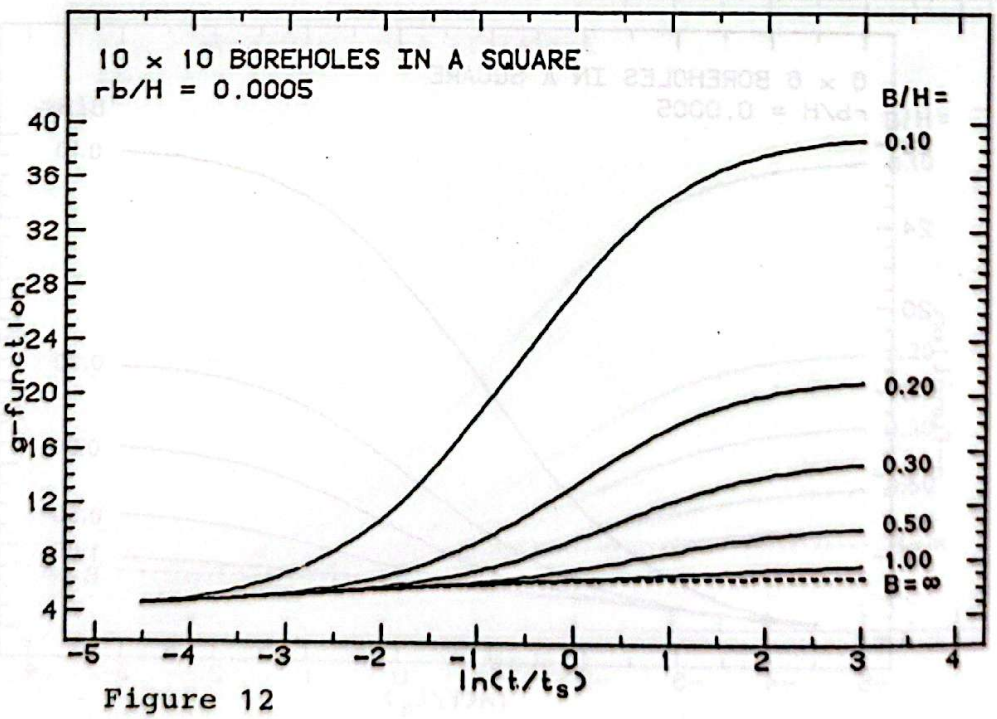

Figure 12

ISBN 91-7900-298-6